

**Mining potential drugs and natural products
from microbial genomes
via improved Red/ET recombineering**

Dissertation

Zur Erlangung des Grades

Des Doktors der Naturwissenschaften

Der Naturwissenschaftlich-Technischen Fakultät

Der Universität des Saarlandes

von

Qiang Tu

Saarbrücken

2016

Tag des Kolloquiums: Freitag, 10. März 2017

Dekan: Prof. Dr. rer. nat. Guido Kickelbick

Berichterstatter: Prof. Dr. R. Müller

Prof. Dr. A. Luzhetskyy

Vorsitz: Prof. Dr. R. W. Hartmann

Akad. Mitarbeiter: Dr. Y. Rebets

Acknowledgements

First and foremost I would like to give my deepest gratitude to my scientific supervisor Prof. Dr. Rolf Müller for all of the precious guidance and the opportunity to work in this remarkable research environment in the laboratory of Department of Pharmaceutical Biotechnology at Saarland University. His inspirational support and encourage during these years are invaluable, such that I have learned so much from his scientific ability and attitude from which I will benefit for my whole research career in my future career.

I also thank Prof. Dr. Jörn Walter for his kind suggestions during my Ph.D. studies.

I owe my sincere gratitude to my co-advisor Prof. Dr. Youming Zhang from State Key Laboratory of Microbial Technology at Shandong University in China, who practically co-advised me to go through the tough research process, especially at the beginning of the Ph.D. study. He taught me many principles and techniques of molecular biology. He provided me very valuable advices and guidance for my research and career. Furthermore, I will also thank Prof. Dr. Xiaoying Bian in Shandong University for his constructive comments and friendly help. In addition, I also would like to show my gratitude to Dr. Youhua Deng for her genuine help during my stay in Germany.

I would like to thank Prof. Dr. A Francis Stewart, Dr. Jun Fu and Dr. Jia Yin from BioInnovationsZentrum, Technische Universität Dresden. Over the past years I had very enjoyable experience to work with them in several collaborated projects. Their ambitions for technology development always inspire me. They are very generous to provide recombineering reagents and advices.

At the same time I am thankful to Dr. Jennifer Herrmann from Helmholtz Institute for

Acknowledgements

Pharmaceutical Research Saarland for bioactivity test of disorazol and writing the manuscript together.

I am grateful to Dr. Stephan Hüttel and Dr. Ritesh Raju in our group who directed me in the isolation, purification and structural elucidation of natural products. Their rich experience in NMR measurement is also very helpful.

I wish to thank all the lab members for their critical and open-minded scientific discussion during the last five years and their contributions to the good working atmosphere. I thank Dr. Silke C. Wenzel for her extremely useful suggestions of my research, Thomas Hoffmann, Eva Luxenburger for LC-MS measurement, and Liujie Huo for protein expression and translation, Dr. Daniel Krug for LC/MS analysis and computer assistance. The administrative assistance of Birgitta Lelarge, Natja Mellendorf, Claudia Thiele and Ellen Merckel is very grateful. I also thank my colleagues Dr. Wei Ding, Dr. Shengbiao Hu, Dr. Yixin Ou, Dr. Shiping Shan, Dr. Chengzhang Fu, Dr. Ronald Garcia, Dr. Hilda Sucipto, Fu Yan, Ying Tang, Srikanth Duddela and Viktoria Schmitt for all their support in various ways as both scientific collaborators and friends.

Last but not least, heartfelt thanks to my parents for their moral support all the years.

Qiang Tu

February, 20th, 2016

Vorveröffentlichungen der Dissertation

Teile dieser Arbeit wurden vorab mit Genehmigung der Naturwissenschaftlich-Technischen Fakultät III, vertreten durch den Mentor der Arbeit, in folgenden Beiträgen veröffentlicht oder sind derzeit in Vorbereitung zur Veröffentlichung:

Publikationen:

Qiang Tu, Jennifer Herrmann, Shengbiao Hu, Ritesh Raju, Xiaoying Bian, Youming Zhang and Rolf Müller. Genetic engineering and heterologous expression of the disorazol biosynthetic gene cluster via Red/ET recombineering. *Scientific Reports*. 2016, 6: 21066.

Qiang Tu*, Jia Yin*, Jun Fu, Jennifer Herrmann, Yuezhong Li, Yulong Yin, A. Francis Stewart, Rolf Mueller and Youming Zhang. Room temperature electrocompetent bacterial cells improve DNA transformation and recombineering efficiency. *Scientific Reports*. 2016, 6: 24648.

Isabel Kolinko, Anna Lohße, Sarah Borg, Oliver Raschdorf, Christian Jogler, **Qiang Tu**, Mihaly Posfai, Eva Tompa, Juergen M. Plitzko, Andreas Brachmann, Gerhard Wanner, Rolf Müller, Youming Zhang and Dirk Schüler. Biosynthesis of magnetic nanostructures in a foreign organism by transfer of bacterial magnetosome gene clusters. *Nature nanotechnology*. 2014, 9:193–197.

Jia Yin, Michael Hoffmann, Xiaoying Bian, **Qiang Tu**, Fu Yan, Liqiu Xia, Xuezhi Ding, A. Francis Stewart, Rolf Müller, Jun Fu and Youming Zhang. Direct cloning and heterologous expression of the salinomycin biosynthetic gene cluster from *Streptomyces albus* DSM41398 in *S. coelicolor* A3 (2). *Scientific Reports*. 2015, 5: 15081.

(*: Authors contributed equally to the work)

Patents

Qiang Tu, Jun Fu, Francis A. Stewart, Rolf Mueller and Youming Zhang.

A new method for DNA transformation.

United States of America patent application No: US 61/730,772 (2012)

International patent application No: PCT/IB2013/071546 (2013)

Conference Contributions

Qiang Tu, Ritesh Raju, Xiaoying Bian, Youming Zhang and Rolf Müller. Reconstruction and heterologous expression disorazol A biosynthetic gene cluster in *Myxococcus xanthus* DK1622 (**Poster**). International VAAM-Workshop 2012: “Biology and Chemistry of Antibiotic-Producing Bacteria and Fungi”. September, 2012, Braunschweig, Germany.

Qiang Tu, Ritesh Raju, Xiaoying Bian, Youming Zhang and Rolf Müller. Engineering and heterologous expression disorazol A biosynthetic gene cluster in *Myxococcus xanthus* DK1622 (**Poster**). 2nd International HIPS Symposium. September, 2012, Saarbrücken, Germany.

Abstract

A great deal of natural product biosynthetic pathways have been detected following the development of bacterial genome-sequencing projects. Reconstruction, genetic modification and heterologous expression of the biosynthetic gene clusters provide an effective approach to discover novel natural product derivatives, while also improving productivities and yields, which sets the stage to expand understanding of their structural diversity and biological activity.

The present thesis copes with several natural product biosynthetic gene clusters of large size (>50kb) and severe complexity with high GC content and repetitive sequences. Typically, it is more challenging to engineer such colossal and complex gene clusters using traditional approaches. Conversely, Red/ET recombineering, without the size and site limitation of DNA engineering established in *E. coli*, appears to enrich the toolbox of molecular biology and break the size and site limitations of DNA manipulation. Here, we have improved the Red/ET recombination method by changing the long-standing protocol of electrocompetent cell preparation from cold conditions to room temperature, such that the DNA transformation efficiency has been greatly increased. This interesting finding should facilitate the cloning of large fragments from genomic DNA preparations and metagenomic samples.

To exemplify this improvement, the core disorazol biosynthetic pathway (~58kb) from *Sorangium cellulosum* So ce12 was cloned by improved Red/ET recombineering and heterologously expressed in *Myxococcus xanthus* DK1622, resulting in an appreciable increase of disorazol production by promoter exchange.

The full-length salinomycin gene cluster (106kb) from *Streptomyces albus* DSM41398 was isolated from the genome by direct cloning and stitching, and this gene cluster was transferred into the heterologous host *S. coelicolor* A3 (2).

As a third example of the efficacy of this technique, the magnetosomes gene clusters within a large genomic magnetosome island (~115kb) from magnetotactic bacteria *Magnetospirillum gryphiswaldense* was cloned and expressed in *Rhodospirillum*

Abstract

rubrum. A visible red spot near the pole of a permanent magnet could be observed at the edge of a culture flask of heterologous mutants, signifying that the magnetosome products had been successfully expressed in the pink-colored heterologous host.

Zusammenfassung

Ein großer Teil der Naturprodukt Biosynthesewege wurden nach der Entwicklung von bakteriellen Genom-Sequenzierungsprojekten entdeckt. Konstruktion, Modifikation und heterologe Expression der Biosynthesegencluster bieten einen effektiven Ansatz an der Entdeckung von neuen Derivaten der Naturstoffe sowie der Verbesserung der Produktionsausbeute. Dies führt zu der Etablierung einer Plattform zur Erweiterung ihrer strukturellen Vielfalt und der biologischen Aktivität.

Die vorliegende Arbeit beschäftigt sich mit mehreren Naturprodukt-Biosynthesegencluster in großen (>50 kb) und komplexen Genclustern mit hohem GC-Gehalt und repetitiven Sequenzen. Herkömmlicherweise ist es kaum möglich, so kolossale und komplexe Gencluster mit traditionellen Ansätzen zu konstruieren. Folglich erschien Red / ET Recombineering die Toolbox der Molekularbiologie zu bereichern und die Begrenzung der DNA-Manipulation aufzulösen. Wir verbesserten die Red/ET-Rekombination durch Optimierung des langjährig verwendeten Protokolls der Vorbereitung elektrokompenter Zellen, welches aus dem kalten Zustand auf Raumtemperatur verändert wurde, so dass die DNA-Transformationseffizienz stark erhöht werden konnte. Diese interessante Erkenntnis sollte das Klonieren von großen Fragmente aus genomischer DNA und Metagenomen erleichtern.

Der Disorazol Biosyntheseweg (*disA-D*, ~58kb) von *Sorangium cellulosum* So ce12 wurde durch diese verbesserte Red/ET Recombineering Methode kloniert und in *Myxococcus xanthus* DK1622 exprimiert. Durch Promoter Austausch war die Erhöhung der Disorazol Produktionsausbeute möglich.

Das gesamte Salinomycin-Gencluster (*salO-orf18*, 106kb) aus *Streptomyces albus* DSM41398 wurde durch direct-cloning ebenfalls kloniert. Das Gencluster wurde in den heterologen Wirt *S. coelicolor* A3 (2) übertragen.

Die Magnetosom-Gene innerhalb eines großen genomischen Magnetosom-Insel (115kb) des magnetotaktischen Bakteriums *Magnetospirillum gryphiswaldense* wurde kloniert und in *Rhodospirillum rubrum* exprimiert. Ein sichtbarer roter Fleck in der Nähe der Pole eines Permanentmagneten konnte am Rande einer Kulturflasche von heterologen Mutanten beobachtet werden.

Table of contents

Acknowledgements.....	I
Abstract.....	II
Zusammenfassung.....	III
Table of contents.....	IV
A. Introduction.....	1
1. Natural products in drug discovery.....	1
2. Biosynthetic logics of microbial natural products.....	2
Polyketide natural products.....	7
Nonribosomal peptide natural products.....	10
PKS/NRPS hybrid systems.....	10
Magnetic particle production in microorganisms.....	11
3. Red/ET Recombineering.....	12
Development of recombineering.....	14
Application of recombineering.....	16
Improvement of recombineering.....	19
4. Heterologous expression of natural products in surrogate hosts.....	20
5. Outline of the dissertation.....	27
B. Publications.....	30
I. Genetic engineering and heterologous expression of the disorazol biosynthetic gene cluster via Red/ET recombineering.	
II. Room temperature electrocompetent bacterial cells improve DNA transformation and recombineering efficiency.	
III. Biosynthesis of magnetic nanostructures in a foreign organism by transfer of bacterial magnetosome gene clusters.	
IV. Direct cloning and heterologous expression of the salinomycin biosynthetic gene cluster from <i>Streptomyces albus</i> DSM41398 in <i>S. coelicolor</i> A3 (2).	

Table of contents

C. Final discussion.....	31
1. Development of a novel improved Red/ET recombination method.....	31
2. Several applications in mining microbial genomes via Red/ET technology, including disorazol, salinomycin and magnetosome product.....	33
3. New molecular technologies are required for construction and modification of large gene cluster in microbial genomes.....	38
D. References.....	40
E. Appendix.....	55

A. Introduction

1. Natural products in drug discovery

Nature has been an immense source of natural products for millennia, with various useful compounds developed from plants and animals.¹⁻³ These molecules have played a considerable and meaningful feature for treating and inhibiting human diseases and agricultural pests across the world over a long time.^{4,5} Following the discovery of penicillin by A. Fleming, H. W. Florey in 1928,⁶ pharmaceutical research began to focus on microbes, triggering a subsequent “golden era” in massive screening efforts to identify a substantial amount of new microbial antibiotics (1945-1960). Over 23, 000 natural products have been characterized, many of which are still used in clinic to date.^{7,8} Currently, approximately 40% of pharmaceuticals in clinical use are either natural products or their derivatives.⁹ Moreover, they are broadly applied not only in clinics, as antibiotics, lipid control agents, immunosuppressive agents, or as compounds exhibiting antitumor or antimalarial properties, but also in agriculture and veterinary applications, including pesticide, insecticides, herbicides, miticides, feed additives, antiparasitic agents and so on (Figure 1-1).¹⁰⁻¹⁴

Natural products from microorganisms are believed to be a dominant source in searching for drug candidates, in comparison with other natural compound producers, such as plants or insects.¹⁵ This perspective is substantiated by the impression that microbial natural products describe the blueprint of an evolutionary optimization process comprising selection for a specific biological activity.¹⁶ However, the diversity of microorganisms is enormous and only a very minor portion (as low as 1%) of bacteria and fungi has been described so far.¹¹ Thus, the identification of novel bacterial secondary metabolite producers is expected to result in the discovery of novel natural products with interesting biological activities in the near future. Moreover, the increasing insights of microbial secondary metabolite biosynthesis and regulation coupled with progresses in molecular genetics drive us to focus on the

discovery and the optimization of natural products in the post-genomic era.

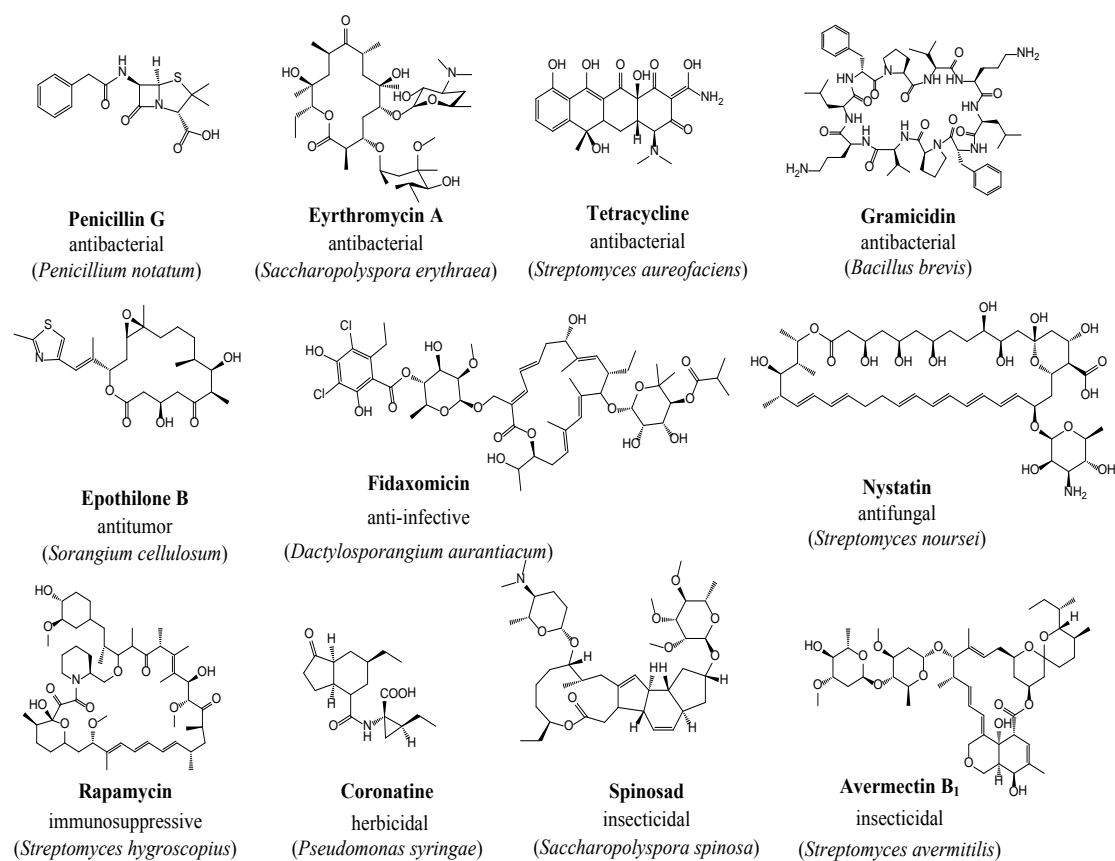


Figure 1-1. Selected examples of natural products derived from microbes used in the clinic/clinical trials, agriculture, and veterinary applications. The structure, name, original producer and type of application are given.

2. Biosynthetic logics of microbial natural products

A wide array of natural products with useful bioactivities and diverse structures are produced by microorganisms via various complex biosynthetic pathways.¹⁷ So far, several important major groups of natural products have already been established by multimodular megasynthase systems such as polyketide synthases (PKS), non-ribosomal peptide synthetases (NRPS), or hybrids thereof.¹⁸⁻²⁰ Additionally, there are also multitudinous bacterial natural products which are derived from other different metabolic routes, such as shikimate or isoprenoid pathway.²¹⁻²³

A great deal of microbial natural products are biosynthesized from simple monomeric building blocks (e.g. amino acids or short chain carboxylic acids) into enormous multifunctional enzymes via PKSs and NRPSs, respectively (Figure 1-2).^{24,25} In PKS

A. Introduction

systems, the vast majority of monomer units incorporated during chain elongation are malonyl-CoA and methylmalonyl-CoA. In some cases, the acyltransferase (AT) domain directly selects the thioesters of monoacyl groups such as acetyl-, propionyl-, and benzoyl-CoAs, or structural variants, such as malonamyl-CoA or methoxymalonyl-CoA to be the start units (Figure 1-3A).²⁶ Meanwhile, in NRPS systems, as well as the typical 20 proteinogenic amino acids, a broad variety of nonproteinogenic amino acids such as aryl acids are utilized as monomer building blocks for oligomerization and diversification during chain elongation and termination (Figure 1-3B).²⁷ Recent studies exhibit that NRP chains can be modified with both *C*-capped and *N*-capped functionalities, such as *C*-capped amines as in bleomycin,²⁸ or *N*-capped acyl groups such as the long-chain β -OH fatty acid in daptomycin.²⁹ Although PKS and NRPS systems employ different building blocks, they manifest remarkable similarities in the modular architecture of various catalytic domains and assembly-like mechanisms.

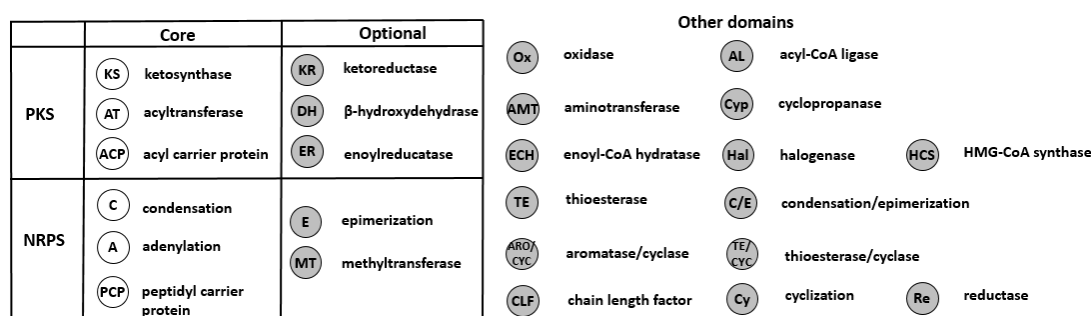


Figure 1-2. Core PKS and NRPS domains. Schematic abbreviations used throughout the whole text are shown³⁰.

In enzymatic machinery, PKS possesses catalytic core domains along with a carrier protein that not only organizes the minimal machinery for chain assembly but also can be post-assembled with additional catalytic domains (Figure 1-3C).¹⁹ In principle, a typical PKS module includes three essential domains: (i) the C–C bond-forming ketosynthase (KS) domain with 45kDa, which performs a decarboxylative claisen thioester condensation of the extender unit (generally malonyl-CoA or methylmalonyl-CoA) with the acyl thioester intermediate from the upstream module,

A. Introduction

(ii) the 50kDa AT domain for extender unit selection and loading, and (iii) the acyl carrier protein (ACP) domain, also known as a thiolation (T) domain with around 8-10kDa, where the acyl chain is assembled and elongated (Figure 1-3C). The typical order of domains is KS-AT-ACP. Additionally, several optional domains could be also involved to modify the polyketide intermediate, such as ketoreductase (KR), dehydratase (DH) and enoyl reductase (ER) domains.^{19,31,32} This process is usually completed with a thioesterase (TE) domain that releases and controls the form of the biosynthetic intermediate, such as in linear, cyclic or branched cyclic forms (Figure 1-2).³³

Similarly, in an NRPS elongation minimal module, the basic machinery also consists of three necessary domains: (i) a 50kDa condensation (C) domain that catalyzes the peptide bond formation, (ii) a 50kDa adenylation (A) domain responsible for amino acid recognition and activation, and also (iii) a 8-10kDa peptidyl carrier protein (PCP) or thiolation (T) domain to which the activated amino acid is covalently attached as thioester (Figure 1-3D).¹⁹ The typical order of domains is C-A-PCP. The specificity of A domains towards corresponding amino acids act crucially in the peptide sequence of the final natural product and the biological activity as well. Nevertheless, the optional domains for modification in NRPS cover epimerase (E), methyltransferase (MT), heterocyclization (HC) and oxidase (Ox) domains.¹⁹ In the same fashion as the PKS system, the TE domain turns out to be the last biosynthetic step in most cases of NRPS by catalyzing the hydrolysis or cyclization of nascent products to constitute linear or cyclic peptides (Figure 1-2).

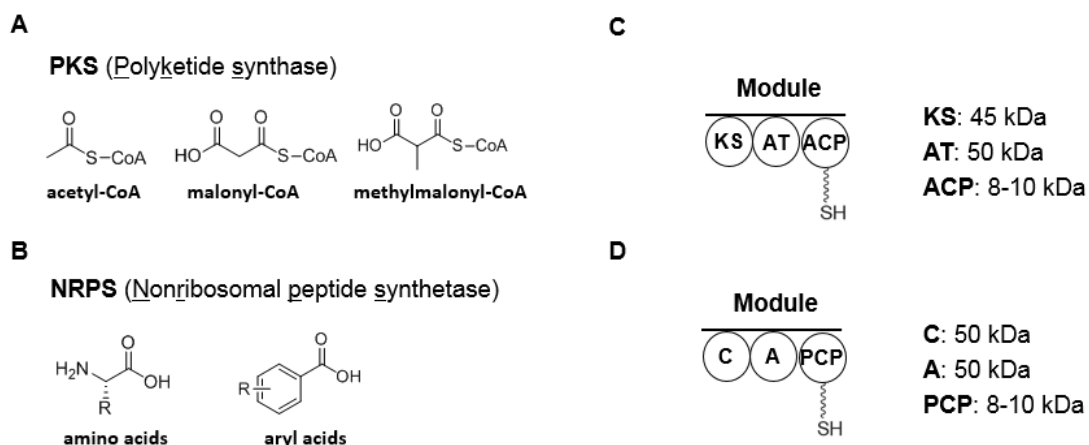


Figure 1-3. Use of thioester monomers and core domains of PKS and NRPS system. (A) Common acyl-CoA thioesters used for chain initiation and elongation by PKSs. (B) Shared amino and aryl acid monomers used for chain initiation and elongation by NRPSs. (C) Core domains of PKS system. A minimal module consists of a KS domain (45 kDa), an AT domain (50 kDa) and an ACP domain (8-10 kDa). (D) Core domains of NRPS system. A minimal module consists of a C domain (50 kDa), an A domain (50 kDa) and a PCP domain (8-10 kDa).

In summary, the core domains of PKS (KS, AT, CP) possess similar counterparts in NRPS (C, A, PCP) which catalyze three main steps as explained previously, covering two catalytic domains and one thiolation domain. The possible combinations of these various domains present thousands of different PKS and NRPS biosynthetic gene clusters in the bacterial chromosome, offering a rich and valuable source of natural products.^{34,35} According to the current sequenced genomes of abundant bacteria, it should be noted that PKS and NRPS clusters are infrequent in bacteria with genomes less than 3 Mb. Conversely, in the bacteria with genomes more than 5 Mb, a linear correlation between the genome size and the number of PKS and NRPS gene clusters is finally discovered.³⁰

The biosynthetic machinery of PKS and NRPS systems can be explained in four strategies: (1) A serine side chain in the carrier protein facilitates the pyrophosphate linkage of coenzyme A. In this case, an important post-translational modification by a phosphopantetheinyl transferase (PPTase) is required for both PKS and NRPS, converting the enzyme from the inactive *apo*- to the active *holo*-form (Figure 1-4).^{36,37} (2) Monomers are supplied into the assembly lines to generate elongated intermediates, and in PKS assembly lines, benzoyl-, butyryl-, cyclohexyl or propionyl-CoAs are employed as starter units²⁶ and malonyl-CoA, methylmalonyl-CoA, alkyl-, hydroxyl or aminomalonyl-CoAs are utilized as the chain extender blocks.³⁸ In contrast, several hundred nonproteinogenic amino acids participate in the biosynthesis of NRP microbial metabolites.³⁹ (3) Chain initiation (including monomer selection, loading and acylation), chain elongation (including claisen, amide and ester condensations) and chain termination are carried out subsequently during the assembly (see detailed description below). (4) Post

assembly-line tailoring of nascent released products (Figure 1-5).

In addition, chain elongation in the step 3 includes three basic reactions:

- (i) Substrate recognition, involving recognition of acyl-CoA thioesters by PKS and aminoacyl-adenylate by NRPS;
- (ii) Covalent binding, e.g. thioester bound to a carrier protein, whether ACP in PKS or PCP in NRPS;
- (iii) Condensation with the acyl- or peptidyl- residues from the upstream module.

Each of these enzymatic modification steps are performed on individual catalytic domains within the module (Figure 1-5).

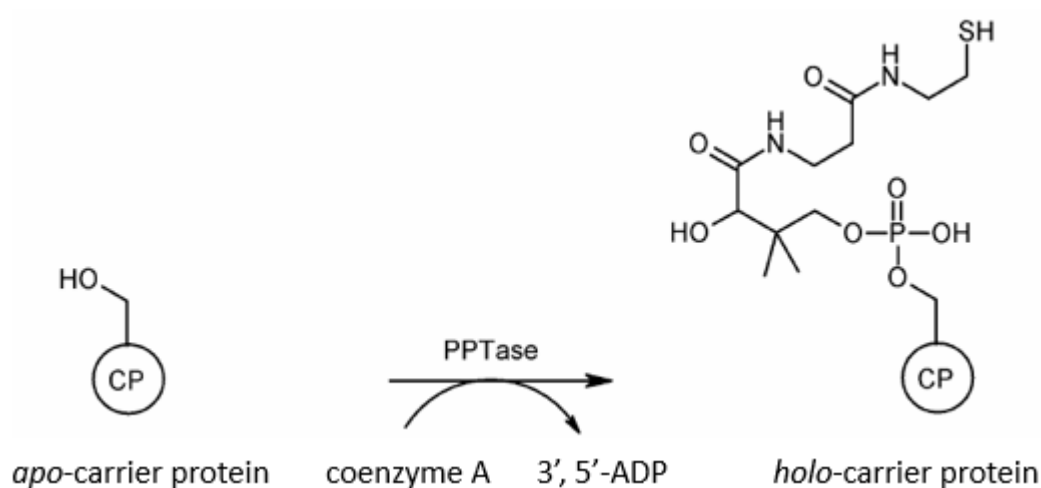


Figure 1-4. Post-translational activation of carrier proteins (CPs) by a phosphopantetheinyl transferase (PPTase).

A. Introduction

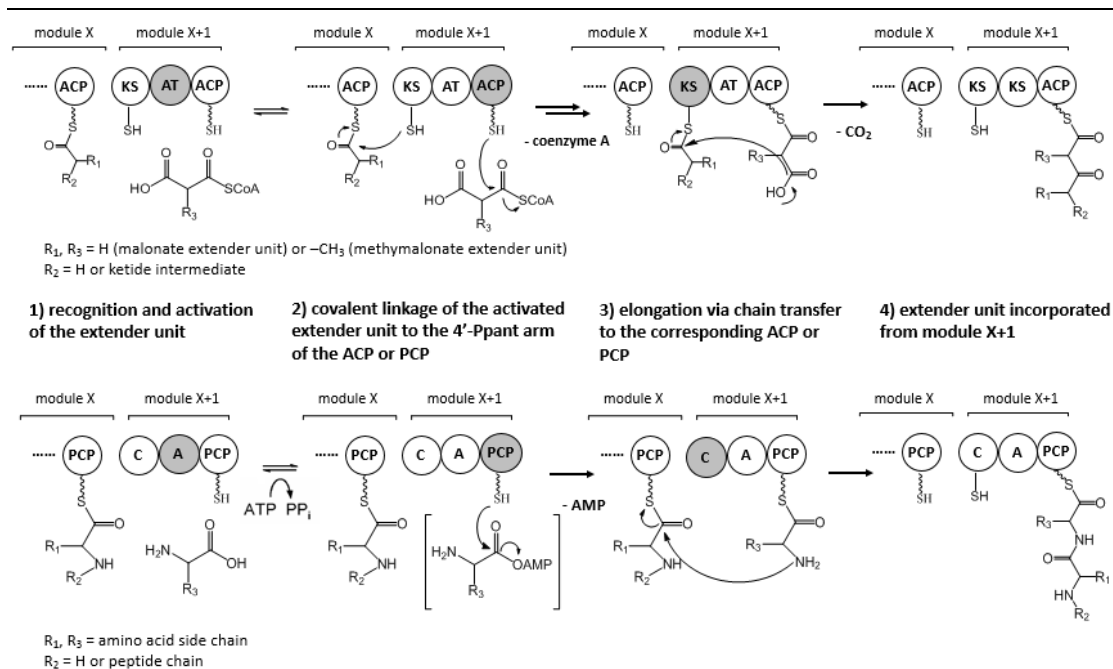


Figure 1-5. Schematic exhibitions of PKS (up) and NRPS (down) biochemistry. Domains involved in the particular reaction steps are highlighted in grey.

2.1 Polyketide natural products

Polyketides are a wide group of natural products occurring in bacteria, fungi, animals and plants, which represent numerous clinical compounds such as macrolide antibiotic erythromycin, polyene immunosuppressant rapamycin, antibiotic tetracycline, anti-cholesterol lovastatin, polyene antifungal amphotericin B and mycotoxin carcinogen aflatoxin B₁.⁴⁰ All of them are biosynthesized from acyl-CoA precursors by PKS enzymes. Much of the research in polyketide biosynthesis in last two decades has focused on biochemistry and genetic studies characterizing that three types of bacterial PKSs.⁴¹ Type I PKSs are large multifunctional enzymes in which both catalytic domains and carrier ACP domains are linked *in cis* to constitute modules that are joined together to form a multimodular assembly line (Figure 1-5 up). Type II PKSs are multienzyme complexes that carry a single set of iteratively acting activities. Contrary to type I PKSs, the catalytic domains and the carrier ACP domains interact *in trans* to achieve acyl- chain elongations in type II PKSs. Lastly, type III PKSs can be distinguished from type I and type II PKSs by this groups preference to utilize malonyl-CoA rather than malonyl-S-pantetheinyl-T species as substrates, and

thus type III PKS do not possess ACP domains.^{31,41} Type I and type II PKSs utilize ACP domain to activate the acyl-CoA substrates and to channel the growing polyketide intermediates, whereas type III PKSs, independent of ACP, act directly on the acyl-CoA substrates.

Type I PKSs are further subdivided into two groups: modular type I PKSs and iterative type I PKSs (iPKSs). iPKSs have nearly been discovered in fungi with reusing domains in a cyclic style.²³⁶ In iPKSs, the KS domain repetitively modifies the growing polyketide chain after each round of condensation and terminates polyketide biosynthesis at a mathematical perform.⁴² Interestingly, the same catalytic domains for multiple rounds of chain extension are repetitively utilized in both iPKSs, type II PKSs and type III PKSs systems.⁴³

Type II PKSs are composed of partite enzymes harboring the minimal PKS module as well as a set of tailoring enzymes.⁴⁴ Each minimal PKS module consists of two KS domains (KS_{α} and KS_{β}) and an ACP domain to catalyze the individual reactions of chain assembly and modification.^{18,45} The subunit KS_{β} has also been known as “chain length factor”.⁴⁶ Additionally, post assembly of the aromatic polyketides in type II PKSs systems require several specialized enzymes which exist in the genetic sequencing scaffold, such as aromatase (ARO), cyclase (CYC) and ketoreductase (KR).⁴⁷

Type III PKSs catalyze the condensation of one to several molecules of extender substrate onto a starter substrate,⁴⁸ and these are mostly found in plants, including stilbene synthases and naringenin-chalcone synthases.^{49,50} However, a lot of studies of have already revealed the fact that type III PKSs can also exist in bacteria, such as quinolone alkaloid aurachins from the myxobacterium *Stigmatella aurantiaca*.⁵¹

It is well known that polyketide elongation depends on at least three enzymatic domains: a KS, an AT and an ACP. Of late the conventional model of complex polyketide biosynthesis was broadened by discovery a special type of modular system named *trans*-AT PKS (Figure 1-6).⁵²⁻⁵⁶ The first report of this *trans*-AT PKS system was from pederin that was produced by an uncultured bacterial symbiont of *Paederus*

beetles.²⁴⁰ Several multimodular systems containing PKS modules lacking proper AT domains were discovered not only in actinomycetes, but also in a wide range of bacteria group.⁵⁷ Previous studies of *trans*-AT phylogeny had emphasized these PKSs undergo a remarkable capacity to develop by horizontal gene transfer, allowing substantial recombination of PKS gene fragments.⁵⁸ Furthermore, with the continuous detections of an increasing number of *trans*-AT PKS-derived polyketides demonstrating significant bioactivities, and a great deal of research had focused on a detailed understanding of *trans*-AT PKS function, including mechanistic and structural insights.⁵⁶ Recent studies indicated that *trans*-AT PKSs possessed several distinct domains only existed in these systems. Some domains were proved to be useless, skipped or even iterative practice.⁵⁶ Moreover, another visible characteristic of *trans*-AT PKS was named β -branching which present a variety of complex modifications in the β -keto position.²⁴¹ Nowadays, with increasing discovery of *trans*-AT PKS-derived compounds from varying microorganisms, more details and specifics in this exceptional system would be understood and disclosed in the near future.

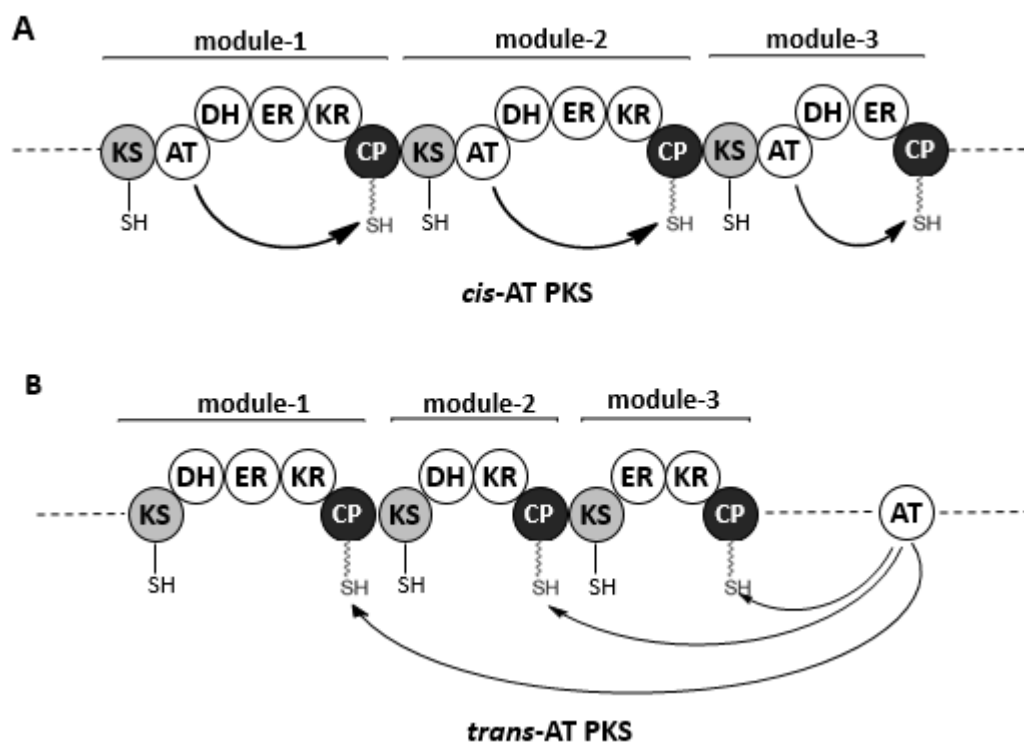


Figure 1-6. Domain organization of *cis*-AT (A) and *trans*-AT (B) PKS. (A) Protein

domains are connected *in cis*. (B) Protein domains interact *in trans*. The figure was reproduced from reference¹⁹.

2.2 Nonribosomal peptide natural products

NRPSs are linear, cyclic or branched peptides with no more than 20 amino residues after various modifications, such as acylation, epimerization, glycosylation, heterocyclization or N-methylation of the amide nitrogen. Hence, the monomers for NRPS assembly are not only proteinogenic but also nonproteinogenic amino acids as well as other carboxylic acids.⁵⁹ There are also many well-known NRP antibiotics including penicillin G, cephamycin C and vancomycin that have already been developed to clinically used drugs.

According to their sphere of activity, the nonribosomal peptides have been separated into several classifications: (1) Antibiotics, such as vancomycin, which is antibiotic of critical importance used when typical antibiotics are found to be ineffective. (2) Antibiotic precursors, such as ACV-tripeptide, which is a precursor of the penicillin and cephalosporine families.⁶⁰ (3) Cytostatics. (4) Immunosuppressive agents. (5) Nitrogen storage polymers. (6) Phytotoxins, such as victorin, a chlorinated cyclic pentapeptide made by the pathogenic fungus *Cochliobolus victoriae*.⁶¹ (7) Pigments, such as indigoidine.⁶² (8) Siderophores, such as *Enterobactin* and *Vibriobactin* are iron-chelating compounds.⁶³ (9) Toxins, such as cyanotoxins from *Cyanobacteria*.⁶⁴

2.3 PKS/NRPS hybrid systems

PKS and NRPS possess such similar catalytic activity and structural organization, that there could therefore be significant potential in the cooperation of these two types of multimodular enzymes, representing an enormous variety of potential structures. For instance, functional interactions between PKS and NRPS modules mean that a PKS-bound acyl intermediate could be directly transferred and subsequently elongated by a NRPS module or a NRPS-bound peptidyl intermediate could be directly transferred and elongated further by a PKS module.^{19,65} Up until to now, a great number of natural products have been expressed following such a hybrid

pathway.⁶⁶⁻⁷⁰ In this case, the intermodular communication is essential for the functionality of the hybrid systems. Although PKS and NRPS have distinct domains to yield metabolic compounds, they share a similar modular organization, and both systems use carrier proteins, such as ACP for PKS and PCP for NRPS to manage the growing chain.⁶⁵ In PKS/NRPS hybrid systems, the critical domains are the ACP domain of PKS and the C domain of NRPS, wherein the C domains in PKS/NRPS hybrids must accept an acyl-S-ACP for chain elongation, instead of an aminoacyl-S-PCP.⁷¹ On the other hand for a NRPS/PKS interface, the key domains are the PCP domain of NRPS and the KS domain of PKS. The KS domain must approve the peptidyl intermediate bound to upstream PCP and condense it with the downstream acyl-S-ACP.⁷²

Moreover, the availability of a PPTase with broad substrate specificity is of paramount importance if both species of CPs (ACPs and PCPs) involved in a functional hybrid system are to be activated (Figure 1-4). To date, previous studies have already stated that several biochemically characterized PPTases (e.g. MtaA, Sfp, Svp) can also activate both ACPs and PCPs.⁷³⁻⁷⁵

2.4 Magnetic particle production in microorganisms

Besides PKSs and NRPSs compounds, microbial natural products arise from a multitude of different types of complex biosynthetic pathways. Among these products, the magnetosome is famous for its magnetotaxis and possible commercialization in bright future. Magnetosome chains are membranous prokaryotic structures, consisting of 15 to 20 magnetite crystals that together act like a compass needle to orient magnetotactic bacteria in geomagnetic fields.⁷⁶

Magnetotactic bacteria are a polyphyletic group of bacteria first reported in 1975⁷⁷ which can utilize the iron from the surrounding environment to assemble an internal chain of nanomagnetic particles within lipid vesicles,^{78,79} allowing the bacteria to orient along the magnetic field lines of Earth's magnetic field. Magnetotactic bacteria usually mineralize either iron oxide magnetosomes, which contain crystals of

magnetite (Fe_3O_4), or iron sulfide magnetosomes, which contain crystals of greigite (Fe_3S_4). Several other iron sulfide minerals have also been identified in iron sulfide magnetosomes — including mackinawite (tetragonal FeS) and a cubic FeS - which are thought to be precursors of Fe_3S_4 .⁷⁹ Magnetosome crystals are typically 35-120 nm long, which make them single-domain crystals, which have the maximum possible magnetic moment per unit volume for a given composition.⁷⁶ Magnetosome biosynthesis in magnetotactic bacteria is controlled by a set of about 30 genes within a large (~115kb) genomic magnetosome island.⁸⁰ However, these microbes are challenging with respect to strain cultivation or genetic modification on a molecular level.

3. Red/ET Recombineering

In modern natural products research, metabolic engineering intrigues scientists to manipulate biosynthetic pathways to yield new analogues as drug candidates. However, it is usually very challenging to manipulate the DNA in the native producing strains, and Red/ET recombineering, which is a highly efficient and straightforward technology established in *E. coli*, has recently emerged as a promising new technique for working with large genomes.⁸¹⁻⁸³

Red/ET recombineering, as a research hotspot studied by several different groups for many years, which is also known as “ λ Red recombination”^{84,85}, “recombineering”^{86,87}, “ET recombination”^{81,82} or “ET cloning”⁸³, relies on *in vivo* homologous recombination mediated by bacteriophage recombinases. The Red operon of the λ phage and the RecET operon of the Rac prophage are basically equivalent in terms of enzymatic function. As can be seen in Figure 1-7,⁸⁸ Red α and RecE are dsDNA exonucleases, while Red β and RecT are single strand DNA annealing proteins (SSAP). In the Red operon the Red γ is an inhibitor of RecBCD which is the major host exonuclease, aggressively degrading dsDNA fragments.⁸⁹

Red α or RecE bind to double-stranded DNA (dsDNA) ends, and progressively degrades linear dsDNA in a 5' to 3' direction, leaving long 3' single strand DNA

(ssDNA) overhangs. Red β or RecT bind to the ssDNA to form ssDNA-SSAP nucleoprotein filaments, which are able to pair their complementary ssDNA. Once aligned, the 3'-end becomes a primer for DNA replication.⁸⁸ The host factors then act an important part in finalizing the recombinant DNA by DNA replication and repair machinery (Figure 1-7).⁹⁰⁻⁹²

Under the effect of recombinases, the chosen DNA regions are amplified in *E. coli*, not in vitro, and thus are subject to review by the *E. coli* replication machinery by a new simple, efficient and more flexible approach. This methodology breaks through the size and site limitation of DNA engineering and allows an extensive range of modifications by insertion, deletion, substitution, fusion, point mutation, subcloning and direct cloning for almost any given DNA molecule at any chosen position. Notably, the homology sequence at the ends of the linear DNA can be as short as 35 bp for efficient homologous recombination, and single-strand oligonucleotides as short as 70 bases can be transformed for direct mutagenesis. These short homology sequences can be easily integrated into synthetic oligonucleotides, greatly expanding the utility of the technology.

Red β was associated in a complex with Red α when it was isolated from the cell.^{93,94} Some of the Red β mutations were found to be defective of not only Red β function, but also the exonuclease activity of Red α .^{95,96} These imply that red α recruits Red β loading onto the single-stranded 3' overhang. A specific protein-protein interaction between RecE and RecT has also been shown in coimmunoprecipitation experiments, suggesting that recombination requires cooperative functions between the exonucleases and the respective DNA annealing proteins.^{88,97-99} It was also shown that substitution of the protein from one system to another can impede function, further confirming protein-protein interaction specificity of each pair.⁸⁸ In this thesis, both Red α /Red β and RecE/RecT systems were investigated for application, and hereby defined as Red/ET recombineering.

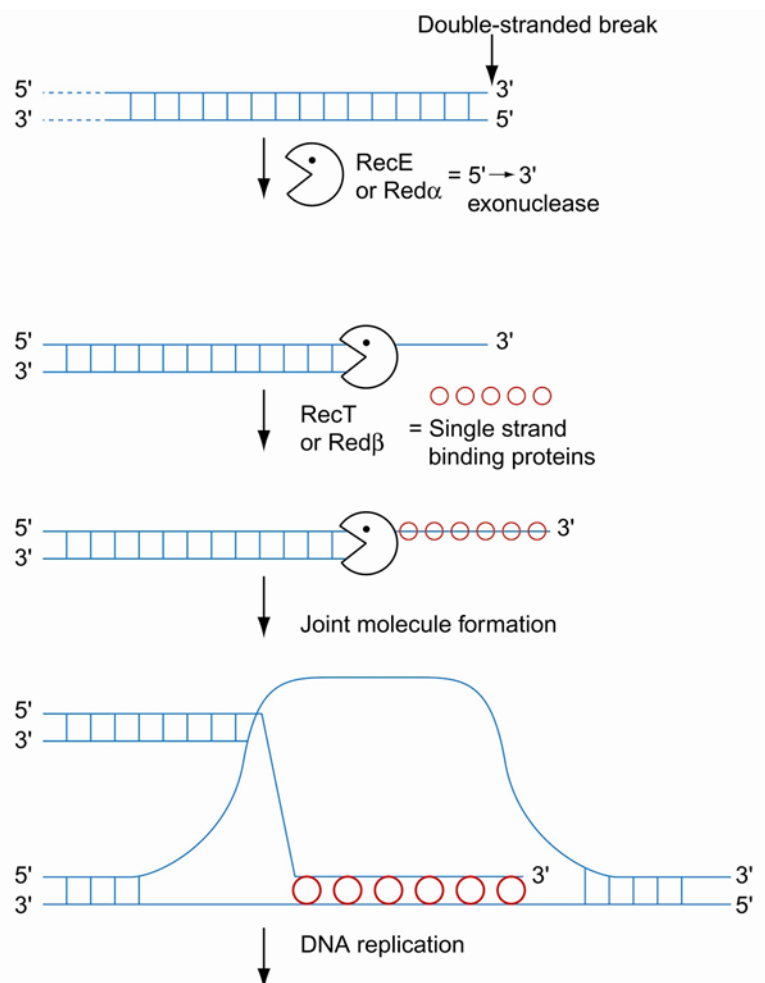


Figure 1-7. Mechanism of Red/ET recombineering. The diagram was reproduced from www.genebridges.com.

3.1 Development of Red/ET recombineering

Conventional methods to generate recombinant DNA use restriction enzymes and T4 DNA ligases,¹⁰⁰ and invention of PCR technology¹⁰¹ greatly expanded the capacity and flexibility of this technology. However, these methods are disable to precisely manipulate DNA fragments larger than 15kb, such as cosmids, fosmids, P1 vectors, bacterial artificial chromosomes (BACs) and bacterial chromosomes.¹⁰²⁻¹⁰⁶

Recombination-mediated genetic engineering was first demonstrated in *Saccharomyces cerevisiae*, using a gapped plasmid for cloning genes off the chromosome and a linear plasmid for targeting genes,^{107,108} with further experiments using single-strand oligonucleotides as short as 20 bp for efficient site-directed mutagenesis.¹⁰⁹ The homology sequence at the ends of the linear DNA were as short

as 35 bp, which could be easily incorporated in oligonucleotide synthesis, and this simplicity encouraged the biologists to establish an equivalent system in *E. coli* strain. However the host RecA-mediated homologous recombination requires much larger homologous sequence and usually resulted in very low efficiency. The first attempt at exploring λ phage Red recombinases used long homology arms (about 1kb) and the recombination was more efficient than that from RecA.¹¹⁰ Independently, Zhang and colleagues in the Stewart laboratory published that either RecE/RecT or Red α /Red β could mediate efficient homologous recombination between very short homology arms (40-50 bps), and the Red $\alpha\beta$ system was much more efficient than the RecET system.⁸³ Thus, Red recombineering has become a popular technology for rapid and precise modification of DNA, including insertion, deletion or replacement by a drug selectable marker,^{81,83} subcloning by gap repair,⁸² oligonucleotide-directed mutagenesis^{111,112} and counter-selection mediated by variable negative selectable markers to recombine DNA sequence without selection.¹¹³⁻¹¹⁵

Subsequently, the differences between the Red system and RecET system were distinguished by biologists. Specifically, when the plasmid replication was required in the homologous recombination, the Red $\alpha\beta$ system was preferred. Conversely, when an unreplicable linear vector was used to recombine with another DNA fragment to form a circular plasmid, RecET was found to be dramatically more efficient. Consequently, a novel RecET-based direct cloning method was invented, using PCR-amplified linear vectors to retrieve sequences of interest from digested genomic DNA, by passing the tedious DNA library construction.¹¹⁶

To date, recombineering has been established not only in *E. coli*, but also in several other species, such as *Agrobacterium tumefaciens*,¹¹⁷ *Mycobacterium tuberculosis*,^{118,119} *Photobacterium luminescens*,¹²⁰ *Xenorhabdus*,¹²⁰ *Salmonella enterica*,¹²¹ *Yersinia pseudotuberculosis*,¹²² *Burkholderia thailandensis* and *Burkholderia pseudomallei*¹²³.

3.2 Application of Red/ET recombineering

Recombineering is now an alternative for conventional recombinant DNA technology, and it is especially favourable for large DNA molecular engineering.^{116,124} Based on the DNA substrate to be recombined, recombineering can be divided into two categories, with each utilizing different phage recombinases. Linear plus circular homologous recombination (LCHR) is typically catalysed by Red α /Red β ,¹²⁵ and is principally used for engineering various vectors and bacterial chromosome. Linear plus linear homologous recombination (LLHR) utilizes RecE/RecT,¹¹⁶ which is primarily exploited for linear DNA cloning (PCR cloning)⁸² and direct cloning.¹¹⁶

The initial step of Red $\alpha\beta$ recombineering is oligonucleotide synthesis, in which the homologous sequence is attached to the PCR primer. The PCR-generated DNA fragment usually contains an antibiotic selectable marker and a terminal sequence identical to the target. After transformation of this DNA fragment in the Red $\alpha\beta$ expressed cell containing the target plasmid, the linear fragment recombines into the plasmid as positioned by the homologous sequence, endowing the cell with new antibiotic resistance (Figure 1-8). Each oligonucleotide for use in recombineering consists of at least two parts, yet could include a third or even fourth part to incorporate restriction enzyme recognition sites, site specific recombinase recognition sites (loxP, FRT, Rox, etc.) or sequence for a short protein tag (His, Strep, Flag, etc.). The target DNA can be a gene locus on the *E. coli* chromosome or any other stretch of DNA in a BAC or plasmid vector.⁸¹⁻⁸³

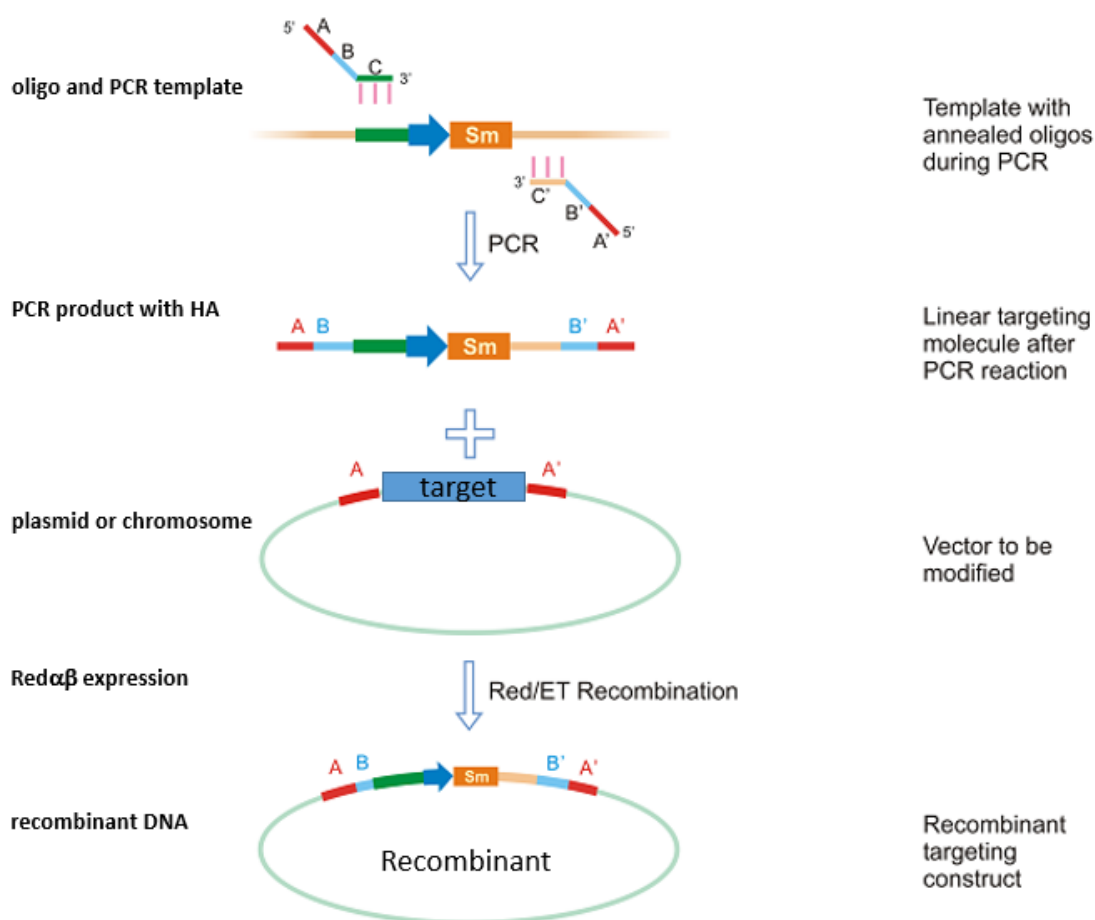


Figure 1-8: Red $\alpha\beta$ recombineering for a circular DNA modification.

This figure illustrates the principle of a circular DNA modification. Sm, selectable marker; the small blue arrow indicates a prokaryotic promoter. Parts A, B and C are the oligonucleotide regions. Part A is the required homology arm in the range of 30-50 bp shared by the target circular molecule and the linear molecule. The sequence of the homology regions can be chosen freely according to the locus on the target circular DNA. Part B is optional (protein tags, restriction sites, site-specific recombination target sites, etc.). Part C is the required primer for PCR, which is usually 18 to 24 nucleotides according to the provided template.²³²

LLHR mediated by RecET is capable of multiple linear DNA fragment assembly, if each fragment has an overlapping region of sequence identity with its neighbour (Figure 1-9A). The final recombination product should contain a plasmid origin for replication and an antibiotic resistance gene for selection. Another merit of RecET recombineering is direct cloning, with application of this technique to the 15.6 kb plu3263 gene providing a good example (Figure 1-9B). Specifically, the genomic

A. Introduction

DNA of *Photobacterium luminescens* is digested with NdeI and PacI to release a fragment containing plu3262. The PCR-generated linear vector is composed of a pBR322 origin, with an ampicillin selectable marker, tetO promoter and its repressor tetR. One homology sequence of the PCR is from the ATG start codon extending 70 bp downstream and another is the PacI site extending 70 bp upstream. After linear plus linear homologous recombination in *E. coli* expressing RecET, the plu3262 is directly cloned under the tetO promoter. Notably, the gene is being directly cloned under a regulated promoter to avoid potential toxicity to the host, and the chosen homologous sequence is designed 552 base pairs inside of the dsDNA end. An additional interesting fact is that RecET is able to align the identical sequences even when they are not exposed.¹¹⁶

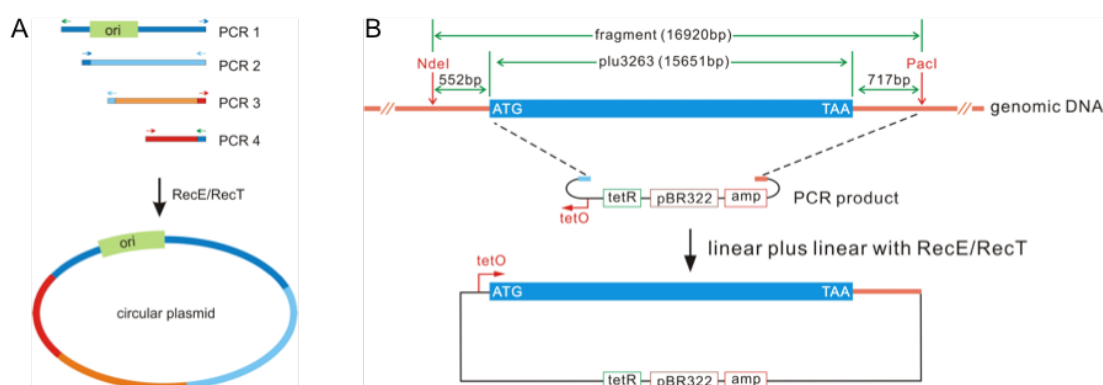


Figure 1-9. RecET recombineering for a circular DNA modification. (A) Schematic illustration of multiple linear DNA recombination to generate a circular plasmid. (B) An example of direct cloning of plu3263 from the *Photobacterium luminescens* genome. The figure was reproduced from reference¹¹⁶.

Natural microbial metabolites with promising medicinal and agricultural values, are always expressed from secondary metabolite pathway gene clusters. These gene clusters are often too large to engineer via conventional arrangements. Hence, components of the gene clusters were reconstituted into a single vector with several essential elements for gene transfer by using recombineering-direct cloning techniques.¹¹⁶ The gene clusters could be shaped further to ensure the successful expression in suitable heterologous hosts.^{124,126,127} Many “unusual” novel compounds have already been synthesized and identified via Red/ET recombineering technology

in the past few years.¹²⁸⁻¹³⁰

3.3 Improvement of Red/ET recombineering

Along with the application of recombineering, technical improvements have been always made in different ways. For instance, the temperature-sensitive pSC101 plasmid was used to express the recombinases. After a temperature shift the expression plasmid will be lost and the recombinant DNA product will not be contaminated.¹²⁹ Another example is that transient co-expression of RecA results in higher survival rate of the cells after electroporation, consequently promoting recombinant yield.⁸⁵

Genetic engineering relies on the transfer of foreign DNA into cells, and optimization of DNA transformation efficiency methods are important. Compared to various methods to prepare chemical competent cells for DNA transformation, electroporation is much more efficient, especially when the DNA molecule is large.¹³¹⁻¹³³ In *E. coli* electroporation procedure, the cells will turn exceptionally competent through high-voltage pulse treatment after rinsing with ice-cold water or 10% glycerol.¹³³⁻¹³⁵ The foreign DNA material will easily and rapidly enter into the permeabilized cell through the holes in the membrane transiently caused by the high voltage (1200-1350V).¹³⁶

According to previous research, electrocompetent cell preparation has to be made at ice-cold conditions and therefore both equipment and washing solutions need to be kept at low temperatures all times.¹³⁷⁻¹³⁹ Holding the cells at chilling conditions is the pivotal aim in the most of the protocols for electroporating Gram-negative bacterial strains involving *E. coli* without an adequate account.¹³⁷

Furthermore, the Red/ET recombineering has also been coordinated with other genetic tools to widen its application scope, for instance site specific recombination¹²⁰ and transposition.¹²⁶ Recently an efficient RNA-guided site-specific DNA cleavage technology has been developed based on the *Streptococcus pyogenes* type II CRISPR (Clustered Regularly Interspaced Short Palindromic Repeats) adaptive immune

system.¹⁴⁰⁻¹⁴² The system contains the CRISPR associated protein Cas9, a trans-activating CRISPR RNA (tracrRNA), and a programmable CRISPR targeting RNA (crRNA), which processes a Cas9-mediated double-stranded break (DSB) at almost any target DNA locus.¹⁴³ CRISPR/Cas9 has caught massive attention for its feasibility, and pioneer data shows that combination of CRISPR-Cas9 and Red/ET recombineering could lead to efficient multigene editing of not only in the *E. coli* genome but also in *Tatumella citrea* with very high efficiency.^{144,145}

4. Heterologous expression of natural products in surrogate hosts

Natural products, exhibiting a broad range of distinct structures and biological activity, are usually synthesized by large multienzymes mega synthetases, such as PKSs, NRPs, hybrid or Ripps. Hence, it is obviously much more economical and time-saving to produce these specified natural products during fermentation. Nevertheless, the ideal approach is not easy to achieve. For instance, the yield of target compounds in native producer is too low to achieve the minimum demands of industrialization or environmentally unfriendly byproducts are generated in the reactions. Furthermore, many native producers harboring these biosynthetic pathways show slow growth rates even in optimized laboratory conditions and are resistant to genetically manipulation.³⁴ Thus, heterologous expression of the corresponding secondary metabolite pathways into a more amenable host organism can play an important role in developing novel derivatives and potential drugs.¹⁴⁶ It also affords a high-level investigative platform for the detailed research of complex biosynthetic mechanisms, allowing careful identification of the products from silent biosynthetic gene clusters, and the generation of fresh analogs through biosynthetic engineering in suitable heterologous hosts which are genetically more tractable and easily cultivated.^{17,127,147-151}

With respect to heterologous expression of increasing number of complex natural products, it is obvious that a general overview of the workflow for cloning and production of large natural product assembly lines has been concluded (Figure

1-10).^{127,128} According to this approach, several general considerations and procedures should be assumed into account:

- 1) *Identification and isolation of the corresponding biosynthetic pathway in the native producer.* In the past dozen years, more and more natural product biosynthetic gene clusters have been investigated, with an accompaniment of a variety of increasing published genome sequencing data.¹⁵² For heterologous expression of a biosynthetic gene cluster, the genes should first be isolated so that they can be mobilized into an appropriate heterologous host, either using traditional ways (a BAC or cosmid library) or by direct cloning, and the clusters from genomic DNA should be transferred to a vector.
- 2) *Identification of a suitable vector for transfer and integration into the chromosome of heterologous host, functional promoter architecture and the corresponding regulatory factors in the related host.* For our direct cloning of large gene clusters, the replication origin and the copy number of the plasmid are two main considerations. We often use several types of vectors: (i) pBR322 plasmids presenting 15-20 copies per cell¹⁵³ with an insert capacity of ~50 kb.¹⁵⁴ (ii) p15A plasmids presenting 10-12 copies per cell¹⁵³ with an insert capacity of ~70 kb.¹¹⁶ (iii) pBAC2015 plasmids presenting a single copy per cell with an insert capacity of ~150kb.¹⁵⁵ Afterwards, the tetracycline inducible promoter (tetR-Ptet) is included in these plasmids to regulate the expression of the gene clusters in order to minimize the potential toxic effect of natural product gene clusters to the host.^{123,156}
- 3) *Heterologous host selection.* An amenable heterologous host is the most crucial aspect to be considered. Firstly, the phylogenetic distance between the native producer and heterologous host is a key consideration. In general, the more closely related the heterologous host is to the native strain, the high success rate of functional transcription of the biosynthetic pathway. Additionally, the codon usage may be similar in comparison between with the closely-related species and the original producer, which may increase the efficiency. In the case of PKSs and

NRPSs heterologous expression, the host must principally contain PPTase, which is required for post-translational activation of PKS-NRPS proteins.¹⁵⁷ Meanwhile, various necessary precursors or substrates, such as CoA-activated short chain carboxylic acids, both proteinogenic and non-proteinogenic amino acids, and short-chain fatty acids must be provided satisfactorily in the parasitifer. Additionally, the genetic engineering availability and cultivation conditions are also very important for heterologous host selection. Higher titer production and lower product cost are the pursuant goals to be achieved through heterologous expression.

- 4) *Genetic engineering of expression constructs.* Following the successful heterologous expression of biosynthetic gene cluster, yield of heterologous expression may be still not satisfactory. Due to this view, promoter exchange, reconstitution of essential clusters and insertion of regulatory regions are entailed for the expression construct. Depending on the host system selected, there are a number of alternative designs for the conservation of the clusters.
- 5) *Transformation into the heterologous hosts.* In the successful heterologous expression, the maintenance of a foreign biosynthetic gene cluster stability in a surrogate host is foundational for sustainable product expression. In principle, there are only two available options for exogenous gene cluster, wherein one is to maintain a steady host-compatible plasmid episomally, and another is direct integration into the chromosome.

Biosynthetic gene clusters can be expressed from self-replicating plasmids, either from a single plasmid with the entire biosynthetic pathway, or from multiple plasmids individually expressing modules *in cis*. For example, the 36kb echinomycin gene cluster from *St. lasaliensis* was expressed in *E. coli* BL21 (DE3) using three pET-derived vectors with the yield of 0.3mg/L.¹⁵⁸ During the plasmid-based expression, increasing the copy number of the biosynthetic gene cluster resulted in improvement of compound production due to an ample supply of precursors.¹⁵⁹ An additional convenience is afforded by the use of shuttle

vectors for the concurrent expression of biosynthetic gene cluster in multiple hosts.^{160,161} However, plasmid-based expression is not suitable to all the heterologous hosts as it depends on the availability of plasmid replicons capable of functioning in the host, and this is a risk for recombination-competent hosts and also for prolonged expression.¹⁶²

In order to secure a stable heterologous expression, the biosynthetic gene clusters should be integrated into the host chromosome. Furthermore, such integration is essential approaches using the plasmid replicons fail in the host. Homologous recombination, transposition and phage-mediated integration are the most popular and frequent applications in chromosomal integrations.

6) *Product analysis and optimization.* The successful expression of target compounds in suitable surrogate hosts is not the destination for our purpose. Often times, an ocean of novel compounds have already been discovered and identified and are in the progress of heterologous expression^{128,163} as are drug candidates. Nowadays, wide array of advanced techniques, involving liquid chromatography-coupled mass spectrometry (LC-MS), fast chromatographic separation (UPLC), electrospray ionization (ESI), high-resolution (HR) time-of-flight mass spectrometry (ToF-MS) and nuclear magnetic resonance (NMR), are employed in the hunt for new natural products to cope with the increasing appearance of novel infectious diseases.

Furthermore, to maximally harvest target metabolites in actual production process, several efficient approaches can be carried out to solve difficulties in the fermentation, such as precursor feeding and growth conditions optimization (in control of concentrations of CO₂ and O₂, pH, stirring rate, reaction time, etc.).^{164,165}

A. Introduction

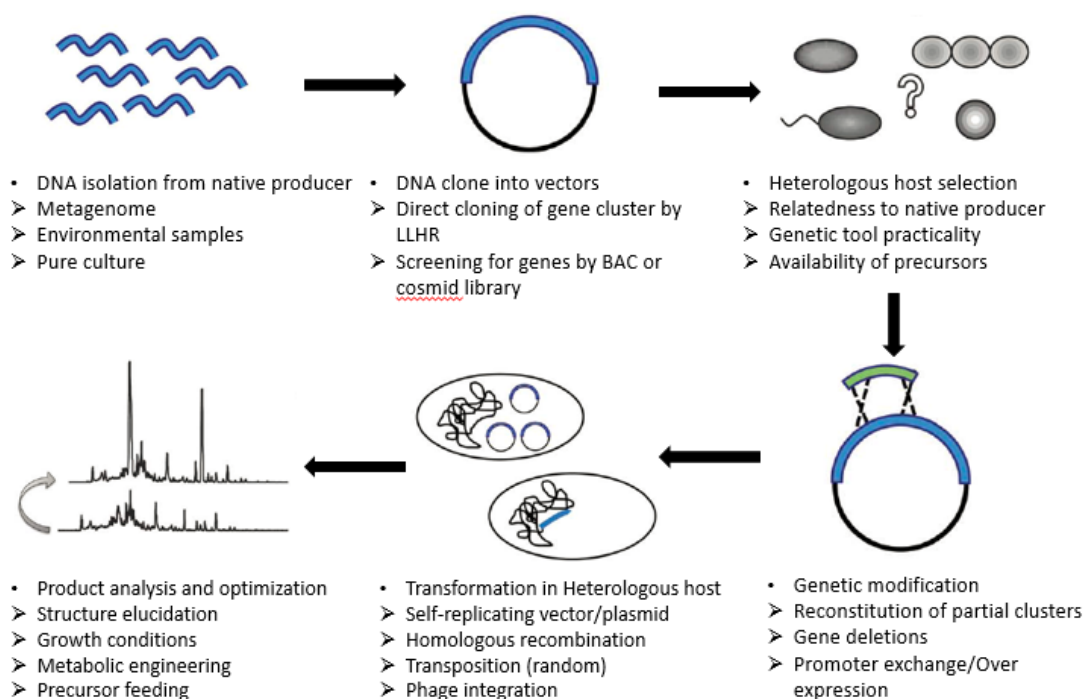


Figure 1-10. Typical strategy for the heterologous expression of natural product biosynthetic gene clusters. Refer to text in the corresponding sections for a specific description of each step. The figure was reproduced from reference.¹²⁸

Heterologous expression is a time-saving method, especially for biosynthetic pathways from slow-growing bacteria, and the biosynthetic pathways can be expressed in a bacterium which cultivates relatively fast. Over the past decade, several complete biosynthetic pathways from fastidious bacteria have already been reassembled by re-construction via Red/ET recombineering and successfully expressed in several different heterologous hosts, such as epothilones in *M. xanthus*,¹²⁶ human alpha-defensin 5 mature peptide in *Pichia pastoris*,¹⁶⁶ nikkomycin in *Streptomyces ansochromogenes*,¹⁶⁷ pretubulysin in *P. putida* and *M. xanthus*,¹⁶⁸ myxochromide S and myxothiazol in *Pseudomonas putida* and *M. xanthus*,^{126,146,165,169} salinomycin in *Streptomyces coelicolor*,¹⁷⁰ luminmycin and glidobactin in *E. coli* Nisse1917,^{129,130} and magnetosome products in *Rhodospirillum rubrum*.¹⁷¹

Additionally, transformation-associated recombination (TAR) cloning, another classic recombineering method, widely uses *in vivo* recombination in *Saccharomyces cerevisiae* to directly and specifically isolate desired large gene clusters from complex genomes.^{172,173} This great technology was discovered in late 1990s but had been

modified and received a high degree of development during the last ten years.¹⁷⁴⁻¹⁷⁶ Fragments up to 250kb can be directly fished out in yeast from multiple samples within 14 days via an optimized TAR cloning approach.¹⁷⁵ Many applications based on this powerful method have been already established in the post-genomic era. According to the protocol, the 56kb Colibactin gene cluster from *Citrobacter koseri* was directly cloned into the vector for heterologous expression.¹⁷⁷ Another good example of the application of TAR cloning is the reconstruction of the evolutionary history of the SPANX gene family in primates.^{178,179} Unfortunately, an obvious disadvantage of TAR cloning is that cloning efficiency drops with a high chromosomal GC content, in both yeast and bacteria.¹⁷⁵

Furthermore, several practical synthetic biological technologies for gene clusters assembly have also been developed recently years, such the Gibson assembly and DNA assembler techniques.¹⁸⁰⁻¹⁸² In comparison with Red/ET recombineering and TAR cloning, they only are capable of assembling small genetic segments prepared by standard PCR or direct chemical synthesis, but for insertions, deletions and point mutations, these methods are flexible and variable during DNA engineering.

Recent research indicates that the challenges of genetic engineering on biosynthetic pathways have been generally solved by Red/ET recombineering plus TAR cloning.^{176,183} The following strategy is to select a suitable surrogate host for expression. An ideal heterologous host should grow fast, be genetically tractable, provide all necessary precursors in sufficient quantities, ensuring functional expression of the required proteins and a low background for native secondary metabolites.¹⁸⁴ It is usually arduous to meet all the requirements above for all natural products, but with better growth and genetic characteristics are the basic goals for our research. According to previous data, several specific strains are good models for expression of heterologous genes, including *E. coli*,¹⁷ *Myxococcus xanthus*,¹²⁶ several *Streptomyces* species (*S. albus*,¹⁸⁵ *S. lividans*¹⁸⁶ and *S. coelicolor*¹⁸⁷), *Pseudomonas putida*¹⁶⁵ and *Rhodospirillum rubrum*.¹⁸⁸

While *E. coli* has been proven to be a powerful and cogent model microorganism for

genetic and metabolic engineering with a quick growth rate and its use for biological products overproduction are also well established.¹⁷ However, original *E. coli* often lacks the essential intracellular machinery to produce natural products. Thus, before heterologous expression, important modifications are required in *E. coli* strain. For example, in order to express luminide via direct cloning, a PPTase from *Stigmatella aurantiaca*⁷³ was introduced into our standard recombinering host, *E. coli* GB05 to form *E. coli* GB05-MtaA.¹¹⁶ Coincidentally, in the heterologous epothilone production, the methylmalonyl-CoA decarboxylase gene (*ygfG*) was replaced by the *pcc* genes to cumulate MM-CoA.¹⁸⁹ All the evidence illuminate that *E. coli* could successfully express large PKS/NRPS gene clusters after selective alterations.

M. xanthus is the best characterized myxobacterium and can be genetically engineered much more easily than any other myxobacteria.¹²⁶ Moreover, in native producers, a variety of PKS/NRPS secondary metabolites are manufactured, such as myxochromid A₂, myxalamid, myxovirescin, myxochelin and DKxanthene,¹⁹⁰ demonstrating the appearances of PPTases, MM-CoA and self-resistance related to bioactive compounds. Furthermore, demonstrating an amazing performance, *M. xanthus* presents a much shorter generation time (5h) than *S. cellulosum* (16h), another major species of myxobacteria harboring miscellaneous antibiotics, such as epothilone. Up until now, the Müller group have established heterologous production of many myxobacterial secondary metabolites involving pretubulylin, myxochromide S, myxothiazol in *M. xanthus*.^{126,168,169} *M. xanthus* can heterologously express not only myxobacterial biosynthetic gene clusters, but also streptomycete-derived biosynthetic gene clusters, e.g. Oxytetracycline yield in *M. xanthus* reached up to a high titer 10 mg/L.¹⁹¹ Those results suggest that *M. xanthus* is a promising candidate for heterologous host to express PKS/NRPS biosynthetic pathways from both myxobacteria and actinomycetes.

Ultimately, the majority of antibiotics and other pharmaceutically relevant bioactive compounds were isolated from actinomycetes (mainly belonging to the genus *Streptomyces*) that had been best analyzed for dozens of years. Several *Streptomyces*

species, such as *S. avermitilis*,¹⁸⁵ *Saccharopolyspora erythraea*¹⁹² and *S. coelicolor*¹⁸⁷ have been sequenced and harnessed as heterologous hosts to produce their own bioactive compounds. Intense efforts of heterologous expression the streptomycete-derived secondary metabolites in these *Streptomyces* hosts have already been reviewed by Baltz.¹⁹³

Rhodospirillum rubrum (*R. rubrum*) is a photosynthetic model organism because of its pink color in the medium.¹⁸⁸ The photosynthesis of *R. rubrum* differs from that of plants as it possesses not chlorophyll, but bacteriochlorophylls. For past decade, *R. rubrum* has already been developed into a modified heterologous host for several natural products, such as *Pseudomonas aeruginosa* membrane protein MscL,¹⁹⁴ various PHA (polyhydroxyalkanoates) synthase genes¹⁹⁵ and magnetosome biosynthetic gene cluster from *Magnetospirillum gryphiswaldense*.¹⁷¹ Based on these achievements, it is believed that more and more natural products are planning to be developed in *R. rubrum*.

5. Outline of the dissertation

The goal of the work described in this thesis is to improve heterologous transformation of genomic DNA, which is related to bacterial natural products, based on the increasing numbers of sequenced microbial genomes. The large gene clusters encoding secondary metabolite biosynthesis pathways can now be rapidly cloned and modified by Red/ET recombineering. In order to enhance the efficiency of recombineering, technical improvement for electrocompetent bacterial cell preparation was described in this thesis. Compared to long-standing ice-cold preparation method, the room temperature electrocompetent bacterial cells have resulted in increased transformation efficiency, which consequently promote the efficiency of Red/ET recombineering. Afterwards, three typical bioactive compound groups had been analyzed: the cytotoxic disorazols from myxobacterium *Sorangium cellulosum* So ce12, the magnetotactic magnetosomes from alphaproteobacterium *Magnetospirillum gryphiswaldense* and the antibacterial and antitumor salinomycin

from *Streptomyces albus* DSM41398.

An important direction of the thesis is to improve the efficiency of Red/ET recombineering by optimization of the conditions for electrocompetent cell preparation. DNA transformation is the routine work in most molecular biology laboratories, and the electroporation has been proven to be more efficient than the chemical transformation. The long-standing protocol for electrocompetent cell preparation is rinsing the cells by ice-cold water or 10% glycerol. However, we found that the electrocompetent *E. coli* cells prepared at room temperature was 5 folds more efficient for transformation of plasmids with different sizes, replication origins and selectable markers. The room temperature electrocompetent *E. coli* cells also resulted in 6-10 folds increased efficiency of RecET recombineering. The beneficial effect of room temperature preparation of electrocompetent cells was not been only shown in *E. coli* but also in several other gram-negative bacteria. Ultimately, these results and data were presented in **publication II**.

Disorazols represent a family of 29 structurally complex macrocyclic polyketides, which were first isolated from the myxobacterium *Sorangium cellulosum* So ce12.¹⁹⁶ These compounds inhibit cancer cell proliferation at picomolar concentrations by preventing tubulin polymerization and inducing destabilization of microtubules, which ultimately leads to the induction of apoptosis.¹⁹⁷⁻¹⁹⁹ According to the biosynthetic model four core genes *disA-D* encode eleven PKS modules and one NRPS module, with an acyltransferase domain is missing in the polyketide synthase modules. The last separate gene *disD* encodes an AT protein revealing the disorazol gene cluster falls into trans-AT PKS family. Thus, we intend to clone and engineer disorazol biosynthetic gene cluster by Red/ET recombineering. Followed by successful expression in heterologous host *Myxococcus xanthus* DK1622, the minor product disorazol A₂ was changed to be prominent in several derivate without significant modifications. Interestingly, the yields of disorazols increased seven times after overexpression the solitary AT domain (*disD* gene) by insertion of a stronger promoter. These results were reported in **publication I**.

The magnetosomes, which are membrane-enclosed crystals of a magnetic iron mineral, are biosynthesized by magnetotactic bacterium *Magnetospirillum gryphiswaldense*.²⁰⁰ Magnetotactic bacteria are a peculiar natural phenomenon that can absorb iron (mostly Fe₃O₄) from the surrounding solution and take it to produce an interior chain of nanomagnetic particles within lipid vesicles which are regarded as magnetosome chains. However, it is difficult to cultivate the bacterium in the optimized laboratory conditions. Through the use of Red/ET recombineering, we directly cloned a set of large genomic magnetosome island (~115kb) into several vectors and transferred them into the photosynthetic bacterium *Rhodospirillum rubrum*, respectively. Small magnetosome particles could be detected by transmission electron microscopy (TEM) and purified from disrupted cells by magnetic separation. Four main gene clusters, either essential *mamAB* or regulatory *mamGFDC*, *mms6* and *mamXY* in magnetosome formation, have been identified and defined through heterologous expression in *Rhodospirillum rubrum*. This biosynthesis of magnetosomes within other organisms enlarges the probability of commercialization of tailored magnetosome production within microorganisms, and these results were recently described in **publication III**.

The natural compound salinomycin, produced by *Streptomyces albus*,²⁰¹ has a potent and selective activity against cancer stem cells and is therefore a potential anti-cancer drug. The salinomycin biosynthetic gene cluster (*salO-orf18*) from *Streptomyces albus* DSM41398 was separately cloned into three plasmids and stitched into an intact gene cluster (106kb) under the native promoter using Red/ET recombineering in *E. coli*. The large gene cluster was transferred in to *Streptomyces coelicolor* A3 (2) for heterologous expression, and this was the first report of such a large genomic region directly cloned from a Gram-positive strain. These studies suggested a new approach to characterization of the relevant functional genes to identify novel analogues by module exchange, and the data and analysis were presented in **publication IV**.

B. Publications

I. Genetic engineering and heterologous expression of the disorazol biosynthetic gene cluster via Red/ET recombineering.

II. Room temperature electrocompetent bacterial cells improve DNA transformation and recombineering efficiency.

III. Biosynthesis of magnetic nanostructures in a foreign organism by transfer of bacterial magnetosome gene clusters.

IV. Direct cloning and heterologous expression of the salinomycin biosynthetic gene cluster from *Streptomyces albus* DSM41398 in *S. coelicolor* A3 (2).

I

Genetic engineering and heterologous expression of the disorazol biosynthetic gene cluster via Red/ET recombineering.

Qiang Tu^{1,2}, Jennifer Herrmann¹, Shengbiao Hu³, Ritesh Raju^{1,†}, Xiaoying Bian², Youming Zhang^{2*} & Rolf Müller^{1*}

¹Department of Microbial Natural Products, Helmholtz Institute for Pharmaceutical Research Saarland, Helmholtz Centre for Infection Research and Department of Pharmaceutical Biotechnology, Saarland University, Campus E8.1, 66123 Saarbrücken, Germany.

²Shandong University – Helmholtz Joint Institute of Biotechnology, State Key Laboratory of Microbial Technology, School of Life Science, Shandong University, Jinan 250100, People's Republic of China.

³College of Life Science, Key Laboratory of Microbial Molecular Biology of Hunan Province, Hunan Normal University, Changsha 410081, Hunan Province, People's Republic of China.

[†]Present address: University of Western Sydney, Department of Pharmacology, School of Medicine, Campbelltown, NSW 2560, Australia.

*Correspondence and requests for materials should be addressed to Y.Z. (email: zhangyouming@sdu.edu.cn) or R.M. (email: rom@helmholtz-hzi.de)

SCIENTIFIC REPORTS



OPEN

Genetic engineering and heterologous expression of the disorazol biosynthetic gene cluster via Red/ET recombineering

Qiang Tu^{1,2}, Jennifer Herrmann¹, Shengbiao Hu³, Ritesh Raju^{1,*}, Xiaoying Bian², Youming Zhang² & Rolf Müller¹

Received: 06 October 2015

Accepted: 18 January 2016

Published: 15 February 2016

Disorazol, a macrocyclic polyketide produced by the myxobacterium *Sorangium cellulosum* So ce12 and it is reported to have potential cytotoxic activity towards several cancer cell lines, including multi-drug resistant cells. The disorazol biosynthetic gene cluster (*dis*) from *Sorangium cellulosum* (So ce12) was identified by transposon mutagenesis and cloned in a bacterial artificial chromosome (BAC) library. The 58-kb *dis* core gene cluster was reconstituted from BACs via Red/ET recombineering and expressed in *Myxococcus xanthus* DK1622. For the first time ever, a myxobacterial *trans*-AT polyketide synthase has been expressed heterologously in this study. Expression in *M. xanthus* allowed us to optimize the yield of several biosynthetic products using promoter engineering. The insertion of an artificial synthetic promoter upstream of the *disD* gene encoding a discrete acyl transferase (AT), together with an oxidoreductase (Or), resulted in 7-fold increase in disorazol production. The successful reconstitution and expression of the genetic sequences encoding for these promising cytotoxic compounds will allow combinatorial biosynthesis to generate novel disorazol derivatives for further bioactivity evaluation.

Natural products from microorganisms, fungi, plants and insects display a broad spectrum of biological activities. Currently, approximately 49% of anti-infectives compounds and 61% of anticancer pharmaceutical agents in clinical use are natural products or their derivatives¹. Over the last decades, myxobacteria have become well known producer organisms, offering a rich and valuable source of natural products^{2,3}. Most of these compounds are biosynthesized by multifunctional megasynthetases, such as polyketide synthases (PKSs)⁴, nonribosomal peptide synthetases (NRPSs)⁵ and hybrids thereof⁶. Genes encoding these PKSs and NRPSs in bacteria are often clustered together on the chromosome, so a gene cluster can be cloned into a vector and then transferred to a heterologous host for functional expression⁷. Recent studies demonstrate the usefulness of heterologously expressed secondary metabolite pathways for the production of natural products⁸. Heterologous expression can improve fermentation yields and generate new natural or synthetic products that can be evaluated as potential pharmacological agents in the course of targeted derivatization or structure-activity relationship studies⁹.

Reconstructing biosynthetic gene clusters in various vectors for heterologous expression in more productive hosts can help show how newly discovered biosynthetic gene clusters function. Derivatives of the new available pharmacologically active compounds can then be produced by biomolecular re-engineering and combinatorial biosynthesis¹⁰.

¹Department of Microbial Natural Products, Helmholtz Institute for Pharmaceutical Research Saarland, Helmholtz Centre for Infection Research and Department of Pharmaceutical Biotechnology, Saarland University, Campus E8.1, 66123 Saarbrücken, Germany. ²Shandong University – Helmholtz Joint Institute of Biotechnology, State Key Laboratory of Microbial Technology, School of Life Science, Shandong University, Jinan 250100, People's Republic of China. ³College of Life Science, Key Laboratory of Microbial Molecular Biology of Hunan Province, Hunan Normal University, Changsha 410081, Hunan Province, People's Republic of China. ^{*}Present address: University of Western Sydney, Department of Pharmacology, School of Medicine, Campbelltown, NSW 2560, Australia. Correspondence and requests for materials should be addressed to Y.Z. (email: zhangyouming@sdu.edu.cn) or R.M. (email: rom@helmholtz-hzi.de)

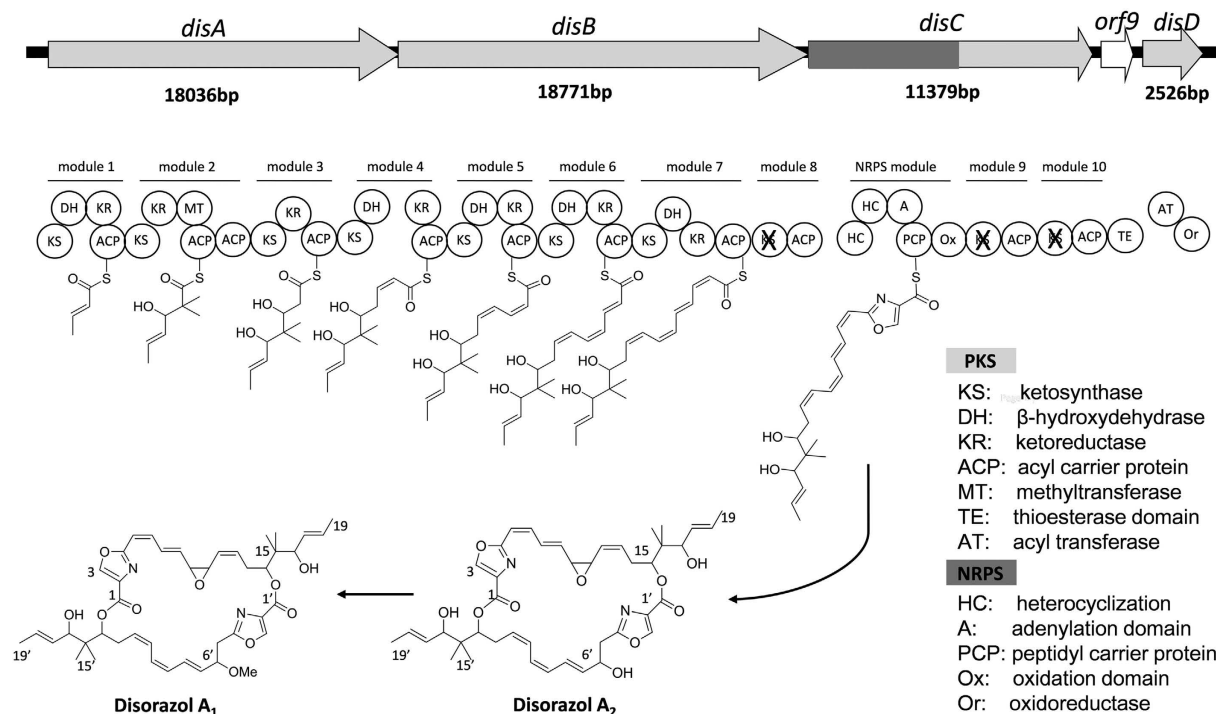


Figure 1. Domain organization of the *dis* biosynthetic gene cluster from *S. cellulosum* So ce12 and a model for biosynthesis of disorazol A₁ (scheme according to Kopp *et al.*).

Large clusters of genes that encode the enzymes for natural product biosynthesis have been difficult to engineer using conventional technology. Red/ET recombineering in combination with TAR (Transformation-associated recombination) cloning is necessary for large biosynthetic gene clusters to be engineered conveniently^{11,12}.

Red/ET recombineering is based on *in vivo* homologous recombination in *E. coli*^{13–15}. The greatest advantage of the technology is that it works regardless of restriction enzyme binding sites or the size of DNA fragments to be shuffled. This technology has made it much easier to genetically manipulate complex biosynthetic pathways in bacteria. Over the past decade, several complete biosynthetic pathways from fastidious bacteria have been heterologously expressed via Red/ET recombineering, e.g. myxochromide S and myxothiazol in *Pseudomonas putida* and *M. xanthus*^{16–19}, epothilones in *M. xanthus*¹⁹, human alpha-defensin 5 mature peptide in *Pichia pastoris*²⁰, nikkomycin in *Streptomyces ansiochromogenes*²¹, pretubulysin in *P. putida* and *M. xanthus*²², luminmycin and glidobactin in *E. coli* Nissle1917^{23,24}, salinomycin in *Streptomyces coelicolor*²⁵ and even a minimal set of genes for magnetosome biosynthesis from the magnetotactic bacterium in *Rhodospirillum rubrum*²⁶.

Secondary metabolite gene clusters in microbes express natural products with potential medicinal and values agricultural qualities²⁷. However, many of the microorganisms hosting these biosynthetic pathways grow slowly even in optimized laboratory conditions and can not be genetically manipulated². Heterologous expression of complete secondary metabolite pathways plays a significant role in hunting for new natural products and developing them into useful drugs¹⁶. Many heterologous expression instruments for secondary metabolite pathways have been reported so far, ranging from targeted expression by shuttle vectors to the random expression of large DNA fragments from chromosomes by transposition⁹.

Disorazols, a family of structurally complex macrocyclic polyketides, are produced by the myxobacterium *Sorangium cellulosum* So ce12 (Fig. S1) and firstly isolated in 1994²⁸. Disorazols inhibit cancer cell proliferation at low picomolar concentrations by preventing tubulin polymerization and inducing destabilization of microtubules, which ultimately leads to the induction of apoptosis^{29–31}. The extraordinary potency of disorazols fostered their development as peptide-conjugates for cancer therapy^{32,33} and encouraged the generation of new and simplified disorazol derivatives by means of chemical synthesis^{34–36}. However, there are no reports to date on genetic engineering approaches for the production of new analogs of the disorazol compound class.

The *dis* biosynthetic gene cluster was identified by transposon mutagenesis. In 2005, the cluster was cloned into a BAC or cosmid library of *S. cellulosum* So ce12 by two independent groups^{37,38}. The clusters showed the anticipated *disA–C* genes encoding hybrid *trans*-AT type I PKS/NRPS megaenzymes, and also another gene, *disD*, that encoded an additional acyl transferase protein (Fig. 1).

According to the biosynthetic model, seven malonyl-CoA units and one serine are incorporated as extender units, forming half of the disorazol bis-lactone core unit. Two polyketide monomers may dimerize to form disorazol via the thioesterase (TE) domain³⁸, possibly requiring an esterase encoded by *orf3*³⁷ (Table S4).

The native strain produces only small amounts of disorazols (~1 mg per liter fermentation medium) and is difficult to cultivate²⁸. Consequently, it is challenging to produce large quantities of disorazol for further

development. Using an amenable heterologous host should be a rational way to assure higher and stable disorazol yields and possibly optimize its structure by molecular engineering.

Here we report the Red/ET recombineering of the *dis* biosynthetic gene cluster into a stable vector containing a p15A replication origin and a MycoMar transposase element. When the *dis* gene cluster was transposed into the chromosome of the heterologous host *M. xanthus* DK1622 several disorazol derivatives were produced. Subsequent gene deletions proved that only the *disA-D* genes and not *orf9* or the putative esterase gene *orf3'* were needed for disorazol production³⁷. Further, we also improved disorazol production in the heterologous host *M. xanthus* DK1622 by replacing the native promoter of the *disD* gene encoding a discrete AT protein with an artificial synthetic promoter.

Results and Discussion

Reconstitution of the disorazol A biosynthetic gene cluster. The disorazol A biosynthetic gene cluster has been cloned, sequenced and identified previously from a BAC library of *So ce12*³⁷. The BAC contained most of the *dis* gene cluster from *disA* to *disD*. However, the BAC pBeloBAC11-*dis* was a large and low copy vector and very difficult to transfer between hosts for heterologous expression. To construct a more efficient expression vector and to insert elements for transfer and expression into different heterologous hosts, we sequentially modified the original BAC (pBeloBAC11-*dis*) by Red/ET recombineering^{13,14}. The backbone of pBeloBAC11-*dis* was replaced by a cassette containing the p15A replication origin (*p15A ori*), the origin of transfer (*oriT*) for conjugation purposes, two inverted repeats (IRs), a MycoMar transposase gene (*Tps*) for transposition, an inducible promoter *tetR-P_{tet}* for driving the *dis* gene cluster upstream of *disA* and a kanamycin resistance gene for selection in *M. xanthus* DK1622.

In the resulting construct p15A-*dis*, the *dis* gene cluster (containing *disA-D* and *orf9*) is in a relatively high copy number vector (20–30 copies per cell in *E. coli*). Instead of the native promoter, expression in this vector is controlled by a tetracycline inducible promoter in this vector works in several heterologous hosts, e.g. *E. coli*, *M. xanthus* and *P. putida*³⁹ (Figs 2 and S2).

We previously found that disorazol production was no longer detectable when an esterase gene (*orf3'*) was mutated by transposon insertion in mutant strain So12_EXI_IE-3³⁷. This mutated esterase gene was implicated in bis-lactone formation during disorazol biosynthesis. We recovered plasmid pTn-Rec_IE2 (Fig. S6), which contained several genes near the transposition in the mutant So12_EXI_IE-3. The transposon was found in the middle of the carboxyl esterase gene *orf3'* (only 6.7 kb upstream of the *disA* start codon).

The plasmid pTn-Rec_IE2 also included a S-adenosyl methionine (SAM) dependent methyl transferase gene *orf2'*³⁷. As the product of *orf2'* may O-methylate the OH group at C-6' adjacent to the *orf3'* gene, it might also be essential for disorazol biosynthesis (Fig. S6, Table S4). Hence, we inserted both, the repaired carboxyl esterase gene *orf3'* and the SAM-dependent methyl transferase gene *orf2'* together into p15A-*dis* to form p15A-*dis-est* by Red/ET recombineering. To gain the fusion plasmid p15A-*dis-est*, firstly, two separate PCR cassette “*cm^R*” and “*spect^R*” with suitable homologous arms to the region (containing two *Hind III* restriction sites in both sides) between the *orf9* and the *disD* genes were introduced into the vector, respectively. After digestion by *Hind III* restriction enzyme in correct clones, the linear fragment “*cm^R-orf2'-orf3'-spect^R*” was integrated to obtain the final construct p15A-*dis-est*. By this, the *cm^R* gene was introduced to drive *orf2'* and *orf3'* genes. Likewise, the *spect^R* gene was introduced to drive the *disD* gene (Figs 2 and S2).

Certain gene products may be toxic to the host cell, potentially limiting the nature of downstream applications when introduced into *E. coli* directly at high copy number⁴⁰. All *E. coli* strains containing the *dis* gene cluster with the native promoter were found to carry mutations after recombineering. Therefore, it was very challenging to obtain the expression construct containing the *dis* gene cluster directly in *E. coli* because the growth of the host was impeded. We reasoned that one of the *dis* proteins interfered with a primary metabolic pathway in *E. coli* to disrupt growth. To address this issue, an inducible promoter *P_{tet}* was used to regulate gene expression. *P_{tet}* is a versatile tetracycline-based regulatory system that is usually used to selectively control expression of downstream genes³⁹. No other promoter system is suitable for so many diverse hosts, including *E. coli*, *M. xanthus* and *P. putida*^{10,22,23,41}. Besides, *P_{tet}* had already enabled several mixed PKS/NRPS natural products to be produced in heterologous hosts unrelated to the native producing organisms, such as myxochromide S from myxobacterium *Stigmatella aurantiaca*, which has been engineered into *P. putida*¹⁹.

The transposon method, which was also applied in this study, is clearly more stable and efficient than using shuttle vectors¹⁹. Several indispensable elements were inserted into the target vectors, for instance *Tps* and *oriT*. The mariner transposon MycoMar is frequently used in Gram-negative hosts for genetic modification^{42,43} and to transfer and integrate a gene cluster into the chromosome of heterologous host strains^{19,22}. The transformation efficiency of large gene sets is higher when using the MycoMar transposon than using homologous recombination, as has been described for the heterologous expression of epothilone and myxochromide S¹⁹. This powerful tool for transforming large genes was used in the disorazol heterologous expression system to make it easier to integrate the *dis* gene cluster into the genome of host strains. The *oriT* was also incorporated for conjugation in other heterologous hosts strains, such as *P. putida*⁴⁴.

Heterologous expression of *dis* gene cluster in *M. xanthus* DK1622. Both expression constructs p15A-*dis* and p15A-*dis-est* (Fig. S2) were introduced into the heterologous host *M. xanthus* DK1622 by electroporation as previously described¹⁹. The *dis* gene cluster was randomly transposed into the chromosome of *M. xanthus*. Transformants were screened on CTT agar containing kanamycin to select for *M. xanthus::p15A-dis* and *M. xanthus::p15A-dis-est* mutants. Six randomly chosen colonies of each mutant were verified by PCR¹⁹, which confirmed that the *dis* gene cluster had been integrated into the *M. xanthus* chromosome in each case. All the checked mutants contained the whole disorazol gene clusters. Several resulting mutants *M. xanthus::p15A-dis* and *M. xanthus::p15A-dis-est* were cultivated (both induction by anhydrotetracycline (AHT)) for compound

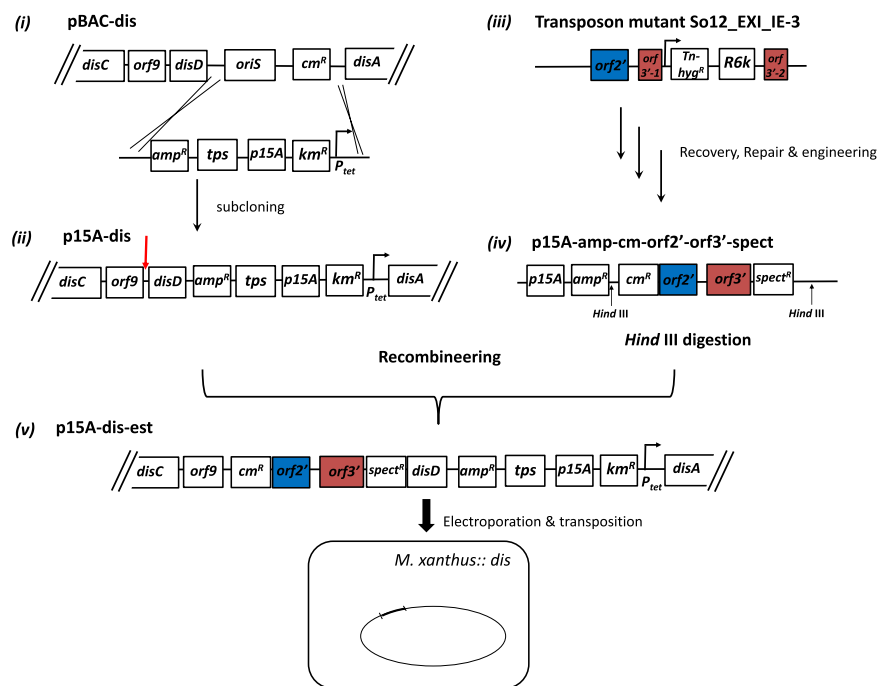


Figure 2. Diagram of disorazol A gene cluster engineering. Firstly, the backbone of plasmid pBeloBAC11-dis (i) was replaced by p15A ori-tps cassette to form p15A-dis (ii) which containing an original MycoMar transposon by Red/ET recombineering. In this way *dis* gene cluster was driven by P_{tet} promoter. Then, the interrupted esterase gene *orf3'* in pTn-Rec_IE2 plasmid (iii) from transposon mutant So12_EXI_IE-3³⁶ was recovered, repaired and engineered to form the vector p15A-amp-cm-*orf2'*-*orf3'*-spect (iv) that contained the whole length of the esterase gene *orf3'*. Next, linear DNA fragment released by *Hind* III was integrated into disorazol vector p15A-dis (ii) to get the final construct p15A-dis-est (v) via Red/ET recombination. Finally, two types of modified vectors p15A-dis (ii) and p15A-dis-est (v) were electroporated into *M. xanthus* respectively and kanamycin-resistant colonies were selected for further analysis. *Hind* III restriction sites used for releasing linear fraction “*cm^R-orf2'-orf3'-spect^R*” were indicated in \uparrow . The insertion site of the linear fragment DNA containing *orf2'* and *orf3'* gene was marked with \downarrow .

extraction and detection. All the mutants produced detectable amounts of disorazols by the analysis of high performance liquid chromatography-tandem mass spectrometry (HPLC-MS)⁴⁵. We have found small amounts of various disorazol compounds (including disorazols A₁, A₂, A₃, A₄, B₂, B₄ and F₂) in both extracts of *M. xanthus*:: *p15A-dis* and *M. xanthus*:: *p15A-dis-est* (Figs 3 and S3, Table S2), upon comparing the secondary metabolite profiles from *M. xanthus* wild type strain and mutants. As expected, these results indicate that the chosen set of genes is sufficient to produce the polyketide-nonribosomal peptide skeleton of the disorazols.

Unexpectedly, without the *orf2'* and the *orf3'* genes, *M. xanthus*:: *p15A-dis* can also produce disorazols. The overall yields of disorazols in *M. xanthus*:: *p15A-dis* (averagely were 0.4 mg/L) match with that in *M. xanthus*:: *p15A-dis-est* (averagely were 0.42 mg/L). Result exhibited that the *orf3'* gene is dispensable in the disorazol biosynthesis in the chosen heterologous host. There might be an enzyme that can substitute for the similar function of the *orf3'* gene product in *M. xanthus* host. The *dis* gene cluster could be inactivated in the transposon mutant So12_EXI_IE-3 due to a strong polar effect³⁷ because it is adjacent to the *disA* gene, possibly preventing downstream genes in an operon from being transcribed^{46,47}.

The HPLC-MS and NMR data showed that the major compound in both mutants *M. xanthus*:: *p15A-dis* and *M. xanthus*:: *p15A-dis-est* was disorazol A₂ which constituted 55% of final product after purification from crude extracts (Figs S3 and S4, Table S3), whereas disorazol A₁ was 20%. But in the native host So ce12, disorazol A₁ was the chief component (nearly 70% after purification, 10 times higher than disorazol A₂) produced among the 29 derivatives²⁸. The most probable explanation was that an *O*-methyl transferase that methylates the OH group at C-6' was absent in the heterologous expression of *dis* gene cluster. This methyl transferase gene could be possibly located elsewhere in the chromosome of the native producer So ce12, which still needs further investigation. Only small amounts of the C-6' methylated disorazols A₁, A₃ and A₄ were produced in *M. xanthus* (Fig. S3), which might be due to partial methylation by a nonspecific *M. xanthus* *O*-methyl transferase. After 5 L fermentation of mutant strain *M. xanthus*::*p15A-dis*, the yield of disorazol A₂ was approximately 0.24 mg/L, which is 5-fold higher than described in the native producer strain So ce12^{28,48}. The result unambiguously demonstrated again that secondary metabolites can be produced in heterologous hosts under the control of the versatile P_{tet} promoter which encouraged further investigation of disorazol formation.

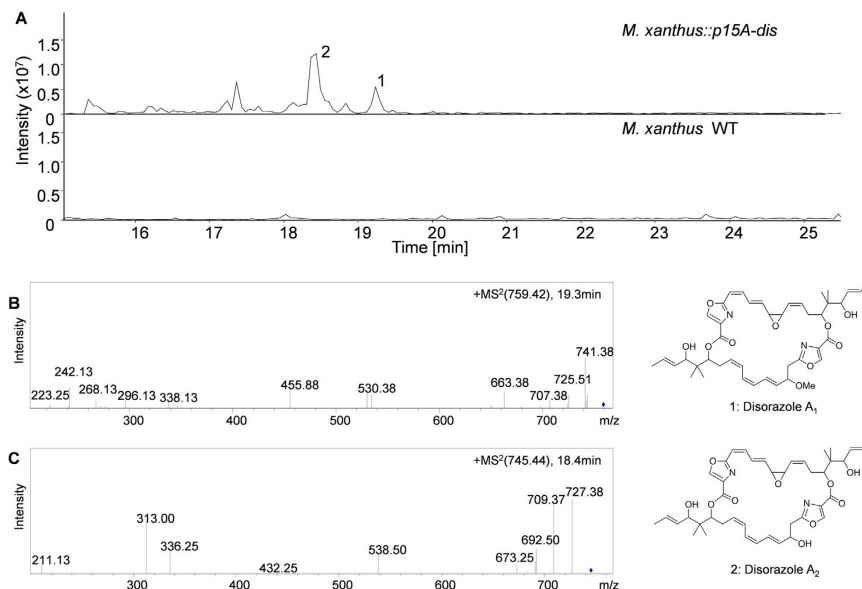


Figure 3. Analysis of disorazol production in *M. xanthus* wildtype (WT) and *M. xanthus::p15A-dis* grown at 30 °C and induced with 0.5 µg/ml AHT. (A) HPLC-MS analysis (base peak chromatogram [BPC] m/z 720–780) of *M. xanthus::p15A-dis* and *M. xanthus* WT. (B) MS² fragmentation pattern of disorazol A₁ (1). (C) MS² fragmentation pattern of disorazol A₂ (2).

Biological activity of disorazol compounds. After having isolated disorazols from our heterologous host *M. xanthus*, biological studies revealed exceptional high cytotoxicity of disorazol A₂ on eukaryotic cells. We determined IC₅₀ values against several established human cancer cell lines from different origin and disorazol A₂ strongly inhibited the growth of these cell lines with IC₅₀ values between 0.05 and 4.9 nM (Table 1). However, compared to disorazol A₁, the antiproliferative activity of disorazol A₂ was less pronounced on most cell lines, except for human U-937 histiocytic lymphoma. Most likely, the higher IC₅₀ values for disorazol A₂ are due to the lack of a methyl group at C-6' compared to disorazol A₁, which in turn might lead to a less favourable binding to the target structure tubulin. Nevertheless, when compared to other anticancer drugs, such as epothilone B or vinblastine, disorazol A₂ is still much more effective *in vitro*^{29,49}.

Optimized production with biomolecular technology. An unusual feature of the disorazol biosynthetic gene cluster is that it has only one discrete AT domain on the DisD module, and hence it is called a *trans*-AT type of PKS⁵⁰. In recent years, *trans*-AT PKSs have been found in an important group of biosynthetic enzymes that produce bioactive natural products, including pederin, rhizoxin, leinamycin, myxovirescin, chivosazol and psymberin^{51,52}. Accessing functionally-optimized polyketides by modifying PKSs through targeted synthase re-engineering is an encouraging approach to optimize natural products for application⁵². However, in contrast to ATs from *cis*-AT PKSs, the mechanisms and structures of *trans*-acting ATs are still unexplored.

The *disD* gene has been modified here to show how *trans*-acting ATs affect the disorazol biosynthesis pathway. In order to enhance the expression of the solitary AT domain, we introduced another strong promoter P_{cp25} upstream of the *disD* gene. P_{cp25} is a highly active, constitutive lactococcal consensus promoter, whose sequence has already been reported^{53,54}. Previous studies have illustrated that overexpression of single genes or multigene transcriptional units by promoter exchange in myxobacteria can improve the production of secondary metabolites^{19,55–57}.

On the other hand, the role of *orf9* gene (showing similarity to hypothetical proteins), which separates the *disC* and *disD* genes, in the *dis* gene cluster has not been defined³⁷. To discover the actual function of the *orf9* gene in disorazol biosynthesis, we inactivated it on the expression construct p15A-dis and then performed heterologous production in *M. xanthus*.

The PCR cassette “P_{cp25}-*spect*^R” (P18–P20 in Table S1), containing promoter P_{cp25} and a spectinomycin resistance gene (*spect*^R), with two different pairs of homologous arms, was inserted into p15A-dis by Red/ET recombineering to form two plasmids p15A-dis-P_{cp25} and p15A-dis-P_{cp25}Δ*orf9* (Figs 4A and S5). In the first plasmid p15A-dis-P_{cp25}, the promoter P_{cp25} was inserted directly upstream of the *disD* gene. In the second plasmid, the *orf9* gene was deleted by using a synthetic promoter cassette with selection for spectinomycin resistance to obtain p15A-dis-P_{cp25}Δ*orf9*. The *disD* gene was thereby controlled by the P_{cp25} promoter in both expression constructs. The recombinants were analyzed after growth on low-salt Luria-Bertani (LB) broth plates plus spectinomycin. The verified constructs were transformed into *M. xanthus* DK1622 and three randomly picked positive transformants of each type of strain were cultivated to analyze the production by HPLC-MS. To clearly identify disorazol, retention times (RT) and the MS² fragmentation pattern were compared to authentic reference substances. The concentration of disorazol A₂ in the culture was determined by UPLC-HRMS. A standard curve between peak area and concentration was established from serial dilutions for disorazol A₂ down to 0.01 µg/mL.

Human Cell line	Origin	IC ₅₀ [nM]	
		Disorazol A ₁	Disorazol A ₂
A-431	epidermoid carcinoma	1.866	4.908
A-549	lung carcinoma	0.072	0.408
HCT-116	colon carcinoma	0.032	0.071
HepG2	hepatocellular carcinoma	0.002	0.051
HL-60	acutemyeloid leukemia	0.058	0.084
K-562	chronicmyeloid leukemia	0.074	0.140
KB-3.1	cervix carcinoma	0.025	0.106
SW480	colonadeno carcinoma	0.030	0.128
U-2 OS	osteosarcoma	0.038	0.206
U-87 MG	glioblastoma-astrocytoma	0.072	0.119
U-937	histiocytic lymphoma	0.293	0.210

Table 1. Activity of disorazol A₁ and disorazol A₂ against human cancer cell lines. IC₅₀ values refer to antiproliferative activities.

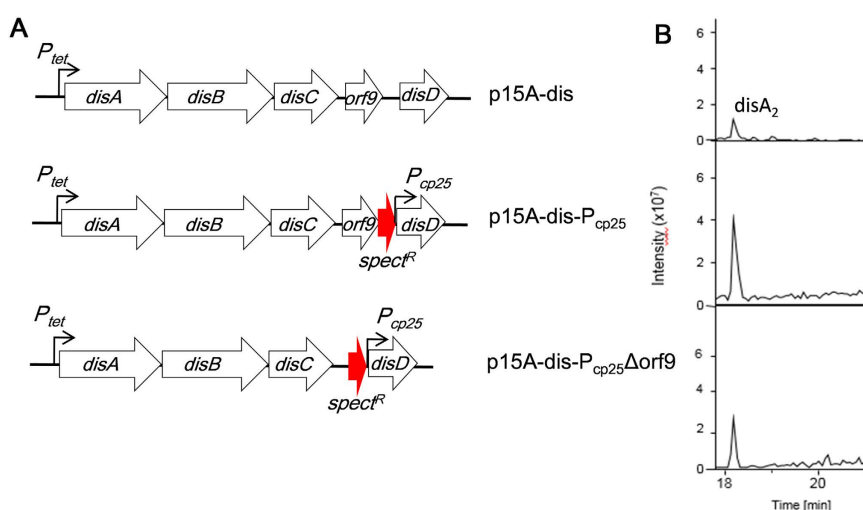


Figure 4. Promoter insertion in front of *disD* gene. (A) Three different types of expression constructs used for disorazol heterologous production. The first one is the original plasmid p15A-dis. The second one was modified via Red/ET recombineering by insertion of promoter P_{cp25} in front of *disD* directly. The third one was deletion *orf9* gene by P_{cp25}-*spect^R* so that P_{cp25} was also upstream *disD*. (B) Quantification of heterologous disorazol production by HPLC-MS analysis of the culture extracts from different *M. xanthus* DK1622 mutant strains. Sections of extracted ion chromatograms at *m/z* = 745.45 corresponding to the [M + H]⁺ ion of disorazol A₂ are illustrated as representative readout of productivity. The *M. xanthus* DK1622 host strains contain one of the three expression constructs shown in (A).

The peak area of disorazol A₂ (base peak chromatograms, BPC + 759.3 ± 0.1, RT = 18.2 min) was calculated by BrukerDaltonics compass data analysis 4.0. The yields of all disorazols were estimated from their relative peak areas in the HPLC-MS chromatogram by comparison with the standard curve for each derivative.

All the resulting host strains still produced disorazols with growing production titres based on HPLC-MS analysis. The generated *M. xanthus*:: p15A-dis-Pcp₂₅ expression host produced on average seven times more disorazol A₂ compared to *M. xanthus*:: p15A-dis and mutant strain *M. xanthus*:: p15A-dis-Pcp₂₅Δ*orf9* produced approximately 2.5-fold when compared to *M. xanthus*:: p15A-dis (Figs 4B and 5). Hence, the *orf9* gene ablation did reduce disorazol production although it was described as having “no functional prediction” in BLAST analysis³⁷. The *orf9* gene, following the TE domain, might affect the biosynthetic formation of the final product by incorporation and cyclization of two sides of the disorazol bis-lactone. The successful enhancement of disorazol heterologous production suggested that re-engineering *trans*-AT PKSs domains on the molecular level was a feasible and practicable approach in investigating the characteristic enzymes.

Trans-AT PKSs are an important but still less known family of biosynthetic systems in comparison to *cis*-AT PKSs^{58,59}. There are significant differences in the existing biosynthetic protocols between *trans*-AT and *cis*-AT PKSs. A single discrete AT DisD recognize and load all molonyl-CoAs for all the *dis* PKS modules. Here we change the native promoter of *disD* gene with a stronger and artificial synthetic P_{cp25} promoter which it would increase the transcription of *disD* gene and most likely raises the amount of DisD protein. Sufficient ATs could

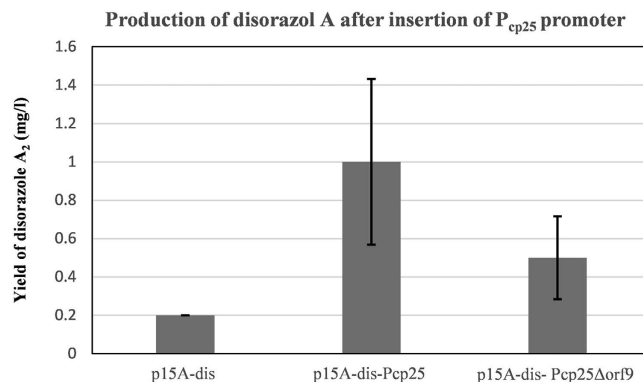


Figure 5. Production of disorazol A after insertion of P_{cp25} promoter. Quantification of disorazol heterologous production by HPLC-MS analysis of the culture extracts from different *M. xanthus* DK1622 mutant strains. All LC-MS- derived area values are normalized to the crude extracts of each sample by method of standard curves. The depicted values are mean values from three independent mutants. Error bars show calculated SDs, yield, control strain.

provide abundant substrates, thus promote the PKS module efficiency for polyketide chain extension of disorazol biosynthesis leading to improved production^{52,60,61}. As *trans*-AT PKSs are a special group of enzymes responsible for natural product biosynthesis in the organisms, it is essential to understand their functions in order to develop more heterologous expression systems for these special polyketides. Here, we have established a pioneer protocol to overexpress an independent AT resulted in increased yield of the final product, which can be used for the production optimization of *trans*-AT directed natural products in the native or heterologous hosts.

Methods

Bacterial strains and culture conditions. All recombinering was performed in *E. coli* strain GB2005 and its derivatives cultured in LB medium and antibiotics (kanamycin [km], 15 μg/ml; ampicillin [amp], 100 μg/ml; spectinomycin [spect], 40 μg/ml; chloramphenicol [cm], 30 μg/ml and tetracycline [tet], 5 μg/ml). The strains used were: GB2005, derived from DH10B by deletion of *fhuA*, *ycbC* and *recET*^{19,62}; GB05-red, derived from GB2005 by insertion of the P_{BAD}-*gbaA* cassette at the *ycbC* locus^{41,62}; GB05-dir, derived from GB2005 by the P_{BAD}-ETgA operon, which was integrated into the *ycbC* locus in GB2005⁴¹. The integration ablates expression of *ycbC*, which encoded a putative exonuclease similar to that encoded by Red α . The heterologous host for PKS/NRPS gene cluster expression was *M. xanthus* DK1622 grown at 30 °C in CTT medium (1% casitone, 8mM MgSO₄, 10mM Tris-HCl, pH 7.6, and 1mM potassium phosphate, pH 7.6)⁶³ with or without km (50 μg/ml) before or after introduction of the disorazol gene cluster.

Red/ET recombinering. All methods were essentially as described previously⁶². By using Red/ET recombinering, 0.3 μg of one linear DNA fragment (either a PCR product or a fragment obtained from restriction enzyme digestion) was electroporated into 50 μl Red/ET-competent *E. coli* cells (such as GB-red cells). After electroporation, colonies grew on the LB-agar plates under selection for the antibiotic resistance gene and then were examined for the intended Red/ET recombination product by restriction analysis with a set of different suitable enzymes.

All PCR reactions carried out using Taq polymerase (Invitrogen GmbH, Karlsruhe, Germany) according to the manufacturer's protocol. For the amplification of the ~1000 bp cassette with high GC content, DMSO was added to a final concentration of 3%. The conditions using an Eppendorf master cyclor were as follows: 10 min at 95 °C to activate the polymerase, denaturation at 95 °C (30 s), annealing at 58 °C (30 s), and extension at 72 °C (35 s); 35 cycles. The PCR product was directly used without any purification.

Reconstitution of *dis* gene cluster. To harvest the full length of the esterase gene *orf3'* in plasmid pTn-Rec_IE2, we first changed the backbone of pTn-Rec_IE2 into p15A-amp-*orf2'*-Tn-hyg in order to get more stable and higher copies of DNA (P3, P4 in Table S1). Then two linear fragments, p15A-amp-*orf2'*-Tn-hyg digested by *Sal* I and primer P5 (see Table S1), were co-transformed into *E. coli* GB05-dir cells⁴¹ to remove *R6k-Tn-hyg^R* genes and recover the whole size of *orf3'* gene. Thus, we obtained plasmid p15A-amp-*orf3'* harboring the full-length esterase gene. In order to insert the whole length *orf2'* and *orf3'* genes into the disorazol plasmid, we inserted two single PCR cassettes "*spect^R*" and "*cm^R*" with suitable homologous arms (P6-P9 Table S1) into the vector to engineer plasmid p15A-amp-*cm-orf2'*-*orf3'*-*spect* and then digested the new construct with *Hind* III to release the linear cassette "*cm^R-orf2'-orf3'-spect^R*" whose *Hind* III restriction site were homologous to p15A-dis vector. In the last step, the "*cm^R-orf2'-orf3'-spect^R*" cassette was transformed into strain GB-red::p15A-dis strain to generate the final plasmid (Figure S7). Two expression constructs p15A-dis and p15A-dis-est were obtained, containing four core-large genes from the disorazol A pathway (ten PKSs and one NRPS, ~58kb), with the P_{tet} promoter located upstream of the first PKS domain (Fig. 2).

Electroporation of *M. xanthus* DK 1622. The engineered gene clusters were introduced into the chromosome of *M. xanthus* DK1622 by electroporation. Briefly, *M. xanthus* cells from 1.7 ml of overnight culture with OD₆₀₀ ~ 0.6 were collected and electrocompetent cells were prepared after washing twice with ice-cold water. A mixture of 50 μ l cell suspension in cold water and 3 μ g DNA was electroporated (Electroporator 2500, Eppendorf AG, Hamburg, Germany) at 1300V using a 0.1 cm cuvette. After electroporation, the cells were resuspended in 1.7 ml fresh CTT medium, and incubated at 30 °C in a 2 ml Eppendorf tube with a hole punched in the lid on a Thermomixer (Eppendorf) at 11000 r.p.m. for 6 h. Then 1 ml 1.5% CTT agar solution at 42 °C was added to the tube and the cells were plated in soft agar for selection on CTT agar plates supplemented with km (50 μ g/ml). Km-resistant colonies appeared after 4 days and were checked by colony PCR as follows. Part of a single colony was washed once in 1 ml H₂O and resuspended in 100 μ l H₂O. Then, 2 μ l of the resulting suspension was used as a PCR template using Taq polymerase according to the manufacturer's protocol. The disorazol-specific primers used to check the integration of the *disC* gene into the *M. xanthus* chromosome were the same as used in a previous study¹⁶. For PCR amplification, primers 10 and 11 were used (see Table S1).

Expression and analysis of disorazol production. Plasmids harboring a core-region or reconstituted *dis* gene cluster were introduced into *M. xanthus* DK1622 by electroporation. The resulting mutants (*M. xanthus* DK1622:: p15A-*dis*) were cultivated in 100 ml shake flasks containing 30 ml CTT medium. The medium was inoculated with 0.5 mL of the overnight culture and incubated at 30 °C on a rotary shaker at 180 rpm. After induction (anhydrotetracycline, final concentration 0.5 μ g/mL) and addition of XAD adsorber resin (2%, 24 h), incubation was continued for 2 more days. The cells and the resin were harvested by centrifugation and extracted with methanol. The extracts were evaporated and then redissolved in 1 mL MeOH. A 5 μ L solution was analyzed by HPLC-MS and analysis was performed on an Agilent 1100 series solvent delivery system that was equipped with a photodiode array detector and coupled to a Bruker HCTultra ion trap mass spectrometer. Chromatographic conditions were as follows: Luna RP-C₁₈ column, 100 \times 2 mm, 2.5 μ m particle size, and precolumn C₁₈, 8 \times 3 mm, 5 μ m. Solvent gradient (with solvents A [water and 0.1% formic acid] and B [CH₃CN and 0.1% formic acid]): 20% B from 0 to 20 min, 20% B-95% B within 10 min, followed by 5 min with 95% B at a flow rate of 0.4 mL/min. Detection was carried out in positive ion mode, auto MSⁿ. Disorazols were identified by comparison to the retention times and the MS² data of disorazols identified from the original producer in our myxo-database (target screening, Table S2)²⁸. The relative production of disorazols was calculated from the peak areas of the extracted ion chromatograms (EICs) of each derivative.

High-resolution mass spectrometry was performed on an Accela UPLC-system (Thermo-Fisher) coupled to a linear trap-FT-Orbitrap combination (LTQ-Orbitrap), operating in positive ionization mode. Separation was achieved on a Waters BEH RP-C₁₈ column (50 \times 2.1 mm; 1.7 μ m particle diameter; flow rate 0.6 mL/min, Waters), with a mobile phase of H₂O/CH₃CN (each containing 0.1% formic acid) and a gradient of 5–95% CH₃CN over 9 mins. UV and MS detection were performed simultaneously. Coupling of HPLC to MS was supported by an Advion Triversa Nanomate nano-ESI system attached to a Thermo Fisher Orbitrap. Mass spectra were acquired in centroid mode at 200–2000 *m/z* with a resolution of R = 30000.

Target screening method. The HPLC-HR-MS data of crude extracts were further analyzed to identify the known compounds present in the extracts using the software Target Analysis (Bruker Daltonik GmbH). The known compounds were identified on the basis of their high resolution mass, isotope pattern and retention time according to the known method⁴⁵. With this approach, re-isolation of known but less interesting compounds could be avoided whereas unknown compounds with potential bioactivity could be identified easily.

Isolation of disorazol A₂. *M. xanthus* containing p15A-*dis* was cultivated in 5 L CTT medium supplemented with 30 μ g/mL kanamycin and 2% XAD 16 resin (after 2 days of incubation) at 30 °C for 5 days⁶³. The resin was collected by sieving, washed with H₂O twice, and then extracted stepwise with acetoacetate (5 L). The extract was concentrated *in vacuo*, followed by suspension in MeOH and extraction with *n*-hexane to defat. The resulting MeOH extract (0.87 g) was fractionated initially on a Sephadex LH-20 column (100 \times 2.5 cm) using MeOH as a mobile phase, and 55 fractions were obtained. Fractions containing disorazol A₂ were subjected to semi-preparative reversed-phase HPLC system (Jupiter Proteo C₁₂, 250 \times 10 mm, 4 μ m, DAD at 254 nm) with an isocratic system of 75% MeOH/H₂O with 0.05% TFA to yield (1.2 mg, *t_R* \approx 22 min).

NMR. NMR spectra were recorded in CD₃OD on a DRx 500 MHz spectrometer (¹H at 500 MHz, ¹³C at 125 MHz) equipped with a 5-mm probe and a Bruker Ascend 700 MHz spectrometer (¹H at 700 MHz, ¹³C at 175 MHz) equipped with a 5-mm TXI cryoprobe system (Bruker Biospin GmbH, Germany). Chemical shift values of ¹H- and ¹³C-NMR spectra are reported in ppm relative to the residual solvent signal given as an internal standard. Multiplicities are described using the following abbreviations: s = singlet, d = doublet, t = triplet, q = quartet, m = multiplet, b = broad; corrected coupling constants are reported in Hz.

References

- Luo, Y., Cobb, R. E. & Zhao, H. Recent advances in natural product discovery. *Curr. Opin. Biotechnol.* **30**, 230–237 (2014).
- Wenzel, S. C. & Müller, R. The impact of genomics on the exploitation of the myxobacterial secondary metabolome. *Nat. Prod. Rep.* **26**, 1385–1407 (2009).
- Schäberle, T. F., Lohr, F., Schmitz, A. & König, G. M. Antibiotics from myxobacteria. *Nat. Prod. Rep.* **31**, 953–972 (2014).
- Gomes, E. S., Schuch, V. & de Macedo Lemos, E. G. Biotechnology of polyketides: new breath of life for the novel antibiotic genetic pathways discovery through metagenomics. *Braz. J. Microbiol.* **44**, 1007–1034 (2014).
- Strieker, M., Tanović, A. & Marahiel, M. A. Nonribosomal peptide synthetases: structures and dynamics. *Curr. Opin. Struct. Biol.* **20**, 234–240 (2010).
- Fischbach, M. A. & Walsh, C. T. Assembly-line enzymology for polyketide and nonribosomal peptide antibiotics: logic, machinery, and mechanisms. *Chem. Rev.* **106**, 3468–3496 (2006).

7. Ongley, S. E. *et al.* High titer heterologous production of Lyngbyatoxin in *E. coli*, a protein kinase C activator from an uncultured marine Cyanobacterium. *ACS Chem. Biol.* **8**, 1888–1893 (2013).
8. Pfeifer, B. A., Admiraal, S. J., Gramajo, H., Cane, D. E. & Khosla, C. Biosynthesis of complex polyketides in a metabolically engineered strain of *E. coli*. *Science* **291**, 1790–1792 (2001).
9. Ongley, S. E., Bian, X., Neilan, B. A. & Müller, R. Recent advances in the heterologous expression of microbial natural product biosynthetic pathways. *Nat. Prod. Rep.* **30**, 1121–1138 (2013).
10. Bian, X. *et al.* Direct cloning, genetic engineering, and heterologous expression of the Syringolin biosynthetic gene cluster in *E. coli* through Red/ET recombineering. *ChemBioChem.* **13**, 1946–1952 (2012).
11. Larionov, V., Kouprina, N., Solomon, G., Barrett, J. C. & Resnick, M. A. Direct isolation of human *BRCA2* gene by transformation-associated recombination in yeast. *Proc. Natl. Acad. Sci. USA* **94**, 7384–7387 (1997).
12. Kouprina, N. *et al.* Functional copies of a human gene can be directly isolated by transformation-associated recombination cloning with a small 3' end target sequence. *Proc. Natl. Acad. Sci. USA* **95**, 4469–4474 (1998).
13. Zhang, Y., Buchholz, F., Muyrers, J. P. P. & Stewart, A. F. A new logic for DNA engineering using recombination in *Escherichia coli*. *Nat. Genet.* **20**, 123–128 (1998).
14. Zhang, Y., Muyrers, J. P. P., Testa, G. & Stewart, A. F. DNA cloning by homologous recombination in *Escherichia coli*. *Nat. Biotechnol.* **18**, 1314–1317 (2000).
15. Zhang, Y., Muyrers, J. P. P., Rientjes, J. & Stewart, A. F. Phage annealing proteins promote oligonucleotide-directed mutagenesis in *Escherichia coli* and mouse ES cells. *Mol. Biol.* **4**, 1 (2003).
16. Wenzel, S. C. & Müller, R. Recent developments towards the heterologous expression of complex bacterial natural product biosynthetic pathways. *Curr. Opin. Biotechnol.* **16**, 594–606 (2005).
17. Gross, F. *et al.* Metabolic engineering of *Pseudomonas putida* for methylmalonyl-CoA biosynthesis to enable complex heterologous secondary metabolite formation. *Chem. Biol.* **13**, 1253–1264 (2006).
18. Perlova, O. *et al.* Reconstitution of the myxothiazol biosynthetic gene cluster by Red/ET recombination and heterologous expression in *Myxococcus xanthus*. *Appl. Environ. Microbiol.* **72**, 7485–7494 (2006).
19. Fu, J. *et al.* Efficient transfer of two large secondary metabolite pathway gene clusters into heterologous hosts by transposition. *Nucleic Acids Res.* **36**, e113 (2008).
20. Wang, A. *et al.* High level expression and purification of bioactive human alpha-defensin 5 mature peptide in *Pichia pastoris*. *Appl. Microbiol. Biotechnol.* **84**, 877–884 (2009).
21. Liao, G. J. *et al.* Cloning, reassembling and integration of the entire nikkomycin biosynthetic gene cluster into *Streptomyces ansochromogenes* lead to an improved nikkomycin production. *Microb. Cell Fact.* **9**, 6 (2010).
22. Chai, Y. *et al.* Heterologous expression and genetic engineering of the tubulysin biosynthetic gene cluster using Red/ET recombineering and inactivation mutagenesis. *Chem. Biol.* **19**, 361–371 (2012).
23. Bian, X., Plaza, A., Zhang, Y. & Müller, R. Luminmycins A–C, cryptic natural products from *Photorhabdus luminescens* identified by heterologous expression in *Escherichia coli*. *J. Nat. Prod.* **75**(9), 1652–1655 (2012).
24. Bian, X. *et al.* Heterologous Production of Glidobactins/Luminmycins in *Escherichia coli* Nissle Containing the Glidobactin Biosynthetic Gene Cluster from *Burkholderia* DSM7029. *ChemBioChem.* **15**, 2221–2224 (2014).
25. Yin, J. *et al.* Direct cloning and heterologous expression of the salinomycin biosynthetic gene cluster from *Streptomyces albus* DSM41398 in *S. coelicolor* A3(2). *Sci. Rep.* **5**, 15081 (2015).
26. Kolinko, I. *et al.* Biosynthesis of magnetic nanostructures in a foreign organism by transfer of bacterial magnetosome gene clusters. *Nat. Nanotech.* **9**, 193–197 (2014).
27. Weissman, K. J. & Müller, R. Myxobacterial secondary metabolites: bioactivities and modes-of-action. *Nat. Prod. Rep.* **27**, 1276–1295 (2010).
28. Jansen, R., Irschik, H., Reichenbach, H., Wray, V. & Höfle, G. Disorazols: highly cytotoxic metabolites from the sorangicin-producing bacterium *Sorangium cellulosum*, strain So ce12. *Liebigs Ann. Chem.* 759–773 (1994).
29. Elnakady, Y. A., Sasse, F., Lünsdorf, H. & Reichenbach, H. Disorazol A₁, a highly effective antimitotic agent acting on tubulin polymerization and inducing apoptosis in mammalian cells. *Biochem. Pharmacol.* **67**, 927–935 (2004).
30. Schäckel, R., Hinkelmann, B., Sasse, F. & Kalesse, M. The synthesis of novel disorazols. *Angew. Chem. Int. Ed.* **49**, 1619–1622 (2010).
31. Lee, C., An, D., Lee, H. & Cho, K. Correlation between *Sorangium cellulosum* subgroups and their potential for secondary metabolite production. *J. Microbiol. Biotechnol.* **23**, 297–303 (2013).
32. Hopkins, C. D. & Wipf, P. Isolation, biology and chemistry of the disorazols: new anti-cancer macrodiolides. *Nat. Prod. Rep.* **26**, 585–601 (2009).
33. Seitz, S. *et al.* Triple negative breast cancers express receptors for LHRH and are potential therapeutic targets for cytotoxic LHRH-analogs, AEZS 108 and AEZS 125. *BMC Cancer* **14**, 847 (2014).
34. Wipf, P. & Graham, T. H. Total synthesis of (-)-disorazol C₁. *J. Am. Chem. Soc.* **126**, 15346–15347 (2004).
35. Xu, F. L. *et al.* Mitotic slippage in non-cancer cells induced by a microtubule disruptor, disorazol C₁. *BMC Chem. Biol.* **10**, 1 (2010).
36. Lazo, J. S. *et al.* Identifying a resistance determinant for the antimitotic natural products disorazol C₁ and A₁. *J. Pharmacol. Exp. Ther.* **332**, 906–911 (2010).
37. Kopp, M., Irschik, H., Pradella, S. & Müller, R. Production of the tubulin destabilizer disorazol in *Sorangium cellulosum*: biosynthetic machinery and regulatory genes. *ChemBioChem.* **6**, 1277–1286 (2005).
38. Carvalho, R. *et al.* The biosynthetic genes for disorazols, potent cytotoxic compounds that disrupt microtubule formation. *Gene* **359**, 91–98 (2005).
39. Stevens, D. C., Hari, T. P. A. & Boddy, C. N. The role of transcription in heterologous expression of polyketides in bacterial hosts. *Nat. Prod. Rep.* **30**, 1391–1411 (2013).
40. Kang, Y. *et al.* Knock-out and pull-out recombineering protocols for naturally transformable *Burkholderia thailandensis* and *Burkholderia pseudomallei*. *Nat. Protoc.* **6**, 1085–1104 (2011).
41. Fu, J. *et al.* Full-length RecE enhances linear-linear homologous recombination and facilitates direct cloning for bioprospecting. *Nat. Biotech.* **30**, 440–446 (2012).
42. Julien, B. & Fehd, R. Development of a mariner-based transposon for use in *Sorangium cellulosum*. *Appl. Environ. Microbiol.* **69**(10), 6299–6301 (2003).
43. Kopp, M. *et al.* Critical variations of conjugational DNA transfer into secondary metabolite multiproducing *Sorangium cellulosum* strains So ce12 and So ce56: development of a mariner-based transposon mutagenesis system. *J. Biotechnol.* **107**, 29–40 (2004).
44. Wenzel, S. C. *et al.* Heterologous expression of a myxobacterial natural products assembly line in pseudomonads via red/ET recombineering. *Chem. Biol.* **12**, 349–356 (2005).
45. Krug, D. & Müller, R. Secondary metabolomics: the impact of mass spectrometry-based approaches on the discovery and characterization of microbial natural products. *Nat. Prod. Rep.* **31**, 768–783 (2014).
46. Moat, A. G., Foster, J. W. & Spector, M. P. *Microbial Physiology*, 4th ed. (New York, Wiley-Liss, Inc. Pub) (2003).
47. Trun, N. & Trempey, J. *Fundamental bacterial genetics*. (Malden, MA: Blackwell Pub.) (2004).
48. Irschik, H., Jansen, R., Gerth, K., Höfle, G. & Reichenbach, H. Disorazol A, an efficient inhibitor of eukaryotic organisms isolated from myxobacteria. *J. Antibiot.* **48**, 31–35 (1995).
49. Hearn, B. R. *et al.* Methanolysis products of disorazol A₁. *J. Nat. Prod.* **69**, 148–150 (2006).

50. Wong, F. T., Jin, X., Mathews, I. I., Cane, D. E. & Khosla, C. Structure and mechanism of the trans-acting acyltransferase from the disorazol synthase. *Biochemistry*. **50**, 6539–6548 (2012).
51. Piel, J. Metabolites from symbiotic bacteria. *Nat. Prod. Rep.* **26**, 338–362 (2009).
52. Till, M. & Race, P. R. Progress challenges and opportunities for the re-engineering of trans-AT polyketide synthases. *Biotechnol. Lett.* **36**, 877–888 (2014).
53. Jensen, P. R. & Hammer, K. The sequence of spacers between the consensus sequences modulates the strength of prokaryotic promoters. *Appl. Environ. Microbiol.* **64**, 82–87 (1998).
54. Kodumal, S. J. *et al.* Total synthesis of long DNA sequences: synthesis of a contiguous 32-kb polyketide synthase gene cluster. *Proc. Natl. Acad. Sci. USA* **101**, 15573–15578 (2004).
55. Richter, C. D., Nietlispach, D., Broadhurst, R. W. & Weissman, K. J. Multienzyme docking in hybrid megasynthetases. *Nat. Chem. Biol.* **4**, 75–81 (2008).
56. Meiser, P. & Müller, R. Two functionally redundant Sfp-type 4-phosphopantetheinyl transferases differentially activate biosynthetic pathways in *Myxococcus xanthus*. *ChemBioChem*. **9**, 1549–1553 (2008).
57. Buntin, K. *et al.* Biosynthesis of thuggacins in myxobacteria: comparative cluster analysis reveals basis for natural product structural diversity. *Chem. Biol.* **17**, 342–356 (2010).
58. Piel, J. Biosynthesis of polyketides by trans-AT polyketide synthases. *Nat. Prod. Rep.* **27**, 996–1047 (2010).
59. Dunn, B. J., Watts, K. R., Robbins, T., Cane, D. E. & Khosla, C. Comparative analysis of the substrate specificity of trans- versus cis-acyltransferases of assembly line polyketide synthases. *Biochemistry*. **53**, pp3796–3806 (2014).
60. Lopanik, N. B. *et al.* *In vivo* and *in vitro* trans-acylation by BryP, the putative bryostatin pathway acyltransferase derived from an uncultured marine symbiont. *Chem. Biol.* **15**, 1175–1186 (2008).
61. Jensen, K. *et al.* Polyketide proofreading by an acyltransferase-like enzyme. *Chem. Biol.* **19**, 329–339 (2012).
62. Fu, J., Teucher, M., Anastassiadis, K., Skarnes, W. & Stewart, A. F. A recombineering pipeline to make conditional targeting constructs. *Meth. Enzymol.* **477**, 125–144 (2010).
63. Meiser, P., Bode, H. B. & Müller, R. The unique DKxanthene secondary metabolite family from the myxobacterium *Myxococcus xanthus* is required for developmental sporulation. *Proc. Natl. Acad. Sci. USA* **103**, 19128–19133 (2006).

Acknowledgements

The authors would like to thank Eva Luxenburger, Dr. Stephan Hüttel and Dr. Thomas Hoffmann (HIPS) for expert assistance with various analytical techniques, Viktoria Schmitt for assistance in biological function experiments and Dr. Jun Fu (Dresden University of Technology) for expert technical assistance in Red/ET recombineering. Research in the laboratory of R.M. was funded by the Deutsche Forschungsgemeinschaft (DFG) and the Bundesministerium für Bildung und Forschung (BMBF). The work in the laboratory of Y. Z. was supported by funding from the Recruitment Program of Global Experts. The authors acknowledge Dr. MA Meredyth Stewart and Dr. Vinothkannan Ravichandran's help in proofreading this manuscript.

Author Contributions

Q.T., S.H. and Y.Z. planned and performed cloning experiments. Q.T. and X.B. performed genetic transfers, cultivation experiments and data analysis. Q.T. and R.R. performed HPLC and compound isolation. R.R. performed NMR experiments and data analysis. J.H. performed biological functional studies. Q.T., Y.Z. and R.M. designed the study and wrote the paper. All authors discussed the results and commented on the manuscript.

Additional Information

Supplementary information accompanies this paper at <http://www.nature.com/srep>

Competing financial interests: The authors declare no competing financial interests.

How to cite this article: Tu, Q. *et al.* Genetic engineering and heterologous expression of the disorazol biosynthetic gene cluster via Red/ET recombineering. *Sci. Rep.* **6**, 21066; doi: 10.1038/srep21066 (2016).



This work is licensed under a Creative Commons Attribution 4.0 International License. The images or other third party material in this article are included in the article's Creative Commons license, unless indicated otherwise in the credit line; if the material is not included under the Creative Commons license, users will need to obtain permission from the license holder to reproduce the material. To view a copy of this license, visit <http://creativecommons.org/licenses/by/4.0/>

Supplemental Information

Genetic Engineering and Heterologous Expression of the Disorazol Biosynthetic Gene Cluster via Red/ET Recombineering

Qiang Tu, Jennifer Herrmann, Shengbiao Hu, Ritesh Raju, Xiaoying Bian, Youming Zhang and Rolf Müller

Inventory of Supplemental Information

Supplemental data

Figure S1. Chemical structures of disorazols.

Structures of all disorazol derivatives mentioned in this paper. On Page 3.

Figure S2. related to Figure 2. Heterologous expression constructs of two type expression plasmids p15A-dis and p15A-dis-est. On Page 9.

Figure S3. related to Figure 3. HPLC-MS analysis of target screening of extracts from *M. xanthus*:: *p15A-dis*. On Page 10.

Figure S4. related to Figure 3. ¹H NMR spectrum data of disorazol A₂. On Page 11.

Figure S5. related to Figure 5. Modify *disD* gene through Red/ET recombineering. On Page 13.

Figure S6. Construct of the recovered plasmid pTn-Rec_IE2. On Page 7.

Table S1 Oligonucleotides used in this study.

Table S2 related to Figure 3. Target screening analysis data of extracts from *M. xanthus* ::*p15A-dis*. On Page 10.

Table S3 related to Figure 3. NMR data for disA₂ comparison with the natural product. On Page 11.

Table S4 Proteins encoded on the recovered plasmid pTn-Rec_IE-2 and their putative function in disorazol biosynthesis. On Page 5.

Supplemental experimental procedures

Supplemental references

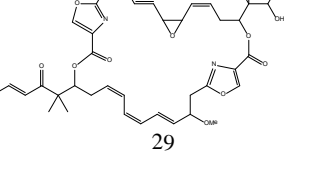
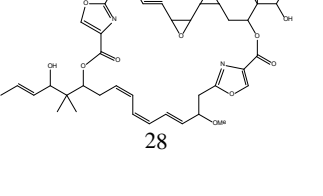
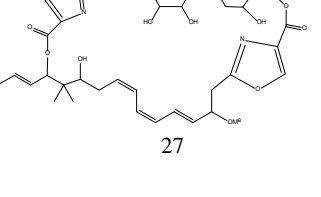
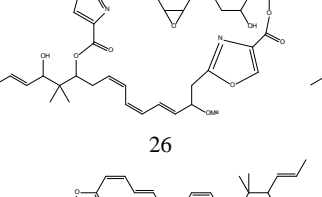
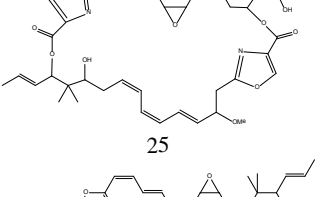
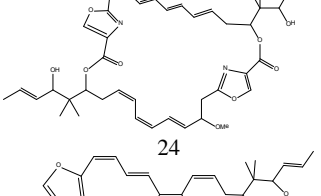
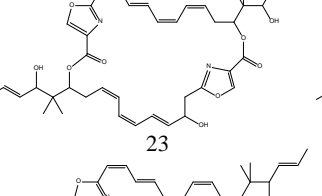
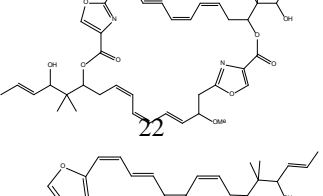
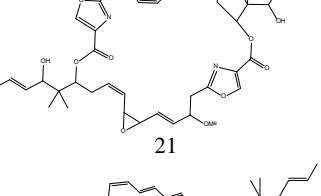
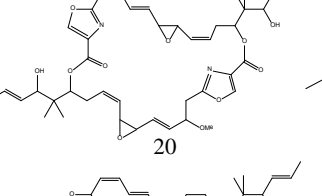
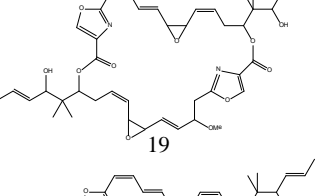
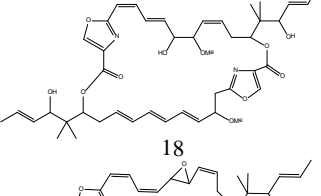
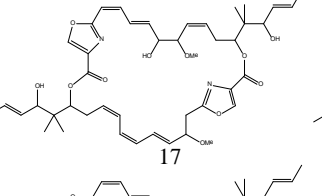
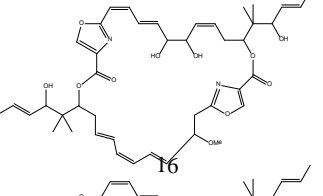
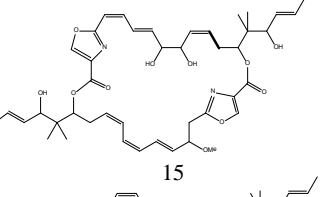
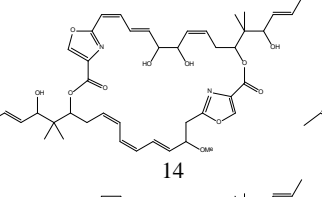
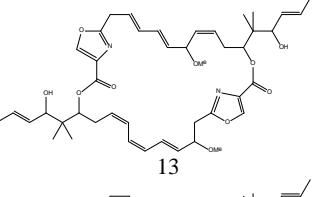
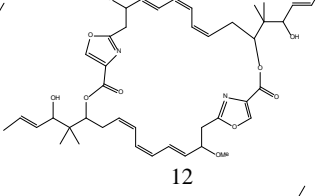
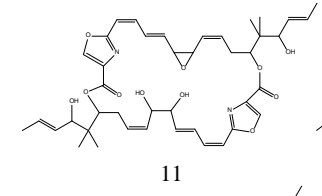
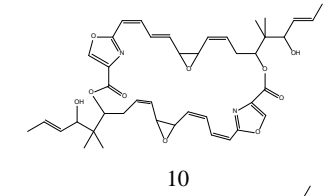
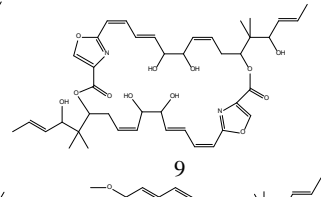
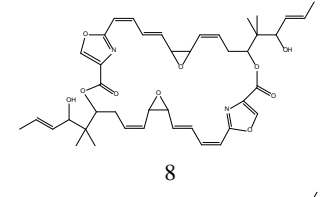
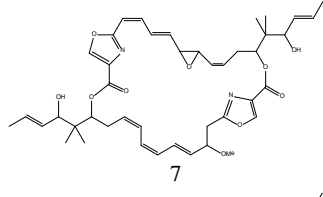
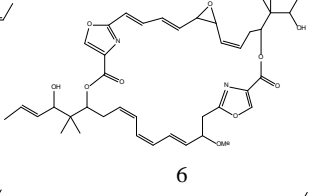
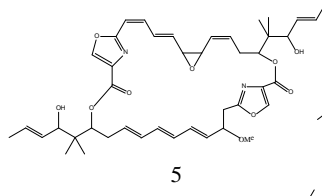
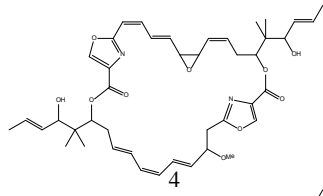
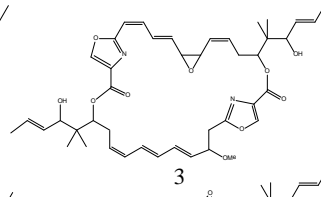
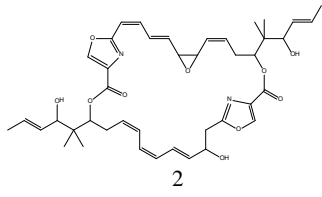
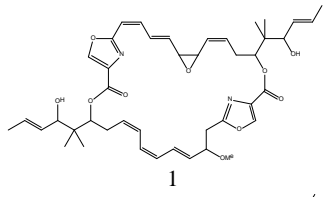


Figure S1. Chemical structures of disorazols.

1. Disorazol A₁
2. Disorazol A₂
3. Disorazol A₃
4. Disorazol A₄
5. Disorazol A₅
6. Disorazol A₆
7. Disorazol A₇
8. Disorazol B₁
9. Disorazol B₂
10. Disorazol B₃
11. Disorazol B₄
12. Disorazol C₁
13. Disorazol C₂
14. Disorazol D₁
15. Disorazol D₂
16. Disorazol D₃
17. Disorazol D₄
18. Disorazol D₅
19. Disorazol E₁
20. Disorazol E₂
21. Disorazol E₃
22. Disorazol F₁
23. Disorazol F₂
24. Disorazol F₃
25. Disorazol G₁
26. Disorazol G₂
27. Disorazol G₃
28. Disorazol H
29. Disorazol I

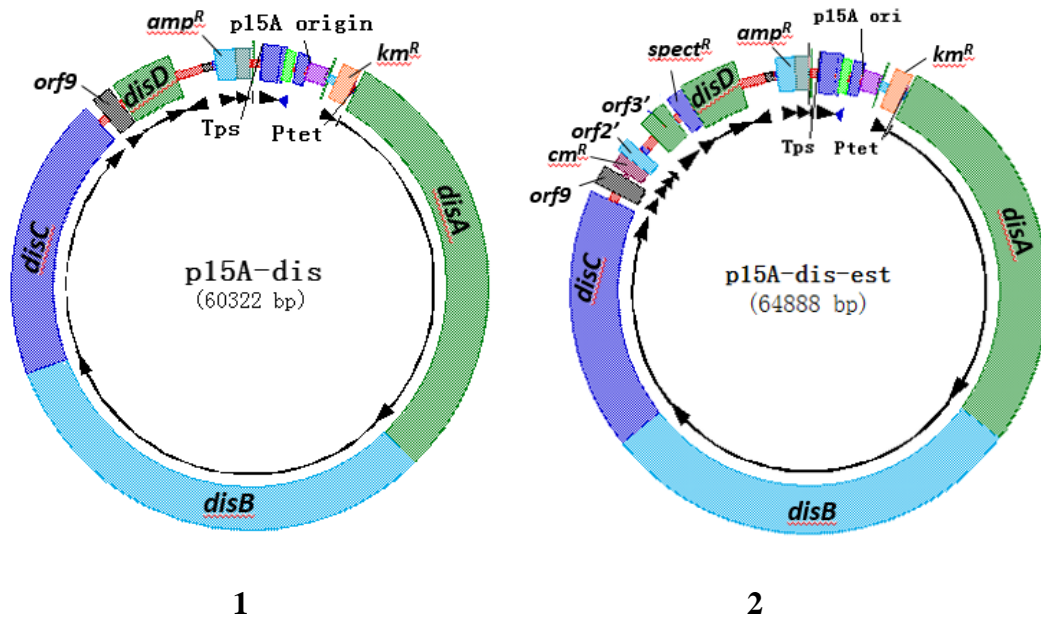


Figure S2. Heterologous expression constructs of two type of expression plasmids p15A-dis and p15A-dis-est.

Construct 1 is p15A-dis. Then we insert the repaired carboxyl esterase gene *orf3'* and the SAM-dependent methyl transferase gene *orf2'* together into p15A-dis by Red/ET recombineering to form construct 2 p15A-dis-est. After insertion, two genes are in the middle of *orf9* gene and *disD* gene.

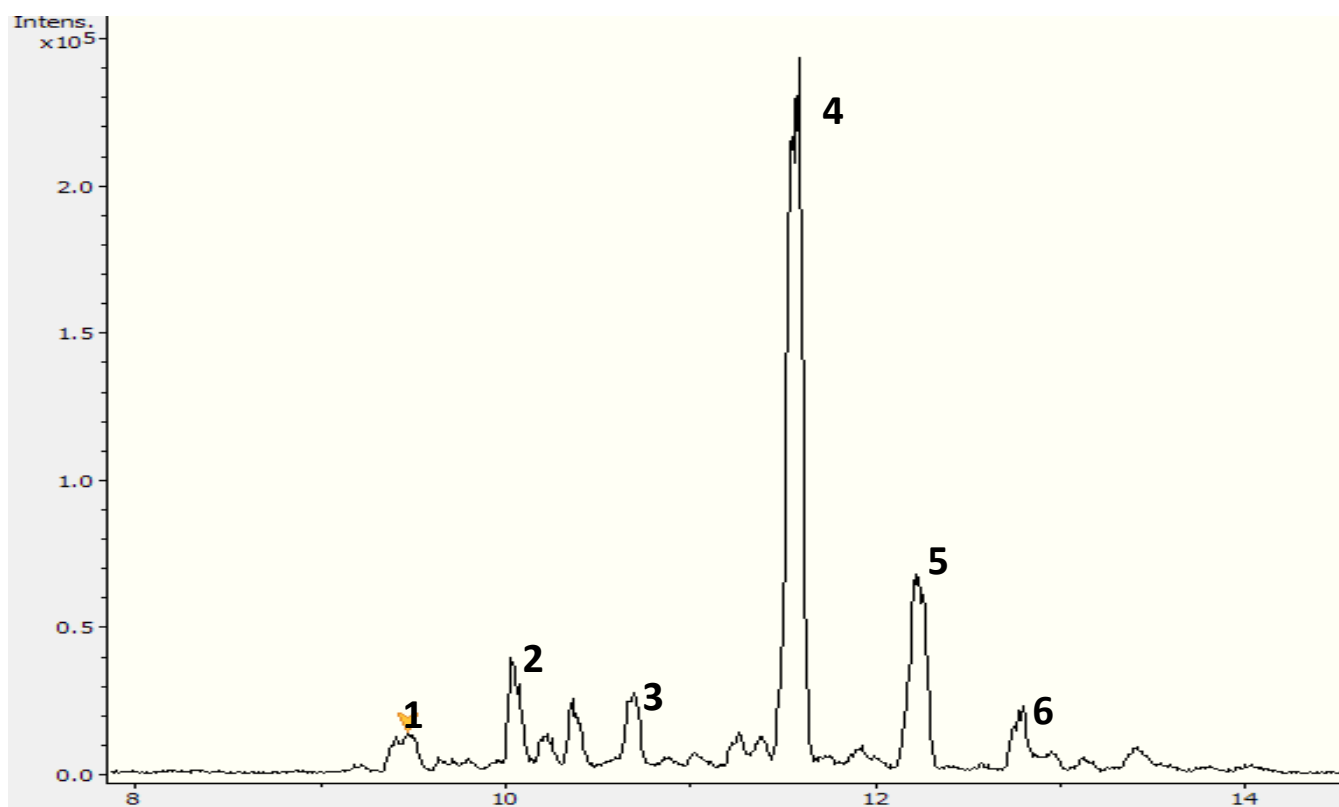


Figure S3. related to Figure 3. HPLC-MS analysis (BPC m/z 720-780) of extracts from *M. xanthus*:: *p15A-dis*.

The peaks are disB₄ (1), m/z 761 [M+H]⁺; dis762 (2), m/z 763 [M+H]⁺; disB₂ (3), m/z 779 [M+H]⁺; disA₂ (4), m/z 745 [M+H]⁺; disA₁ (5), m/z 759 [M+H]⁺; disF₂ (6), m/z 729 [M+H]⁺.

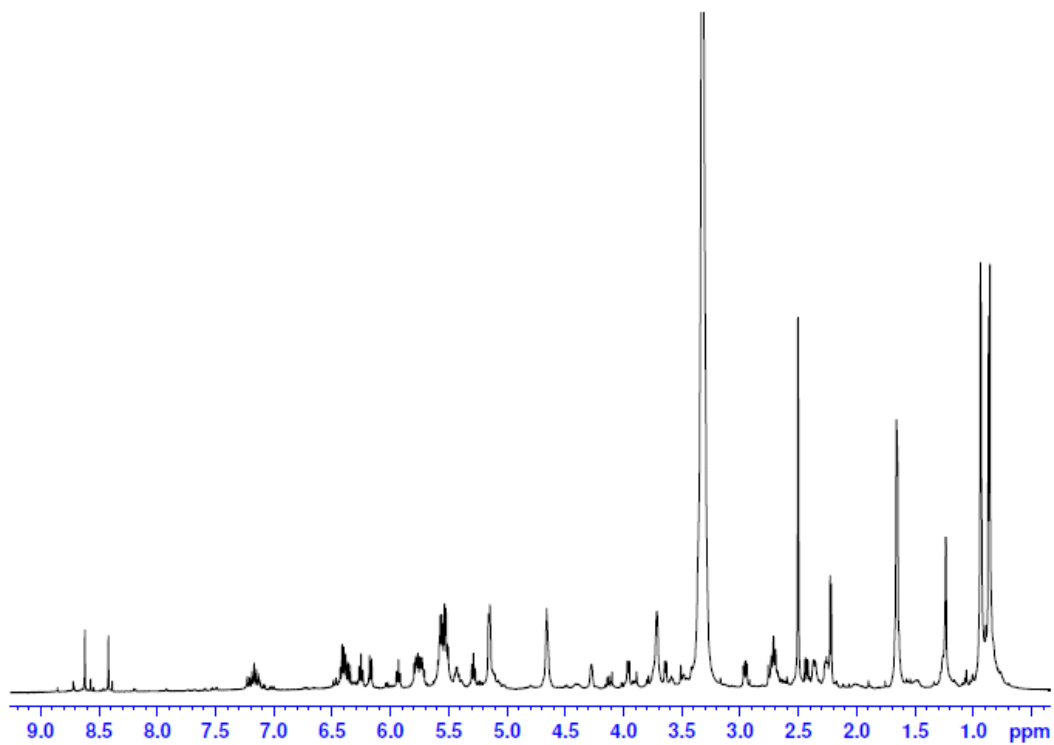
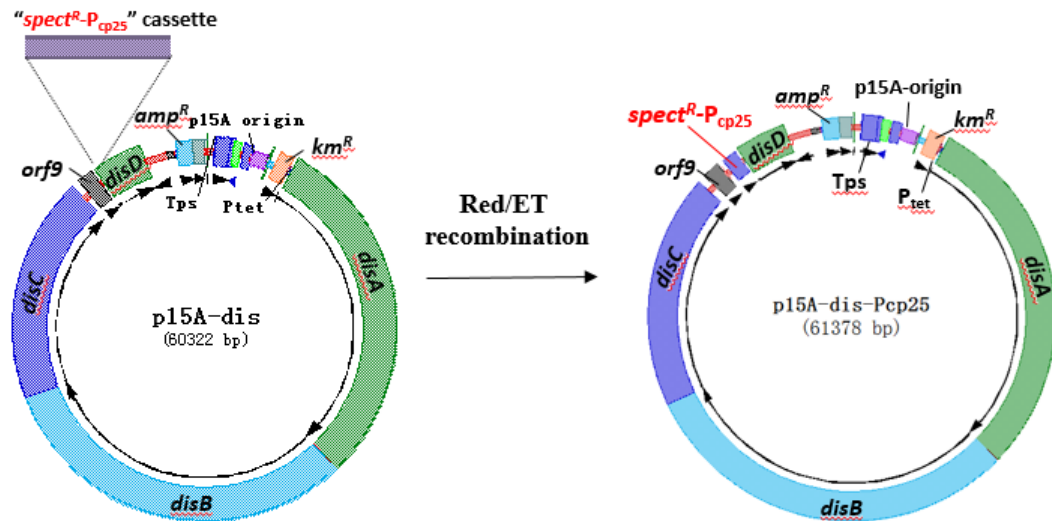
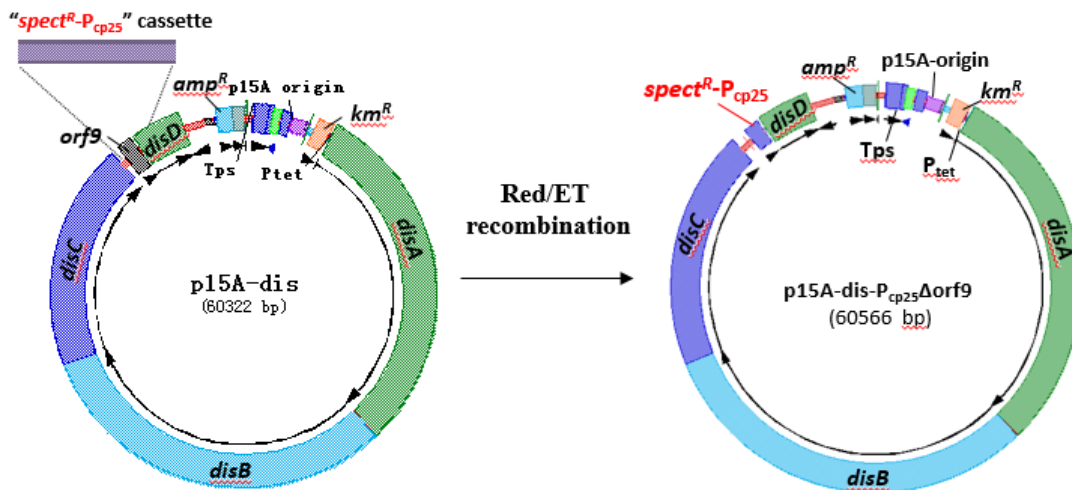


Figure S4. ^1H NMR spectrum of disorazol A₂.



1



2

Figure S5. Modify *disD* gene through Red/ET recombineering.

1: only insert promoter P_{cp25} in front of *disD* gene.

2: insert promoter P_{cp25} in front of *disD* gene by deletion *orf9* gene.

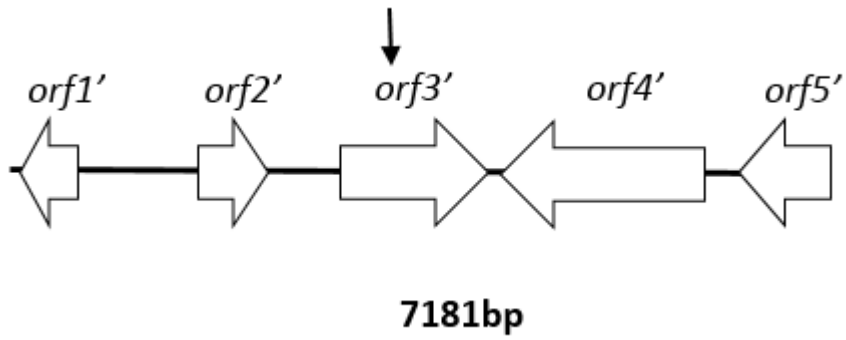


Figure S6. Construct of the recovered plasmid pTn-Rec_IE2. (data according to Kopp et al.)

Diagram of the genes encoded adjacent to the transposition site of mutant

So12_EXI_IE-3 that was cloned into the recovered plasmid pTn-Rec_IE-2. ↓ is the location of the transposon insertion site.

Table S1 Oligonucleotides used in this study

name	sequences(5'-3')	Notes
P1	AATGTGCGACAATGTGCGCCATTTTTTC ACTTCACAGGTCAACGCTCACGCTGA CGCTGTCCGCCGAGACCGACTTGGGC TTCTACCTGCGGATCCTGGTGATGATG GCGGGATCGTTG	Used to replace the backbone of disBAC plasmid
P2	AATGAATAGTTCGACAAAAATCTAGA TAACGAGGATCAACGATGGAGCAGGA CGCCATTGCGATCATCGGCGTAGCGT GCCGATTTCCCGGGATCCTGTGACGG AAGATCACTTCG	
P3	TCCGCTGCATCCTGGATCTGGATATGG ACAGGAAGGCGTTTGAAGAAGTCGAG TTTGAACAAAACAACCTTATATCG	Used to replace the backbone of pTn- Rec_IE2 plasmid
P4	CTCAGCCCGCGTCGAGCGCGTAGACG GCCGTGGCCGTCTTTCGCCCCGTCAGG TCTTACCAATGCTTAATCAGTGAG	
P5	TACCGTCGCGGCCACGCGCATCTGGG GCCCCCTCGGCATGAACGATACGATG TACAACCCGCCCGCGGAGCTCCACGA GCGCGTGGCGGCCACGGGCTACTCGA CC	Used to delete R6k-Tn-hyg genes in order to form full length of esterase gene
P6	CAGATCGCTGAGATAGGTGCCTCACT GATTAAGCATTGGTAAGCTTGAGACC CTTGCCCGGAAACATGTATGCTTTCA TCGGTTCTTCCTCTTATAATTTTTTTAA TCTGTTA	Used to form the homology arm to p15A-dis plasmid
P7	CCTCAGCCCGCGTCGAGCGCGTAGAC GGCCGTGGCCGTCTTTCGCCTAACGTG ACTGGCAAGAGATAT	
P8	TGACCTCCGGCTCGAGCACGCGCGCC AGCGACATGCTCGCATCCTTCTCCGTT ACGCCCCGCCCTGCCACTC	Used to form the homology arm to p15A-dis plasmid
P9	TCAGCCCCATACGATATAAGTTGTTTT GTTCAAACCTCGACTTCAAGCTTGCGCC GAGGCGAGCCCCTGGCGGGCACGTCG TGGCGGCGCGCCTCCTGGTGTCCTGT TGATACC	
P10	TGGAAAGCGCGATGACCATCCAGGAG TTTGCCAACTTGTCTGCGGAG	Used to verify <i>M. xanthus</i> :p15A-dis mutant.
P11	TGTGGGAGGCGAGGGCCTCGGCGAAG AGGGTGAGGAGCAGGGCCGTCGG	

P12	TGGAGGTCCGCCCGATCGCCGAGGGC GAGCTGCACGAGCGCCTCGCGCGGCA GGAGCCCTTACGCCCCGCCCTGCCACT CATCGCAG	Used to inactivate <i>disA</i> gene
P13	TGATAGAGAAAAGTGAAATGAATAGT TCGACAAAAATCTAGGAGGATGATGA CGCCAACTTTTGGCGAAAATGAGAC	
P14	CGTAGGACACCCGGTTGGCGATCGAC GAGTAATCGGCGCTCGCGATCACGGG GTTTCCCTTGTGGAGCTCGTCCTGTTA CGCCCCGCCCTGCCACTCATCGCA	Used to inactivate <i>disB</i> gene
P15	TGCGCCGCTCGGCTATTACCAATCGAC CTGGACCAGAAGCGCGCTTTGAACGT CGGGGTAACCTCCCAACTTTTGGCGA AAATGAGAC	
P16	CGGCTCGGTGAGCGAGAGCCGCAGCT CGAAGAAGGGCCACTGATCCAGGGGG AATACCCTTTACGCCCCGCCCTGCCAC TCATCGCAG	Used to inactivate <i>disC</i> gene
P17	TGGCCGGCGTACCGGGCGAGGAGCTG ACTCGGCTCTACGCCATCCTGCAAGA GGAATGATGACCAACTTTTGGCGAAA ATGAGAC	
P18	TGAGACCCTTGCCCGGGAAACATGTA TGCTTTCATCGGTTCTTCTCTCTATCA CTGATAGGGAGTGGTAAAATAACTCT ATCAATGATAGAGTGTCAACAGTACT ATGTGATTATACC	Used to insert P _{cp25} promoter in front of <i>disD</i> gene
P19	CGCGCCGAGGCGAGCCCCCTGGCGGGC ACGTCTGTGGCGGCGCGCTCCTCCCCG CGAGCACGTGTTGACAATTAATC	
P20	TGCGTTTGATATCGAGCGATCCGCATG ATAGACGACCCCGCGCTGAACCGAGC ACGTGTTGACAATTAATC	Used to delete <i>orf9</i> gene by insertion of P _{cp25} promoter in front of <i>disD</i> gene

Table S2 related to Figure 3. Target screening analysis data of extracts from *M. xanthus::p15A-dis*.

RT [min]	m/z	Compound	sum formula
4.36	335.16205	Ar001-23-2	C ₁₄ H ₂₇ N ₂ O ₅ S ₁
12.48	384.28846	AS_DK1622_383-1	C ₂₅ H ₃₈ N ₁ O ₂
12.48	384.28846	AS_DK1622_383-2	C ₂₅ H ₃₈ N ₁ O ₂
5.1	631.27543	Cittilin A	C ₃₄ H ₃₉ N ₄ O ₈
12.81	729.37322	Disorazol F2	C₄₂H₅₂N₂O₉
11.58	745.36879	Disorazol A2	C₄₂H₅₃N₂O₁₀
12.24	759.38345	Disorazol A1	C₄₃H₅₅N₂O₁₀
12.24	759.38345	Disorazol A3	C₄₃H₅₅N₂O₁₀
12.24	759.38345	Disorazol A4	C₄₃H₅₅N₂O₁₀
7.77	779.37324	Disorazol B2	C₄₂H₅₅N₂O₁₂
9.49	761.36162	Disorazol B4	C₄₂H₅₃N₂O₁₁
10.04	763.37894	Disorazol 762	C₄₂H₅₄N₂O₁₁
7.44	519.25799	DKxanthen-518	C ₂₉ H ₃₅ N ₄ O ₅
7.8	519.25783	DKxanthen-518	C ₂₉ H ₃₅ N ₄ O ₅
7.18	535.25311	DKxanthen-534	C ₂₉ H ₃₅ N ₄ O ₆
7.54	535.25281	DKxanthen-534	C ₂₉ H ₃₅ N ₄ O ₆
8.07	549.26825	Dkxanthen-548	C ₃₀ H ₃₇ N ₄ O ₆
3.56	183.09128	Marinoquinoline A	C ₁₂ H ₁₁ N ₂
5.36	225.13794	Marinoquinoline B	C ₁₅ H ₁₇ N ₂
5.84	259.12181	Marinoquinoline C	C ₁₈ H ₁₅ N ₂
2.55	197.12852	Mediacompound-Amb-001	C ₁₀ H ₁₇ N ₂ O ₂
3.56	245.12887	Mediacompound-Amb-002	C ₁₄ H ₁₇ N ₂ O ₂
4.01	245.12862	Mediacompound-Amb-003	C ₁₄ H ₁₇ N ₂ O ₂
3.51	211.14406	Mediacompound-Amb-004	C ₁₁ H ₁₉ N ₂ O ₂
13.01	416.31467	Myxalamid A	C ₂₆ H ₄₂ N ₁ O ₃
12.59	402.2989	Myxalamid B	C ₂₅ H ₄₀ N ₁ O ₃
11.84	388.28299	Myxalamid C	C ₂₄ H ₃₈ N ₁ O ₃
13.83	430.33012	Myxalamid-430	C ₂₇ H ₄₄ N ₁ O ₃
5.4	405.16444	Myxochelin A	C ₂₀ H ₂₅ N ₂ O ₇
3.93	404.18101	Myxochelin B	C ₂₀ H ₂₆ N ₃ O ₆
13	624.4456	Myxovirescin A	C ₃₅ H ₆₂ N ₁ O ₈
12.73	622.42858	Myxovirescin B	C ₃₅ H ₆₀ N ₁ O ₈
16.86	632.44647	Myxovirescin C	C ₃₅ H ₆₃ N ₁ Na ₁ O ₇
11.03	642.45472	Myxovirescin Variante KP641	C ₃₅ H ₆₄ N ₁ O ₉
2.3	261.12324	Tyr-Pro Dioxopiperazin	C ₁₄ H ₁₇ N ₂ O ₃
2.41	261.1234	Tyr-Pro Dioxopiperazin	C ₁₄ H ₁₇ N ₂ O ₃

The shadow part are disorazol and its derivatives (in bold in the table).

Table S3 related to Figure 3. NMR data for disA₂ comparison with the natural product.

pos	δ_{H} , mult (<i>J</i> in Hz) Disorazol ¹ A ₂	δ_{H} , mult (<i>J</i> in Hz) Disorazol ² A ₂
3-H	8.34, s br	8.42, s
5-H	6.18, d br (11.7)	6.17, d (11.9)
6-H	6.47, dd (11.7, 11.9)	6.41, m
7-H	7.36, dd (11.9, 15)	7.16, dd (11.4, 14.7)
8-H	5.71, m	5.75, m
9-H	3.66, dd (4.2, 9.9)	3.64, dd (4.4, 9.9)
10-H	4.06, dd (4.2, 9.7)	3.96, dd (4.2, 10.0)
11-H	5.34, dd (9.7, 11.5)	5.28, dd (9.0, 11.2)
12-H	5.86, ddd (5.5, 11, 11)	5.77, m
13-Ha	2.88, m	2.71, m
13-Hb	2.46, ddbr	2.43, dd (3.2, 14.6)
14-H	5.35, dd (2.5, 11)	5.15, m
16-H	3.88, d (7.5)	3.73
17-H	5.64, m	5.74, m
18-H	5.71, m	5.15, m
19-H ₃	1.74, d (1, 6)	1.65
20-H ₃	1.07 ^a , s	0.94 ^a , s
21-H ₃	1.03 ^a , s	0.93 ^a , s
3'-H	8.49, s	8.62, s
5'-Ha	3.11, dd (5.4, 14.9)	2.95, dd (6.0, 14.7)
5'-Hb	2.65, dd (3.8, 14.9)	2.43, dd (3.3, 14.4)
6'-H	4.42, m	4.66, m
7'-H	5.88, dd (9, 15.1)	5.93, dd (9.4, 12.0)
8'-H	6.43, dd (11, 15.1)	6.39, m
9'-H	6.01, dd (11, 11)	6.17, d (11)
10'-H	6.37, dd(11, 11)	6.36, m
11'-H	6.48, dd(11, 11)	6.40, m
12'-H	5.55, ddd (5.5, 11, 11)	5.54, m
13'-Ha	2.88, m	2.72, m
13'-Hb	2.36, m	2.26, m
14'-H	5.35, dd (2.5, 11.6)	5.15, m
16'-H	3.88, d (7.5)	3.72, m
17'-H	5.64, m	5.54, m
18'-H	5.71, m	5.50, m
19'-H ₃	1.74, d	1.65
20'-H ₃	1.02 ^b , s	0.85 ^b , s
21'-H ₃	1.01 ^b , s	0.87 ^b , s

¹NMR data taken in MeOH-*d*₄, ² DMSO-*d*₆ ^{a,b} overlapping signals.

Table S4 Proteins encoded on the recovered plasmid pTn-Rec_IE-2 and their putative function in disorazol biosynthesis (data according to Kopp et al.)

Gene	Size (bp)	Proposed function of the similar protein	Similarity/ Identity
<i>orf1</i> '	522	arylesterase-related protein	29%/ 43%
<i>orf2</i> '	591	SAM- dependent methyl transferase	48%/ 58%
<i>orf3</i> '	1284	putative esterase β -lactamase	35%/ 51%
<i>orf4</i> '	1782	adenylate cyclase	31%/ 51%
<i>orf5</i> '	854	outer membrane protein (incomplete)	36%/ 46%

Genetic inactivation of the disorazol biosynthetic genes

As mentioned earlier, ten PKS modules and one NRPS module are encoded in the genes *disA-C* in the conserved disorazol biosynthetic gene cluster. To confirm that *disA-C* is involved in the biosynthesis of disorazol, the module was inactivated by disrupting the gene, including the PKS modules 1 and 5 and the NRPS module, on the p15A-dis expression construct (Figure 1). A 1100 bp fragment conferring chloramphenicol resistance (cm) to the linker region between these modules was separately inserted into the p15A-dis construct by homologous recombination in *E. coli*. The modified deletion constructs pDisA, pDisB and pDisC were screened using low-salt LB plates plus chloramphenicol and then verified by restriction analysis (Table S1). The successfully modified constructs were then transformed into *M. xanthus* DK1622, and the production profile of positive recombinants was analyzed by HPLC-MS (Figure S6-I).

The mutant strains no longer produced disorazols. The missing peaks indicate that all these modules and genes are vital for the disorazol biosynthetic pathway. Without any one of these genes, no disorazols are produced. It is, however, still possible that the significant changes in the cluster architecture that were caused by the gene inactivation may have affected the expression of the biosynthetic enzymes (Figure S6-II).

Biological evaluation

Cell lines were obtained from the German Collection of Microorganisms and Cell Cultures (*Deutsche Sammlung für Mikroorganismen und Zellkulturen*, DSMZ) or were part of our internal collection and were cultured under conditions recommended by the depositor. Half-inhibitory concentrations (IC₅₀) in terms of growth inhibition were determined as described previously¹. In brief, cells were treated in 96-well plates with serial dilutions of disorazol A₁ and A₂ for 5 d. Cell viability was assessed via tetrazolium salt reduction and average IC₅₀ values were obtained in two independent experiments by sigmoidal curve fitting.

Supplemental references

1. Herrmann, J., Hüttel, S., & Müller R. Discovery and biological activity of new chondramides from *Chondromyces* sp. *ChemBioChem*. **14**, 1573-1580 (2013).

Publication I


Genetic engineering and heterologous expression of the disorazol biosynthetic gene cluster via Red/ET recombineering.


Qiang Tu, Jennifer Herrmann, Shengbiao Hu, Ritesh Raju, Xiaoying Bian, Youming Zhang[†] & Rolf Müller[†]


Author Contributions


Q.T., S.H. and Y.Z. planned and performed cloning experiments. **Q.T.** and X.B. performed genetic transfers, cultivation experiments and data analysis. **Q.T.** and R.R. performed HPLC and compound isolation. R.R. performed NMR experiments and data analysis. J.H. performed biological functional studies. **Q.T.**, Y.Z. and R.M. designed the study and wrote the paper. All authors discussed the results and commented on the manuscript.

Signatures:


Qiang Tu: 

Jennifer Herrmann: 

Shengbiao Hu: 

Ritesh Raju: 

Xiaoying Bian: 

Youming Zhang: 

Rolf Müller: 

II

Room temperature electrocompetent bacterial cells improve DNA transformation and recombineering efficiency.

Qiang Tu^{1,2,4,*}, Jia Yin^{1,3,4,*}, Jun Fu^{1,3}, Jennifer Herrmann², Yuezhong Li¹, Yulong Yin⁴, A. Francis Stewart^{3#}, Rolf Müller^{2#} & Youming Zhang^{1#}

¹Shandong University–Helmholtz Institute of Biotechnology, State Key Laboratory of Microbial Technology, School of Life Sciences, Shandong University, Shanda Nanlu 27, 250100 Jinan, People’s Republic of China.

²Department of Microbial Natural Products, Helmholtz Institute for Pharmaceutical Research Saarland, Helmholtz Centre for Infection Research and Department of Pharmaceutical Biotechnology, Saarland University, Campus E8.1, 66123 Saarbrücken, Germany.

³Department of Genomics, Dresden University of Technology, BioInnovations-Zentrum, Tatzberg 47-51, 01307 Dresden, Germany.

⁴Animal Nutrition and Human Health Laboratory, College of Life Science of Hunan Normal University, 410081 Changsha, People’s Republic of China.

*These authors contributed equally to this work.

#Correspondence and requests for materials should be addressed to A.F.S. (email: francis.stewart@biotec.tu-dresden.de) or R.M. (email: Rolf.Mueller@helmholtz-hzi.de) or Y.M.Z. (email: zhangyouming@sdu.edu.cn)

SCIENTIFIC REPORTS



OPEN

Room temperature electrocompetent bacterial cells improve DNA transformation and recombineering efficiency

Received: 08 December 2015

Accepted: 04 April 2016

Published: 20 April 2016

Qiang Tu^{1,2,4,*}, Jia Yin^{1,3,4,*}, Jun Fu^{1,3}, Jennifer Herrmann², Yuezhong Li¹, Yulong Yin⁴, A. Francis Stewart³, Rolf Müller² & Youming Zhang¹

Bacterial competent cells are essential for cloning, construction of DNA libraries, and mutagenesis in every molecular biology laboratory. Among various transformation methods, electroporation is found to own the best transformation efficiency. Previous electroporation methods are based on washing and electroporating the bacterial cells in ice-cold condition that make them fragile and prone to death. Here we present simple temperature shift based methods that improve DNA transformation and recombineering efficiency in *E. coli* and several other gram-negative bacteria thereby economizing time and cost. Increased transformation efficiency of large DNA molecules is a significant advantage that might facilitate the cloning of large fragments from genomic DNA preparations and metagenomics samples.

Usage of various competent cells in different molecular biology techniques such as cloning, amplification of plasmid DNA, construction of genomic libraries, gene expression, and mutagenesis are the routine procedures in each laboratory. Most commonly and extensively used bacterial strain is the Gram-negative bacterium *Escherichia coli*^{1,2}.

E. coli cells can be made competent by washing with divalent cations such as Ca²⁺ at 0 °C or under ice-cold conditions^{3,4}. However, such metal ion liquids washed competent cells would have lower transformation efficiency than using the electroporation method. In the electroschock methods (electroporation transformation), high-voltage pulse treated *E. coli* cells become exceptionally competent after washing with ice-cold 10% glycerol or water^{4–8}. The high voltage causes the cellular membrane to be transiently permeabilized, allowing the foreign material to enter into the cells⁹. High efficient electrocompetent cells are mainly used in library construction, mutagenesis and recombineering¹⁰. Protocols for electroporating Gram-negative bacteria including *E. coli* have already been described by many researchers^{4–6,9,11,12}. Generally, cells are grown up to a suitable density, harvested, and followed by a series of washes to remove culture medium. Several factors have been identified to cause potential impact on the efficiency of electroporation transformation process. These factors include the electrical field strength, pulse decay time, pulse shape, temperature, type of cell, type of suspension buffer, concentration and size of the nucleic acid to be transferred^{9,13}. According to the methods reported earlier, electrocompetent cell preparation have to be performed at ice-cold temperature and the equipment and washing solutions have to be maintained at the same temperature as well^{14–16}.

Recombineering is now an alternative technology for conventional recombinant DNA engineering, a unique tool for large size DNA engineering, as well as the most appealing method of choice for bacterial genome engineering^{17,18}. There are two main recombineering activities: one is based on linear plus circular homologous

¹Shandong University–Helmholtz Institute of Biotechnology, State Key Laboratory of Microbial Technology, School of Life Sciences, Shandong University, Shanda Nanlu 27, 250100 Jinan, People's Republic of China. ²Department of Microbial Natural Products, Helmholtz Institute for Pharmaceutical Research Saarland, Helmholtz Centre for Infection Research and Department of Pharmaceutical Biotechnology, Saarland University, Campus E8.1, 66123 Saarbrücken, Germany. ³Department of Genomics, Dresden University of Technology, BiInnovations-Zentrum, Tatzberg 47-51, 01307 Dresden, Germany. ⁴Animal Nutrition and Human Health Laboratory, College of Life Science of Hunan Normal University, 410081 Changsha, People's Republic of China. *These authors contributed equally to this work. Correspondence and requests for materials should be addressed to A.F.S. (email: francis.stewart@biotec.tu-dresden.de) or R.M. (email: Rolf.Mueller@helmholtz-hzi.de) or Y.M.Z. (email: zhangyouming@sdu.edu.cn)

recombination (LCHR) initiated by the Red operon from λ phage¹⁹, and the other is the linear plus linear homologous recombination (LLHR) which is initiated by RecE/RecT from Rac phage¹⁷. LCHR is mainly applied to engineer plasmids which includes Bacterial Artificial Chromosome (BAC) while LLHR is primarily applied to linear DNA cloning (PCR cloning)²⁰ and direct cloning¹⁷. Direct cloning is a shortcut for cloning of a large DNA fragments from genomic DNA without library construction and screening. For accomplishing the direct cloning, the DNA segment of interest should meet the linear cloning vector in one cell and then recombine each other. Therefore, the transformation efficiency and homologous recombination efficiency in the RecET proficient cells become the major limitation.

Keeping the cells cold was the pivotal point in the most of the protocols for electroporating Gram-negative bacterial strains including *E. coli* but there was no detailed explanations why this is important¹⁶. However, an improved transformation efficacy in the pathogen *Pseudomonas aeruginosa* when cells were washed at room temperature (RT) had previously been reported²¹. We surprisingly discovered that electrocompetent cells could be prepared at room temperature so that the cooling steps would be omitted. This was really astonishing because the conventional preparation method of electrocompetent cells for Gram-negative bacteria must be performed at 4 °C or preferably at 0–2 °C. Additionally, we found that the efficiency of direct cloning which was mediated by RecET recombineering would be dramatically improved by using the electrocompetent cells prepared at room temperature (named as room temperature competent cells). This astonishing discovery permitted the preparation and distribution of electrocompetent cells at a higher temperature. Here we present a novel DNA transformation method that is simplified, fast, efficient, convenient, and cost effective. This simple procedure does not only improve electroporation transformation efficiency in *E. coli* but also has implications for other bacterial hosts, e.g. *Agrobacterium*²², *Burkholderia*¹³, *Photobacterium*²³ and *Xenorhabdus*²³.

Results

Effect of temperature shift on electrocompetent cells. It was inconvenient to maintain low temperature conditions for preparation, storage and transport of the electrocompetent cells. We intended to test the transformation efficiency of the electrocompetent cells prepared at room temperature. A large plasmid pGB-amp-Ptet-plu1880 (27.8 kb) was transformed into *E. coli* GB2005 strain^{17,24} at various temperature. The warm electrocompetent cells showed 10 times higher transformation efficiency than the cold electrocompetent cells (Fig. 1a). After placing the cold electrocompetent cells at room temperature for 15 minutes, the transformation efficiency increased by 5 folds (Fig. S1a). In contrast, after the room temperature electrocompetent cells were placed on ice for 15 minutes before electroporation, there was a significant decrease in transformation efficiency (Fig. S1b).

The room temperature in our laboratory was set at 24 °C. To determine the range of optimum temperature for the preparation of competent cells, we prepared the cells at different temperature ranges and revealed that the best temperature for electrocompetent cell preparation was in the range of 24–28 °C (Fig. S2).

Effect of different plasmids on electrocompetent cells. Plasmids were varied in the size, selection marker and origins of replication. Initially we tested three plasmids with different sizes. Two of them were p15A origin plasmids with ampicillin (amp) or chloramphenicol (cm) resistance. Another one was a pBR322 origin based plasmid with ampicillin resistance. All the plasmids gained higher transformation efficiency with room temperature electrocompetent cells (Fig. 1b, column 1–3). We also tested BAC vectors with different size and selection markers. All BACs gained higher transformation efficiency when room temperature electrocompetent *E. coli* GB2005 cells were used (Fig. 1b, column 4–6). These results indicated that for electrocompetent transformation, room temperature electrocompetent cells were more efficient than cold electrocompetent cells irrespective of their size, selection marker and origins of replication. Therefore the room temperature electrocompetent cells could be a better candidate for gene cloning, construction of DNA libraries and mutagenesis than cold electrocompetent ones.

Effect of different strains on electrocompetent cells. The *E. coli* GB2005 was an optimized strain for plasmid transformation and propagation^{17,25}. Along with this strain, several other commonly used *E. coli* strains were also tested for room temperature transformation as well. Results revealed that although different *E. coli* strains varied in their relative transformation efficiencies, all of them exhibited higher transformation efficiency when their electrocompetent cells were prepared at room temperature (Fig. 1c). We also tested the improving approach in a few of other Gram-negative bacterial strains. *Burkholderia glumae* PG1 was an industrial strain for detergent lipase production²⁶, which could also be the heterologous host used for PKS/NRPS gene clusters expression (unpublished data). An oriV origin plasmid pRK₂-apra-kan based on plasmid pBC301^{27,28}, was utilized for transformation. When PG1 competent cells were prepared at room temperature, the electroporation efficiency of RK₂ plasmid was around three times higher than the cells prepared on ice (Fig. S3a). Other Gram-negative bacterial strains, such as *Agrobacterium*²², *Burkholderia*¹³, *Photobacterium*²³ and *Xenorhabdus*²³, were tested for RK₂ plasmid transformation by using room temperature and cold temperature protocols. All the results indicated that room temperature competent cells had higher transformation efficiency than cold competent cells (Fig. S3b).

Improvement of recombineering by using room temperature electrocompetent cells.

The plasmid transformation efficiency significantly increased by room temperature electrocompetent cells was not the destination. It was necessary to evaluate the improvement of the room temperature protocol on lambda Red or Rac RecET mediated recombineering. A simple assay using a PCR product of linear vector (p15A ori plus cm or pBR322 ori plus cm) and a PCR product with kanamycin (kan) was built to test LLHR efficiency¹⁷. *E. coli* strain GB05-dir with *recET* on its chromosome was used for LLHR test²⁵. The results showed that LLHR in room temperature competent cells was 6–10 times more efficient than the cells prepared on ice. Both p15A origin and

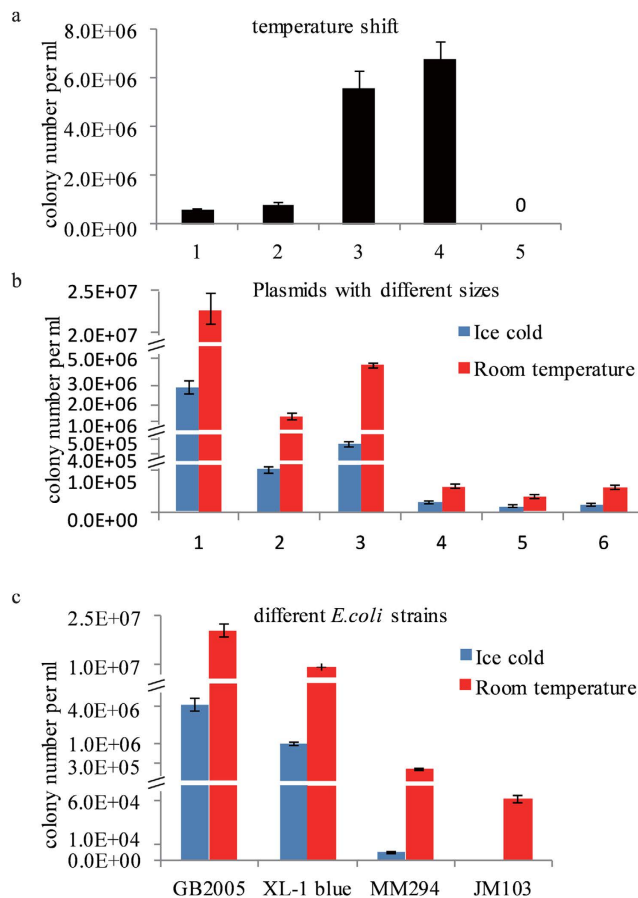


Figure 1. Transformation efficiency of competent cells. (a) Effect of temperature, *E. coli* GB2005 cells transformed by $\sim 0.1 \mu\text{g}$ of pGB-amp-Ptet-plu1880 (27.8 kb) were plated on Amp plates. 1, the normal ice-cold method for preparing electrocompetent cells; 2, as for 1 but the cells were kept on ice for 15 min before electroporation; 3, as for 1 but the cells were placed at room temperature (RT) for 15 min before electroporation; all cuvettes were used at RT; 4, every step was done at RT; 5, no plasmid DNA. (b) RT prepared cells were transformed with different plasmids. 1, pBR322 origin with ampicillin resistance (27.8 kb); 2, p15A origin with chloramphenicol resistant (54.7 kb); 3, p15A origin with ampicillin resistance (54.7 kb); 4, BAC with chloramphenicol resistant (>120 kb); 5, BAC with kanamycin resistant (91.7 kb); 6, BAC with ampicillin resistant (91.7 kb). (c) Different *E. coli* strains tested for electroporation transformation. Cells were transformed by $0.1 \mu\text{g}$ of pGB-amp-Ptet-plu1880 and plated on Amp plates. Error bars, SD; $n = 3$.

pBR322 origin plasmids gained the same fold increase (Fig. 2a,b). A direct cloning experiment to fish out the thailandepsin gene cluster (~ 39 kb) from *Burkholderia thailandensis* had been performed, around 150 colonies were obtained by using cold electrocompetent cells, but by using room temperature electrocompetent cells more than 600 colonies were obtained. This improvement leads to a higher chance to clone large DNA fragments from genomic DNA pools directly.

PCR cloning is a routine exercise in every molecular biology laboratory²⁰. It is thus our interest to find out an easy and inexpensive way to clone PCR products. Since the electrocompetent cells prepared at room temperature improves the LLHR efficiency around 10 folds, it is essential to find out the minimum homology sequences needed for LLHR. Previously, we identified 20 bp as the minimum length of sequence homology required for recombineering^{29,30}. To test whether the minimal length could be further shortened, pBAD24 vector was digested with EcoR I/Hind III as linear recipient, and PCR product cassette (Tn5-neo) flanked with short homology arms to the ends of digested pBAD24 vector was used as linear donor fragment (Fig. S4). Seven PCR products with different sizes of homology arms (HA) were designed to test the LLHR efficiency. Results revealed that only 8 bp of terminal homology was sufficient via room temperature protocol (Fig. S5). When ice-cold cells were used, the minimum homology arms required for recombineering were found 12 bp. These data indicated that LLHR might be used to generate a kit for PCR product or small DNA fragment cloning by using homology arms as short as 8 bp.

In contrast to the LLHR experiment, LCHR efficiency was not increasing in the room temperature protocol when compared to the cold protocol (Fig. 2c). However, we discovered that LCHR efficiency would be significantly raised when freshly prepared cold electrocompetent cells were placed at room temperature for 3 minutes (Fig. 2d), suggesting that transient swelling of the cells had a beneficial effect.

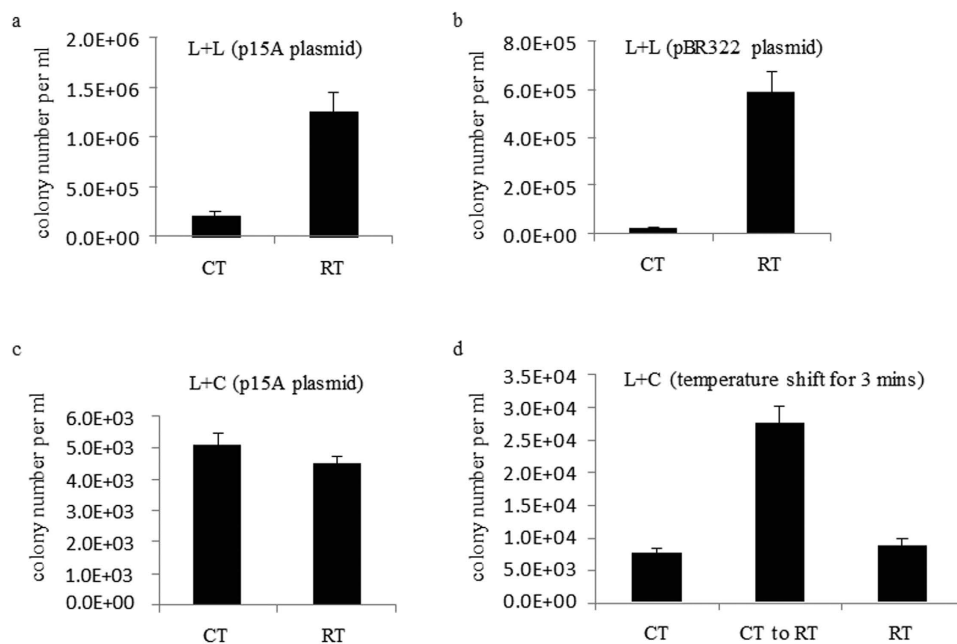


Figure 2. Recombineering using room temperature electrocompetent cells. (a) Colony number of a standard LLHR assay¹⁷ in GB05-dir from the normal and the cold method in *E. coli*. (b) As for A, but with pBR322 origin. (c) As for A, but with a standard LCHR assay in GB05-red. (d) The electrocompetent cells were prepared on ice first. After adding PCR product kan cassette into the ice-cold electrocompetent cells, the cells plus DNA mixture were shifted to RT for 3 minutes before electroporation (middle column). CT, Cold temperature; RT, Room temperature. Error bars, SD; n = 3.

Stability of room temperature electrocompetent cells. Normally, after 2.5–3.0 hours cultivation at 37 °C, *E. coli* GB2005 reached OD₆₀₀ 0.4–0.6 which was in the log phase, the period with the best transformation efficiency of the cells. When bacterial cells were overgrown, the transformation efficiency dropped down (Fig. S6a), and the transformation efficiency of the cold electrocompetent cells was completely lost after 4 hours or 6 hours (only 18 and 5 colonies respectively) (Fig. S6a). But room temperature electrocompetent cells still kept relatively high efficiency even after 4 or 6 hours cultivation. *E. coli* GB2005 cultured for 4 hours at 37 °C reached OD₆₀₀ 1.0~1.2 and cultured for 6 hours reached OD₆₀₀ > 1.8 which was at the plateau phase. It was noteworthy that over-grown or even overnight cultured bacterial cells could still be used for transformation when room temperature protocol was used for preparing competent cells.

To predigest the transformation process, we had tested whether the recovery step could be omitted. For simple plasmid transformation, the recovery step could be omitted when the electrocompetent cells were prepared by using room temperature protocol (Fig. S6b). Although the transformation efficiency in the un-recovery room temperature group was around 30% less than in the recovery room temperature group, it was still at least 5 times higher comparing to the cold temperature group, either recovery or not. Results suggested that plasmid or ligation transformation could be performed in a few minutes after electroporation by using room temperature competent cells. Previous results concluded that the room temperature electrocompetent cells had much better transformation efficiency than cold electrocompetent cells. Furthermore we wanted to know how long the competent cells could stay at room temperature without any significant loss of transformation efficiency. Results showed that room temperature competent cells lost around 30% efficiency after 1 hour storage at room temperature, around 60% lost after 4 hours and around 80% lost after one day (Fig. S7). These results indicated that the room temperature competent cells lost their transformation efficiency to the maximum when stored in room temperature more than one day. To avoid this efficiency loss, room temperature competent cells were prepared by using 10% glycerol¹¹ and dried by vacuum and stored at 4 °C till three days. Result showed that dried room temperature competent cells prepared in 10% glycerol lost their 55% efficiency as compared to the room temperature competent cells without dry (Table S2). But interestingly, the dried competent cells prepared in 10% glycerol could keep the LLHR efficiency up to 3 days without any further efficiency loss (Table S3). This ability gives us an opportunity in the future to deliver the competent cells in routine cooling pack, which is easier and cost effective.

Electron microscopy analysis of competent cells. To find the reasons of higher efficiency in room temperature protocol, electron microscopy was used for comparative analysis of the morphological shapes of cold competent cells and room temperature competent cells of *E. coli*. Their comparative analysis showed that cold competent cells appeared to shrink more than room temperature cells, and the surface of room temperature competent cells was found smoother (Fig 3a–d). Shrunken cells might be more difficult to transform, and the bacterial cell membrane and wall could be more permeable for foreign DNA entry at a higher temperature. Additionally, it may be difficult for the shrunken cells to form pores that allow DNA transfer through the cell membrane under

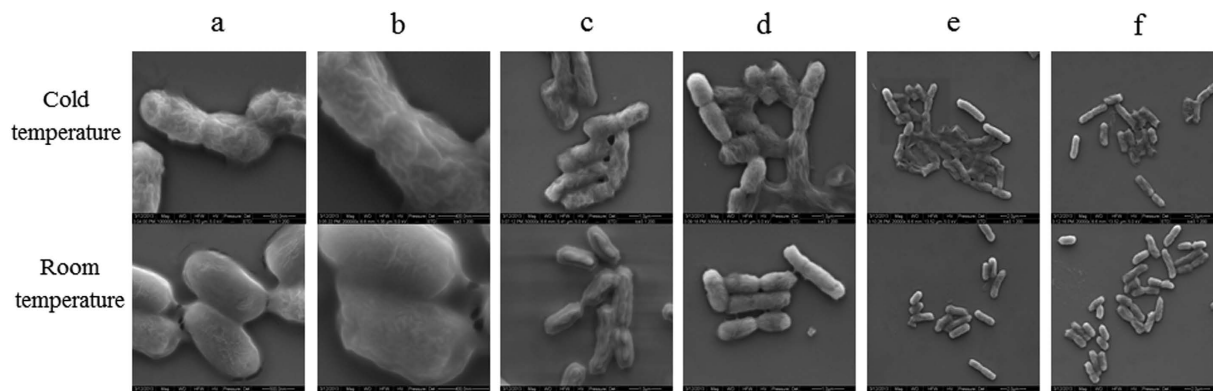


Figure 3. Phenotypes of the cells by room temperature and cold protocols and also electroporated the cells for subsequent analysis by electron microscopy. (a–d): micrograph of the cells washed with cold and room temperature protocols with different magnifications. (e–f): micrograph of the electroporated cells mixture with episomal insertion DNA.

electroporation conditions, and after electroporation most of the cold competent cells were found to be lysed. (Fig. 3e,f). From this we assume that the bacterial cell membrane/cell wall might have better permeability for foreign material to enter into the cell.

Discussion

The ability to introduce exogenous DNA molecules into the cells plays key role in the development of molecular biology techniques, such as mutagenesis and genetic engineering of microorganisms. Several methods have been reported to introduce exogenous DNA molecules into the cells which includes chemical treatment, electroporation, utilization of a biolistic gun, polyethylene glycol, ultrasound, microwave, and hydrogel³¹. In those methods, electroporation has been often demonstrated to be more efficient and convenient way to transform a large number of microorganisms used for genetic studies³², and many efforts have been performed to increase its efficiency^{33–36}.

The phage-derived homologous recombination systems have been developed into very useful DNA engineering technologies, well known as recombineering which has also been performed in electrocompetent cells^{10,20}. This suggests that a crucial step in recombineering is the transformation of *E. coli* by electroporation.

In conventional electroporation transformation, the electrocompetent cells were prepared on ice and the other supplies were also in cold environment, including pre-chilled cuvette, buffer, and centrifuge. The cells must be repeatedly washed before electroporation to remove conductive solutes. If the conductivity of a cell mixture is too high, then arcing will occur during electroporation, which will ruin the experiment. The washing process can elicit a stress response that can lead to decrease in transformation efficiency. If the cells are kept at 4 °C then they are inactive and this stress response is prevented. However, current studies reveals that the electroporation transformation efficiency is decreased at ice-cold temperature (Fig. 1). This decreased efficiency might be due to ice cold temperature which alters the cell membrane topology. The cell membrane mainly consists of phospholipids and proteins³⁷ and the phospholipid bilayer forms a stable barrier between two aqueous compartments. Embedded proteins of phospholipid bilayer carry out the specific functions of the plasma membrane, including the selective transportation of molecules across the membrane and cell-cell recognition³⁸. At ice-cold temperature, the fatty acid tails of the phospholipids become more rigid. This affects the fluidity, permeability, and the cell's ability to live³⁹. Therefore, cold temperatures may be not favourable for the survival and thus decreases the transformation efficiency. Additionally, during electroporation process due to externally applied electric field there is a significant increase in the permeability of cell's plasma membrane, which is used to introduce exogenous DNA into bacterial cell³². Previous reports revealed that if the environmental conditions were changed, including the temperature, the cell membranes undergoes a gross morphological changes⁴⁰. These structural perturbations were associated with characteristic disturbances of functions such as loss of selective permeability. Similar results were observed in this study that cold competent cells were appeared to shrink more than room temperature cells, and additionally more cold competent cells were found lysed after electroporation (Fig. 3).

The temperature effects on electroporation transformation could be explained by thermal effects during electro pore formation^{41–43}. According to the electroporation theory, hydrophobic pores in the cell membrane were formed spontaneously by lateral thermal fluctuations of the lipid molecules³⁹, which suggested that hydrophobic pores formation would be enhanced by increased temperature conditions. To improve recombination efficiency many parameters had been described previously^{17,44,45} except the transformation efficiency. This study showed that LLHR efficiency in room temperature competent cells was higher than in the same cells prepared on ice (Fig. 2a,b), but the room temperature protocol did not increase LCHR efficiency when compared to the cold protocol (Fig. 2c). The Red recombinases (Red alpha and beta) might be not stable while preparing the competent cells at room temperature.

In conclusion, this study reports an unexpected finding, that is contrary to common assumption, that it is better to prepare bacterial cells at room temperature than on ice for electroporation. In addition, this study also

shows that this is not only efficient for *E. coli* but also for several other gram-negative and gram-positive hosts. However, further research will be essential to confirm the transfer and principle of membrane in competent cells.

Methods

Strains, plasmids and reagents. The bacterial strains and plasmids used in this study were listed in Table S1. The antibiotics were purchased from Invitrogen. *E. coli*, *Agrobacterium*, *Photobacterium* and *Xenorhabdus* were cultured in Luria–Bertani (LB) broth or on LB agar plates (1.2% agar) with ampicillin [*amp*] (100 µg/mL), kanamycin [*kan*] (15 µg/mL) or chloramphenicol [*cm*] (15 µg/mL) as required. *Burkholderia glumae* PG1 was cultured in MME medium (5 g/L K₂HPO₄, 1.75 g/L Na(NH₄)HPO₄ × 4H₂O, 1 g/L Citrate, 0.1 g/L MgSO₄ × 7H₂O, 8 g/L Glucose, pH7.0). *Burkholderia* DSM7029 was cultured in CYCG medium (6g/L Casitone, 1.4g/L CaCl₂ × 2H₂O, 2g/L Yeast extract and 20 ml/L Glycerol).

Preparation of electrocompetent cell at cold and room temperature conditions. The electrocompetent cells at cold temperature were prepared according to the protocol established previously in our lab⁴⁶. For electrocompetent cells at room temperature, overnight culture were diluted into 1.4 mL LB medium and again cultured at 37 °C at 900 rpm in an Eppendorf ThermoMixer. After 2 hours of incubation when OD₆₀₀ was approximately reached up to 0.6, the bacterial cells were centrifuged at 9000 rpm at room temperature (24 °C). The supernatant was then discarded and the cells were resuspended in 1 mL of dH₂O at room temperature, and washing step was repeated. The bacterial cells were again resuspended in about 30 µl of dH₂O (24 °C) and the tubes were placed at room temperature. 300 ng of the each plasmid DNA or PCR products were added into the prepared cells. The DNA-cell mixture were then transferred into 1 mm-gap cuvette (24 °C) for electroporation at 1250 volts. The cuvette was then flushed with 1 ml fresh medium and the cells were recovered by the incubation at 37 °C for 1 hour. In the end, the culture was streaked on the LB plates containing appropriate antibiotics.

Preparation of electrocompetent cell to test the effect of different temperature range. *E. coli* GB2005 strain was cultured at 37 °C till OD₆₀₀ was reached at 0.6. The cells were pelleted and washed by dH₂O at different temperature range (2, 15, 20, 22, 24, 26, 28, 30, 32, 34 and 37 °C). The cuvettes were also kept at these temperatures. After electroporation with pGB-amp-Ptet-plu1880 plasmid, 1 ml LB was added into the cuvette to recover the transformed cells and then incubated at 37 °C. After 1 hour incubation 0.004 µl of cells (diluted by fresh LB) were streaked on LB plates containing ampicillin (100 µg/mL). The colonies were counted after 24 hours of cultivation.

Recombineering assays. In LCHR assay we used a 2 kb p15A-cm plasmid carrying the chloramphenicol resistance gene and a 2 kb kan-PCR product carrying the kanamycin resistance gene. Each end of the kan-PCR product had a 50-bp homology arm to the p15A-cm plasmid between the chloramphenicol gene (cm) and the p15A origin. The circular plasmid (200 ng) and the PCR product (200 ng) were co-electroporated into *E. coli* GB2005 expressing the lambda Red recombinase to generate the chloramphenicol plus kanamycin-resistant plasmid p15A-cm-kan (4 kb). The expression plasmid was pSC101-BAD-gbaA-tet. The recombinants were selected on LB plates with double antibiotic selection.

One of LLHR assays was just like above mentioned setup except the p15A-cm plasmid was linearized between the two 50-bp homology arms. The linear plasmid backbone (200 ng) and the kan-PCR product (200 ng) were co-electroporated into *E. coli* GB2005 expressing the *recET* recombinase to generate the plasmid p15A-cm-kan. Another LLHR assay used EcoR I and Hind III digested 4.5 kb pBAD24 plasmid (450 ng) and 1.7 kb Tn5-neo PCR (170 ng) to generate the ampicillin plus kanamycin-resistant plasmid pBAD24-neo (6.2 kb). The expression plasmid was pSC101-BAD-ETgA-tet. The recombinants were selected on LB plates with double antibiotic selection.

Both kan-PCR and Tn5-neo-PCR were amplified from suicide R6K plasmid to avoid the selection background from the carryover of the PCR template (any residual circular plasmid). The negative control with DNA electroporation into uninduced cells was done to indicate the sufficient selection pressure. After colony counting, 8 clones from each of the triplicate experiments were picked up for plasmid DNA preparation and restriction analysis to prove the successful accomplishment of the recombineering experiment.

Preparation of dried room temperature electrocompetent cell. The electrocompetent cells were washed twice with dH₂O or 10% glycerol at room temperature, cells were pelleted once again and remaining dH₂O or 10% glycerol was removed by pipetting. Cell pellet was dried under the vacuum for 30 min and stored at 4 °C. For transformation, dried cells were resuspended in 25 µL dH₂O (without glycerol) at room temperature and DNA was added into the cells. Cells and DNA were electroporated at 1250 v by using 1 mm-gap electroporation cuvette and Eppendorf electroporator as usual.

Cells preparations for Electron Microscope. *E. coli* cells were harvested by centrifugation and were fixed in 2% paraformaldehyde/1% glutaraldehyde for 20 min at room temperature. After repeated washing with ultrapure water the cell pellet was resuspended and a small aliquot of the samples in water was placed on a silicon waver and was dried under ambient conditions. Next, the *E. coli* cells were investigated with secondary electrons under high-vacuum conditions in an ESEM type FEI Quanta400 FEG at 5 kV accelerating voltage.

References

1. Cohen, S. N., Chang, A. C. Y. & Hsu, L. Nonchromosomal antibiotic resistance in bacteria: genetic transformation of *Escherichia coli* by R-Factor DNA. *Proc. Natl. Acad. Sci. USA* **69**, 2110–2114 (1972).
2. Cohen, S. N., Chang, A. C., Boyer, H. W. & Helling, R. B. Construction of biologically functional bacterial plasmids *in vitro*. *Proc. Natl. Acad. Sci. USA* **70**, 3240–3244 (1973).

3. Hanahan, D. Studies on transformation of *Escherichia coli* with plasmids. *J. Mol. Biol.* **166**, 557–580 (1983).
4. Hanahan, D., Jessee, J. & Bloom, R. B. Plasmid transformation of *Escherichia coli* and other bacteria. *Methods Enzymol.* **204**, 63–113 (1991).
5. Dower, W. J., Miller, J. F. & Ragsdale, C. W. High efficiency transformation of *E. coli* by high voltage electroporation. *Nucleic Acids Res.* **16**, 6127–6145 (1988).
6. Fiedler, S. & Wirth, R. Transformation of bacteria with plasmid DNA by electroporation. *Anal. Biochem.* **170**, 38–44 (1988).
7. Taketo, A. DNA transfection of *Escherichia coli* by electroporation. *Biochim. Biophys. Acta* **949**, 318–324 (1988).
8. Sambrook, J. & Russell, D.W. *Molecular Cloning: A Laboratory Manual*. 3rd ed, Vol. 1 & 3 (Cold Spring Harbor Laboratory Press, New York, 2001).
9. Andreason, G. L. & Evans, G. A. Introduction and expression of DNA molecules in eukaryotic cells by electroporation. *Biotechniques* **6**, 650–660 (1988).
10. Zhang, Y., Buchholz, F., Muyrers, J. P. P. & Stewart, A. F. A new logic for DNA engineering using recombination in *Escherichia coli*. *Nat. Genet.* **20**, 123–128 (1998).
11. Nikoloff, J.A. Animal cell electroporation and electrofusion protocols. *Methods in molecular biology*, Vol. 48 (Humana Press, Totowa, New Jersey, 1995).
12. Harlander, S.K. Transformation of *Streptococcus lactis* by electroporation. In: Ferretti J. J., Curtiss III R. (eds), *Streptococcal Genetics*, pp 229–233 (ASM Press, Washington DC, 1987).
13. Oka M. *et al.* Glidobactins A, B and C, new antitumor antibiotics. II. Structure elucidation. *J. Antibiot.* **41**, 1338–1350 (1988).
14. Aune, T. E. V. & Aachmann, F. L. Methodologies to increase the transformation efficiencies and the range of bacteria that can be transformed. *Appl. Microbiol. Biot.* **85**, 1301–1313 (2010).
15. Yoshida, N. & Sato, M. Plasmid uptake by bacteria: a comparison of methods and efficiencies. *Appl. Microbiol. Biot.* **83**, 791–798 (2009).
16. Chassy, B. M. & Flickinger, J. L. Transformation of *Lactobacillus casei* by electroporation. *FEMS Microbiol. Lett.* **44**, 173–177 (1987).
17. Fu, J. *et al.* Full-length RecE enhances linear-linear homologous recombination and facilitates direct cloning for bioprospecting. *Nat. Biotechnol.* **30**, 440–446 (2012).
18. Thomason, L. *et al.* Recombineering: genetic engineering in bacteria using homologous recombination. *Curr. Protoc. Mol. Biol.* Section V. **1** 16.1–1.16.24 (2007).
19. Maresca, M. *et al.* Single-stranded heteroduplex intermediates in lambda Red homologous recombination. *BMC Mol. Biol.* **29**, 11–54 (2010).
20. Zhang, Y., Muyrers, J. P. P., Testa, G. & Stewart, A. F. DNA cloning by homologous recombination in *Escherichia coli*. *Nat Biotechnol.* **18**, 1314–1317 (2000).
21. Liang, R. & Liu, J. Scarless and sequential gene modification in *Pseudomonas* using PCR product flanked by short homology regions. *BMC Microbiol.* **10**, 209–209 (2010).
22. Hu, S. *et al.* Genome engineering of *Agrobacterium tumefaciens* using the lambda Red recombination system. *Appl. Environ. Microbiol.* **98**, 2165–2172 (2014).
23. Yin, J. *et al.* A new recombineering system for *Photobacterium* and *Xenorhabdus*. *Nucleic Acids Res.* **43** (6), e36 (2015).
24. Bian, X., Plaza, A., Zhang, Y. & Müller, R. Luminmycins A–C, cryptic natural products from *Photobacterium luminescens* identified by heterologous expression in *Escherichia coli*. *J. Nat. Prod.* **75** (9), 1652–1655 (2012).
25. Bian, X. *et al.* Direct cloning, genetic engineering, and heterologous expression of the syringolin biosynthetic gene cluster in *E. coli* through Red/ET recombineering. *ChemBioChem* **13**, 1946–1952 (2012).
26. Frenken, L. G. *et al.* Cloning of the *Pseudomonas glumae* lipase gene and determination of the active site residues. *Appl. Environ. Microbiol.* **58**, 3787–3791 (1992).
27. Xiang, C., Han, P., Lutziger, I., Wang, K. & Oliver, D. A mini binary vector series for plant transformation. *Plant Mol. Biol.* **40**, 711–717 (1999).
28. Yang. Functional Modulation of the Geminivirus AL2 Transcription Factor and Silencing Suppressor by Self-Interaction. *J. Virol.* **81**, 11972–11981 (2007).
29. Erler, A. *et al.* Conformational adaptability of Red β during DNA annealing and implications for its structural relationship with Rad52. *J. Mol. Biol.* **391**, 586–598 (2009).
30. Yin, J. *et al.* Direct cloning and heterologous expression of the salinomycin biosynthetic gene cluster from *Streptomyces albus* DSM41398 in *Streptomyces coelicolor* A3(2). *Sci. Rep.* **5**, 15081 (2015).
31. Singh, M., Yadav, A., Ma, X. & Amoah, E. Plasmid DNA Transformation in *Escherichia Coli*. Effect of Heat Shock Temperature, Duration, and Cold Incubation of CaCl₂ Treated Cells. *International Journal of Biotechnology and Biochemistry* **6**, 561–568 (2010).
32. Miller, J. F., Dower, W. J. & Tompkins, L. S. High-voltage electroporation of bacteria: genetic transformation of *Campylobacter jejuni* with plasmid DNA. *Proc. Natl. Acad. Sci. USA* **85**, 856–860 (1988).
33. Nováková, J., Izsáková, A., Grivalský, T., Ottmann, C. & Farkašovsky, M. Improved method for high-efficiency electrotransformation of *Escherichia coli* with the large BAC plasmids. *Folia Microbiol.* **59**, 53–61 (2014).
34. Cui, B., Smooker, P. M., Rouch, D. A. & Deighton, M. A. Enhancing DNA electro-transformation efficiency on a clinical *Staphylococcus capitis* isolate. *J. Microbiol. Meth.* **109**, 25–30 (2015).
35. Welker, D. L., Hughes, J. E., Steele, J. L. & Broadbent, J. R. High efficiency electrotransformation of *Lactobacillus casei*. *FEMS Microbiol. Lett.* **362**, 1–6 (2015).
36. Ma, Z., Liu, J., Shentu, X., Bian, Y. & Yu, X. Optimization of electroporation conditions for toyocamycin producer *Streptomyces diastatochromogenes* 1628. *J. Basic Microb.* **54**, 278–284 (2014).
37. Singer, S. J. The structure and function of membranes—A personal memoir. *J. Membrane Biol.* **129**, 3–12 (1992).
38. GM, C. Structure of the Plasma Membrane. 2 edn, (Sinauer Associates, 2000).
39. Kandušer, M., Šentjurc, M. & Miklavčič, D. The temperature effect during pulse application on cell membrane fluidity and permeabilization. *Bioelectrochemistry* **74**, 52–57 (2008).
40. Quinn. A lipid-phase separation model of low-temperature damage to biological membranes. *Cryobiology* **22**, 128–146 (1985).
41. Weaver, J. C. & Chizmadzhev, Y. A. Theory of electroporation: A review. *Bioelectrochem. Bioenerg.* **41**, 135–160 (1996).
42. Kotnik, T. & Miklavčič, D. Theoretical evaluation of the distributed power dissipation in biological cells exposed to electric fields. *Bioelectromagnetics* **21**, 385–394 (2000).
43. Pavlin, M., Kotnik, T., Miklavčič, D., Kramar, P. & Maček Lebar, A. In *Advances in Planar Lipid Bilayers and Liposomes* Vol. 6 (ed Leitmannova Liu) 165–226 (Academic Press, 2008).
44. Gray, M. & Honigberg, S. M. Effect of chromosomal locus, GC content and length of homology on PCR-mediated targeted gene replacement in *Saccharomyces*. *Nucleic Acids Res.* **29**, 5156–5162 (2001).
45. Cobb, R. E. & Zhao, H. Direct cloning of large genomic sequences. *Nat. Biotechnol.* **30**, 405–406 (2012).
46. Fu, J., Teucher, M., Anastassiadis, K., Skarnes, W. & Stewart, A. F. In *Methods in Enzymology* Vol. 477 (eds M., Wassarman Paul & M., Soriano Philippe) 125–144 (Academic Press, 2010).

Acknowledgements

This research was supported by the funding of Y. Z. from the Recruitment Program of Global Experts and Shandong Innovation and Transformation of Achievements Grant (2014ZZCX02601) and the Program of Introducing Talents of Discipline to Universities (B16030), funding of R.M. from the Deutsche Forschungsgemeinschaft (DFG) and the Bundesministerium für Bildung und Forschung (BMBF), funding of A. F. S. from the TUD Elite University Support the Best program, funding of J. F. from the International S&T Cooperation Program of China (ISTCP 2015DFE32850) and National Natural Science Foundation of China (31570094), funding of J. Y. from China/Shandong University International Postdoctoral Exchange Program and China Postdoctoral Science Foundation (2015M582081). The authors acknowledge Mr. Nazeer Abbasi's help in proofreading this manuscript and Dr. Marcus Koch for ESEM scanning.

Author Contributions

Q.T. and J.Y. participated in the design of this study, performed data collection analysis, and drafted the manuscript; J.F, J.H, Y.L. and Y.Y. participated in interpretation data; A.F.S. and R.M. gave the advice for experimental design and discussed the data, also helped in the revision of the final manuscript. Y.Z. designed and oversaw the study, performed data interpretation and drafted the manuscript. All authors read and approved the final manuscript.

Additional Information

Supplementary information accompanies this paper at <http://www.nature.com/srep>

Competing financial interests: The authors declare no competing financial interests.

How to cite this article: Tu, Q. *et al.* Room temperature electrocompetent bacterial cells improve DNA transformation and recombineering efficiency. *Sci. Rep.* **6**, 24648; doi: 10.1038/srep24648 (2016).



This work is licensed under a Creative Commons Attribution 4.0 International License. The images or other third party material in this article are included in the article's Creative Commons license, unless indicated otherwise in the credit line; if the material is not included under the Creative Commons license, users will need to obtain permission from the license holder to reproduce the material. To view a copy of this license, visit <http://creativecommons.org/licenses/by/4.0/>

Supplemental Information

Room temperature electrocompetent bacterial cells improve DNA transformation and recombineering efficiency

Qiang Tu, Jia Yin, Jun Fu, Jennifer Herrmann, Yuezhong Li, Yulong Yin, A. Francis Stewart, Rolf Müller and Youming Zhang

Inventory of Supplemental Information

Supplemental data

Figure S1. Temperature shift effect on the competent cells for transformation. On Page 5.

Figure S2. Effect of different temperature on electrocompetent cells. On Page 5.

Figure S3. Transformation efficiency comparison of warm and cold temperature in different gram-negative strains. On Page 6.

Figure S4. Diagram of LLHR by using short homology arms. On Page 7.

Figure S5. Effect of the length of homology arms on room temperature electrocompetent cells (warm cells). On Page 7.

Figure S6. Effect of over-grown cells on transformation efficiency and electroporation without recovery step. On Page 8.

Figure S7. Stability of room temperature electrocompetent cells stored at room temperature. On Page 8.

Table S1 Strains and plasmids.

Table S2 Transformation efficiency (colonies on plates with ampicillin ($\times 10^4$)) using cells prepared in dH₂O or 10% glycerol. On Page 9.

Table S3 LLHR efficiency (colonies on plates with ampicillin and kanamycin) using cells prepared in dH₂O or 10% glycerol. On Page 9.

Supplemental references

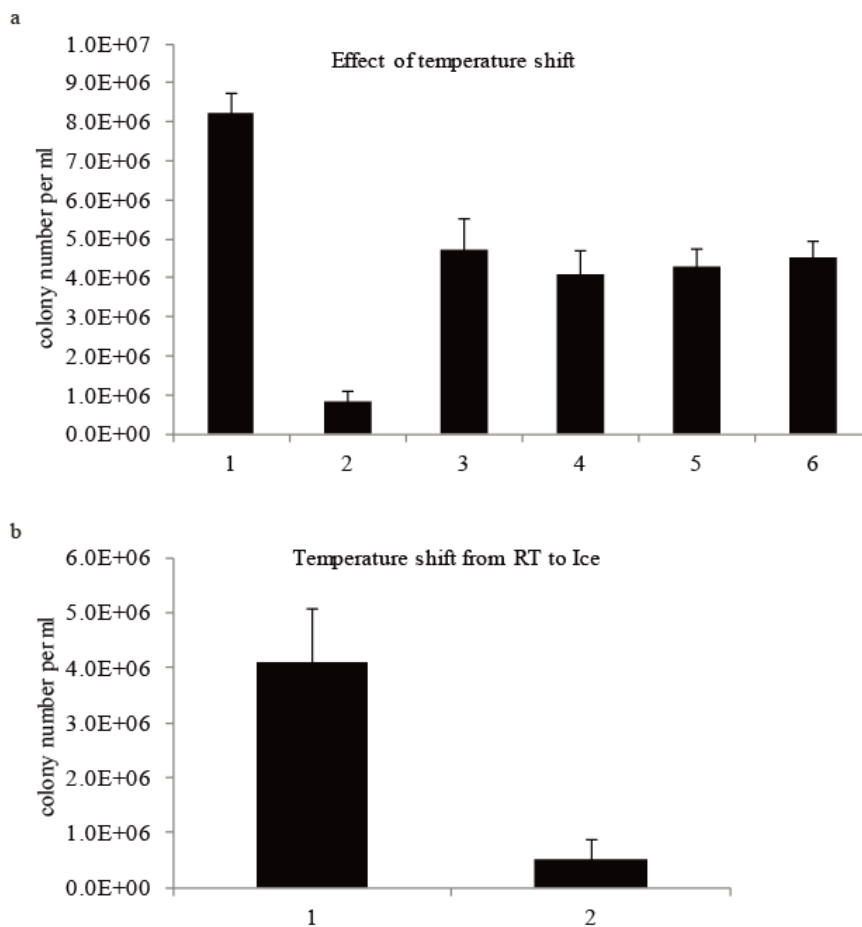


Figure S1. Temperature shift effect on the competent cells for transformation. (a) GB2005 cells transformed by $\sim 0.1\mu\text{g}$ of pGB-Ptet-plu1880 (27.8kb) and plated on Amp plates. 1 -cells prepared at RT; 2 -cells prepared on ice; 3 -cells prepared on ice first then left at RT for 2.5min before electroporation; 4 -same as 3 but at RT for 4min; 5 -same as 4 but at RT for 10min; 6 -same as 3 but at RT for 15min. (b) 1 -cells prepared at RT; 2 -cells prepared at RT, then placed on ice for 15min before electroporation. Error bars, SD; $n = 3$.

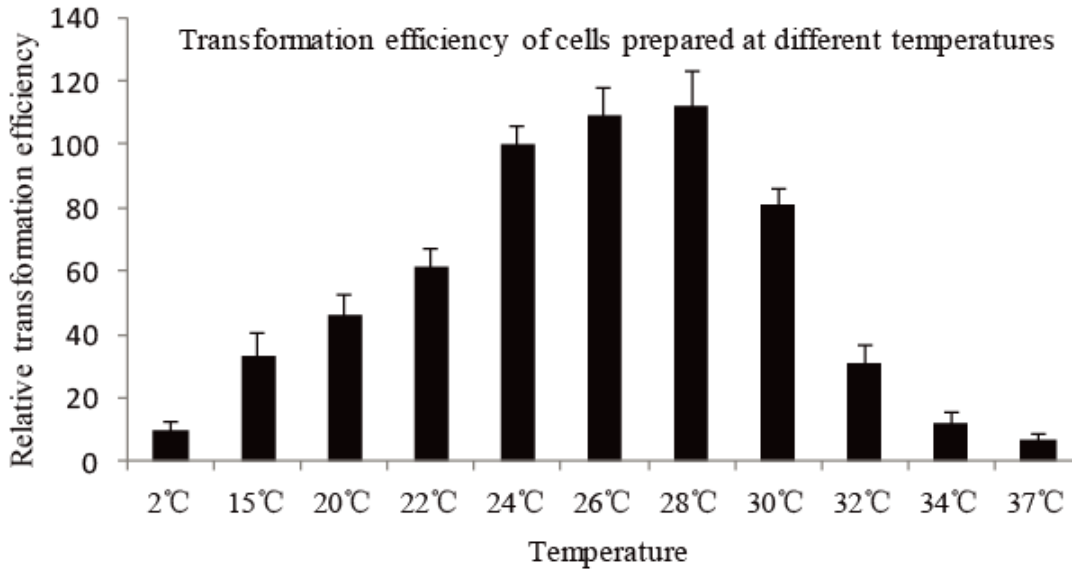


Figure S2. Effect of different temperature on electrocompetent cells. GB2005 cells were transformed by ~0.1µg of pGB-Ptet-plu1880 (27.8kb) and plated on Amp plates. Ice to 37°C were used for preparing competent cells and electroporation. It shows the results in relative transformation efficiency using the transformants at 24°C (room temperature) as standard (100%). Transformants from different temperatures were divided by standard to give the relative transformation efficiency. It also shows that significant results were obtained by preparing competent cells between 24°C-28°C. This confirms that preparation of electrocompetent cells can be made as simple as possible. Error bars, SD; n = 3.

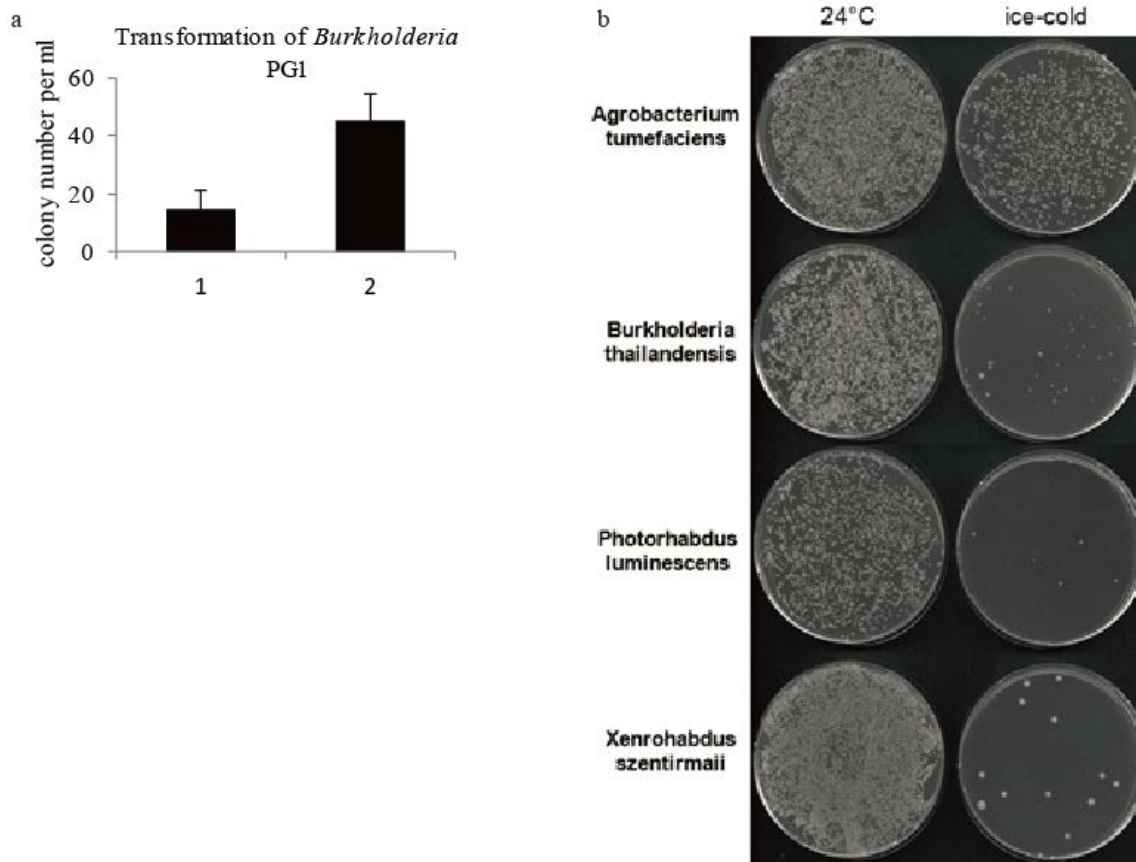


Figure S3. Transformation efficiency comparison of warm and cold temperature in different gram-negative strains. (a) pRK2-apra-km plasmid was used to transform into *Burkholderia* PG1. The transformants were Km resistant. (b) A few bacterial strains: *Agrobacterium* (G^-), *Burkholderia* DSM7029 (G^-), *Photorhabdus* (G^-), and *Xenorhabdus* (G^-) were used to perform the transformation experiment. Error bars, SD; n = 3.

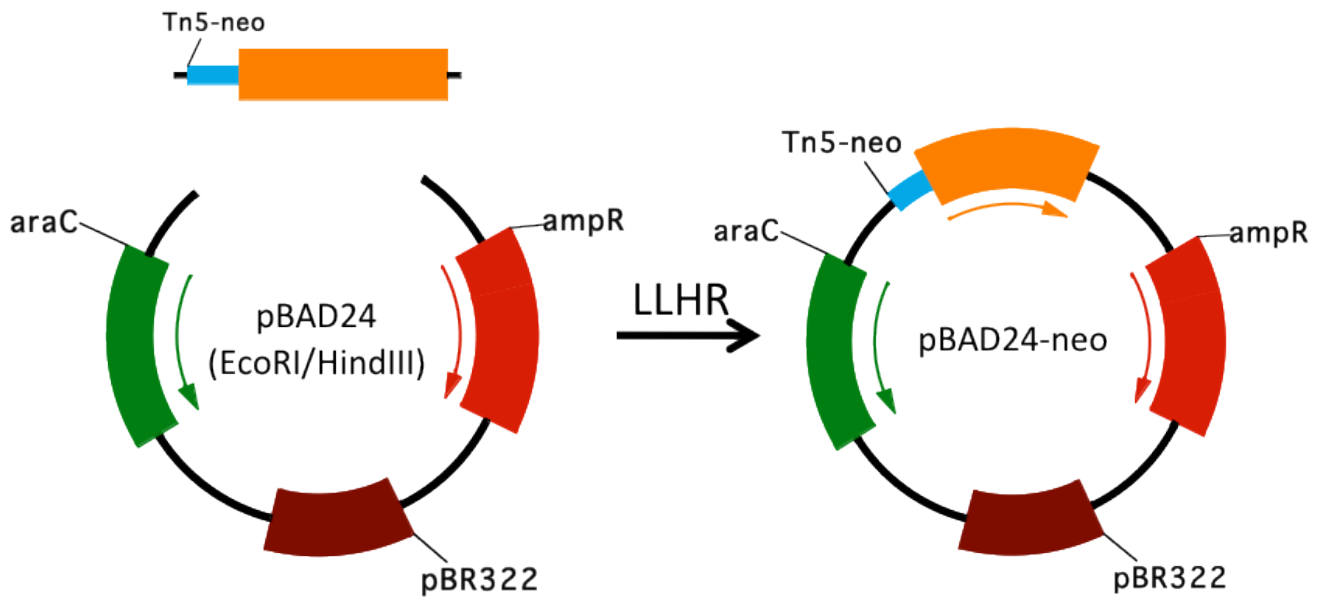


Figure S4. Diagram of LLHR by using short homology arms. pBAD24 circle vector digested by EcoRI plus Hind III was used as linear recipient vector. The homology sequences are exactly exposed at the ends. Tn5-neo PCR product flanked with short homology arms to the ends of digested pBAD24 vector is used as linear donor fragment.

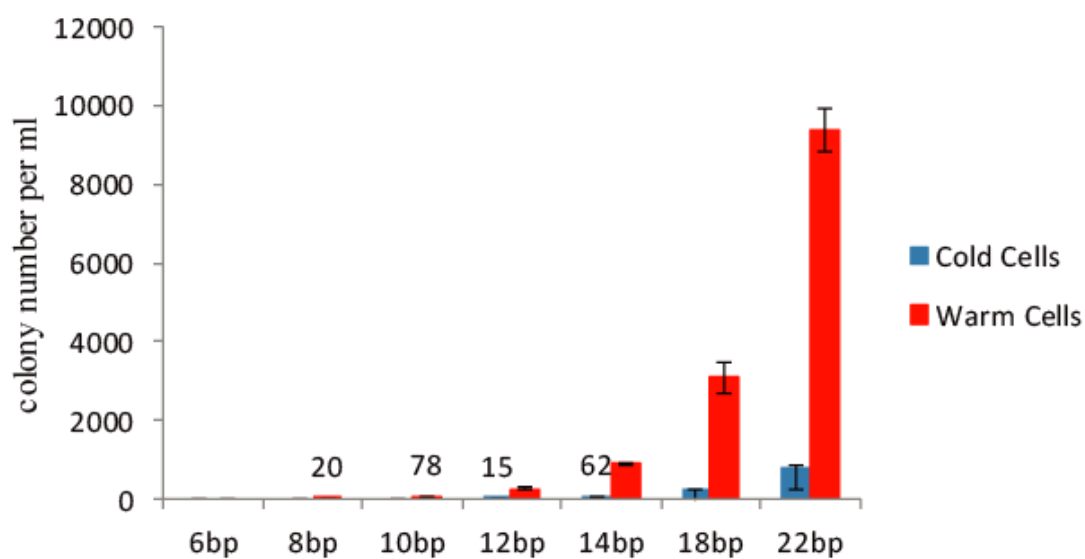


Figure S5. Effect of the length of homology arms on room temperature electrocompetent cells (warm cells). Seven PCR products with different homology arms (HA) were used for testing the LLHR efficiency. The homology arms can be as short as 8bp for LLHR to occur when cells were prepared at RT. When ice-cold cells used, the minimum homology arms are 12bp. Error bars, SD; n = 3.

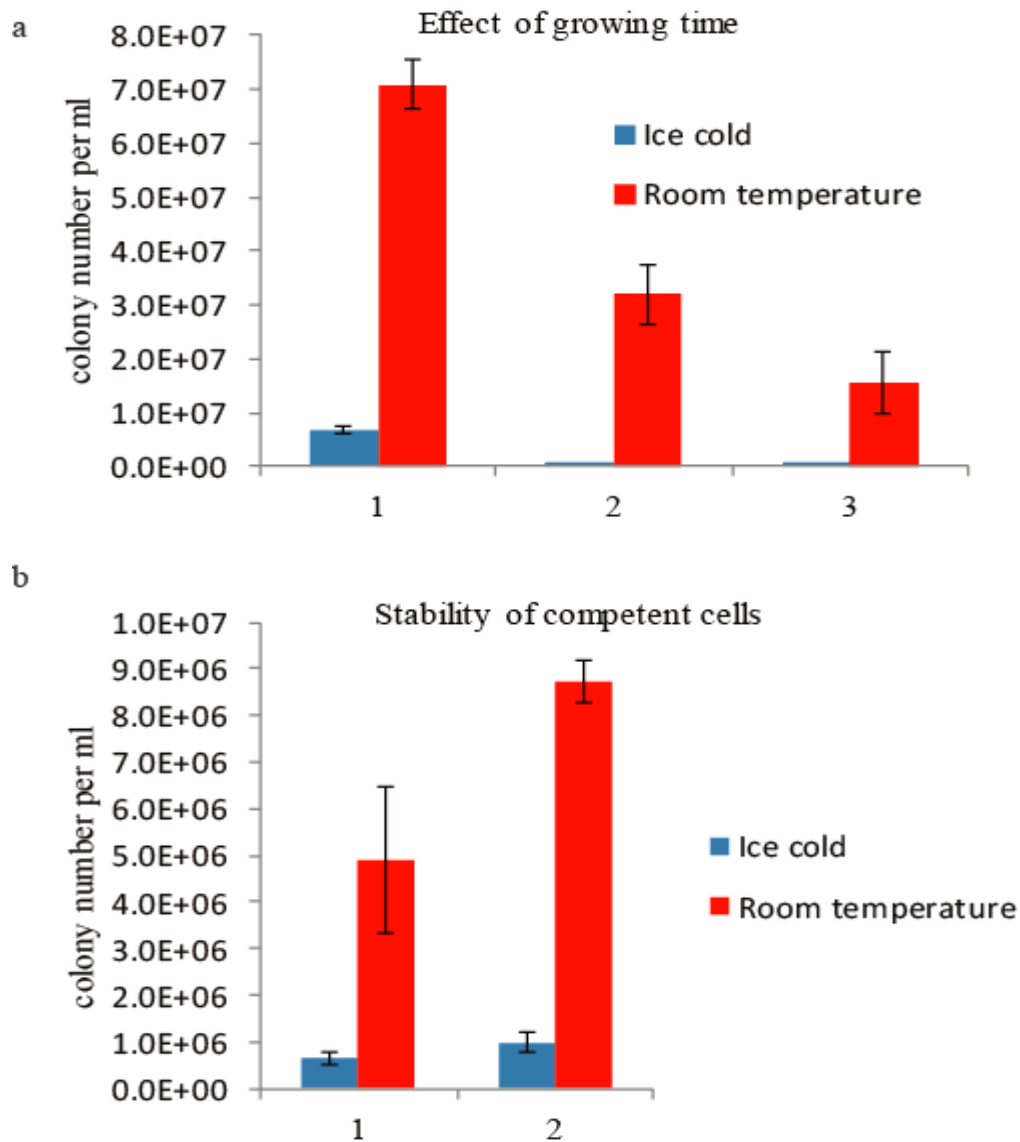


Figure S6. Effect of over-grown cells on transformation efficiency and electroporation without recovery step. (a) 35 μ L overnight cultured GB2005 cells were diluted into 1.4mL LB medium and cultured at 37°C for different time courses. Electrocompetent cells were transformed by 0.1 μ g of pGB-Ptet-plu1880 and plated on LB plates plus amp. 1 -cells growing for 2.5 hours, OD600=0.4; 2 -cells growing for 4 hours, OD600=1.2; 3 -cells growing for 6 hours, OD600=1.8. (b) GB2005 cells transformed by 0.1 μ g of pGB-Ptet-plu1880 and plated on Amp plates. 1 -cells plated directly after electroporation; 2 - same as 1 but after 1 hour recovery at 37°C. Error bars, SD; n = 3.

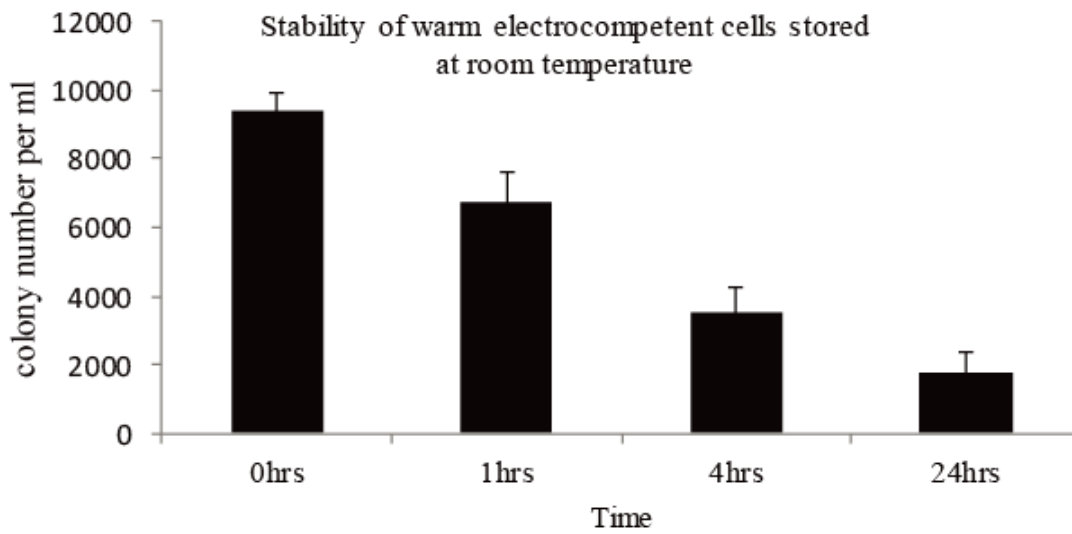


Figure S7. Stability of room temperature electrocompetent cells stored at room temperature. The room temperature competent cells lost around 30% of efficiency after 1 hour of storage at room temperature, 60% after 4 hours and approximately 80% after 1 day. Error bars, SD; n = 3.

Table S1 Strains and plasmids.

Strain or plasmid	Characteristics	References or sources
Strains		
<i>E. coli</i> GB05	F- <i>mcrA</i> Δ (<i>mrr-hsdRMS-mcrBC</i>) ϕ 80 <i>lacZ</i> Δ M15 Δ <i>lacX74 recA1 endA1 araD139 Δ(<i>ara, leu</i>)7697 <i>galU galK</i> λ <i>rpsLnupGfhuA::IS2 recET reda</i>, phage T1-resistant</i>	1
<i>E. coli</i> GB05-dir	GB2005, <i>araC</i> -BAD-ET γ A	2
<i>E. coli</i> GB05-red	GB2005, <i>araC</i> -BAD- γ β α A	1
<i>Burkholderia glumae</i> PG1	lipidase -producing wild-type strain, host for heterologous expression of PKS/NRPS gene clusters	3
<i>Agrobacterium tumefaciens</i>	gram-positive strain	4
<i>Burkholderia</i> DSM7029	gram-negative strain	3
<i>Photorhabdus luminescens</i>	gram-negative strain	5
<i>Xenorhabdus stockiae</i>	gram-negative strain	5
Plasmid		
pGB-amp-Ptet-plu1880	pBR322 replicon, ampR	6
pRK2-apra-km	oriV origin, kmR	This study
pBC301	oriV origin	7,8
pBeloBAC11-dis	BAC, kmR	This study
p15A-cm	p15A replicon, cmR	2
p15A-cm-km	p15A replicon, cmR, kmR	2
pBAD24	pBR322 replicon, ampR	9
pBAD24-neo	pBR322 replicon, ampR, kmR	This study

Table S2 Transformation efficiency (colonies on plates with ampicillin ($\times 10^4$)) using cells prepared in dH₂O or 10% glycerol.

	Cells before dry	Dried cells day 0	Dried cells day 1	Dried cells day 3
dH ₂ O	640	0	0	0
10% glycerol	468	196	212	188

Table S3 LLHR efficiency (colonies on plates with ampicillin and kanamycin) using cells prepared in dH₂O or 10% glycerol.

	Cells before dry	Dried cells day 0	Dried cells day 1	Dried cells day 3
dH ₂ O	420	0	0	0
10% glycerol	360	298	272	284

References

- 1 Fu, J., Teucher, M., Anastassiadis, K., Skarnes, W. & Stewart, A. F. in *Methods in Enzymology* Vol. 477 (eds M. Wassarman Paul & M. Soriano Philippe) 125-144 (Academic Press, 2010).
- 2 Fu, J. *et al.* Full-length RecE enhances linear-linear homologous recombination and facilitates direct cloning for bioprospecting. *Nat. Biotechnol.* **30**, 440-446 (2012).
- 3 M, O. *et al.* Glidobactins A, B and C, new antitumor antibiotics. II. Structure elucidation. *J. Antibiot.* **41**, 1338–1350 (1988).
- 4 Hu, S. *et al.* Genome engineering of *Agrobacterium tumefaciens* using the lambda Red recombination system. *Appl. Environ. Microbiol.* **98**, 2165-2172 (2014).
- 5 Yin, J. *et al.* A new recombineering system for *Photobacterium* and *Xenorhabdus*. *Nucleic Acids Res.* **43** (6), e36 (2015).
- 6 Bian, X. *et al.* Direct cloning, genetic engineering, and heterologous expression of the syringolin biosynthetic gene cluster in *E. coli* through Red/ET recombineering. *ChemBioChem* **13**, 1946-1952 (2012).
- 7 Xiang. A mini binary vector series for plant transformation. *Plant Mol. Biol.* **40**, 711-717 (1999).
- 8 Yang. Functional modulation of the geminivirus AL₂ transcription factor and silencing suppressor by self-interaction. *J. Virol.* **81**, 11972–11981 (2007).
- 9 Guzman, L.M., *et al.* Tight regulation, modulation, and high-level expression by vectors containing the arabinose pBAD promoter. *J. Bacteriol.* **177**, 4121-4130 (1995).

Publication II


Room temperature electrocompetent bacterial cells improve DNA transformation and recombineering efficiency.

Qiang Tu*, Jia Yin*, Jun Fu, Jennifer Herrmann, Yuezhong Li, Yulong Yin, A. Francis Stewart[‡], Rolf Müller[‡] and Youming Zhang[‡]

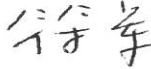
Author Contributions

Q.T. and **J.Y.** participated in the design of this study, performed data collection analysis, and drafted the manuscript; **J.F.**, **J.H.**, **Y.L.** and **Y.Y.** participated in interpretation data; **A.F.S.** and **R.M.** gave the advice for experimental design and discussed the data, also helped in the revision of the final manuscript. **Y.Z.** designed and oversaw the study, performed data interpretation and drafted the manuscript. All authors read and approved the final manuscript.

Signatures:


Qiang Tu: 


Jia Yin: 

Jun Fu: 


Jennifer Herrmann: 

Yuezhong Li: 

Yulong Yin: 

A. Francis Stewart: 

Rolf Müller: 

Youming Zhang: 

III

Biosynthesis of magnetic nanostructures in a foreign organism by transfer of bacterial magnetosome gene clusters.

Isabel Kolinko¹, Anna Lohße¹, Sarah Borg¹, Oliver Raschdorf^{1,2}, Christian Jogler^{1, †}, **Qiang Tu**^{3,4}, Mihály Pósfai⁵, Éva Tompa⁵, Jürgen M. Plitzko^{2,6}, Andreas Brachmann¹, Gerhard Wanner¹, Rolf Müller³, Youming Zhang^{4*} and Dirk Schüler^{1*}

¹Ludwig-Maximilians-Universität München, Department of Biology I, Großhaderner Straße 2-4, 82152 Martinsried, Germany.

²Max Planck Institute of Biochemistry, Department of Molecular Structural Biology, Am Klopferspitz 18, 82152 Martinsried, Germany.

³Helmholtz Institute for Pharmaceutical Research Saarland, Helmholtz Centre for Infection Research and Department of Pharmaceutical Biotechnology, Saarland University, PO Box 151150, 66041 Saarbrücken, Germany.

⁴Shandong University – Helmholtz Joint Institute of Biotechnology, State Key Laboratory of Microbial Technology, Life Science College, Shandong University, Jinan 250100, China.

⁵University of Pannonia, Department of Earth and Environmental Sciences, Veszprém, H-8200 Hungary.

⁶Bijvoet Center for Biomolecular Research, Utrecht University, 3584 CH Utrecht, The Netherlands.

[†]Present address: Leibniz Institute DSMZ, Department of Microbial Cell Biology and Genetics, Inhoffenstraße 7B, 38124 Braunschweig, Germany.

*e-mail: dirk.schueler@lmu.de; zhangyouming@sdu.edu.cn

Biosynthesis of magnetic nanostructures in a foreign organism by transfer of bacterial magnetosome gene clusters

Isabel Kolinko¹, Anna Lohße¹, Sarah Borg¹, Oliver Raschdorf^{1,2}, Christian Jogler^{1†}, Qiang Tu^{3,4}, Mihály Pósfai⁵, Éva Tompa⁵, Jürgen M. Pitzko^{2,6}, Andreas Brachmann¹, Gerhard Wanner¹, Rolf Müller³, Youming Zhang^{4*} and Dirk Schüler^{1*}

The synthetic production of monodisperse single magnetic domain nanoparticles at ambient temperature is challenging^{1,2}. In nature, magnetosomes—membrane-bound magnetic nanocrystals with unprecedented magnetic properties—can be biomineralized by magnetotactic bacteria³. However, these microbes are difficult to handle. Expression of the underlying biosynthetic pathway from these fastidious microorganisms within other organisms could therefore greatly expand their nanotechnological and biomedical applications^{4,5}. So far, this has been hindered by the structural and genetic complexity of the magnetosome organelle and insufficient knowledge of the biosynthetic functions involved. Here, we show that the ability to biomineralize highly ordered magnetic nanostructures can be transferred to a foreign recipient. Expression of a minimal set of genes from the magnetotactic bacterium *Magnetospirillum gryphiswaldense* resulted in magnetosome biosynthesis within the photosynthetic model organism *Rhodospirillum rubrum*. Our findings will enable the sustainable production of tailored magnetic nanostructures in biotechnologically relevant hosts and represent a step towards the endogenous magnetization of various organisms by synthetic biology.

The alphaproteobacterium *M. gryphiswaldense* produces uniform nanosized crystals of magnetite (Fe₃O₄), which can be engineered by genetic^{6,7} and metabolic means⁸ and are inherently biocompatible. The stepwise biogenesis of magnetosomes involves the invagination of vesicles from the cytoplasmic membrane, magnetosomal uptake of iron, and redox-controlled biomineralization of magnetite crystals, as well as their self-assembly into nanochains along a dedicated cytoskeletal structure to achieve one of the highest structural levels in a prokaryotic cell^{3,9}.

We recently discovered genes controlling magnetosome synthesis to be clustered within a larger (115 kb) genomic magnetosome island, in which they are interspersed by numerous genes of unrelated or unknown functions^{6,10}. Although the smaller *mamGFDC*, *mms6* and *mamXY* operons have accessory roles in the biomineralization of properly sized and shaped crystals^{6,11}, only the large *mamAB* operon encodes factors essential for iron transport, magnetosome membrane (MM) biogenesis, and crystallization of

magnetite particles, as well as their chain-like organization and intracellular positioning^{6,10,12}. However, it has been unknown whether this gene set is sufficient for autonomous expression of magnetosome biosynthesis.

Using recombineering (recombinogenic engineering) based on phage-derived Red/ET homologous recombination, we stitched together several modular expression cassettes comprising all 29 genes (26 kb in total) of the four operons in various combinations (Supplementary Fig. 1), but lacking the tubulin-like *ftsZm*. This gene was omitted from its native *mamXY* operon because of its known interference with cell division during cloning. Regions 200–400 bp upstream of all operons were retained to ensure transcription from native promoters¹³. Transposable expression cassettes comprising the MycoMar (*tps*) or Tn5 transposase gene, two corresponding inverted repeats, the origin of transfer *oriT*, and an antibiotic resistance gene were utilized to enable transfer and random chromosomal integration in single copy^{14,15} (Supplementary Tables 3 and 4). Chromosomal reintegration of all cassettes into different non-magnetic single-gene and operon deletion strains of *M. gryphiswaldense* resulted in stable wild type-like restoration of magnetosome biomineralization, indicating that transferred operons maintained functionality upon cloning and transfer (Supplementary Fig. 2).

We next attempted the transfer of expression cassettes to a foreign non-magnetic host organism (Fig. 1). We chose the photosynthetic alphaproteobacterium *R. rubrum* as a first model because of its biotechnological relevance and relatively close relationship to *M. gryphiswaldense*^{16–18} (16S rRNA similarity to *M. gryphiwaldense* = 90%). Although the *mamAB* operon alone has been shown to support some rudimentary biomineralization in *M. gryphiswaldense*⁶, neither genomic insertion of the *mamAB* operon alone (pTps_AB) nor in combination with the accessory *mamGFDC* genes (pTps_ABG) had any detectable phenotypic effect (Supplementary Table 1). We also failed to detect a magnetic response (C_{mag}) in the classical light scattering assay¹⁹ after insertion of pTps_ABG6 (*mamAB* + *mamGFDC* + *mms6*). However, the cellular iron content of *R. rubrum*_ABG6 increased 2.4-fold compared with the untransformed wild type (Supplementary Table 1). Transmission electron microscopy (TEM) revealed a loose chain

¹Ludwig-Maximilians-Universität München, Department of Biology I, Großhaderner Straße 2-4, 82152 Martinsried, Germany, ²Max Planck Institute of Biochemistry, Department of Molecular Structural Biology, Am Klopferspitz 18, 82152 Martinsried, Germany, ³Helmholtz Institute for Pharmaceutical Research Saarland, Helmholtz Centre for Infection Research and Department of Pharmaceutical Biotechnology, Saarland University, PO Box 151150, 66041 Saarbrücken, Germany, ⁴Shandong University – Helmholtz Joint Institute of Biotechnology, State Key Laboratory of Microbial Technology, Life Science College, Shandong University, Jinan 250100, China, ⁵University of Pannonia, Department of Earth and Environmental Sciences, Veszprém, H-8200 Hungary, ⁶Bijvoet Center for Biomolecular Research, Utrecht University, 3584 CH Utrecht, The Netherlands, [†]Present address: Leibniz Institute DSMZ, Department of Microbial Cell Biology and Genetics, Inhoffenstraße 7B, 38124 Braunschweig, Germany. *e-mail: dirk.schueler@lmu.de; zhangyouming@sdu.edu.cn

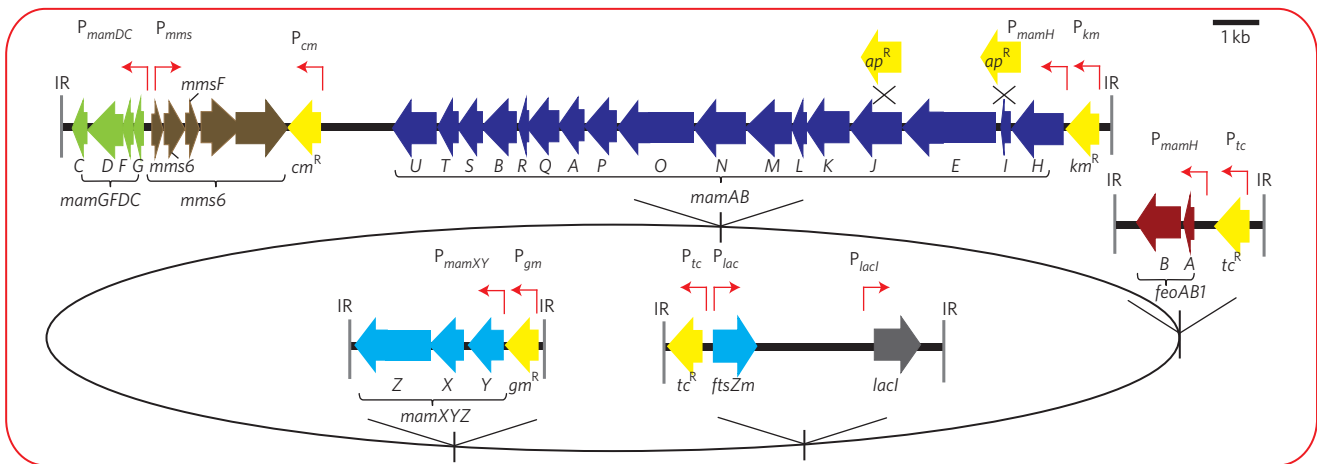


Figure 1 | Schematic representation of molecular organization of gene cassettes inserted into the chromosome of *R. rubrum* in a stepwise manner. Broad arrows indicate the extensions and transcriptional directions of individual genes. Different colours illustrate the cassettes inserted into the chromosome (oval shape, not to scale) as indicated by their gene names in the figure. Shown in yellow are antibiotic resistance genes (km^R , kanamycin resistance; tc^R , tetracycline resistance; ap^R , ampicillin resistance; gm^R , gentamicin resistance). Thin red arrows indicate different promoters (P) driving transcription of inserted genes (P_{km} , P_{gm} , P_{tc} , promoters of antibiotic resistance cassettes; P_{lac} , promoter lac repressor; P_{mms} , P_{mamDC} , P_{mamH} , P_{mamXY} native promoters of the respective gene clusters from *M. gryphiswaldense*; P_{lac} , lac promoter). Crossed lines indicate sites of gene deletions of *mamI* and *mamJ* in strains *R. rubrum*_ABG6X-dl and *R. rubrum*_ABG6X-dJ, respectively. IR, inverted repeat defining the boundaries of the sequence inserted by the transposase.

of small (~12 nm) irregularly shaped electron-dense particles (Fig. 2a,ii), identified as poorly crystalline hematite (Fe_2O_3) by analysis of the lattice spacings in high-resolution TEM images (Supplementary Fig. 3), much as in the hematite particles previously identified in *M. gryphiswaldense* mutants affected in crystal formation^{11,20}. To further enhance biomineralization, we next transferred pTps_XYZ, an insertional plasmid harbouring *mamX*, *Y* and *Z* from the *mamXY* operon, into *R. rubrum*_ABG6 (Supplementary Fig. 1). The resulting strain ABG6X encompassed all 29 relevant genes of the magnetosome island except *ftsZm*. Intriguingly, cells of ABG6X exhibited a significant magnetic response (Supplementary Table 1) and were 'magnetotactic', that is, within several hours accumulated as a visible pellet near a magnet at the edge of a culture flask (Fig. 2b). TEM micrographs revealed the presence of electron-dense particles identified as magnetite (Fe_3O_4) (Fig. 2d, Supplementary Fig. 8 and Table 1), which were aligned in short, fragmented chains loosely dispersed within the cell (Fig. 2a,iii). Despite their smaller sizes (average, 24 nm) the particles strongly resembled the magnetosomes of the donor strain in terms of their projected outlines and thickness contrast, suggestive of cubooctahedral or octahedral crystal morphologies (Fig. 2d). Additional insertion of the *ftsZm* gene under control of the inducible *lac* promoter had no effect on the cellular iron content and the number and size of magnetite crystals in the resulting *R. rubrum*_ABG6X_ftsZm (Fig. 2a,iv, Supplementary Table 1). Magnetite biomineralization occurred during microoxic chemotrophic as well as anoxic photoheterotrophic cultivation. Medium light intensity, 50 μM iron and 23 °C supported the highest magnetic response (C_{mag}) and robust growth of the metabolically versatile *R. rubrum*_ABG6X, which was indistinguishable from the untransformed wild type (Supplementary Figs 4 and 5). The magnetic phenotype remained stable for at least 40 generations under non-selective conditions, with no obvious phenotypic changes.

To test whether known mutation phenotypes from *M. gryphiswaldense* could be replicated in *R. rubrum*, we constructed variants of expression cassettes in which single genes were omitted from the *mamAB* operon by deletion within the cloning host *Escherichia coli*. The small (77 amino acids) MamI protein was previously implicated in MM vesicle formation and found to be essential for magnetosome

synthesis¹². *R. rubrum*_ABG6X-dI failed to express magnetosome particles (Supplementary Fig. 10), which phenocopied a *mamI* deletion in the related *M. magneticum*¹². Another tested example was MamJ, which is assumed to connect magnetosome particles to the cytoskeletal magnetosome filament formed by the actin-like MamK²¹. Much as in *M. gryphiswaldense*, deletion of *mamJ* caused agglomeration of magnetosome crystals in ~65% of *R. rubrum*_ABG6X-dJ cells (Fig. 2a,v, Supplementary Fig. 10 and Table 1). Together, these observations indicate that magnetosome biogenesis and assembly within the foreign host are governed by very similar mechanisms and structures as in the donor, which are conferred by the transferred genes.

As magnetosomes in *R. rubrum*_ABG6X were still smaller than those of *M. gryphiswaldense*, we wondered whether full expression of biomineralization may depend on the presence of further auxiliary functions, possibly encoded outside the canonical magnetosome operons. For instance, deletion of *feoB1* encoding a constituent of a ferrous iron transport system specific for magnetotactic bacteria caused fewer and smaller magnetosomes in *M. gryphiswaldense*²². Strikingly, insertion of *feoAB1* into *R. rubrum* strain ABG6X resulted in even larger, single-crystalline and twinned magnetosomes and longer chains (440 nm) (Fig. 2a,vi, Supplementary Table 1). The size (37 nm) of the crystals approached that of the donor, and cellular iron content was substantially increased (0.28% of dry weight) compared with *R. rubrum*_ABG6X (0.18%), although still lower than in *M. gryphiswaldense* (3.5%), partly because of the considerably larger volume of *R. rubrum* cells (Fig. 2c).

Magnetosome particles could be purified from disrupted cells by magnetic separation and centrifugation²³ and formed stable suspensions (Fig. 3). Isolated crystals were clearly enclosed by a layer of organic material resembling the MM attached to magnetosomes of *M. gryphiswaldense*. Smaller, immature crystals were surrounded by partially empty vesicles (Fig. 3c, inset), which were also seen in thin-sectioned cells (Supplementary Fig. 8) and on average were smaller (66 ± 6 nm) than the abundant photosynthetic intracytoplasmic membranes (ICMs) (93 ± 34 nm; Fig. 3a, Supplementary Fig. 8).

Organic material of the putative MM could be solubilized from isolated magnetite crystals of *R. rubrum*_ABG6X by various detergents (Fig. 3d), in a similar manner to that reported for MM of

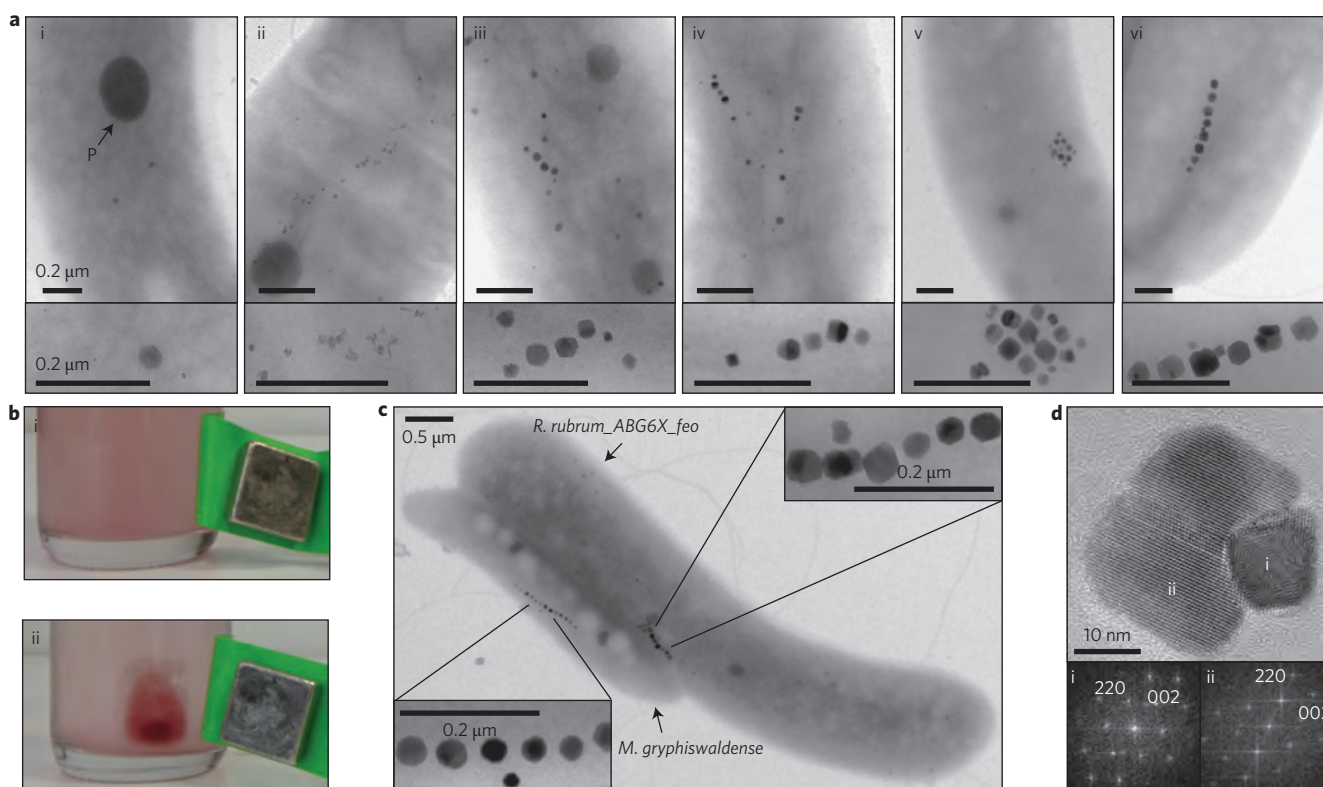


Figure 2 | Phenotypes of *R. rubrum* strains expressing different magnetosome gene clusters and auxiliary genes. **a**, TEM images: *R. rubrum* wild type (i), containing a larger phosphate inclusion (P) and some small, non-crystalline, electron-dense particles; *R. rubrum_ABG6* (ii); *R. rubrum_ABG6X* (iii); *R. rubrum_ABG6X_ftsZm* (iv); *R. rubrum_ABG6X_dJ* (v); *R. rubrum_ABG6X_feo* (vi). Insets: Magnifications of non-crystalline electron-dense particles (i) or heterologously expressed nanocrystals (ii–vi). All insets are of the same particles/crystals as in their respective main images, except for (v). For further TEM micrographs see Supplementary Fig. 10. **b**, Unlike the untransformed *R. rubrum* wild type, cells of *R. rubrum_ABG6X* accumulated as a visible red spot near the pole of a permanent magnet at the edge of a culture flask. **c**, TEM micrograph of a mixed culture of the donor *M. gryphiswaldense* and the recipient *R. rubrum_ABG6X_feo*, illustrating characteristic cell properties and magnetosome organization. Insets: Magnifications of magnetosomes from *M. gryphiswaldense* and *R. rubrum_ABG6X_feo*. **d**, High-resolution TEM lattice image of a twinned crystal from *R. rubrum_ABG6X*, with Fourier transforms (i) and (ii) showing intensity maxima consistent with the structure of magnetite.

*M. gryphiswaldense*²³. Proteomic analysis of the SDS-solubilized MM revealed a complex composition (Supplementary Fig. 6), and several genuine magnetosome proteins (MamKCJAFDMBYOE, Mms6, MmsF) were detected among the most abundant polypeptides (Supplementary Table 2). An antibody against MamC, the most abundant protein in the MM of *M. gryphiswaldense*²³, also recognized a prominent band with the expected mass (12.4 kDa) in the MM of *R. rubrum_ABG6X* (Supplementary Fig. 6).

The subcellular localization of selected magnetosome proteins in *R. rubrum* depended on the presence of further determinants encoded by the transferred genes. For example, MamC tagged with a green fluorescent protein, which is commonly used as magnetosome chain marker in *M. gryphiswaldense*²⁴ displayed a punctuate pattern in the *R. rubrum* wild type background. In contrast, a filamentous fluorescent signal became apparent in the majority of cells (79%) of the *R. rubrum_ABG6X* background, in which the full complement of magnetosome genes is present (Supplementary Fig. 7), reminiscent of the magnetosome-chain localization of these proteins in *M. gryphiswaldense*²⁴.

Our findings demonstrate that one of the most complex prokaryotic structures can be functionally reconstituted within a foreign, hitherto non-magnetic host by balanced expression of a multitude of structural and catalytic membrane-associated factors. This also provides the first experimental evidence that the magnetotactic trait can be disseminated to different species by only a single event, or a few events, of transfer, which are likely to occur also

under natural conditions by horizontal gene transfer as speculated before^{18,25,26}.

The precise functions of many of the transferred genes have remained elusive in native magnetotactic bacteria, but our results will now enable the dissection and engineering of the entire pathway in genetically more amenable hosts. The approximately 30 transferred magnetosome genes constitute an autonomous expression unit that is sufficient to transplant controlled synthesis of magnetite nanocrystals and their self-assembly within a foreign organism. However, further auxiliary functions encoded outside the *mam* and *mms* operons are necessary for biomineralization of donor-like magnetosomes. Nevertheless, this minimal gene set is likely to shrink further as a result of systematic reduction approaches in different hosts.

Importantly, the results are promising for the sustainable production of magnetic nanoparticles in biotechnologically relevant photosynthetic hosts. Previous attempts to magnetize both prokaryotic and eukaryotic cells by genetic and metabolic means (for example, refs 27,28) resulted in only irregular and poorly crystalline iron deposits. This prompted ideas to borrow genetic parts of the bacterial magnetosome pathway for the synthesis of magnetic nanoparticles within cells of other organisms^{4,29}. Our results now set the stage for synthetic biology approaches to genetically endow both uni- and multicellular organisms with magnetization by biomineralization of tailored magnetic nanostructures. This might be exploited for instance in nanomagnetic actuators or *in situ* heat

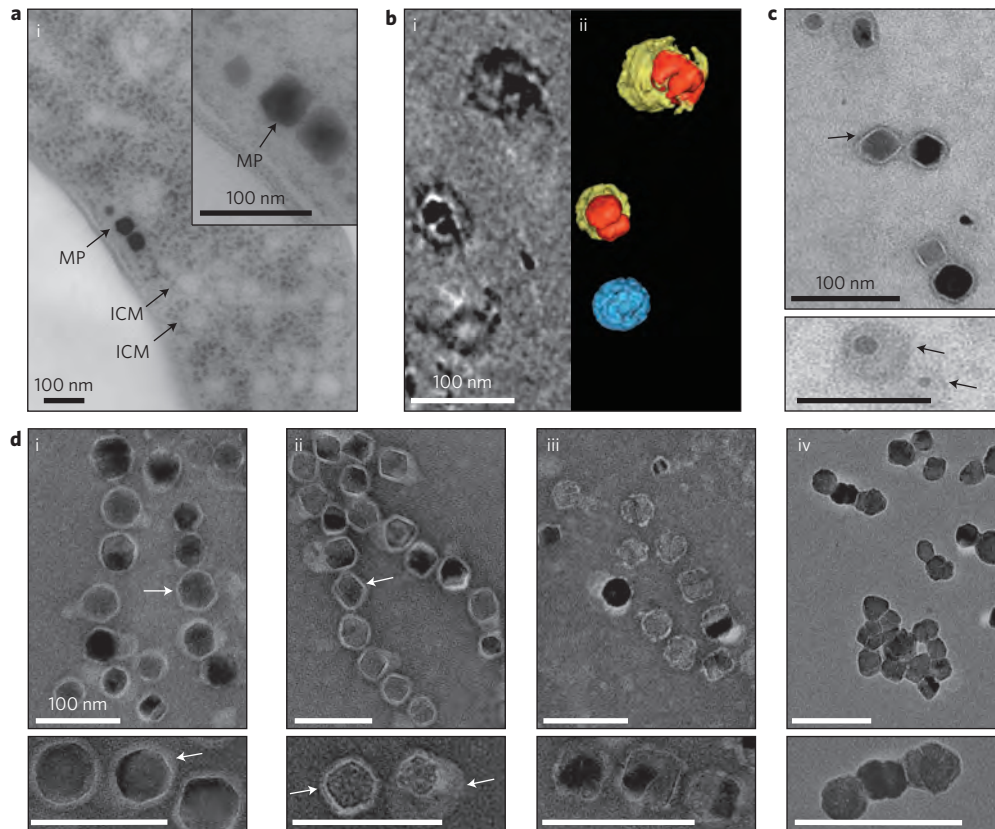


Figure 3 | Ultrastructural analysis of *R. rubrum_ABG6X* and isolated crystals. a, Cryo-fixed, thin-sectioned *R. rubrum_ABG6X* contained intracytoplasmic membranes (ICMs) (93 ± 34 nm, $n = 95$) and magnetic particles (MP). Inset: Magnification of the magnetite crystals. **b**, Cryo-electron tomography of isolated magnetic particles of *R. rubrum_ABG6X*: *x-y* slice of a reconstructed tomogram (i) and surface-rendered three-dimensional representation (ii). A membrane-like structure (yellow, thickness 3.4 ± 1.0 nm, $n = 6$) surrounds the magnetic particles (red). (Blue, empty vesicle.) **c,d**, TEM images of isolated magnetosomes from *R. rubrum_ABG6X* (**c** and **d**, i, iii, iv) and *M. gryphiswaldense* (**d**, i) negatively stained by uranyl acetate (**c**) or phosphotungstic acid (**d**). Insets: Higher-magnification images of magnetic particles; these are of different particles to those shown in the main images, except for (iv). Scale bars, 100 nm. Arrows indicate the magnetosome membrane, which encloses magnetic crystals of *M. gryphiswaldense* (thickness 3.2 ± 1.0 nm, $n = 103$) and *R. rubrum_ABG6X* (thickness 3.6 ± 1.2 nm, $n = 100$). Organic material could be solubilized from magnetite crystals of *R. rubrum_ABG6X* with SDS (sodium dodecyl sulfate, iv) and less effectively also with Triton X-100 (iii).

generators in the emerging field of magnetogenetics³⁰, or for endogenous expression of magnetic reporters for bioimaging³¹.

Methods

Bacterial strains, media and cultivation. The bacterial strains are described in Supplementary Table 4. *E. coli* strains were cultivated as previously described³². A volume of 1 mM DL- α,ϵ -diaminopimelic acid was added for the growth of auxotrophic strains BW29427 and WM3064. *M. gryphiswaldense* strains were cultivated in flask standard medium (FSM), in liquid or on plates solidified by 1.5% agar, and incubated at 30 °C under microoxic (1% O₂) conditions³³. Cultures of *R. rubrum* strains were grown as specified (Supplementary Fig. 3).

Construction of magnetosome gene cluster plasmids and conjugative transfer. The oligonucleotides and plasmids used in this study are listed in Supplementary Tables 4 and 5. Red/ET (Lambda red and RecET) recombination was performed as described previously¹⁴. Briefly, a cloning cassette was amplified by polymerase chain reaction (PCR) and transferred into electrocompetent *E. coli* cells (DH10b) expressing phage-derived recombinases from a circular plasmid (pSC101-BAD-gbaA). After transfer of the cassette, recombination occurred between homologous regions on the linear fragment and the plasmid.

To stitch the magnetosome gene clusters together into a transposon plasmid (Supplementary Fig. 1) we used triple recombination¹⁴ and co-transformed two linear fragments, which recombined with a circular plasmid. Recombinants harbouring the correct plasmids were selected by restriction analysis³².

Conjugations into *M. gryphiswaldense* were performed as described before³³. For conjugation of *R. rubrum*, cultures were incubated in ATCC medium 112. Approximately 2×10^9 cells were mixed with 1×10^9 *E. coli* cells, spotted on American Type Culture Collection (ATCC) 112 agar medium and incubated for 15 h. Cells were flushed from the plates and incubated on ATCC 112 agar medium supplemented with appropriate antibiotics for 7–10 days ($T_c = 10 \mu\text{g ml}^{-1}$;

$K_m = 20 \mu\text{g ml}^{-1}$; $G_m = 10 \mu\text{g ml}^{-1}$, where T_c , tetracycline; K_m , kanamycin; G_m , gentamicin). Sequential transfer of the plasmids resulted in 1×10^{-6} to 1×10^{-8} antibiotic-resistant insertants per recipient, respectively. Two clones from each conjugation experiment were chosen for further analyses. Characterized insertants were indistinguishable from wild type with respect to motility, cell morphology or growth (Supplementary Fig. 5).

Analytical methods. The optical density of *M. gryphiswaldense* cultures was measured turbidimetrically at 565 nm as described previously¹⁹. The optical density of *R. rubrum* cultures was measured at 660 nm and 880 nm. The ratio of 880/660 nm was used to determine yields of chromatophores within intact cells (Supplementary Fig. 4). Furthermore, *bacteriochlorophyll a* was extracted from cultures with methanol. Absorption spectra (measured in an Ultrospec 3000 photometer, GE Healthcare) of photoheterotrophically cultivated *R. rubrum_ABG6X* cells were indistinguishable from that of the wild type (Supplementary Fig. 4). The average magnetic orientation of cell suspensions (C_{mag}) was assayed with a light scattering assay as described previously¹⁹. Briefly, cells were aligned at different angles to a light beam by application of an external magnetic field.

Microscopy. For TEM of whole cells and isolated magnetosomes, specimens were directly deposited onto carbon-coated copper grids. Magnetosomes were stained with 1% phosphotungstic acid or 2% uranyl acetate. Samples were viewed and recorded with a Morgagni 268 microscope. Sizes of crystals and vesicles were measured with ImageJ software.

Chemical fixation, high-pressure freezing and thin sectioning of cells were performed as described previously¹⁷. Processed samples were viewed with an EM 912 electron microscope (Zeiss) equipped with an integrated OMEGA energy filter operated at 80 kV in the zero loss mode. Vesicle sizes were measured with ImageJ software. High-resolution TEM was performed with a JEOL 3010 microscope,

operated at 297 kV and equipped with a Gatan Imaging Filter for the acquisition of energy-filtered compositional maps. For TEM data processing and interpretation, DigitalMicrograph and SingleCrystal software were used²⁰. Cryo-electron tomography was performed as described previously²¹. Fluorescence microscopy was performed with an Olympus IX81 microscope equipped with a Hamamatsu Orca AG camera using exposure times of 0.12–0.25 s. Image rescaling and cropping were performed with Photoshop 9.0 software.

Received 9 September 2013; accepted 16 January 2014;
published online 23 February 2014

References

- Prozorov, T., Bazylinski, D. A., Mallapragada, S. K. & Prozorov, R. Novel magnetic nanomaterials inspired by magnetotactic bacteria: topical review. *Mater. Sci. Eng. R* **74**, 133–172 (2013).
- Baumgartner, J., Bertinetti, L., Widdrat, M., Hirt, A. M. & Faivre, D. Formation of magnetite nanoparticles at low temperature: from superparamagnetic to stable single domain particles. *PLoS ONE* **8**, e57070 (2013).
- Bazylinski, D. A. & Frankel, R. B. Magnetosome formation in prokaryotes. *Nature Rev. Microbiol.* **2**, 217–230 (2004).
- Goldhawk, D. E., Rohani, R., Sengupta, A., Gelman, N. & Prato, F. S. Using the magnetosome to model effective gene-based contrast for magnetic resonance imaging. *Wiley Interdiscip. Rev. Nanomed. Nanobiotechnol.* **4**, 378–388 (2012).
- Murat, D. Magnetosomes: how do they stay in shape? *J. Mol. Microbiol. Biotechnol.* **23**, 81–94 (2013).
- Lohsse, A. *et al.* Functional analysis of the magnetosome island in *Magnetospirillum gryphiswaldense*: the *mamAB* operon is sufficient for magnetite biomineralization. *PLoS ONE* **6**, e25561 (2011).
- Pollithy, A. *et al.* Magnetosome expression of functional camelid antibody fragments (nanobodies) in *Magnetospirillum gryphiswaldense*. *Appl. Environ. Microbiol.* **77**, 6165–6171 (2011).
- Staniland, S. *et al.* Controlled cobalt doping of magnetosomes *in vivo*. *Nature Nanotech.* **3**, 158–162 (2008).
- Jogler, C. & Schüler, D. Genomics, genetics, and cell biology of magnetosome formation. *Annu. Rev. Microbiol.* **63**, 501–521 (2009).
- Ullrich, S., Kube, M., Schübbe, S., Reinhardt, R. & Schüler, D. A hypervariable 130-kilobase genomic region of *Magnetospirillum gryphiswaldense* comprises a magnetosome island which undergoes frequent rearrangements during stationary growth. *J. Bacteriol.* **187**, 7176–7184 (2005).
- Raschdorf, O., Müller, F. D., Pósfai, M., Plietzko, J. M. & Schüler, D. The magnetosome proteins MamX, MamZ and MamH are involved in redox control of magnetite biomineralization in *Magnetospirillum gryphiswaldense*. *Mol. Microbiol.* **89**, 872–886 (2013).
- Murat, D., Quinlan, A., Vali, H. & Komeili, A. Comprehensive genetic dissection of the magnetosome gene island reveals the step-wise assembly of a prokaryotic organelle. *Proc. Natl Acad. Sci. USA* **107**, 5593–5598 (2010).
- Schübbe, S. *et al.* Transcriptional organization and regulation of magnetosome operons in *Magnetospirillum gryphiswaldense*. *Appl. Environ. Microbiol.* **72**, 5757–5765 (2006).
- Fu, J. *et al.* Efficient transfer of two large secondary metabolite pathway gene clusters into heterologous hosts by transposition. *Nucleic Acids Res.* **36**, e113 (2008).
- Martinez-Garcia, E., Calles, B., Arevalo-Rodriguez, M. & de Lorenzo, V. pBAM1: an all-synthetic genetic tool for analysis and construction of complex bacterial phenotypes. *BMC Microbiol.* **11**, 38 (2011).
- Richter, M. *et al.* Comparative genome analysis of four magnetotactic bacteria reveals a complex set of group-specific genes implicated in magnetosome biomineralization and function. *J. Bacteriol.* **189**, 4899–4910 (2007).
- Jogler, C. *et al.* Conservation of proteobacterial magnetosome genes and structures in an uncultivated member of the deep-branching *Nitrospira* phylum. *Proc. Natl Acad. Sci. USA* **108**, 1134–1139 (2011).
- Lefèvre, C. T. *et al.* Monophyletic origin of magnetotaxis and the first magnetosomes. *Environ. Microbiol.* **15**, 2267–2274 (2013).
- Schüler, D. R., Uhl, R. & Bäuerlein, E. A simple light scattering method to assay magnetism in *Magnetospirillum gryphiswaldense*. *FEMS Microbiol. Ecol.* **132**, 139–145 (1995).
- Uebe, R. *et al.* The cation diffusion facilitator proteins MamB and MamM of *Magnetospirillum gryphiswaldense* have distinct and complex functions, and are involved in magnetite biomineralization and magnetosome membrane assembly. *Mol. Microbiol.* **82**, 818–835 (2011).
- Scheffel, A. *et al.* An acidic protein aligns magnetosomes along a filamentous structure in magnetotactic bacteria. *Nature* **440**, 110–114 (2006).
- Rong, C. *et al.* Ferrous iron transport protein B gene (*feoB1*) plays an accessory role in magnetosome formation in *Magnetospirillum gryphiswaldense* strain MSR-1. *Res. Microbiol.* **159**, 530–536 (2008).
- Grünberg, K. *et al.* Biochemical and proteomic analysis of the magnetosome membrane in *Magnetospirillum gryphiswaldense*. *Appl. Environ. Microbiol.* **70**, 1040–1050 (2004).
- Lang, C. & Schüler, D. Expression of green fluorescent protein fused to magnetosome proteins in microaerophilic magnetotactic bacteria. *Appl. Environ. Microbiol.* **74**, 4944–4953 (2008).
- Jogler, C. *et al.* Comparative analysis of magnetosome gene clusters in magnetotactic bacteria provides further evidence for horizontal gene transfer. *Environ. Microbiol.* **11**, 1267–1277 (2009).
- Jogler, C. *et al.* Toward cloning of the magnetotactic metagenome: identification of magnetosome island gene clusters in uncultivated magnetotactic bacteria from different aquatic sediments. *Appl. Environ. Microbiol.* **75**, 3972–3979 (2009).
- Nishida, K. & Silver, P. A. Induction of biogenic magnetization and redox control by a component of the target of rapamycin complex 1 signaling pathway. *PLoS Biol.* **10**, e1001269 (2012).
- Kim, T., Moore, D. & Fussenegger, M. Genetically programmed superparamagnetic behavior of mammalian cells. *J. Biotechnol.* **162**, 237–245 (2012).
- Murat, D. *et al.* The magnetosome membrane protein, MmsF, is a major regulator of magnetite biomineralization in *Magnetospirillum magneticum* AMB-1. *Mol. Microbiol.* **85**, 684–699 (2012).
- Huang, H., Delikanli, S., Zeng, H., Ferkey, D. M. & Pralle, A. Remote control of ion channels and neurons through magnetic-field heating of nanoparticles. *Nature Nanotech.* **5**, 602–606 (2010).
- Westmeyer, G. G. & Jasanoff, A. Genetically controlled MRI contrast mechanisms and their prospects in systems neuroscience research. *Magn. Reson. Imaging* **25**, 1004–1010 (2007).
- Sambrook, J. & Russell, D. *Molecular Cloning: A Laboratory Manual* Vol. 3 (Cold Spring Harbor Laboratory Press, 2001).
- Kolinko, I., Jogler, C., Katzmann, E. & Schüler, D. Frequent mutations within the genomic magnetosome island of *Magnetospirillum gryphiswaldense* are mediated by *RecA*. *J. Bacteriol.* **193**, 5328–5334 (2011).

Acknowledgements

This work was supported by the Human Frontier Science Foundation (grant RGP0052/2012), the Deutsche Forschungsgemeinschaft (grants SCHU 1080/12-1 and 15-1) and the European Union (Bio2MaN4MR1). The authors thank F. Kiemer for expert help with iron measurements and cultivation experiments.

Author contributions

I.K., D.S., Y.Z., Q.T., C.J. and R.M. planned and performed cloning experiments. I.K. and A.L. performed genetic transfers and cultivation experiments. G.W. prepared cryo- and chemically fixed cells. S.B., O.R. and G.W. performed TEM and I.K. analysed the data. J.P. and O.R. performed cryo-electron tomography experiments. E.T. and M.P. took high-resolution TEM micrographs and analysed the data. I.K. and A.L. took fluorescence micrographs and performed phenotypization experiments. I.K. performed western blot experiments and analysed proteomic data. A.B. performed Illumina genome sequencing and I.K. analysed the data. I.K. and D.S. designed the study and wrote the paper. All authors discussed the results and commented on the manuscript.

Additional information

Supplementary information is available in the [online version](#) of the paper. Reprints and permissions information is available online at www.nature.com/reprints. Correspondence and requests for materials should be addressed to Y.Z. and D.S.

Competing financial interests

I.K. and D.S. (LMU Munich) have filed a patent application on the process described in this work (Production of magnetic nanoparticles in recombinant host cells, EP13193478).

Biosynthesis of magnetic nanostructures in a foreign organism by transfer of bacterial magnetosome gene clusters

6 Construction of Tn5 transposon plasmids

7 For construction of translational (C-terminal) gene fusions, the *mamDC* promoter
8 (XbaI, BamHI restriction sites added) was cloned in front of either the *mamGFDC*
9 operon or the *mamJ* gene (NdeI, KpnI), which were followed by the *egfp* gene (KpnI,
10 EcoRI). The resulting construct was cloned into pBAM1¹ modified by a tetracycline
11 resistance cassette (exchange of *km^R* against *tc^R* with SanDI and AatII). The
12 replicative plasmid pFM211 (Frank Müller, unpublished) harboring *ftsZm* with a
13 *mCherry* fusion under control of an inducible lac promoter was recombined with
14 pBAM1 to construct pBAM-ftsZm_mcherry. The resident *km^R* was replaced by *tc^R*
15 using ET-recombination. For construction of pBAM_feoAB1, a fragment with P_{*mamH*}
16 and *feoAB1* was amplified by PCR from pRU1feoAB (XbaI, EcoRI) and cloned into
17 Tet-pBAM1.

18

19 Intracellular iron measurements

20 Cellular iron contents were determined after incubation under photoheterotrophic
21 conditions in 10 ml Hungate tubes using a modified version of the ferrozine assay².
22 To this end, 4 ml cultures were centrifuged for 1 min at 11.000 rpm, resuspended in
23 90 µl HNO₃ (65%) and incubated for 3 h at 99 °C.

24

25 Sequencing

26 For whole genome sequencing of strain *R. rubrum*_ABG6X a genomic DNA library
27 was generated with the Nextera Kit (Illumina). Sequencing (1.25 Mio clusters, 2x 250
28 bp) was performed with a MiSeq sequencer (Illumina). Data analysis with CLC
29 Genomics Workbench (CLCbio) confirmed single-site integration of both expression
30 cassettes without mutations, except for a spontaneous deletion (aa 169-247) within
31 the hypervariable non-essential CAR domain of *mamJ* which was shown to be
32 irrelevant for protein function³.

33 **Magnetosome isolation, electrophoresis and immuno-chemical detection**

34 For magnetosome isolation and expression analysis, cultures of *R. rubrum* were
35 grown photoheterotrophically in sealed 5 liter flasks illuminated by white light, 1000
36 lux intensity. Cells were harvested, washed and resuspended into HEPES buffer⁴.
37 Cell suspensions were lysed by sonication and cellular debris was removed by low-
38 speed centrifugation. Magnetic separation of magnetosome particles, solubilization of
39 the enclosing organic layer and fractionation of non-magnetic membrane fraction and
40 soluble proteins were performed as previously described^{5,6}. Polyacrylamide gels
41 were prepared according to the procedure of Laemmli⁷. Protein samples from
42 different cellular fractions (magnetosome membrane, soluble fraction, non-magnetic
43 membrane fraction) were resuspended in electrophoresis sample buffer and
44 denatured at 98 °C for 5 min⁸. 10 µg of protein extracts were separated on a 15%
45 SDS-polyacrylamide gel. Protein bands were visualized by Coomassie brilliant blue
46 staining. Western blot analysis for detection of MamC was performed as previously
47 described⁶.

48

49 **Mass spectrometry**

50 For mass spectrometry 25 µg solubilised proteins were tryptically in-gel digested as
51 described previously⁹. The resulting fragments were separated on a C18 reversed-
52 phase column and analyzed by nano-electrospray ionization-LC tandem MS (ESI-LC-
53 MS/MS), recorded on an Orbitrap mass spectrometer⁹. Spectra were analyzed via
54 MascotTM software using the NCBI nr Protein Database and a database from
55 *M. gryphiswaldense*¹⁰.

56

57
58 1 Martinez-Garcia, E., Calles, B., Arevalo-Rodriguez, M. & de Lorenzo, V. pBAM1: an all-
59 synthetic genetic tool for analysis and construction of complex bacterial phenotypes. *BMC*
60 *Microbiol.* **11**, 38 (2011).
61 2 Viollier, E., Inglett, P. W., Hunter, K., Roychoudhury, A. N. & Van Cappellen, P. The ferrozine
62 method revisited: Fe(II)/Fe(III) determination in natural waters. *Appl. Geochem.* **15**, 785-790
63 (2000).
64 3 Scheffel, A. & Schüler, D. The acidic repetitive domain of the *Magnetospirillum*
65 *gryphiswaldense* MamJ protein displays hypervariability but is not required for
66 magnetosome chain assembly. *J. Bacteriol.* **189**, 6437-6446 (2007).
67 4 Uebe, R. *et al.* The cation diffusion facilitator proteins MamB and MamM of
68 *Magnetospirillum gryphiswaldense* have distinct and complex functions, and are involved in
69 magnetite biomineralization and magnetosome membrane assembly. *Mol. Microbiol.* **82**,
70 818-835, doi:10.1111/j.1365-2958.2011.07863.x (2011).
71 5 Grünberg, K. *et al.* Biochemical and proteomic analysis of the magnetosome membrane in
72 *Magnetospirillum gryphiswaldense*. *Appl. Environ. Microbiol.* **70**, 1040-1050 (2004).
73 6 Lang, C. & Schüler, D. Expression of green fluorescent protein fused to magnetosome
74 proteins in microaerophilic magnetotactic bacteria. *Appl. Environ. Microbiol.* **74**, 4944-4953
75 (2008).
76 7 Laemmli, U. K. Cleavage of structural proteins during the assembly of the head of
77 bacteriophage T4. *Nature* **227**, 680-685 (1970).
78 8 Uebe, R. *et al.* The cation diffusion facilitator proteins MamB and MamM of
79 *Magnetospirillum gryphiswaldense* have distinct and complex functions, and are involved in
80 magnetite biomineralization and magnetosome membrane assembly. *Mol. Microbiol.* **82**,
81 818-835 (2011).
82 9 Klein, A. *et al.* Characterization of the insertase for beta-barrel proteins of the outer
83 mitochondrial membrane. *J. Cell Biol.* **199**, 599-611 (2012).
84 10 Richter, M. *et al.* Comparative genome analysis of four magnetotactic bacteria reveals a
85 complex set of group-specific genes implicated in magnetosome biomineralization and
86 function. *J. Bacteriol.* **189**, 4899-4910 (2007).

87

88

Biosynthesis of magnetic nanostructures in a foreign organism by transfer of bacterial magnetosome gene clusters

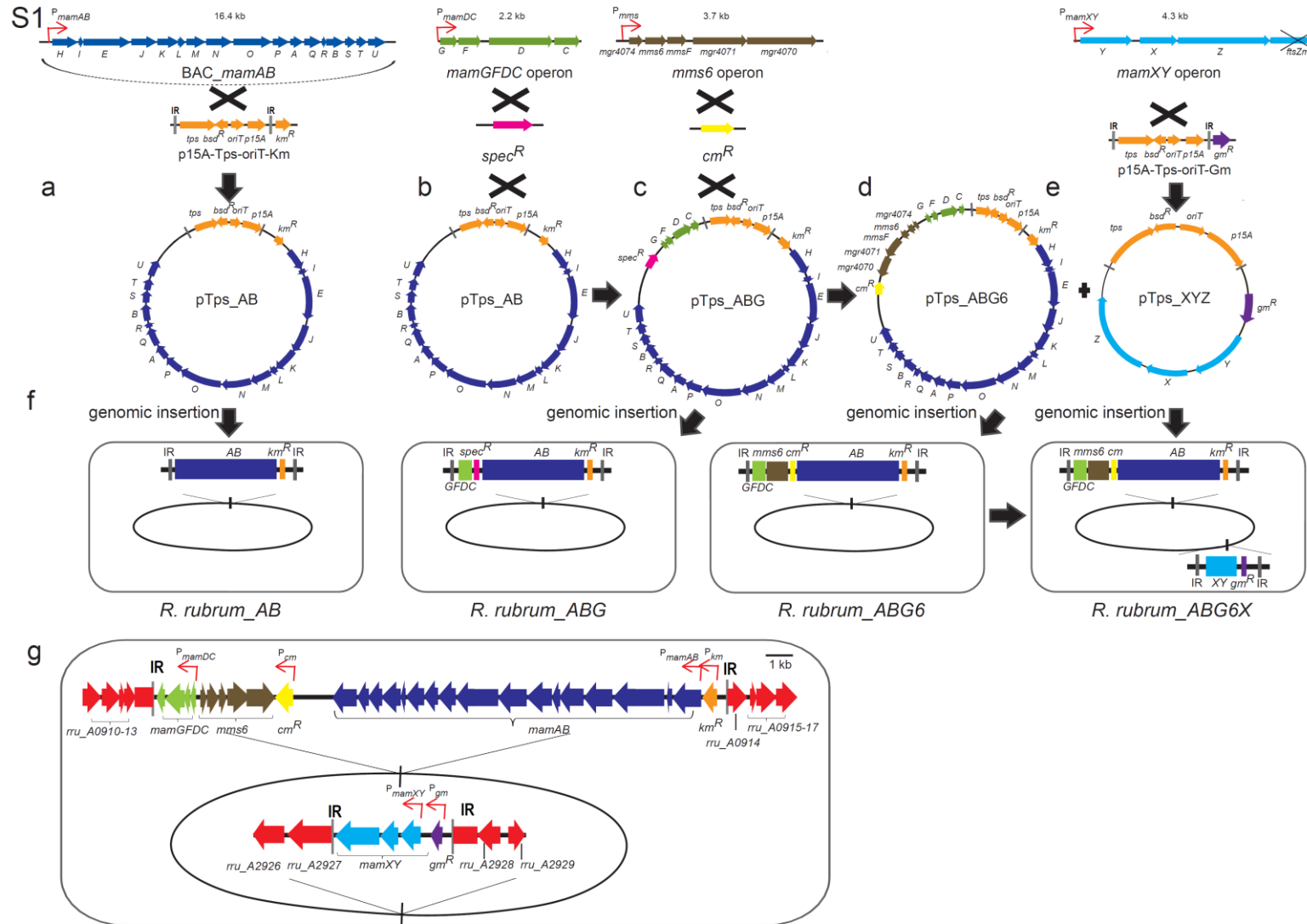


Fig. S1: Construction scheme of insertion cassettes for modular expression of the *mam* and *mms* operons. (a) Recombineering of a BAC containing the *mamAB* operon (blue) and a vector backbone (Km-p15A-Tps-oriT-Km, orange) harboring a MycoMar transposase gene (*tps*), inverted repeats (IR), origin of transfer (*oriT*), p15A origin of replication (*p15A*) and a *kanamycin*^R cassette (*km*^R, orange). (b) Insertion of a *spectinomycin*^R cassette (*spec*^R, pink) and the *mamGFDC* operon (green) into pTps_AB by triple recombination. (c & d) Stitching of pTps_ABG by insertion of the *mms6* operon and a *chloramphenicol*^R cassette. (e) pTps_XYZ consisting of a Tps vector backbone (orange), *mamXYZ* (pale blue) and a *gentamicin*^R gene (*gm*^R, purple) was constructed. (f) Plasmids were transferred by conjugation into *R. rubrum*. Transposition of the DNA-fragments within the IR sequences occurred at random positions at TA dinucleotide insertion sites by a “cut and paste” mechanism¹. (g) Chromosomal insertion sites of the transposed constructs in *R. rubrum*_ABG6X are shown with adjacent genes (red) as revealed by whole genome sequencing performed with a MiSeq sequencer (Illumina) (accession number of *R. rubrum* ATCC 11170: NC_007643). pTps_ABG6 inserted within a gene encoding a putative aldehyd dehydrogenase (YP_426002), and pTps_XYZ inserted within *rru_A2927*, encoding a putative acriflavin resistance protein (protein accession number YP_428011). Sequences of inserted magnetosome operons matched those of the donor (*M. gryphiswaldense*) with no detectable mutations, except for a deletion (aa 169-247) within the hypervariable non-essential CAR domain of *mamJ*, which was shown to be irrelevant for protein function².

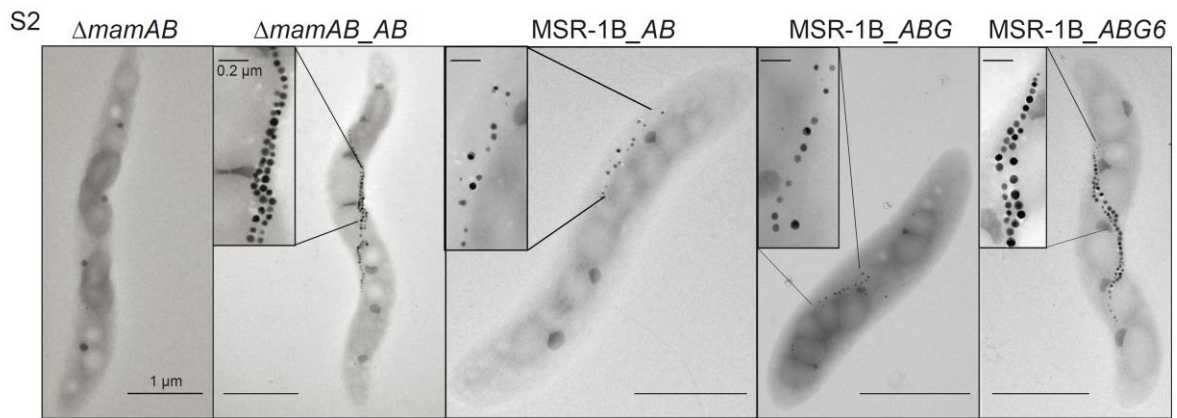


Fig. S2: Transmission electron micrographs of MSR mutants expressing various insertional transposon constructs. The plasmids pTps_ AB , pTps_ ABG and pTps_ $ABG6$ were transferred into the non-magnetic *M. gryphiswaldense* mutants $\Delta mamAB^3$ and MSR-1B, the latter lacking most of the magnetosome genes except of the *mamXY* operon^{3,4}. After transfer of pTps_ AB , a wt-like phenotype was restored in $\Delta mamAB_AB$ as revealed by C_{mag} (1.2 ± 0.2) and measured crystal sizes (37 ± 10 nm) in comparison with *M. gryphiswaldense* wt (36 ± 9 nm, $C_{mag}=1.4 \pm 0.2$) (see also Table S1). Mutant MSR-1B was only partly complemented after insertion of pTps_ AB and pTps_ ABG , that is, C_{mag} and crystal sizes were still lower than in the wt (Table S1). Transfer of pTps_ $ABG6$ restored nearly wt-like magnetosome formation in MSR-1B (35 ± 8 nm, $C_{mag}=0.9 \pm 0.1$). \pm = s.d. Scale bar: 1 μ m, insets: 0.2 μ m.

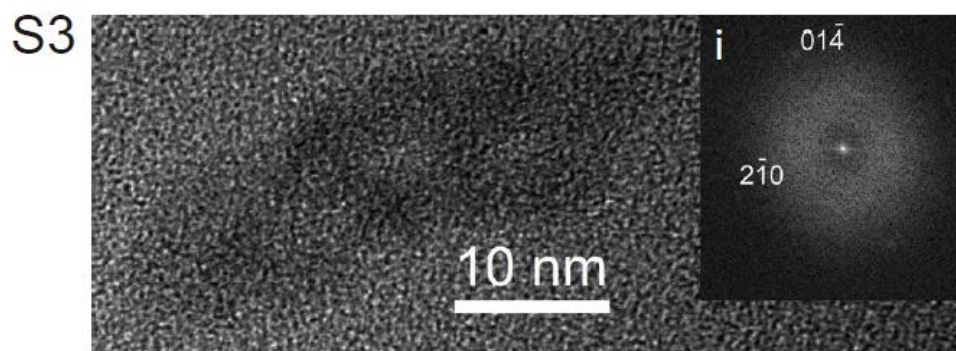


Fig. S3: HRTEM image of a poorly crystalline iron oxide particle from *R. rubrum_ABG6* with the corresponding Fourier transform (i) that shows diffuse, faint intensity maxima consistent with the structure of hematite.

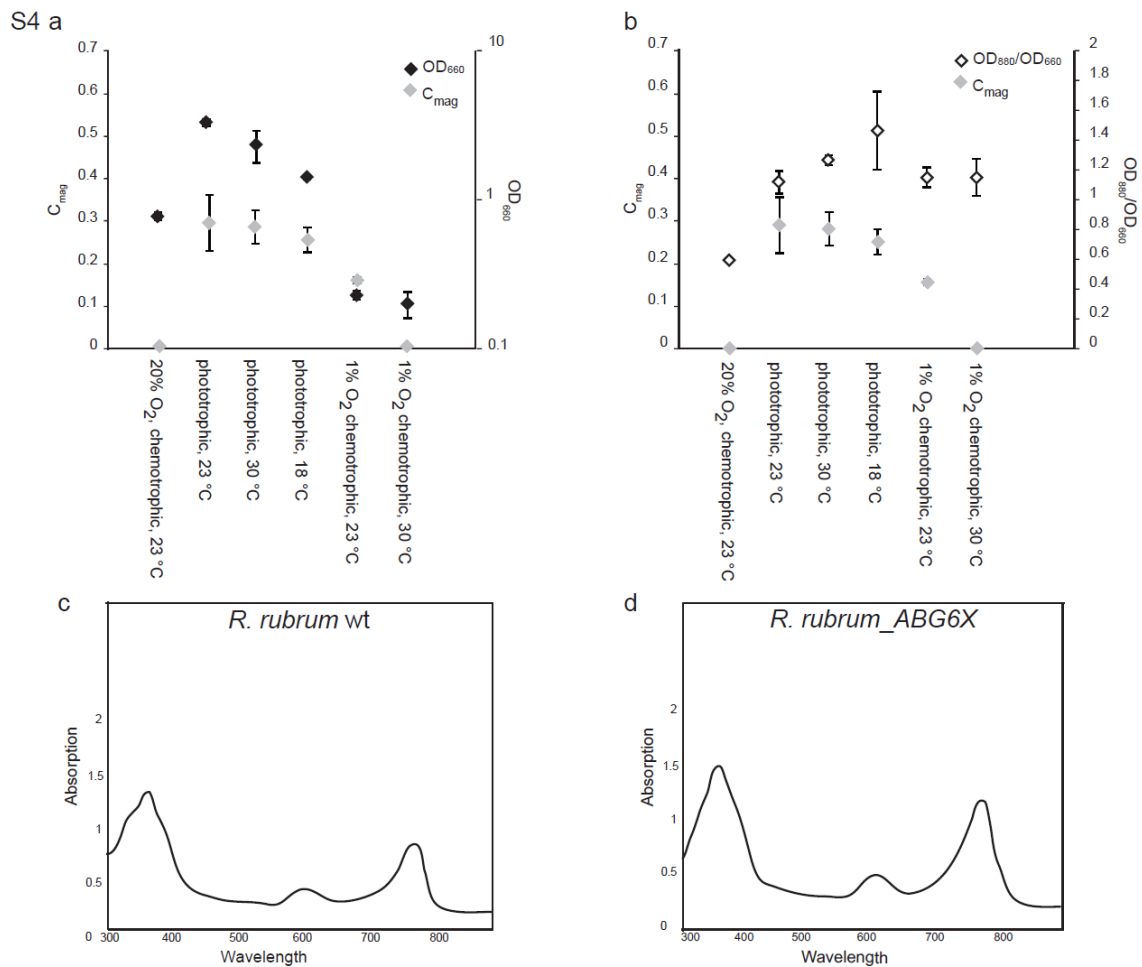


Fig. S4: Growth, magnetic response and ICM/Bchl a production of *R. rubrum_ABG6X*. (a & b) Cells were grown in ATCC 112 (chemotrophic, 20% O_2), Sistrom A (phototrophic, anoxygenic) and M2SF (chemotrophic, 1% O_2) medium for 3 (30 °C), 4 (23 °C) or 10 (18 °C) days. Optical density at 660 nm (minimal Bchl a absorption, black diamonds), 880 nm (maximal Bchl a absorption) and magnetic response (grey diamonds) were measured. The ratio OD_{880}/OD_{660} (white diamonds) correlates with the amount of chromatophores produced in the cells⁵ (median values $n=3$, error bars indicate s.d.). No C_{mag} was detectable under aerobic and microaerobic conditions at 30 °C. (c & d) Absorption spectra of extracted bacteriochlorophylls from *R. rubrum wt* (c) and *R. rubrum_ABG6X* (d) (phototrophic growth, 30 °C).

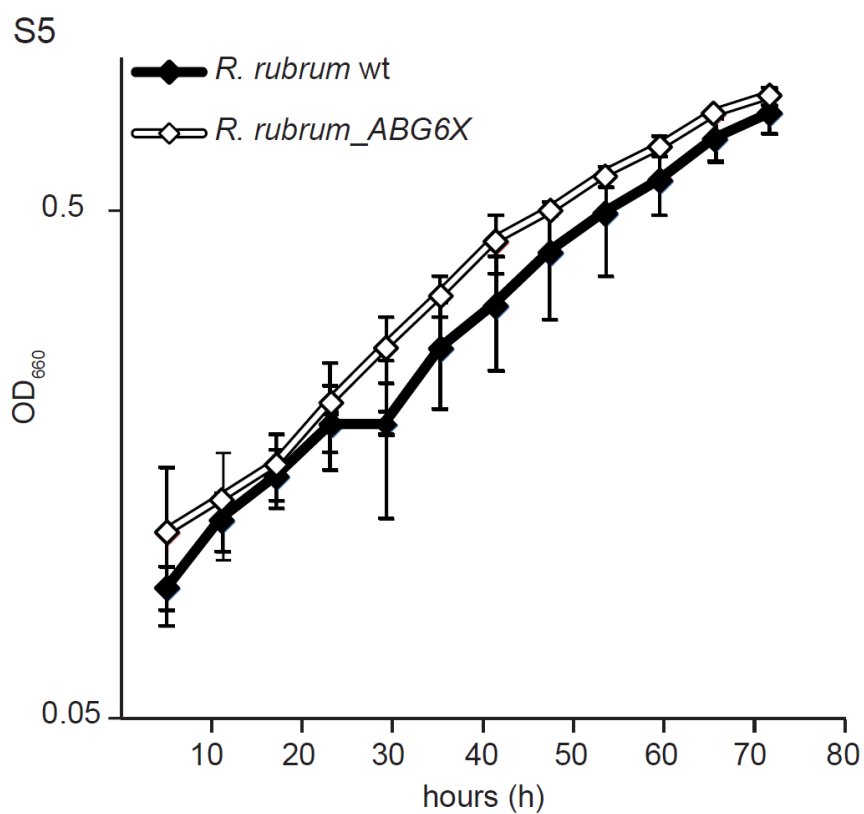


Fig. S5: Growth of *R. rubrum* wt and *R. rubrum_ABG6X* (OD₆₆₀). Cells of *R. rubrum* (Sistrom A medium, 1000 lux) were incubated in Sistrom A medium (1000 lux) for 3 days at 23 °C under anaerobic conditions. No major growth differences between wt (n=3) and mutant strain *ABG6X* (median values n=3, error bars indicate s.d.) were detectable .

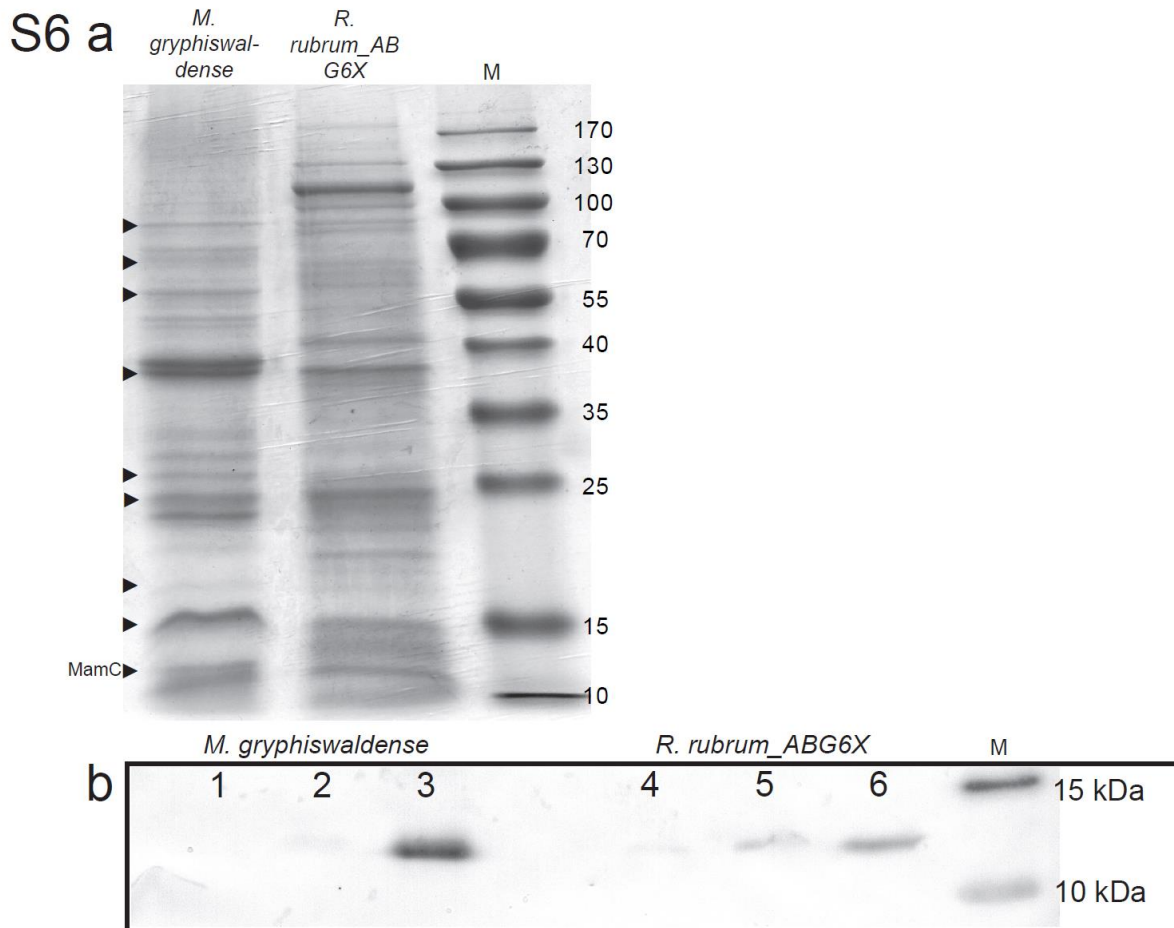


Fig. S6: Proteomic analysis of magnetosomes from *R. rubrum_ABG6X*. (a) 1D SDS-PAGE of Coomassie blue stained proteins solubilized from isolated magnetosome particles of *M. gryphiswaldense* and *R. rubrum_ABG6X*. Bands of the same size are indicated (arrowheads). (b) Immunodetection of MamC (12.4 kDa) in blotted fractions of *M. gryphiswaldense* and *R. rubrum_ABG6X* using an anti-MamC antibody⁶. A signal for MamC was detectable in the magnetic membrane fraction of *R. rubrum_ABG6X* (6), which was absent from the soluble fraction, but faintly present also in the non-magnetic membrane fraction (5), possibly originating from empty membrane vesicles or incomplete magnetic separation during isolation. Protein extracts from *M. gryphiswaldense*: 1. soluble fraction, 2. non-magnetic membrane fraction, 3. magnetosome membrane. Protein extracts from *R. rubrum_ABG6X*: 4. soluble fraction, 5. non-magnetic membrane fraction, 6. magnetic (“magnetosome”) membrane fraction. M: Marker.

S7

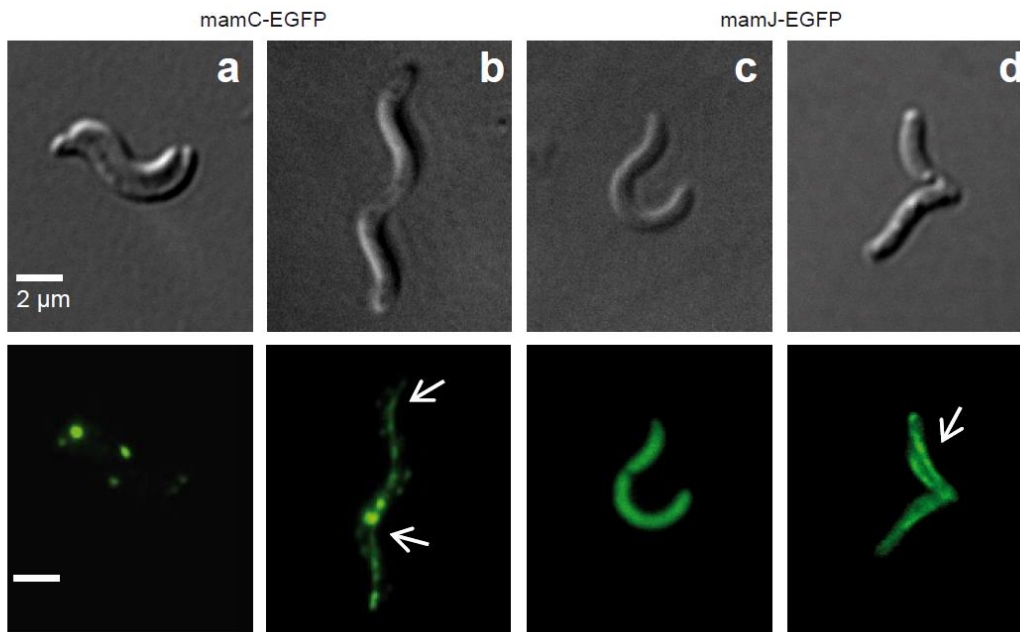


Fig. S7: Fluorescence microscopy of *R. rubrum* wt and *R. rubrum*_ABG6X cells expressing different EGFP-tagged magnetosome proteins. For localization studies of fluorescently labeled magnetosome proteins, strains were cultivated in ATCC medium overnight at 30 °C with appropriate antibiotics (Table S3). **(a & b)** MamGFDC with a C-terminal MamC-EGFP fusion expressed in *R. rubrum* wt (n=151) **(a)**, and *R. rubrum*_ABG6X (n=112) **(b)**. In the transformed strain, a filamentous structure is visible for 79% of the cells (n=89). **c & d**, MamJ-EGFP expressed in *R. rubrum* wt (n=109) **(c)**, and in *R. rubrum*_ABG6X (n=89) displaying a chain-like fluorescence signal in 63% of the cells (n=56) **(d)**. Scale bar: 2 μm.

S8

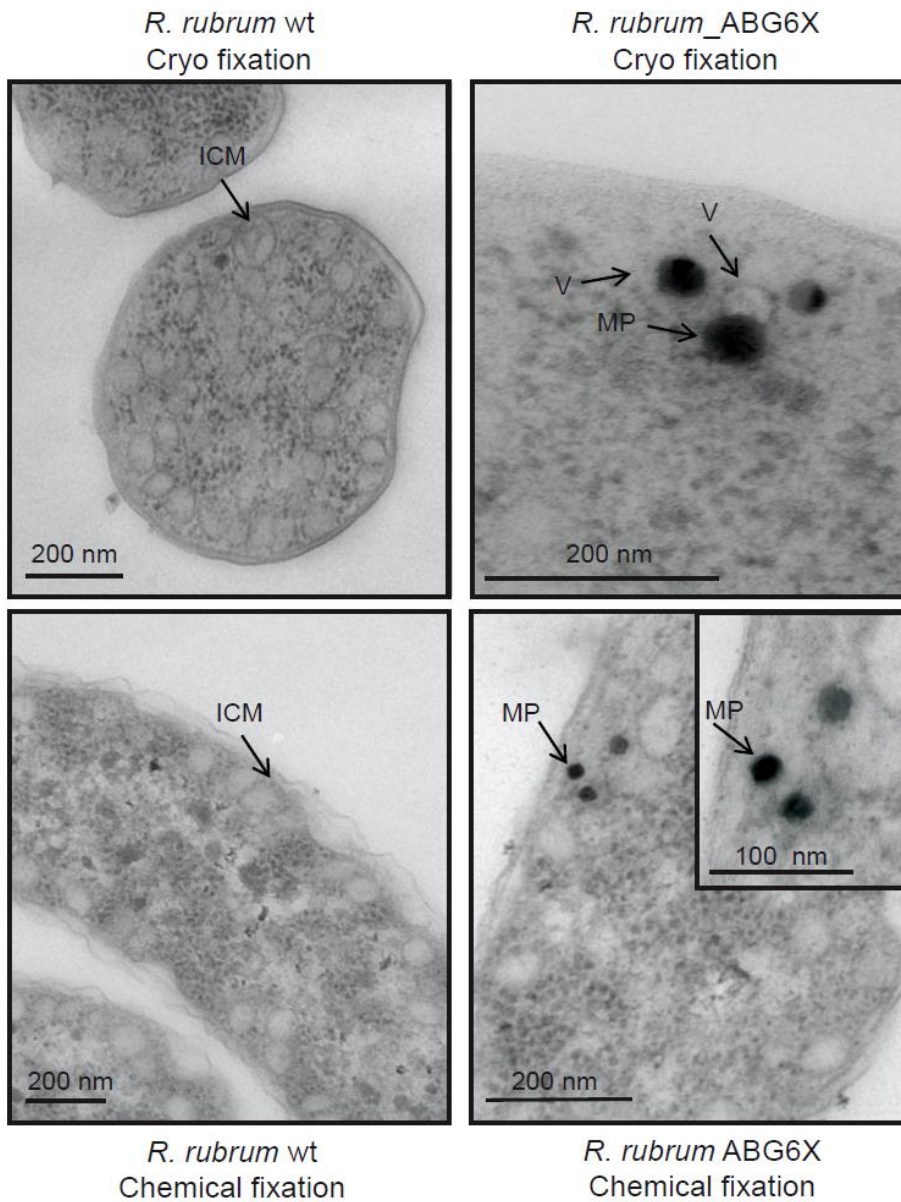


Fig. S8: TEM of cryo- or chemically fixed, thin sectioned *R. rubrum* strains.

Cells were cultivated under photo-heterotrophic conditions. ICM sizes of cryo-fixed *R. rubrum* wt (93 ± 34 nm, $n=95$) and vesicles surrounding immature magnetosomes of cryo-fixed *R. rubrum*_ABG6X (66 ± 6 nm, $n=6$) were measured.

S9

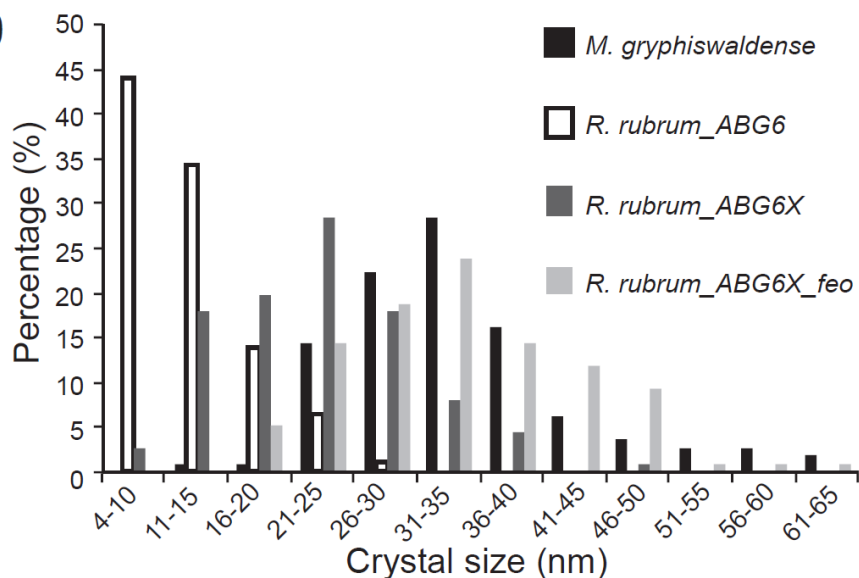


Fig. S9: Size distribution of magnetosome crystals in *M. gryphiswaldense* and different *R. rubrum* strains. Whereas crystals of *R. rubrum_ABG6* (n=303) and *R. rubrum_ABG6X* (n=306) were smaller than those of the donor *M. gryphiswaldense* (n=310), crystal sizes of *R. rubrum_ABG6X_feo* (n=301) were significantly larger, approaching those of the donor strain (see also Supplementary Table 1).

S10

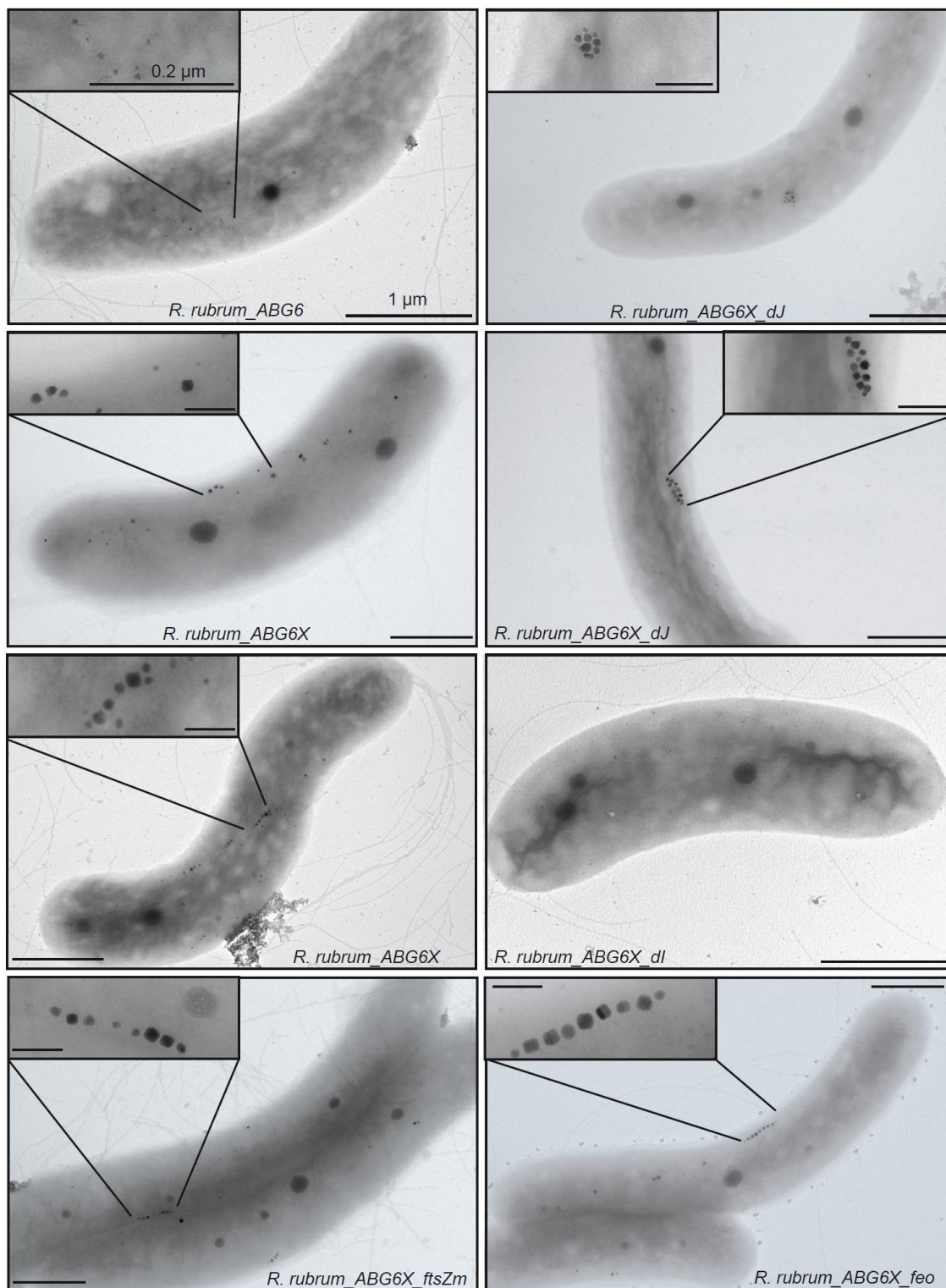


Figure S10: Transmission electron micrographs of whole cells of different *R. rubrum* strains expressing magnetosome gene clusters. Scale bar: 1 μ m, inset: 0.2 μ m.

- 1 Rubin, E. J. *et al.* *In vivo* transposition of *mariner*-based elements in enteric bacteria and mycobacteria. *Proc. Natl. Acad. Sci. U S A* **96**, 1645-1650 (1999).
- 2 Scheffel, A. & Schüler, D. The acidic repetitive domain of the *Magnetospirillum gryphiswaldense* MamJ protein displays hypervariability but is not required for magnetosome chain assembly. *J. Bacteriol.* **189**, 6437-6446 (2007).
- 3 Lohsse, A. *et al.* Functional analysis of the magnetosome island in *Magnetospirillum gryphiswaldense*: the *mamAB* operon is sufficient for magnetite biomineralization. *PLoS One* **6**, e25561 (2011).
- 4 Schübbe, S. *et al.* Characterization of a spontaneous nonmagnetic mutant of *Magnetospirillum gryphiswaldense* reveals a large deletion comprising a putative magnetosome island. *J. Bacteriol.* **185**, 5779-5790 (2003).
- 5 Ghosh, R., Hardmeyer, A., Thoenen, I. & Bachofen, R. Optimization of the Siström Culture Medium for Large-Scale Batch Cultivation of *Rhodospirillum rubrum* under Semiaerobic Conditions with Maximal Yield of Photosynthetic Membranes. *Appl. Environ. Microbiol.* **60**, 1698-1700 (1994).
- 6 Lang, C. & Schüler, D. Expression of green fluorescent protein fused to magnetosome proteins in microaerophilic magnetotactic bacteria. *Appl. Environ. Microbiol.* **74**, 4944-4953 (2008).

Biosynthesis of magnetic nanostructures in a foreign organism by transfer of bacterial magnetosome gene clusters

Table S1: Summary of magnetic responses (“C_{mag}”), intracellular iron content and crystal size and number of various strains (median values, ± = standard deviation). If not indicated otherwise, cells were grown in the presence of 50 µM ferric citrate. Magnetic response and total iron content measurements were performed with (n) biological replicates under identical conditions (see also material & methods). For determination of crystal size and number per cell, cells of one clone were analyzed by TEM (n=sample size). The Mann-Whitney test (<http://elegans.som.vcu.edu/~leon/stats/utest.html>) was performed for crystal size comparison of *R. rubrum_ABG6X* and *R. rubrum_ABG6X_feo*: the difference was highly significant ($p < 0.001$, two tailed test). Crystal size comparison of *R. rubrum_ABG6X_feo* and *M. gryphiswaldense* revealed no significant difference ($p \geq 0.05$, two tailed test).

Strain	Magnetic response (“C _{mag} ”)	Iron content (% dry weight)	Crystal size (nm)	Crystal number per cell
<i>M. gryphiswaldense</i> MSR-1	1.4 ± 0.2 (n=3)	3.5 (n=3)	36 ± 9 (n=310)	24 ± 8 (n=52)
<i>M. gryphiswaldense</i> Δ mamAB_AB	1.2 ± 0.2 (n=3)	n.d.	37 ± 10 (n=112)	23 ± 7 (n=24)
<i>M. gryphiswaldense</i> MSR-1B_AB	0.2 (n=3)	n.d.	17 ± 6 (n=112)	16 ± 6 (n=20)
<i>M. gryphiswaldense</i> MSR-1B_ABG	0.6 ± 0.1, (n=3)	n.d.	25 ± 6 (n=104)	13 ± 6 (n=20)
<i>M. gryphiswaldense</i> MSR-1B_ABG6	0.9 ± 0.2 (n=3)	n.d.	35 ± 8 (n=103)	18 ± 8 (n=22)
<i>R. rubrum</i> ATCC 11170	-	0.07 ± 0.04 (n=3)	-	-
<i>R. rubrum</i> _AB	-	0.08 (n=3)	-	-
<i>R. rubrum</i> _ABG	-	0.10 ± 0.01 (n=3)	-	-
<i>R. rubrum</i> _ABG6	-	0.17 (n=4)	12 ± 6 (n=304)	26 ± 10 (n=50)
<i>R. rubrum</i> _ABG6X	0.3 ± 0.2 (n=3)	0.17 ± 0.02 (n=4)	24 ± 7 (n=307)	10 ± 4 (n=50)
<i>R. rubrum</i> _ABG6X 500 µM ferric citrate	0.3 (n=4)	n. d.	25 ± 7 (n=301)	11 ± 5 (n=51)
<i>R. rubrum</i> _ABG6X 100 µM ferrous sulfate	0.2 (n=4)	n.d.	24 ± 8 (n=312)	10 ± 5 (n=52)

<i>R. rubrum</i> _ABG6X_ftsZm	0.6 ± 0.1* (n=3)	0.18 ± 0.03 (n=3)	26 ± 9 (n=300)	11 ± 4 (n=51)
<i>R. rubrum</i> _ABG6X_dJ	0.2 (n=3)	0.18 ± 0.01 (n=3)	27 ± 9 (n=300)	9 ± 4 (n=50)**
<i>R. rubrum</i> _ABG6X_dI	-	0.09 ± 0.07 (n=3)	-	-
<i>R. rubrum</i> _ABG6X_feo	0.8 ± 0.1 (n=3)	0.28 ± 0.07 (n=3)	37 ± 10 (n=300)	10 ± 4 (n=52)

*The slightly increased C_{mag} is likely due to effects of the genuine cell division protein FtsZm on cell morphology, as no difference in iron content and crystal size or number per cell was detectable.

**64% of mutant cells (n=32) harbored clustered magnetosomes, whereas 36% still showed a chain-like alignment of magnetosomes (n=18).

Table S2: Magnetosome proteins identified in the MM of strain *R. rubrum*_ABG6X by nano-electrospray ionization-LC tandem MS (ESI-LC-MS/MS). Spectra were analyzed via Mascot™ software using the NCBI nr Protein Database and a database from *M. gryphiswaldense*¹ (asterisks). Proteins are listed in the order of their exponentially modified protein abundance index (emPAI). The data have been deposited to ProteomeXchange with identifier PXD000348 (DOI 10.6019/PXD000348).

Protein	Accession number	Coverage (%)	No. of spectrum matches	No. of sequence peptides	Molecular weight (kDa)	Calculated pI	emPAI	Putative function
MamK	MGR_4093	57	9	9	39.6	5.4	1.51	Magnetosome chain assembly/positioning ^{2,3}
MamC	MGR_4078	32	4	3	12.4	5.1	1.01	Crystal size and shape control ⁴
MamJ	MGR_4092	32	10	6	48.6	4.0	0.76	Magnetosome chain assembly ⁵
MamA	MGR_4099	37	1	1	23.9	5.7	0.65	TPR-like protein associated with the magnetosome membrane ^{6,7}
MamF	MGR_4076	17	1	1	12.4	9.1	0.60	Magnetosome size and shape control ⁴
Mms6	MGR_4073	19	1	1	12.7	9.5	0.58	Magnetosome crystallization ^{8,9}
MamD	MGR_4077	20	3	3	30.2	9.8	0.49	Crystal size and shape control ⁴
MamM*	MGR_4095	15	3	3	34.7	5.8	0.42	Iron transport/MM assembly ¹⁰
MmsF*	MGR_4072	8	2	1	13.9	9.3	0.23	Crystal size and shape control ¹¹
MamB*	MGR_4102	7	1	1	32.1	5.4	0.21	Iron transport/MM assembly ¹⁰
MamY*	MGR_4150	18	2	2	40.9	4.8	0.16	Tubulation and magnetosome membrane formation ¹²
MamO*	MGR_4097	6	3	3	65.3	6.5	0.15	Magnetosome crystallization ^{13,14}
MamE	MGR_4091	4	2	2	78.3	8.1	0.08	Magnetosome crystallization ^{13,14}

Table S3: Strains and plasmids used in this study. Km^R= kanamycin resistance, Tc^R= tetracycline resistance, Ap^R= ampicillin resistance, BSD^R= blasticidin S resistance, Cm^R= chloramphenicol resistance, Gm^R= gentamicin resistance, Spec^R= spectinomycin resistance.

Strain or plasmid	Characteristics	Reference(s) or source
<i>Magnetospirillum gryphiswaldense</i> strains		
<i>M. gryphiswaldense</i> MSR-1	Wild-type (wt)	DSM-6361, ¹⁵
<i>M. gryphiswaldense</i> MSR-1B	spontaneous unmagnetic mutant lacking parts of the MAI	¹⁶
<i>M. gryphiswaldense</i> Δ <i>mamAB</i>	<i>mamAB</i> deletion mutant	¹⁷
<i>M. gryphiswaldense</i> Δ <i>mamAB</i> _AB	Km ^R , transposon mutant with inserted <i>mamAB</i> operon	This study
<i>M. gryphiswaldense</i> MSR-1B_AB	Km ^R , transposon mutant with inserted <i>mamAB</i> operon	This study
<i>M. gryphiswaldense</i> MSR-1B_ABG	Km ^R , Spec ^R , transposon mutant with inserted <i>mamAB</i> and <i>mamGFDC</i> operon	This study
<i>M. gryphiswaldense</i> MSR-1B_ABG6	Km ^R , Cm ^R , transposon mutant with inserted <i>mamAB</i> , <i>mamGFDC</i> and <i>mms6</i> operon	This study
<i>Rhodospirillum rubrum</i> strains		
<i>R. rubrum</i> ATCC 11170	wt	¹⁸ (kindly provided by H. Grammel, Magdeburg)
<i>R. rubrum</i> _AB	Km ^R , transposon mutant with inserted <i>mamAB</i> operon	This study
<i>R. rubrum</i> _ABG	Km ^R , Spec ^R , transposon mutant with inserted <i>mamAB</i> and <i>mamGFDC</i> operon	This study
<i>R. rubrum</i> _ABG6	Km ^R , Cm ^R , transposon mutant with inserted <i>mamAB</i> , <i>mamGFDC</i> and <i>mms6</i> operon	This study
<i>R. rubrum</i> _ABG6X	Km ^R , Cm ^R , Gm ^R transposon mutant with inserted <i>mamAB</i> , <i>mamGFDC</i> , <i>mms6</i> and <i>mamXY</i> operon (without <i>ftsZm</i>)	This study
<i>R. rubrum</i> _ABG6X_dJ	Km ^R , Cm ^R , Gm ^R , Ap ^R transposon mutant with inserted <i>mamAB</i> (<i>mamJ</i> deletion), <i>mamGFDC</i> , <i>mms6</i> and <i>mamXY</i> operon (without <i>ftsZm</i>)	This study
<i>R. rubrum</i> _ABG6X_dI	Km ^R , Cm ^R , Gm ^R , Ap ^R transposon mutant with inserted <i>mamAB</i> (<i>mamI</i> deletion), <i>mamGFDC</i> , <i>mms6</i> and <i>mamXY</i> operon (without <i>ftsZm</i>)	This study
<i>R. rubrum</i> _ABG6X_ftsZm	Km ^R , Cm ^R , Gm ^R , Tc ^R transposon mutant with inserted <i>mamAB</i> , <i>mamGFDC</i> , <i>mms6</i> and <i>mamXY</i> operon (without <i>ftsZm</i>) and <i>ftsZm</i>	This study

	under control of an inducible lac promoter	
<i>R. rubrum</i> _ABG6X_feo	Km ^R , Cm ^R , Gm ^R , Tc ^R transposon mutant with inserted with inserted <i>mamAB</i> , <i>mamGFDC</i> , <i>mms6</i> , <i>mamXY</i> and <i>feoAB1</i> operon	This study
<i>R. rubrum</i> _GFDC-EGFP	Tc ^R transposon mutant with inserted <i>mamGFDC-EGFP</i>	This study
<i>R. rubrum</i> _ABG6X_GFDC-EGFP	Km ^R , Cm ^R , Gm ^R , Tc ^R transposon mutant with inserted <i>mamAB</i> , <i>mamGFDC</i> , <i>mms6</i> and <i>mamXY</i> operon (without <i>ftsZm</i>) and <i>mamGFDC-EGFP</i>	This study
<i>R. rubrum</i> _J-EGFP	Tc ^R transposon mutant with inserted <i>mamGFDC-EGFP</i>	This study
<i>R. rubrum</i> _ABG6X_J-EGFP	Km ^R , Cm ^R , Gm ^R , Tc ^R transposon mutant with inserted <i>mamAB</i> , <i>mamGFDC</i> , <i>mms6</i> and <i>mamXY</i> operon (without <i>ftsZm</i>) and <i>mamJ-EGFP</i>	This study
<i>Escherichia coli</i> strains		
DH10b	<i>F</i> - <i>mcrA</i> Δ (<i>mrr-hsdRMS-mcrBC</i>) Φ 80 <i>lacZ</i> Δ M15 Δ <i>lacX74</i> <i>recA1</i> <i>endA1</i> <i>araD139</i> Δ (<i>ara leu</i>) 7697 <i>galU</i> <i>galK</i> <i>rpsL</i> <i>nupG</i> λ -	Invitrogen
BW29427	<i>dap</i> auxotroph derivative of <i>E. coli</i> strain B2155	K. Datsenko and B. L. Wanner, unpublished
WM3064	<i>thrB1004</i> <i>pro thi rpsL hsdS</i> <i>lacZ</i> Δ M15 RP4-1360 Δ (<i>araBAD</i>)567 Δ <i>dapA1341::[erm pir]</i>	W. Metcalf, kindly provided by J. Gescher, KIT Karlsruhe
Plasmids		
pSC101-BAD-gbaA	Tc ^R , replicative plasmid containing <i>redα/redβ</i> recombinases under the control of a L-Arabinose inducible promoter, temperature sensitive origin of replication	19
p15A-Tps-oriT-Km	Km ^R , BSD ^R , oriT, p15A origin of replication, mariner tps, cloning cassette	20
pSSK18 (BAC_ <i>mamAB</i>)	BAC containing the <i>mamAB</i> operon from <i>M. gryphiswaldense</i>	16
pTps_AB	Km ^R , BSD ^R , mariner tps vector containing <i>mamAB</i> operon	This study
pTps_ABG	Spec ^R , Km ^R , BSD ^R , mariner tps vector with <i>mamAB</i> and <i>mamGFDC</i> operon	This study
pTps_ABG6	Cm ^R , Km ^R , BSD ^R , mariner tps vector with <i>mamAB</i> , <i>mamGFDC</i> , and <i>mms6</i> operon	This study
pTps_XYZ	Gm ^R , BSD ^R , mariner Tps vector with <i>mamY</i> , <i>mamX</i> and <i>mamZ</i>	This study

pTps_ABG6_dJ	Cm ^R , Km ^R , BSD ^R , Ap ^R , mariner tps vector with <i>mamAB</i> , <i>mamGFDC</i> , and <i>mms6</i> operon, (<i>mamJ</i> deletion)	This study
pTps_ABG6_dl	Cm ^R , Km ^R , BSD ^R , Ap ^R , mariner tps vector with <i>mamAB</i> , <i>mamGFDC</i> , and <i>mms6</i> operon, (<i>mamI</i> deletion)	This study
pBAM1	Km ^R , Ap ^R , γ R6K origin of replication, oriT, Tn5 vector	21
Tet-pBAM1	Tc ^R , Ap ^R , γ R6K origin of replication, oriT, Tn5 vector	This study
Tet-pBam_mamGFDC-EGFP	Tc ^R , Ap ^R , <i>mamGFDC</i> operon under control of P _{<i>mamDC</i>} with a C-terminal EGFP fusion, Tn5 vector	This study
Tet-pBam_MamJ-EGFP	Tc ^R , Ap ^R , <i>mamJ</i> under control of P _{<i>mamDC</i>} with a C-terminal EGFP fusion, Tn5 vector	This study
pRU-1feoAB	Km ^R , broad host range pBBRMCS2, <i>feoAB1</i> operon under the control of P _{<i>mamH</i>}	R. Uebe, unpublished
Tet-pBam_feoAB1	Tc ^R , Ap ^R , <i>feoAB1</i> operon under the control of P _{<i>mamH</i>} , Tn5 vector	This study
Tet-pBam-ftsZm_mCherry	Tc ^R , Ap ^R , <i>ftsZm</i> , <i>lacI</i> with a C-terminal mCherry fusion under control of inducible P _{<i>lac</i>} , Tn5 vector	This study
pFM211	Km ^R , broad host range pBBRMCS2, <i>lacI</i> , <i>ftsZm</i> with C-terminal <i>mCherry</i> fusion, <i>mamK</i> with N-terminal EGFP fusion	F. Müller, unpublished

Table S4: Oligonucleotides used in this study.

Primer	Nucleotide sequence (5'-3') ^a	Product
Mam-tps5	AATTCGCACGGACTATAGCAACGAATCGAGGTCGGTTGAC AAGCCATAAATCAGAAGAACTCGTCAAGAAGGC	p15A-Tps-oriT-Km, ET-recombination with BAC_ <i>mamAB</i> , pTps_AB
Mam-tps3	GAACGAAGATGAGACAGAAATCCGTGGCGCCGAGCGTAA GCATCCGGTGAGAACCCTCATTCCCTCATGATACAG	
mamGFC3	TATCATGAGGGAATGAGGTTCTCACC GGATGCTTACGCTC GGCGCCAGAGCACATCGGGGTGAATGACGAC	<i>mamGFDC</i> operon, ET-recombination with pTps_AB
mamGFC5	CGCTAGCTGCGGGTTATTTCGCATTTGC	
spectMam3	TCAAACCCGCGCAGAGGCAAATGCGAATAACCCGCAGCT AGCGTTATAATTTTTTAACTCTGTATT	Spectinomycin resistance cassette, ET-recombination with pTps_AB
spectMam5	TGATCCGCTATGGTAAGCGCATCATGTCCGGATCCCATGG CGTTCCGCTCGTAACGTGACTGGCAAGAGATATT	
mms6cm5	TACTGCGATGAGTGGCAGGGCGGGCGTAAGCTTACAATT TCCATTGCGCCATTC	<i>mms6</i> operon, ET- recombination with pTps_ABG
mms6mam3	GTGCTTCGCTGTGTCCACAAGAACC	
cm-mms6-3	TGGCGAATGGA AATTGTAAGCTTACGCCCGCCCTGCCAC TC	Chloramphenicol resistance cassette, ET-recombination with pTps_ABG
cm-mms6-5	TGATCCGCTATGGTAAGCGCATCATGTCCGGATCCCATGG CGTTCCGCTCGTCTGTGTCCCTGTTGATACC	
IK097	TCTAGAGGGCCCAACTTTTTCGCTTTACTAGCTCTTAGTT CTCCAATAAATTCCTGCGTCGA	<i>P_{mamDC}</i> in pBAM1
IK098	CATATGCTGATCTCCGGCAAGTGTATGCACGATTCCCTCTC TGCCCTTAAAATCGACGCAGGGAAT	
IK107	CATATGATCAAGGGCATCGCGGG	<i>mamGFDC</i> operon in pBAM1
IK101	GGTACCGGCCAATTCTTCCCTCAGAA	
IK102	GGTACCGGAGGCGGAGGCGGT	<i>egfp</i> in pBAM1
IK103	GAATTCCTTACTTGTACAGCTCGTCCATG	
IK163	GAATTCCTTAGCCGATTTCGCGAG	<i>mamXY</i> -operon (without <i>ftsZm</i>), ET- recombination with p15A-Tps-oriT-Gm
IK164	GAGCTCGGCAGCCTCATTTAA	
IK173	CCGGAATTGCCAGCTGGGGCGCCCTCTGGTAAGGTTGGG AAGCCCTGCAACGTATAATTTGCCCATG	Gentamicin resistance cassette, ET-Recombination with p15A-Tps-oriT- Km
IK174	AGGCGATAGAAGGCGATGCGCTGCGAATCGGGAGCGGCG ATACCGTAAAGCGATCTCGGCTTGAA	
IK208	CCCGGTACCCAGCTTTTGTTCCTTTAGTGAGGGTTAATTG CGCGCTTGGCCTCATTCCCTCATGATACAGAGAC	p15A-Tps-oriT-Gm, ET-recombination with <i>mamXY</i>
IK209	GGCGTTACCCAACCTTAATCGCCTTGACGACATCCCCCTTT CGCCAGCTGTCTCGGCTTGAACGAATTG	
IK213	GACGTCGAGCCACGGCGG	Tetracycline resistance cassette in pBAM1
IK214	GGGTCCCTCAGGTCGAGGTGGC	
IK215	TCTAGACTACAAGAATGTCCCGC	<i>feoAB1</i> operon+ <i>P_{mamH}</i> in pBAM1
IK216	GAATTCGGCATCCTGATCGGT	
IK217	CATATGATGGCAAAAACCGG	<i>mamJ</i> in pBAM1
IK218	GGCGGTACCTTTATTCTTATCTTCAGCATCAC	
IK235	GGGTGGAGCGGGATAATGGCAAAAACCGGCGTGATCGC GGCACGGCTAAATACATTCAAATATGTATCC	Ampicillin resistance cassette insertion into <i>mamJ</i> of pTps_ABG6
IK236	CTATTTATTCTTATCTTCAGCATCACATTTGCGGATGAACA ACTACCTTACCAATGCTTAATCAGTG	
IK239	CGCCGCTTGTGTTCTGTATCAAGACTGGAGAACGTTTATG CCAATAAATACATTCAAATATGTATCC	Ampicillin resistance cassette Insertion into <i>mamI</i> of pTps_ABG6
IK240	TCAACCATCGATGTTAGGGTCTGAGTTCGCCCTTTACCG GCAGGTTACCAATGCTTAATCAGTG	
IK251	AAACCGCCCAGTCTAGCTATCGCCATGTAAGCCCCTGCA AGCTACCTGCCCTCATTCCCTCATGATACA	Tet-pBAM1, ET- recombination with

IK252	CAGCACATCCCCCTTTGCGCCAGCTGGCGTAATAGCGAAGA GGCCCGCACCGGATTTTGAGACACAAGACGTC	recombination with pFM211
-------	---	------------------------------

References

- 1 Richter, M. *et al.* Comparative genome analysis of four magnetotactic bacteria reveals a complex set of group-specific genes implicated in magnetosome biomineralization and function. *J. Bacteriol.* **189**, 4899-4910 (2007).
- 2 Katzmann, E. *et al.* Magnetosome chains are recruited to cellular division sites and split by asymmetric septation. *Mol. Microbiol.* **82**, 1316-1329 (2011).
- 3 Draper, O. *et al.* MamK, a bacterial actin, forms dynamic filaments *in vivo* that are regulated by the acidic proteins MamJ and LimJ. *Mol. Microbiol.* **82**, 342-354 (2011).
- 4 Scheffel, A., Gardes, A., Grünberg, K., Wanner, G. & Schüler, D. The major magnetosome proteins MamGFDC are not essential for magnetite biomineralization in *Magnetospirillum gryphiswaldense* but regulate the size of magnetosome crystals. *J. Bacteriol.* **190**, 377-386 (2008).
- 5 Scheffel, A. *et al.* An acidic protein aligns magnetosomes along a filamentous structure in magnetotactic bacteria. *Nature* **440**, 110-114 (2006).
- 6 Zeytuni, N. *et al.* Self-recognition mechanism of MamA, a magnetosome-associated TPR-containing protein, promotes complex assembly. *Proc. Natl. Acad. Sci. U S A* **108**, E480-487 (2011).
- 7 Komeili, A., Vali, H., Beveridge, T. J. & Newman, D. K. Magnetosome vesicles are present before magnetite formation, and MamA is required for their activation. *Proc. Natl. Acad. Sci. U S A* **101**, 3839-3844, doi:10.1073/pnas.0400391101 (2004).
- 8 Arakaki, A., Webb, J. & Matsunaga, T. A novel protein tightly bound to bacterial magnetic particles in *Magnetospirillum magneticum* strain AMB-1. *J. Biol. Chem.* **278**, 8745-8750 (2003).
- 9 Prozorov, T. *et al.* Protein-Mediated Synthesis of Uniform Superparamagnetic Magnetite Nanocrystals. *Adv. Funct. Mater.* **17**, 951-957 (2007).
- 10 Uebe, R. *et al.* The cation diffusion facilitator proteins MamB and MamM of *Magnetospirillum gryphiswaldense* have distinct and complex functions, and are involved in magnetite biomineralization and magnetosome membrane assembly. *Mol. Microbiol.* **82**, 818-835 (2011).
- 11 Murat, D. *et al.* The magnetosome membrane protein, MmsF, is a major regulator of magnetite biomineralization in *Magnetospirillum magneticum* AMB-1. *Mol. Microbiol.* (2012).
- 12 Tanaka, M., Arakaki, A. & Matsunaga, T. Identification and functional characterization of liposome tubulation protein from magnetotactic bacteria. *Mol. Microbiol.* **76**, 480-488 (2010).
- 13 Yang, W. *et al.* *mamO* and *mamE* genes are essential for magnetosome crystal biomineralization in *Magnetospirillum gryphiswaldense* MSR-1. *Res. Microbiol.* **161**, 701-705 (2010).
- 14 Quinlan, A., Murat, D., Vali, H. & Komeili, A. The HtrA/DegP family protease MamE is a bifunctional protein with roles in magnetosome protein localization and magnetite biomineralization. *Mol. Microbiol.* **80**, 1075-1087 (2011).
- 15 Schleifer, K. *et al.* The genus *Magnetospirillum* gen. nov., description of *Magnetospirillum gryphiswaldense* sp. nov. and transfer of *Aquaspirillum magnetotacticum* to *Magnetospirillum magnetotacticum* comb. nov. *Syst. Appl. Microbiol.* **14**, 379-385 (1991).
- 16 Schübbe, S. *et al.* Characterization of a spontaneous nonmagnetic mutant of *Magnetospirillum gryphiswaldense* reveals a large deletion comprising a putative magnetosome island. *J. Bacteriol.* **185**, 5779-5790 (2003).
- 17 Lohsse, A. *et al.* Functional analysis of the magnetosome island in *Magnetospirillum gryphiswaldense*: the *mamAB* operon is sufficient for magnetite biomineralization. *PLoS One* **6**, e25561 (2011).
- 18 Pfenning, N. & Trüper, H. G. Type and Neotype Strains of the Species of Phototrophic Bacteria Maintained in Pure Culture. *Int. J. Syst. Bacteriol.* **21**, 19-24 (1971).

- 19 Wang, J. *et al.* An improved recombineering approach by adding RecA to lambda Red recombination. *Mol Biotechnol* **32**, 43-53 (2006).
- 20 Fu, J. *et al.* Efficient transfer of two large secondary metabolite pathway gene clusters into heterologous hosts by transposition. *Nucleic Acids Res.* **36**, e113 (2008).
- 21 Martinez-Garcia, E., Calles, B., Arevalo-Rodriguez, M. & de Lorenzo, V. pBAM1: an all-synthetic genetic tool for analysis and construction of complex bacterial phenotypes. *BMC Microbiol.* **11**, 38 (2011).

Publication III


Biosynthesis of magnetic nanostructures in a foreign organism by transfer of bacterial magnetosome gene clusters.

Isabel Kolinko, Anna Lohße, Sarah Borg, Oliver Raschdorf, Christian Jogler, **Qiang Tu**, Mihály Pósfai, Éva Tompa, Jürgen M. Plitzko, Andreas Brachmann, Gerhard Wanner, Rolf Müller, Youming Zhang[‡] and Dirk Schüler[‡]

Author contributions

I.K., D.S., Y.Z., Q.T., C.J. and R.M. planned and performed cloning experiments. I.K. and A.L. performed genetic transfers and cultivation experiments. G.W. prepared cryo- and chemically fixed cells. S.B., O.R. and G.W. performed TEM and I.K. analysed the data. J.P. and O.R. performed cryo-electron tomography experiments. E.T. and M.P. took highresolution TEM micrographs and analysed the data. I.K. and A.L. took fluorescence micrographs and performed phenotypization experiments. I.K. performed western blot experiments and analysed proteomic data. A.B. performed Illumina genome sequencing and I.K. analysed the data. I.K. and D.S. designed the study and wrote the paper. All authors discussed the results and commented on the manuscript.

Signatures:

Isabel Kolinko: 

Anna Lohße: 

Sarah Borg: 


Oliver Raschdorf: 

Christian Jogler: 

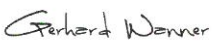
Qiang Tu: 

Mihály Pósfai: 


Éva Tompa: 

Jürgen M. Plitzko: 

Andreas Brachmann: 

Gerhard Wanner: 

Rolf Müller: 

Youming Zhang: 

Dirk Schüler: 

IV

Direct cloning and heterologous expression of the salinomycin biosynthetic gene cluster from *Streptomyces albus* DSM41398 in *S. coelicolor*A3(2).

Jia Yin^{1,2,3,4}, Michael Hoffmann³, Xiaoying Bian¹, **Qiang Tu**^{1,3}, Fu Yan³, Liqiu Xia⁴, Xuezhi Ding⁴, A. Francis Stewart², Rolf Müller^{3*}, Jun Fu^{1,2*} & Youming Zhang^{1*}

¹Shandong University–Helmholtz Institute of Biotechnology, State Key Laboratory of Microbial Technology, School of Life Science, Shandong University, Shanda Nanlu 27, Jinan, 250100, People's Republic of China.

²Department of Genomics, Dresden University of Technology, BioInnovations-Zentrum, Tatzberg 47-51, Dresden, 01307, Germany.

³Helmholtz Institute for Pharmaceutical Research, Helmholtz Centre for Infection Research and Department of Pharmaceutical Biotechnology, Saarland University, PO Box 151150, Saarbrücken, 66041, Germany.

⁴Hunan Provincial Key Laboratory for Microbial Molecular Biology-State Key Laboratory Breeding Base of Microbial Molecular Biology, College of Life Science, Hunan Normal University, Changsha, 410081, People's Republic of China.

*Correspondence and requests for materials should be addressed to R.M. (email: Rolf.Mueller@helmholtzhi.de) or J.F. (email: fujun@sdu.edu.cn) or Y.M.Z. (email: zhangyouming@sdu.edu.cn)

SCIENTIFIC REPORTS



OPEN

Direct cloning and heterologous expression of the salinomycin biosynthetic gene cluster from *Streptomyces albus* DSM41398 in *Streptomyces coelicolor* A3(2)

Jia Yin^{1,2,3,4}, Michael Hoffmann³, Xiaoying Bian¹, Qiang Tu^{1,3}, Fu Yan³, Liqiu Xia⁴, Xuezhi Ding⁴, A. Francis Stewart², Rolf Müller³, Jun Fu^{1,2} & Youming Zhang¹

Received: 09 July 2015

Accepted: 24 August 2015

Published: 13 October 2015

Linear plus linear homologous recombination-mediated recombineering (LLHR) is ideal for obtaining natural product biosynthetic gene clusters from pre-digested bacterial genomic DNA in one or two steps of recombineering. The natural product salinomycin has a potent and selective activity against cancer stem cells and is therefore a potential anti-cancer drug. Herein, we separately isolated three fragments of the salinomycin gene cluster (*salO-orf18*) from *Streptomyces albus* (*S. albus*) DSM41398 using LLHR and assembled them into intact gene cluster (106 kb) by Red/ET and expressed it in the heterologous host *Streptomyces coelicolor* (*S. coelicolor*) A3(2). We are the first to report a large genomic region from a Gram-positive strain has been cloned using LLHR. The successful reconstitution and heterologous expression of the salinomycin gene cluster offer an attractive system for studying the function of the individual genes and identifying novel and potential analogues of complex natural products in the recipient strain.

Red/ET recombineering in *E. coli*^{1,2}, is a powerful technique for the genetic engineering of natural product biosynthetic pathways, especially for large polyketide synthetase (PKS) as well as nonribosomal peptide-synthetase (NRPS)^{3–6}. Recently, this technique was used to clone large biosynthetic gene clusters from a complex DNA source into a vector by linear plus linear homologous recombination (LLHR)⁷. LLHR is mediated by the full-length Rac prophage protein RecE, an exonuclease, its partner RecT, a single-strand DNA-binding protein, and Red γ , an inhibitor of the major exonuclease. RecA, a repair protein, is also included⁸. Fu *et al.*, 2012 cloned ten hidden biosynthetic pathways from digested genomic DNA of Gram-negative *P. luminescens* using LLHR, and two of these have been successfully expressed in *E. coli*^{7,9}. Many gene clusters have also been cloned by this method, including the syringolin, glidobactin, and colibactin gene clusters^{10–12}, and all are from Gram-negative strains.

¹Shandong University–Helmholtz Institute of Biotechnology, State Key Laboratory of Microbial Technology, School of Life Science, Shandong University, Shanda Nanlu 27, Jinan, 250100, People's Republic of China. ²Department of Genomics, Dresden University of Technology, BioInnovations-Zentrum, Tatzberg 47-51, Dresden, 01307, Germany. ³Helmholtz Institute for Pharmaceutical Research, Helmholtz Centre for Infection Research and Department of Pharmaceutical Biotechnology, Saarland University, PO Box 151150, Saarbrücken, 66041, Germany. ⁴Hunan Provincial Key Laboratory for Microbial Molecular Biology-State Key Laboratory Breeding Base of Microbial Molecular Biology, College of Life Science, Hunan Normal University, Changsha, 410081, People's Republic of China. Correspondence and requests for materials should be addressed to R.M. (email: Rolf.Mueller@helmholtz-hzi.de) or J.F. (email: fujun@sdu.edu.cn) or Y.M.Z. (email: zhangyouming@sdu.edu.cn)

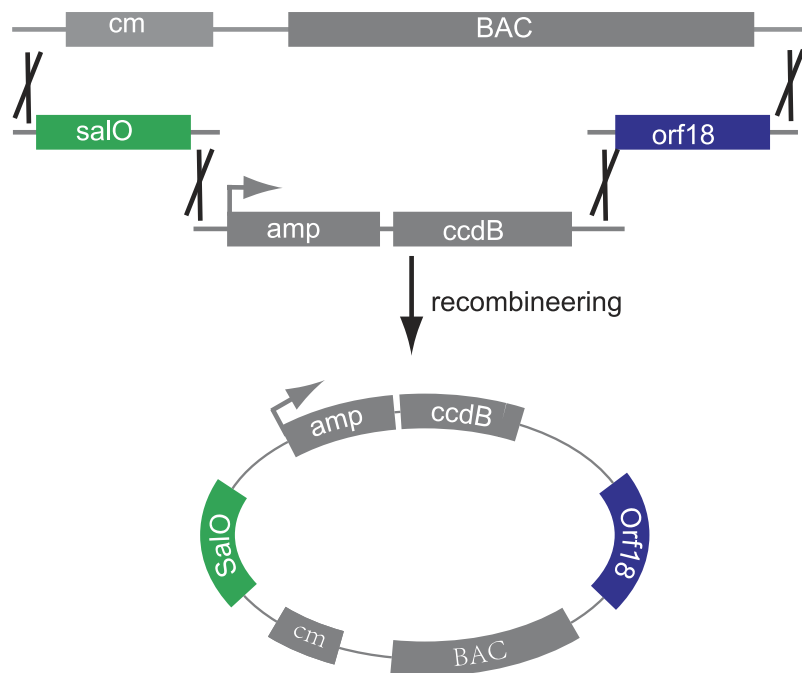


Figure 1. Quadruple recombineering of the BAC vector for direct cloning of the salinomycin gene cluster. pBeloBAC11 was linearized by *Bam*HI, and three fragments (*salO*, *amp-ccdB*, and *orf18*) were obtained by PCR. An ampicillin resistance gene and *ccdB* were co-expression under the same promoter.

An emerging idea in cancer biology is that tumors harbor a group of cells, known as cancer stem cells (CSCs), which have the unique ability to regenerate cancers^{13,14}. In addition to promoting tumor growth, growing evidence indicates that CSCs may be responsible for cancer recurrence, resistance to conventional treatments and metastasis^{15–18}. Recently, Lander *et al.*, 2009 showed that salinomycin can selectively kill breast CSCs after screening 16,000 compounds¹⁹. Further studies revealed that salinomycin has potent and selective activity against other cancer cell lines^{20,21}. *In vitro* data revealed that salinomycin pre-treatment reduced the tumor-seeding ability of cancer cell lines greater than 100-fold over the chemotherapy drug paclitaxel. Furthermore, salinomycin reduced mammary tumor size in mice to a greater extent than paclitaxel¹⁹.

Salinomycin is produced by *Streptomyces albus*²² and has been used to prevent *Coccidioidomycosis* in poultry and alter gut flora to improve nutrient absorption in ruminants²³. The compound interferes with potassium transport across mitochondrial membranes, thus reducing intracellular energy production. It may also disrupt $\text{Na}^+/\text{Ca}^{2+}$ exchange in skeletal and, in some cases, cardiac muscle, allowing a fatal accumulation of intracellular calcium²⁴.

Earlier results revealed that the polyketide chain of salinomycin is synthesized by an assembly line of nine PKS multienzymes (*salAI–IX*). The nine PKS genes are collinearly arranged in the cluster. Four of these multienzymes (*salAIV*, *salAVI*, *salAVII*, and *salAIX*) each catalyze a single extension module, while the other five (*salAI*, *salAII*, *salAIII*, *salAV*, and *salAVIII*) encode two extension modules. In addition to the nine PKS genes, some other genes play vital roles in salinomycin biosynthesis^{25,26}. Upstream of the PKS genes, the adjacent *orf1*, *orf2*, and *orf3* do not belong to the salinomycin cluster, but *salN* and *salO* encode putative regulatory proteins. *SalP* and *SalQ* are involved in the formation of the butyrate extender unit for salinomycin biosynthesis, and inactivation of *salP* and *salQ* reduced the yields of salinomycin by 10% and 36%, respectively when compared to wild-type²⁶. Downstream of the PKS genes, *orf18* is predicted to encode a peptidyl carrier protein, and targeted inactivation of *orf18* results in a 50–60% reduction in salinomycin production compared to wild-type²⁵.

Herein, we report the cloning of the 106-kb salinomycin gene cluster (*salO–orf18*) from the genomic DNA of *Streptomyces albus* DSM41398 by three rounds of direct cloning followed by assembling. All of the genes are oriented in the same direction and under the original promoters. The gene cluster was introduced into *S. coelicolor* A3(2) for successful heterologous production of salinomycin.

Results

Constructing a BAC vector for direct cloning of the salinomycin gene cluster by quadruple recombineering. In order to construct a vector for direct cloning of the salinomycin gene cluster, the four fragments (backbone of pBeloBAC11, *amp-ccdB*, *salO*, and *orf18*) each had a 50-bp overlapping sequence, as illustrated in Fig. 1, and were co-electroporated into GB05dir-*gyrA*₄₆₂⁵, a *CcdB*-resistant *E.*

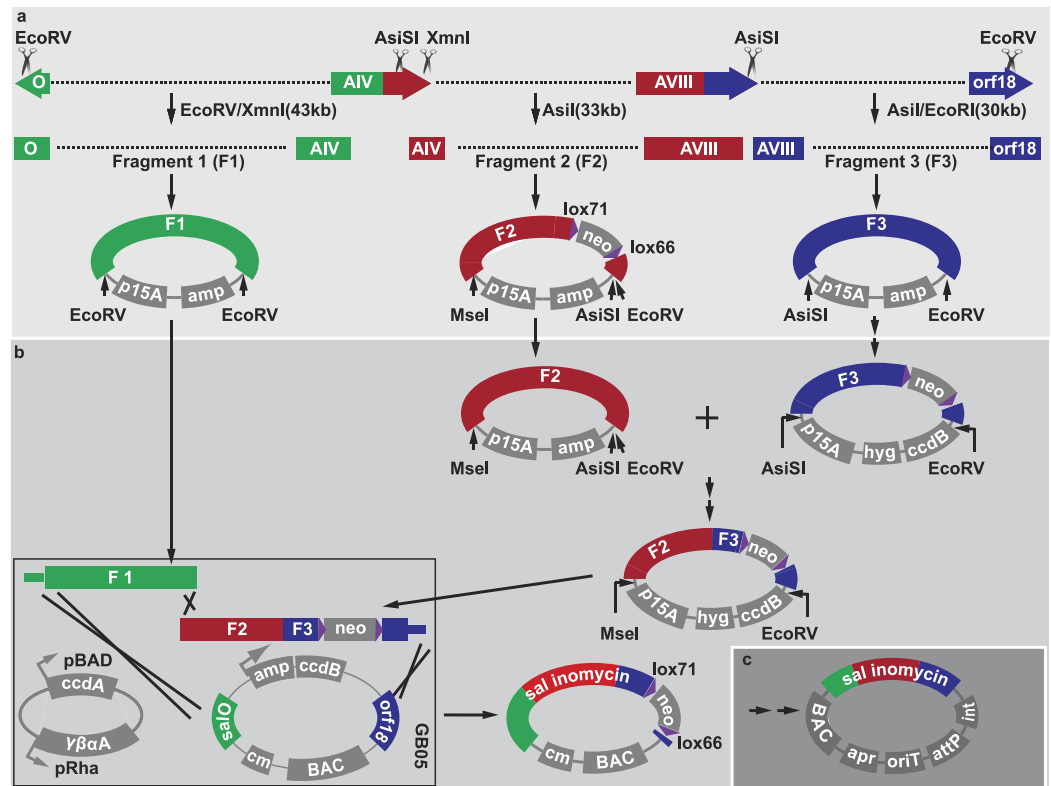


Figure 2. Diagram of direct cloning and assembling of the salinomycin gene cluster and engineering for conjugation and integration. (a) Genomic DNA was digested by restriction enzymes to produce three fragments, which were recombined with p15A-amp after direct cloning. Fragment F2 was isolated using the neomycin selection marker. (b) Three fragments were assembled. Fragments F2 and F3 were assembled by a ligation reaction. F1 and F2&3 were assembled together by triple recombineering to produce pBeloBAC11-sal-*lox71-neo-lox66*. (c) The neomycin selection marker was deleted by Cre from the pBeloBAC11-sal-*lox71-neo-lox66* plasmid, and the integrase-attP-oriT-apramycin cassette was inserted into the noncoding sequence to generate the final construct, pBeloBAC-sal-int-attP-oriT-apr. hyg, hygromycin resistance gene; amp, ampicillin resistance gene; neo, neomycin resistance gene.

coli strain containing the mutation GyrA R462M^{27,28} and LLHR-proficient recombinase (RecET, Red γ , and RecA), to form the BAC vector by quadruple recombineering.

The BAC vector contained a homology arm to *salO* (292 bp) and *orf18* (238 bp) and a cassette of the counterselection marker CcdB, which can be used to delete the background from the original BAC vector for direct cloning. A CcdB function test was performed as described previously⁵.

Direct cloning of the salinomycin gene cluster. As mentioned above, *salO* encodes putative regulatory protein and *orf18* is an essential factor for salinomycin production. Additionally, the restriction site (*EcoRV*), which can be utilized for direct cloning, is located in *salO* and *orf18*. Thus, we attempted to directly clone the 106-kb fragment (*salO-orf18*) using one and two-step recombination reactions⁷ with the BAC vector but were unsuccessful.

Hence, we divided the gene cluster into three fragments for direct cloning (Fig. 2a). We directly cloned the fragments of *salO-salAIV* (F1) and *salAIX-orf18* (F3) using one step of LLHR⁷ with an efficiency of 4/24 and 1/24, respectively (Fig. S1a,c). We directly cloned the fragment of *salAIV-salAVIII* (F2) by a two-step recombination with an efficiency of 8/24 (Fig. S1b). Due to the repeated sequence in *salAIV-salAVIII* (Fig. S2), we were unable to directly clone this fragment by one step of LLHR. Therefore, this fragment was isolated using a neomycin selection marker flanked by *lox71-lox66*, which could be utilized to delete the selection marker conveniently in the assembling procedure. The three desired fragments were inserted in plasmids p15A-amp-F1, p15A-amp-F2-*lox71-neo-lox66*, and p15A-amp-F3, respectively.

Assembling of the salinomycin gene cluster and engineering for conjugation and integration. Figure 2b shows the assembling procedure to reconstitute the entire cluster. F2 and F3 were ligated using the original restriction site of *AsiSI/EcoRV* in the gene cluster, which did not cause any open reading frame shift. The neomycin selection marker was deleted by Cre from the plasmid

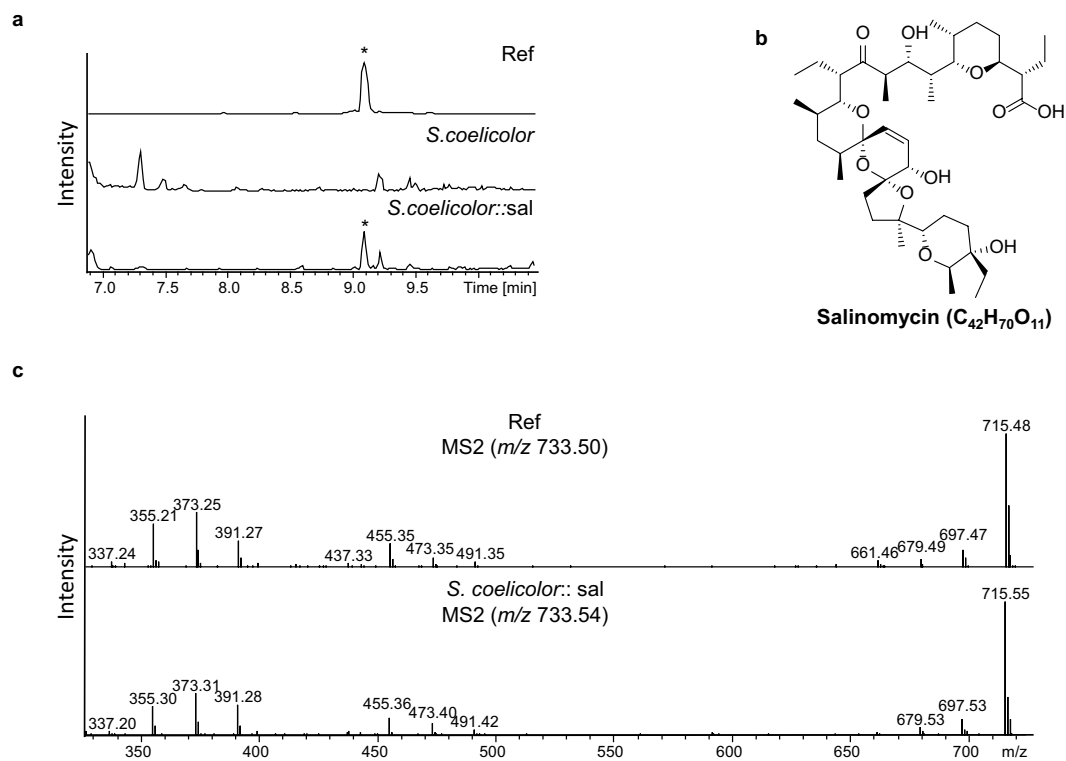


Figure 3. Heterologous salinomycin production. (a) HPLC-MS analysis (base peak chromatograms (BPC) m/z 200–2000+ All MS) of the salinomycin standard (Ref), the wild-type *S. coelicolor* A3(2) and mutant *S. coelicolor::sal*. Salinomycin is indicated by an asterisk. (b) MS² fragmentation patterns of precursor m/z 733.5 [M–H₂O+H]⁺ in standard salinomycin and in *S. coelicolor::sal* mutant.

p15A-amp-F2-lox71-neo-lox66 to produce p15A-amp-F2. Modifications were made to p15A-amp-F3 with two steps of recombineering. The neomycin selection marker flanked by lox71-lox66 was inserted into the non-coding sequence of F3 in the first recombineering step. The second recombineering step replaced the ampicillin selection marker with the *hyg-ccdB* cassette to produce p15A-*hyg-ccdB*-F3-lox71-neo-lox66. F3 was excised by *AsiI/EcoRV* and inserted into the *AsiI/EcoRV* site in p15A-amp-F2 by ligation to produce p15A-amp-F2&3-lox71-neo-lox66.

The ampicillin selection marker of the previous ligation product was replaced by the *hyg-ccdB* cassette to produce the plasmid p15A-*hyg-ccdB*-F2&3-lox71-neo-lox66. The plasmid p15A-amp-F1 was digested by *EcoRV* to release the fragment F1, and p15A-*hyg-ccdB*-F2&3-lox71-neo-lox66 was digested by *EcoRV/MseI* to excise F2&3-lox71-neo-lox66. The two fragments overlapped by 592bp, and each fragment had a homologous arm with previously constructed BAC vector. The BAC vector was transformed into GB05 cells harboring the plasmid pSC101-*ccdA-gbaA*. As CcdB is toxic, we induced CcdA, that inactivates the CcdB toxin, by rhamnose in the liquid medium or culture plates. The two previous linearize fragments were co-transformed into GB05 cells containing the BAC vector and the expression plasmid (pSC101-*ccdA-gbaA*) to produce pBeloBAC11-*sal-lox71-neo-lox66*. We verified pBeloBAC11-*sal-lox71-neo-lox66* using three restriction enzymes, the results (Fig. S3) showed that the pBeloBAC11-*sal-lox71-neo-lox66* was correct.

To introduce the gene cluster into a heterologous expression host, few necessary elements were engineered before conjugation. The two step engineering procedure for conjugation and integration is diagrammed in Fig. 2c. Finally, the gene cluster was introduced into *S. coelicolor* A3(2) by conjugation and integrated into its chromosome.

Heterologous production of salinomycin in *S. coelicolor* A3(2). The genetic organization and promoters of the obtained salinomycin gene cluster are identical to those of the original producer *S. albus* DSM41398. After conjugation, the exconjugant colonies were confirmed by PCR and subsequently analyzed for heterologous salinomycin production. The salinomycin gene cluster was successfully inserted into the attB site of *S. coelicolor* A3(2) (Fig. S4).

The metabolite profiles of the wild-type *S. coelicolor* and the mutant strains *S. coelicolor::sal* were analyzed by HPLC-MS and compared with the salinomycin standard (Fig. 3a (Ref)). Thus, we were able to identify Salinomycin in extracts of the mutant strains *S. coelicolor::sal* via HPLC-MS (Fig. 3a,b) and

heterologous expression could be unambiguously confirmed by comparing MS² fragmentation pattern (Fig. 3c).

Discussion

Over the past several decades, numerous multifunctional megasynthases have been identified, cloned, sequenced, engineered, and heterologously expressed in suitable hosts. Traditionally, natural product biosynthetic gene clusters were retrieved from a single cosmid or reconstructed from several cosmids within a genomic library of the natural producer strain, which was time consuming due to subsequent cloning steps following the screening process from a genomic library^{4,29}.

LLHR-mediated recombineering was ideal for direct cloning of the salinomycin gene cluster from pre-digested genomic DNA after one or two steps of recombineering⁷. Red/ET recombineering has traditionally been applied for heterologous expression of biosynthetic pathways to modify the biosynthetic pathways³⁰.

The failure to directly clone the 106-kb fragment with the BAC vector may have resulted from several considerations. First, the recombineering efficiency is very low for large fragments. Although the developed method of direct cloning is efficient for cloning up to ~52-kb fragments from a bacterial genome⁷, it is limited by inefficient co-transformation of two linear molecules, especially for long fragments (106 kb). Moreover, the gene cluster contains GC-rich sequences. We studied the impact of the GC content on the recombineering efficiency and found that it was decreased for sequences with high GC content (data not shown). Second, enrichment of the target DNA is difficult after extracting the genomic DNA. Genomic DNA is susceptible to shearing forces associated with mechanical destruction and degradation by nuclease activity. Therefore, it is difficult to obtain the intact salinomycin biosynthesis gene cluster, especially for *S. albus* DSM 41398, the gram-positive strain. Third, previous data revealed that the Red β monomer anneals ~11 bp of DNA, and the smallest stable annealing intermediate requires only 20 bp of DNA and two Red β monomers³¹. In this study, we found that most of the colonies resulted from self-circularization of the vector used for direct cloning after recombineering although there were no obvious homologous regions in the backbone of the vector. As a result, it is difficult to screen the correct clone from thousands of self-circularized vectors.

In parallel to our LLHR-mediated direct cloning, the other DNA cloning methods for bioprospecting have their distinct merits. LLHR-mediated RecET direct cloning was not accessible to metagenomic DNA. Bioprospecting of metagenomics needs DNA synthesis and assembly method. *Streptomyces* phage ϕ BT1 integrase-mediated *in vitro* site-specific recombination could assemble the 56 kb epothilone biosynthetic gene cluster using modules as units. The authors didn't prove that the complete gene cluster with *att* site scars could be expressed in a heterologous host³². The incorrect linker between modules might affect the biosynthesis³³. An intact DNA sequence can be obtained by the Gibson assembly^{34,35}, which is the most efficient 'chew back and anneal' method^{36–38}. The Gibson assembly was also proved to be capable of direct cloning of a 41 kb conglobatin biosynthetic gene cluster³⁹. Much larger DNA fragment can be directly cloned by transformation-associated recombination (TAR) in yeast *Saccharomyces cerevisiae*^{40,41}. However unregulated yeast homologous recombinase might cause rearrangement of repetitive PKS/NRPS biosynthetic DNA sequences. The *oriT*-directed cloning for Gram-negative bacteria relies on available genetic tools to insert conjugation elements on the genome by two elaborated vectors. Although it is not straight forward, it has a capacity of cloning regions up to 140 kb from the genome of *Burkholderia pseudomallei*⁴². The phage ϕ BT1 integrase-mediated direct cloning was developed for Gram-positive bacteria *Streptomyces*. It has the similar logic to *oriT*-directed cloning, which starts with integration of a capture vector by genome engineering at two spots, but both excision and circularization happen in the original bacteria⁴³. If *Bacillus subtilis* is justified as a suitable heterologous host for a biosynthetic gene cluster, its genome can be used as a vector for direct cloning of giant DNA, which has the potential to overcome the capacity limit of the BAC vector⁴⁴.

Compare to above methods our LLHR-mediated direct cloning has a significant feature. It is a genetic tool in *E. coli*, which is simple, convenient and cost-effective. The important improvement in this study is to combine RecET mediated direct cloning and *lambda* Red mediated plasmids stitching to hierarchically clone the intact 106kb salinomycin gene cluster. The reliability of the cloning method has been proved by subsequently successful heterologous expression in *S. coelicolor* A3(2). Our results represent a potent approach to mine the function of the individual genes and identify novel and potentially useful analogues of the complex natural products through module exchange in the recipient.

Methods

Strains, plasmids and culture conditions. The bacterial strains and plasmids used in this study are shown in Table S1. All primers were synthesized by Sigma-Genosys (Germany) (Table S2). All restriction enzymes, Taq polymerase, and DNA markers were purchased from New England Biolabs (UK).

E. coli cells were cultured in Luria-Bertani (LB) liquid media or on LB agar (1.2% agar). Ampicillin (amp, 100 μ g mL⁻¹), kanamycin (km, 15 μ g mL⁻¹), chloramphenicol (cm, 15 μ g mL⁻¹), hygromycin (hyg, 30 μ g mL⁻¹), apramycin (apr, 15 μ g mL⁻¹), and tetracycline (tet, 5 μ g mL⁻¹) were added to the media as required.

For sporulation and conjugation, *S. coelicolor* A3(2) was grown on mannitol salt (MS) agar plates for 10 days. If necessary for conjugation, apr (50 μ g mL⁻¹) and nalidixic acid (NA, 50 μ g mL⁻¹) were added.

S. albus DSM41398, *S. coelicolor* A3(2), and mutant strains were cultivated in M1 medium (10 g L⁻¹ starch, 4 g L⁻¹ yeast extract, 2 g L⁻¹ peptone) at 30 °C with constant agitation at 180 rpm.

Bacterial genomic DNA isolation. *S. albus* DSM41398 was cultured in 30 mL medium (4 g L⁻¹ glucose, 4 g L⁻¹ yeast extract, 10 g L⁻¹ malt extract, pH 7.2) at 30 °C for two days. After centrifugation, the cells were resuspended in 5 mL SET buffer (75 mM NaCl, 25 mM EDTA, 20 mM Tris, pH 7.5). After adding lysozyme to a final concentration of 1 mg mL⁻¹ and incubating at 37 °C for 0.5–1 h, 500 μL 10% SDS and 125 μL 20 mg mL⁻¹ proteinase K were added, and the mixture was incubated at 55 °C with occasional inversion for 2 h until the solution became clear. The solution was combined with 2 mL 5 M NaCl and 8 mL phenol:chloroform:isoamyl alcohol (25:24:1) and incubated at room temperature for 0.5 h with frequent inversion. After centrifuging at 4500 × *g* for 15 min, the aqueous phase was transferred to a new tube using a blunt-ended pipette tip, and the DNA was precipitated by adding one volume of isopropanol and gently inverting the tube. DNA was transferred to a microfuge tube, rinsed with 75% ethanol, dried under vacuum, and dissolved in ddH₂O.

Preparation of electrocompetent cells for recombineering. Recombineering and direct cloning were performed as described previously⁷ with several small modifications. The linear cloning vector p15A-amp, flanked with homology arms to target genes, was amplified by PCR using p15A-amp-ccdB⁵ as a template. Digested genomic DNA (10 μg) was mixed with 2 μg linear cloning vector and co-transformed into competent cells by electroporation.

Conjugation. Conjugation between *E. coli* and *S. coelicolor* A3(2) was performed as described previously with minor modifications⁴⁵. The plasmid containing the salinomycin gene cluster and elements for conjugation and integration was transformed into the donor strain *E. coli* ET12567 (pUZ8002). The donor strain was prepared by growth overnight at 37 °C in LB supplemented with antibiotics. The overnight culture was diluted 100-fold in 15 mL fresh LB plus antibiotic and grown at 30 °C to an OD₆₀₀ of 0.3. The *E. coli* cells were washed twice with an equal volume of LB and resuspended in 0.1 volume LB. *S. coelicolor* A3(2) mycelia fragments were harvested from a four-day-old culture in TSB medium and served as the recipient strain. The donor strain and recipient strain were mixed with equal volumes, the mixture was centrifuged, and the supernatant was discarded. Finally, the pellet was resuspended in the residual liquid. The mating mixture was spread on MS plates and incubated at 30 °C. After 24 h, the cells were collected and spread on MS plates with NA (50 μg mL⁻¹) and apr (50 μg mL⁻¹) and further incubated at 30 °C until exconjugant colonies appeared.

Extraction and analysis of the compound. *S. coelicolor::sal* gene cluster cells were cultivated in 300-mL flasks containing 30 mL M1 medium supplemented with apr (25 μg mL⁻¹). The culture was grown at 30 °C with constant agitation at 180 rpm. After 13 days, the biomass was harvested by centrifugation, and 2% resin Amberlite XAD-16 was added to the supernatant before the resin was extracted with methanol. The received extracts were evaporated and dissolved in methanol and used for HPLC-MS analysis. The HPLC-MS measurement was performed on a Dionex Ultimate 3000 LC system utilizing a Waters Acquity BEHC-18 column (50 × 2 mm, 1.7-μm particle size). Separation of 2 μL sample was obtained using a linear gradient of A (water and 0.1% formic acid) and B (acetonitrile and 0.1% formic acid) at a flow rate of 600 μL min⁻¹ at 45 °C. The gradient was initiated by a 0.5-min isocratic step at 5% B followed by an increase to 95% B over 9 min and a final 1.5-min step at 95% B before reequilibration with initial conditions. UV spectra were recorded by a DAD from 200–600 nm. MS measurement was carried on an amaZon speed mass spectrometer (Bruker Daltonics, Bremen, Germany) using the standard ESI source. Mass spectra were acquired in centroid mode ranging from 200–2000 *m/z* in positive ionization mode with auto MS² fragmentation.

References

- Zhang, Y., Buchholz, F., Muirers, J. P. P. & Stewart, A. F. A new logic for DNA engineering using recombination in *Escherichia coli*. *Nat. Genet.* **20**, 123–128 (1998).
- Zhang, Y., Muirers, J. P. P., Testa, G. & Stewart, A. F. DNA cloning by homologous recombination in *Escherichia coli*. *Nat. Biotechnol.* **18**, 1314–1317 (2000).
- Gross, F. *et al.* Metabolic engineering of *Pseudomonas putida* for methylmalonyl-CoA biosynthesis to enable complex heterologous secondary metabolite formation. *Chem. Biol.* **13**, 1253–1264 (2006).
- Fu, J. *et al.* Efficient transfer of two large secondary metabolite pathway gene clusters into heterologous hosts by transposition. *Nucleic Acids Res.* **36**, e113 (2008).
- Wang, H. *et al.* Improved seamless mutagenesis by recombineering using ccdB for counterselection. *Nucleic Acids Res.* **42**, e37 (2014).
- Wenzel, S. C. *et al.* Heterologous Expression of a Myxobacterial Natural Products Assembly Line in *Pseudomonads* via Red/ET Recombineering. *Chem. Biol.* **12**, 349–356 (2005).
- Fu, J. *et al.* Full-length RecE enhances linear-linear homologous recombination and facilitates direct cloning for bioprospecting. *Nat. Biotechnol.* **30**, 440–446 (2012).
- Wang, J. *et al.* An improved recombineering approach by adding RecA to lambda Red recombination. *Mol. Biotechnol.* **32**, 43–53 (2006).
- Bian, X., Plaza, A., Zhang, Y. & Müller, R. Luminmycins A–C, Cryptic Natural Products from *Photorhabdus luminescens* Identified by Heterologous Expression in *Escherichia coli*. *J. Nat. Prod.* **75**, 1652–1655 (2012).

10. Bian, X. *et al.* Heterologous Production of Glidobactins/Luminomycins in *Escherichia coli* Nissle Containing the Glidobactin Biosynthetic Gene Cluster from *Burkholderia* DSM7029. *Chembiochem* **15**, 2221–2224 (2014).
11. Bian, X. *et al.* Direct cloning, genetic engineering, and heterologous expression of the syringolin biosynthetic gene cluster in *E. coli* through Red/ET recombineering. *Chembiochem* **13**, 1946–1952 (2012).
12. Bian, X. *et al.* *In Vivo* Evidence for a Prodrug Activation Mechanism during Colibactin Maturation. *Chembiochem* **14**, 1194–1197 (2013).
13. Reya, T., Morrison, S. J., Clarke, M. F. & Weissman, I. L. Stem cells, cancer, and cancer stem cells. *Nature* **414**, 105–111 (2001).
14. Al-Hajj, M., Wicha, M. S., Benito-Hernandez, A., Morrison, S. J. & Clarke, M. F. Prospective identification of tumorigenic breast cancer cells. *Proc. Nat. Acad. Sci. USA*. **100**, 3983–3988 (2003).
15. Noirot, P. & Kolodner, R. D. DNA Strand Invasion Promoted by *Escherichia coli* RecT Protein. *J. Biol. Chem.* **273**, 12274–12280 (1998).
16. Dean, M., Fojo, T. & Bates, S. Tumour stem cells and drug resistance. *Nat. Rev. Cancer* **5**, 275–284 (2005).
17. McIntosh, J. A., Donia, M. S. & Schmidt, E. W. Ribosomal peptide natural products: bridging the ribosomal and nonribosomal worlds. *Nat. Prod. Rep.* **26**, 537–559 (2009).
18. Lobo, N. A., Shimono, Y., Qian, D. & Clarke, M. F. The biology of cancer stem cells. *Annu. Rev. Cell Dev. Biol.* **23**, 675–699 (2007).
19. Gupta, P. B. *et al.* Identification of selective inhibitors of cancer stem cells by high-throughput screening. *Cell* **138**, 645–659 (2009).
20. Kim, J.-H. *et al.* Salinomycin sensitizes cancer cells to the effects of doxorubicin and etoposide treatment by increasing DNA damage and reducing p21 protein. *Br. J. Pharmacol.* **162**, 773–784 (2011).
21. Lu, D. *et al.* Salinomycin inhibits Wnt signaling and selectively induces apoptosis in chronic lymphocytic leukemia cells. *Proc. Nat. Acad. Sci. USA*. **108**, 13253–13257 (2011).
22. Mitani, M., Yamanishi, T. & Miyazaki, Y. Salinomycin: A new monovalent cation ionophore. *Biochem. Biophys. Res. Commun.* **66**, 1231–1236 (1975).
23. Miyazaki, Y. *et al.* Salinomycin, a new polyether antibiotic. *J. Antibiot.* **27**, 814–821 (1974).
24. Story, P. & Doube, A. A case of human poisoning by salinomycin, an agricultural antibiotic. *New Zeal. Med. J.* **117**, U799 (2004).
25. Jiang, C., Wang, H., Kang, Q., Liu, J. & Baia, L. Cloning and characterization of the polyether salinomycin biosynthesis gene cluster of *Streptomyces albus* XM211. *Appl. Environ. Microbiol.* **78**, 994–1003 (2012).
26. Yurkovich, M. E. *et al.* A Late-Stage Intermediate in Salinomycin Biosynthesis Is Revealed by Specific Mutation in the Biosynthetic Gene Cluster. *Chembiochem* **13**, 66–71 (2012).
27. Bernard, P. Positive selection of recombinant DNA by CcdB. *Biotechniques* **21**, 320–323 (1996).
28. Bernard, P. & Couturier, M. Cell killing by the F plasmid CcdB protein involves poisoning of DNA-topoisomerase II complexes. *J. Mol. Biol.* **226**, 735–745 (1992).
29. Ongley, S. E. *et al.* High-Titer Heterologous Production in *E. coli* of Lyngbyatoxin, a Protein Kinase C Activator from an Uncultured Marine Cyanobacterium. *ACS Chem. Biol.* **8**, 1888–1893 (2013).
30. Kolinko, I. *et al.* Biosynthesis of magnetic nanostructures in a foreign organism by transfer of bacterial magnetosome gene clusters. *Nat. Nano.* **9**, 193–197 (2014).
31. Erler, A. *et al.* Conformational adaptability of Red β during DNA annealing and implications for its structural relationship with Rad52. *J. Mol. Biol.* **391**, 586–598 (2009).
32. Zhang, L., Zhao, G. & Ding, X. Tandem assembly of the epothilone biosynthetic gene cluster by *in vitro* site-specific recombination. *Sci. Rep.* **1** (2011).
33. Yuzawa, S., Kapur, S., Cane, D. E. & Khosla, C. Role of a Conserved Arginine Residue in Linkers between the Ketosynthase and Acyltransferase Domains of Multimodular Polyketide Synthases. *Biochemistry* **51**, 3708–3710 (2012).
34. Gibson, D. G. *et al.* Enzymatic assembly of DNA molecules up to several hundred kilobases. *Nat. Methods* **6**, 343–345 (2009).
35. Shih, S. C. C. *et al.* A Versatile Microfluidic Device for Automating Synthetic Biology. *ACS Synth. Biol.* (2015).
36. Ellis, T., Adie, T. & Baldwin, G. S. DNA assembly for synthetic biology: from parts to pathways and beyond. *Integr. Biol.* **3**, 109–118 (2011).
37. Zhu, B., Cai, G., Hall, E. O. & Freeman, G. J. In-FusionTM assembly: seamless engineering of multidomain fusion proteins, modular vectors, and mutations. *Biotechniques* **43**, 354–359 (2007).
38. Sleight, S. C., Bartley, B. A., Lieviant, J. A. & Sauro, H. M. In-Fusion BioBrick assembly and re-engineering. *Nucleic Acids Res.* **38**, 2624–2636 (2010).
39. Zhou, Y. *et al.* Iterative Mechanism of Macrodilide Formation in the Anticancer Compound Conglobatin. *Chem. Biol.* **22**, 745–754 (2015).
40. Larionov, V., Kouprina, N., Gregory Solomon \ddagger , Barrett, J.C. & Resnick, M.A. Direct isolation of human BRCA2 gene by transformation-associated recombination in yeast. *Proc. Nat. Acad. Sci. USA*. **94**, 7384–7387 (1997).
41. Yamanaka, K. *et al.* Direct cloning and refactoring of a silent lipopeptide biosynthetic gene cluster yields the antibiotic taromycin A. *Proc. Nat. Acad. Sci. USA*. **111**, 1957–1962 (2014).
42. Kvitko, B. H., McMillan, I. A. & Schweizer, H. P. An Improved Method for oriT-Directed Cloning and Functionalization of Large Bacterial Genomic Regions. *Appl. Environ. Microbiol.* **79**, 4869–4878 (2013).
43. Du, D. *et al.* Genome engineering and direct cloning of antibiotic gene clusters via phage ϕ BT1 integrase-mediated site-specific recombination in *Streptomyces*. *Sci. Rep.* **5** (2015).
44. Itaya, M., Nagata, T., Shiroishi, T., Fujita, K. & Tsuge, K. Efficient Cloning and Engineering of Giant DNAs in a Novel *Bacillus subtilis* Genome Vector. *J. Biochem.* **128**, 869–875 (2000).
45. Hou, Y., Li, F., Wang, S., Qin, S. & Wang, Q. Intergeneric conjugation in holomycin-producing marine *Streptomyces* sp. strain M095. *Microbiol. Res.* **163**, 96–104 (2008).

Acknowledgments

This work was supported by funding to Y.Z. from the Recruitment Program of Global Experts, funding to J.Y. from China/Shandong University International Postdoctoral Exchange Program, funding to J.F. from the International S&T Cooperation Program of China (ISTCP 2015DFE32850), funding to A.F. S. from the TUD Elite University Support the Best program. The authors acknowledge Vinothkannan Ravichandran's help in proofreading this manuscript.

Author Contributions

J.Y. participated in the design of this study, performed data collection analysis, and drafted the manuscript; H.M., X.Y., T.Q., F.Y., L.Q. and X.Z. participated in interpretation data; A.F.S. and R.M.

helped with the revision of the final manuscript. J.F. and Y.Z. designed and oversaw the study, performed data interpretation and drafted the manuscript.

Additional Information

Supplementary information accompanies this paper at <http://www.nature.com/srep>

Competing financial interests: The authors declare no competing financial interests.

How to cite this article: Yin, J. *et al.* Direct cloning and heterologous expression of the salinomycin biosynthetic gene cluster from *Streptomyces albus* DSM41398 in *Streptomyces coelicolor* A3(2). *Sci. Rep.* 5, 15081; doi: 10.1038/srep15081 (2015).



This work is licensed under a Creative Commons Attribution 4.0 International License. The images or other third party material in this article are included in the article's Creative Commons license, unless indicated otherwise in the credit line; if the material is not included under the Creative Commons license, users will need to obtain permission from the license holder to reproduce the material. To view a copy of this license, visit <http://creativecommons.org/licenses/by/4.0/>

1 **Supplemental Information**

2

3 **Direct cloning and heterologous expression of the salinomycin biosynthetic gene cluster from *Streptomyces albus* DSM41398**

4 **in *S. coelicolor* A3(2)**

5

6 **Jia Yin, Michael Hoffmann, Xiaoying Bian, Qiang Tu, Fu Yan, Liqui Xia, Xuezhi Ding, A. Francis Stewart, Rolf Müller, Jun Fu and**

7 **Youming Zhang**

8

9

10

11

12

13

14

15

16

17

18

19

20

21

22

23

24

25

Table S1 Strains and plasmids

Strain or plasmid	Characteristics	References or sources
<i>E. coli</i>		
GB05	F- <i>mcrA</i> Δ (<i>mrr</i> - <i>hsdRMS</i> - <i>mcrBC</i>) ϕ 80/ <i>lacZ</i> Δ M15 Δ <i>lacX74</i> <i>recA1</i> <i>endA1</i> <i>araD139</i> Δ (<i>ara</i> , <i>leu</i>)7697 <i>galU</i> <i>galK</i> λ <i>rpsL</i> <i>nupG</i> <i>fhuA</i> ::IS2 <i>recET</i> <i>redα</i> , phage T1-resistant	1
GB06	<i>endA1</i> <i>glnV44</i> <i>thi-1</i> <i>relA1</i> <i>gyrA96</i> <i>recA1</i> <i>mcrB</i> + Δ (<i>lac-proAB</i>) <i>e14</i> - [F' <i>traD36</i> <i>proAB</i> + <i>lacIq</i> <i>lacZ</i> Δ M15] <i>hsdR17</i> (rK-mK+) <i>rpsL</i> <i>recET</i> phage T1-resistant	
GB05-dir	GB2005, <i>araC</i> -BAD-ET γ A	2
GB05-red	GB2005, <i>araC</i> -BAD- γ β α A	1
GB05dir- <i>gyrA462</i>	GB05dir, <i>gyrA462</i> (<i>ccdB</i> resistant)	3
GB05red- <i>gyrA462</i>	GB05red, <i>gyrA462</i> (<i>ccdB</i> resistant)	3
ET12567(pUZ8002)	<i>recF</i> , <i>dam</i> -, <i>dcm</i> -, CmR, KmR	4
<i>Streptomyces</i>		
<i>S. albus</i> DSM41398	Salinomycin-producing wild-type strain	DSMZ
<i>S. coelicolor</i> A3(2)	Recipient strain of gene cluster	5
<i>S. coelicolor</i> :: <i>sal</i>	Salinomycin gene cluster in the chromosome, <i>aprR</i>	This study
Plasmid		
pSC101-BAD-Cre-tet	Cre under BAD promoter, tetR	6
pSC101-rha-ETgA-tet	RecET, <i>redγ</i> and RecA under rha promoter, tetR	This study
pBeloBAC11-amp- <i>ccdB</i> -4Sal	pBeloBAC11, the vector for direct cloing, ampR	This study
p15A-amp-F1	p15A replicon, contained the fragment of <i>salO</i> - <i>salAIV</i> , ampR	This study
p15A-amp-F2-lox71-neo-lox66	p15A replicon, contained the fragment of <i>salAIV</i> - <i>salAVIII</i> and the cassette of <i>lox71</i> - <i>neo</i> - <i>lox66</i> , ampR, kmR	This study
p15A-amp-F3	p15A replicon, contained the fragment of <i>salAIX</i> - <i>orf18</i> , ampR	This study

p15A-amp-F2	p15A replicon, the neo selection marker was deleted by Cre from the p15A-amp-F2-lox71-neo-lox66, ampR	This study
p15A-hyg-ccdB-F3-lox71-neo-lox66	p15A replicon, two cassettes of hyg-ccdB and lox71-neo-lox66 was integrated into the p15A-amp-salAIX-orf18, hygR, kmR	This study
p15A-amp-F2&3-lox71-neo-lox66	p15A replicon, contained the fragment of salAIV-orf18 and the cassette of lox71-neo-lox66, ampR, kmR	This study
pBeloBAC11-sal-lox71-neo-lox66	pBeloBAC11, contained the whole salinomycin PKS and the cassette of lox71-neo-lox66, kmR	This study
pBeloBAC-sal-int-attP-oriT-apr	pBeloBAC11, contained the whole salinomycin PKS, an origin of transfer(oriT), attP sequence and integrase gene, aprR	This study

26

27

28

29

30

31

32

33

34

35

36

37

38

39

40

41

42

43

44

Table S2. Oligonucleotides

Gene	Primer name	Primer sequence 5'-3'	Restriction enzymes sites	application
<i>saO</i>	saO-5	<u>AGTGAATTGTAATACGACTCACTATAGGGCGAATTCGAGCTCGGTACCCGGTGGACGAGACCCGACCGCG</u>		BAC vector
	saO-3	GGCCCCCAGCGGTCCATCA		BAC vector
<i>orf18</i>	Orf18-5	<u>CTAATGAGCGGGCTTTTTTTTGAACAAAACAACCTTATATCGTATGGGGCTGGATCC</u> ttATGACCCGCCCGCCCCCTG	<i>Bam</i> HI	BAC vector
	Orf18-3	<u>GTGACACTATAGAATACTCAAGCTTGCATGCCTGCAGGTCGACTCTAGAG</u> aTCACCACGGCCACCCCTCGG		BAC vector
<i>Amp-ccdB</i>	Amp-ccdB-5	<u>ATGCAGAGCGAACTGGCCACCCTGATGGACCGCTGGCGGGCCCGCCGCGCCGGGAGTTGAGGATCC</u> TTTGT	<i>Bam</i> HI	BAC vector
		TTTTCTAAATA		
	Amp-ccdB-3	AGCCCCATACGATATAAGTT		BAC vector
<i>saO-saAIV</i>	saO-saAIV-3	<u>CGCTCGCGCCGGGAGCCGGTTCGCGCTCCCGGCCGACCATGTGGATCTGCGAGAGGTAGCGGACCGCGCCG</u>	<i>Eco</i> RV	Direct cloning
	saO-saAIV-5	<u>GATATC</u> TTACCAATGCTTAATCAGTG CCAGCTGGAGGCGGACCTGCTGTCCGTCGCCCTGGACAAGGACGAACGAACCTCACCCGGCGCCTCGAA	<i>Eco</i> RV	
<i>saAIV-saAVIII</i>	saAIV-saAV III-3	<u>TCCGAGAGCAGCGGGCGGGTTCGCGCGGAGGTGAACAGCGGCCAGAACCCTCCAGTCCACGTCCGCGACG</u>	<i>M</i> seI	Direct cloning
	saAIV-saAV III-5	<u>GCGATTAAT</u> ACAACCTTATATCGTATGGGG CGACGCGCTCCTCGAGCTCGGCGCCCGCCGGTTCGGCGAGACGGCCGCGCAGCAACCCGACGAG	<i>Asi</i> SI& <i>Eco</i> RV	
	saAIV-saAV III-5	<u>GCCGCGGCGATCGC</u> ACTGTAGATATC TTACCAATGCTTAATCAGTG		
<i>saAIX-orf18</i>	saAIX-orf18-3	<u>TCCGCTCCACGGGCGCGTCAGGAGTTGCTGTTGTGCGAGGGCCAGCGAGACGAGGGCGTTCGACGTC</u>	<i>Asi</i> SI	Direct cloning
	saAIX-orf18-5	<u>CATCTCGGCGATCGC</u> ACAACCTTATATCGTATGGGG TCGAGGACGACTTCGGCCTCGCCGTCGACCCCGCCTCGCCCGCGAACTCCCCACCGTGACCGCCCTCGCCGG	<i>Eco</i> RV	
	saAIX-orf18-5	<u>ATATC</u> TTACCAATGCTTAATCAGTG		
<i>lox71-neo-lox66</i>	sal-km-5	<u>CCTGCTCGACGACGAACTCGAAACGAAATAACCCATGAACGGCGCCGCTT</u> TACCGTTCGTATAATGTATGCTATACG AAGTTATTCAGAAGAACTCGTCAAGAAG		Direct cloning
	sal-km-3	<u>AACTCAGTCACCTACCGAAACAGGACCGGGCACGGGAAGCGGAAGGCCG</u> TACCGTTCGTATAGCATAATTATAC GAAGTTATGCTTGCACTGGGCTTACAT		
<i>Hyg-ccdB</i>	hygccdb-5	<u>TTACCAATGCTTAATCAGTGAGGCACCTATCTCAGCGATCTGTCTATTT</u> CCTAGGTTATATTTCCCAGAACATCA		Assembling
	hygccdb-3	<u>ATGTATCCGCTCATGAGACAATAACCCTGATAAATGCTTCAATAATTTGAGGAGG</u> CCCTAGGTATGAAAAAGCCTGAA CTCAC		
<i>lox71-neo-lox66</i>	kan-5	<u>GTAGAGCGCCACCATCAGATGCGCGTGGAACCTCCTCGCGCAGCGGGA</u> ACTTACCGTTCGTATAGCATAATTATAC		Assembling

		GAAGTTATGCTTGCAAGTGGGCTTACAT	
	kan-3	<u>GACGAGGAGGATGTTCTCGGGCGGGCACCTCGAACTCCTCGGGCGATCAGCATACCGTTTCGTATAATGTATGCTATAC</u>	
		GAAGTTATTCAGAAGAAGTTCGTCGAAGAAG	
Integrase-attP-o	intApSal5	<u>TAGAGCGCCACCATCAGATGCGCGTGGAAGTCCCTCGCGCAGCGGGAACTTAGATCAGGCTTCCCGGGTGTC</u>	Engineering
riT-Apramycin	intApSal3	<u>CGCGGGCCGTGTCCCTCAAGTCCAGCAGGTCCGCGCGCAGTTGGCGGGTCTGACGCTCAGTGGAACG</u>	
	attB-L	CAGGTTCACCCACAGCTG	Verification
	attB-R	CTCAACTAAAGTGGGGCG	Verification
	attP-dn	AAATGCCCGACGAACCTGAA	Verification
	attP-up	TCGCTATAATGACCCCGAAGCAG	Verification

45 Underlined sequences indicate homology arms.

46 Bold letters represent restriction enzyme sites.

47

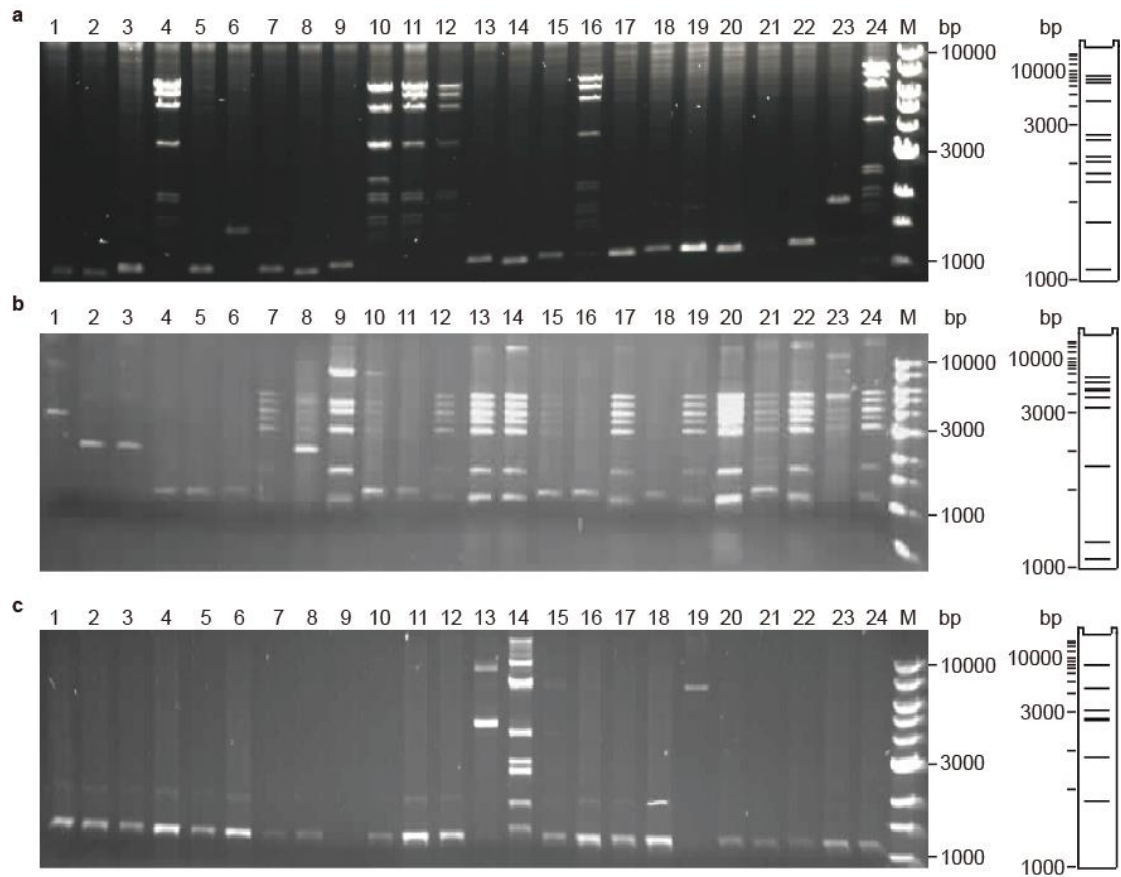


Figure S1 Digestion of the direct cloning products. **(a)** Products of fragment F1 were digested by *Nco*I. M, 1-kb NEB ladder. 1–24, clones obtained from direct cloning. **(b)** Products of fragments F2 and **(c)** F3 digested by *Pvu*II. M, 1-kb NEB ladder. 1–24, clones obtained from direct cloning.

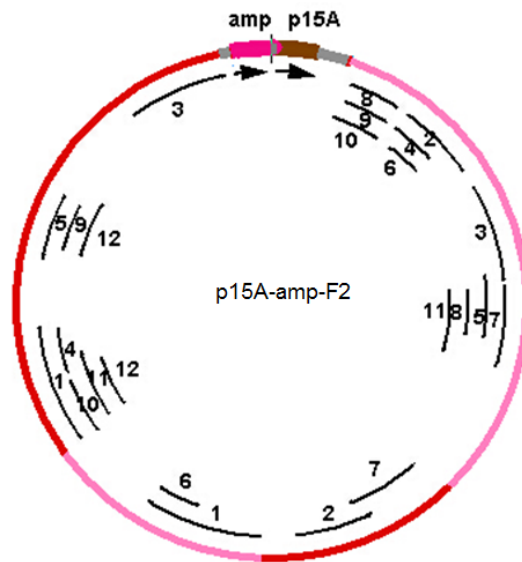


Figure S2 Alignment analysis of the F2 fragment and itself. The repetitive sequences were marked as same numbers.

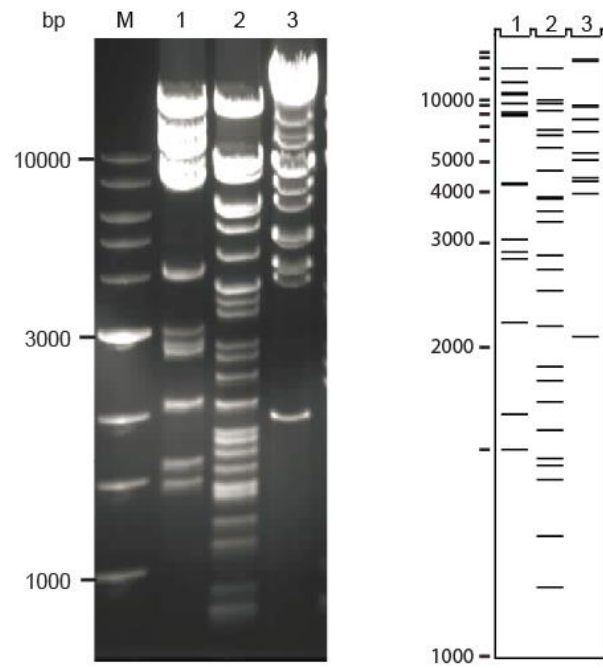


Figure S3 Digestion of pBeloBAC11-sal-lox71-neo-lox66. The three fragments were stitched into pBeloBAC11, and the correct clone was **confirmed** by three restriction enzymes: *AscI* (1), *ApaLI* (2), and (*BgIII*) (3). M: Marker (NEB 1-kb DNA ladder).

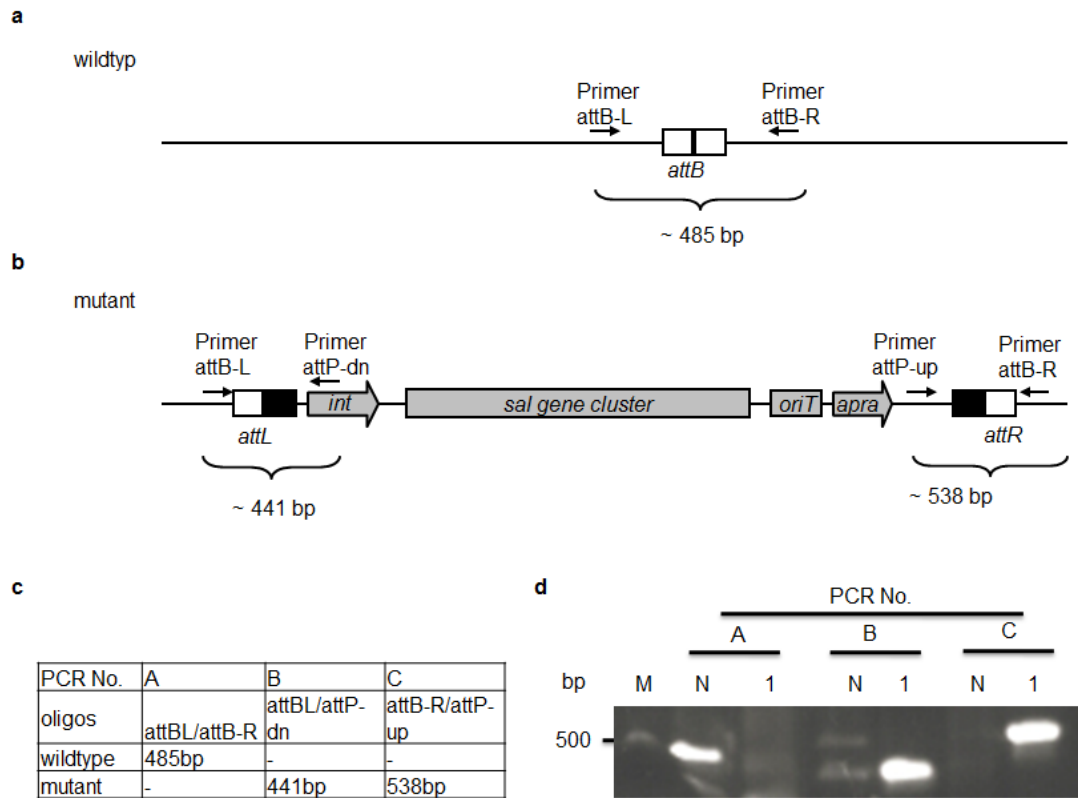


Figure S4 PCR verification of salinomycin gene cluster integration into the *attB* site in *S. coelicolor* A3(2). **(a, b)** Diagram of the PCR procedure in the wild-type **(a)** and mutant **(b)** strains using the indicated primers. Primers attB-L and attB-R were dependent on the sequence of *S. coelicolor* A3(2). Primers attP-down and attP-up were based on the BAC sequence. **(c)** PCR products and primer pairs. **(d)** Agarose gel containing PCR-amplified DNA fragments using to the primer pairs in **(c)**. M, Marker; N, wild-type *S. coelicolor* A3(2); 1, exconjugant colonies.

References

1. Fu, J., Teucher, M., Anastassiadis, K., Skarnes, W. & Stewart, A.F. A Recombineering Pipeline to Make Conditional Targeting Constructs, Vol. 477. (Academic Press, Unit State; 2010).
2. Fu, J. *et al.* Full-length RecE enhances linear-linear homologous recombination and facilitates direct cloning for bioprospecting. *Nat. Biotechnol.* **30**, 440-446 (2012).
3. Wang, H. *et al.* Improved seamless mutagenesis by recombineering using ccdB for counterselection. *Nucleic Acids Res.* **42**, e37 (2014).
4. Paget, M.S.B., Chamberlin, L., Atrih, A., Foster, S.J. & Buttner, M.J. Evidence that the extracytoplasmic function sigma factor sigmaE is required for normal cell wall structure in *Streptomyces coelicolor* A3(2). *J. Bacteriol.* **181**, 204-211 (1999).
5. Huo, L., Rachid, S., Stadler, M., Wenzel, S.C. & Muller, R. Synthetic biotechnology to study and engineer ribosomal bottromycin biosynthesis. *Chem. Biol.* **19**, 1278-1287 (2012).
6. Anastassiadis, K. *et al.* Dre recombinase, like Cre, is a highly efficient site-specific recombinase in *E. coli*, mammalian cells and mice. *Dis. Model. Mech.* **2**, 508-515 (2009).

Publication IV

Direct cloning and heterologous expression of the salinomycin biosynthetic gene cluster from *Streptomyces albus* DSM41398 in *S. coelicolor*A3(2).

Jia Yin, Michael Hoffmann, Xiaoying Bian, **Qiang Tu**, Fu Yan, Liqiu Xia, Xuezhi Ding, A. Francis Stewart, Rolf Müller[†], Jun Fu[†] & Youming Zhang[†]

Author Contributions

J.Y. participated in the design of this study, performed data collection analysis, and drafted the manuscript; H.M., X.Y., T.Q., F.Y., L.Q. and X.Z. participated in interpretation data; A.F.S. and R.M. helped with the revision of the final manuscript. J.F. and Y.Z. designed and oversaw the study, performed data interpretation and drafted the manuscript.

Signatures:

Jia Yin: 尹佳

Michael Hoffmann:

Xiaoying Bian:

Qiang Tu:

Fu Yan:

Liqiu Xia:

Xuezhi Ding:

A. Francis Stewart:

Rolf Müller:

Jun Fu:

Youming Zhang:

C. Final discussion

1. Development of a novel improved Red/ET recombination method

Introduction of foreign DNA into *E. coli* (transformation) is a basic and essential step for mutagenesis and genetic engineering of microorganisms. In order to enhance transformation efficacy, several methods have been reported in the literature to introduce exogenous DNA into the cells, including chemical treatment (using divalent cations like Ca^{2+}), electroporation, polyethylene glycol, utilization of a biolistic gun, ultrasound, hydrogel, and microwave techniques.²⁰² Among these methods, electroporation has been proven to be most useful and convenient to genetically transform a number of microorganisms used for genetic studies.²⁰³

The phage-derived homologous recombination systems, well known as recombineering, have been developed into very helpful DNA engineering technologies performing in electrocompetent cells,^{83,204} and it is very important to increase the transformation efficiency which means the number of cells transformed out of one microgram DNA.

The novel transformation of electrocompetent cells presented here, prepared at room temperature (named as room temperature competent cells), showed almost 10 times higher transformation efficiency than the conventional ice-cold electrocompetent cells in our research (Figure 3-1). As is well known, the electrocompetent cells were always prepared on ice in the conventional electroporation transformation, including other supplies, such as cold pre-chilled cuvette, buffer, and centrifuge. At such low temperatures, cell membrane topology would be modified for electrocompetent cells, and the fatty acid tails of the phospholipids in the cell membrane become more rigid, which that impacts membrane fluidity and permeability, and in turn, cell survival.²⁰⁵ In addition, a remarkable raise occurred in the permeability of cell's plasma membrane, which was used to introduce exogenous DNA into bacterial cell during electroporation process due to externally applied electric field.²⁰³ These structural perturbations were associated with characteristic disturbances of function such as loss

of selective permeability. Afterwards, according to the electroporation theory, hydrophobic pores in the cell membrane were formed spontaneously by lateral thermal fluctuations of the lipid molecules,²⁰⁵ which suggested that hydrophobic pores formation would be enhanced at higher temperatures. Moreover, previous research found that the cell membranes underwent major morphological changes with respect to constantly changing environmental conditions, including temperature.²⁰⁶

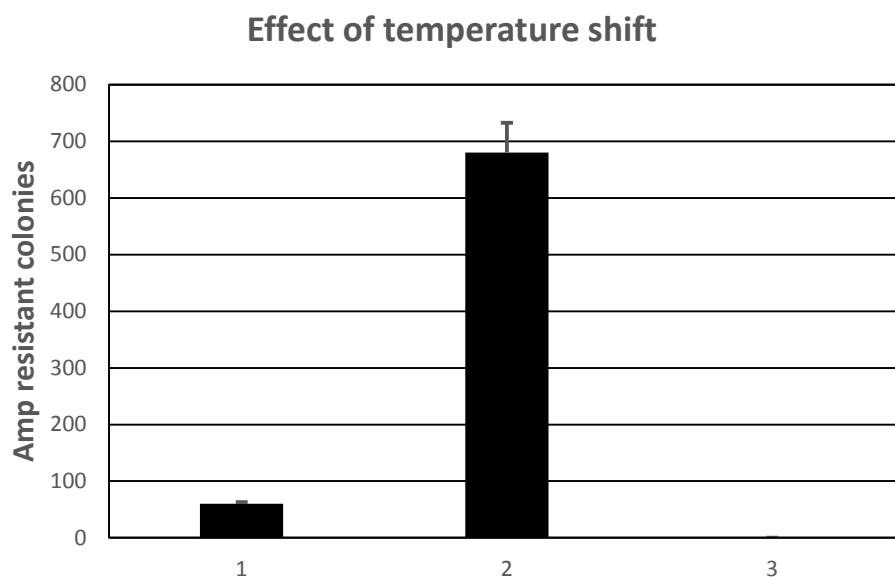


Figure 3-1. Transformation efficiency of competent cells with temperature shift, *E. coli* GB2005 cells transformed by plasmid pGB-amp-Ptet-plu1880 (27.8 kb) were plated on Amp plates. 1, the normal ice-cold method for preparing electrocompetent cells; 2, every step was done at RT; 5, no plasmid DNA. Error bars, s.d.; n = 3.²³⁷

Recombineering is now a central technology for recombinant DNA engineering, as well as the method of choice for bacterial genome engineering.¹¹⁶ In order to improve recombination efficiency, many parameters had been described previously.^{116,207,208} For our Red/ET recombineering, whether LLHR by RecET or LCHR by Red $\alpha\beta$, the recombineering efficiency tests were also performed at room temperature. Interestingly, the situation in these two types of recombineering were not as good as we expected and the result was different. The reason was attributed to the instability of the Red recombinases (Red alpha and beta), which are related to LCHR recombineering while preparing the competent cells at room temperature. In a word, no one protocol was best for all the DNA manipulation.

Using improved Red/ET recombineering with room temperature competent cells, the secondary metabolite pathways can be more easily and rapidly performed in *E. coli*. We can take the appropriate procedure in the complex different cases, whether using room temperature competent cells in transformation, LLHR or cold temperature competent cells in LCHR. Additionally, in some cases, it is more deliberate in the construction of metabolite biosynthetic gene clusters because of knowing the minimum homology arms for recombineering. DNA transformation and recombineering are very critical steps in the study of synthetic biology in the recent revolution for discovering thousands of biosynthetic gene clusters and novel natural compounds. The transformation of exogenous DNA by room temperature competent cells in several other Gram-negative bacteria (*Agrobacterium*, *Burkholderia*, *Photorhabdus* and *Xenorhabdus*) have also been accomplished by our group, which demonstrates the powerful capability and wide adaptability of room temperature competent cells for potential bioprospecting. The improved approach will be a new guide and standard for our Red/ET recombineering in the future.

2. Several applications in mining microbial genomes via Red/ET technology, including disorazol, salinomycin and magnetosome product

Next, we used this developed transformation technique combined with direct cloning and other Red/ET methods for cloning and engineering of known disorazol gene cluster from *Sorangium cellulosum* So ce12 and salinomycin gene cluster from *S. albus* DSM41398, and for the challenging magnetosome gene clusters from *M. gryphiswaldense*.

2.1 Disorazol

Disorazol, initially isolated from the fermentation broth of the myxobacterium *Sorangium cellulosum* So ce12 in 1994,¹⁹⁶ represents a class of antibiotics exhibiting inhibitory activity on cancer cell proliferation at low picomolar concentrations.^{197,198,209} Disorazols are the third group of myxobacterial secondary metabolites that interfere with tubulin polymerization following behind epothilones²³⁸

and tubulysins.²³⁹ Because of this extraordinary potency, disorazols were fostered for development as peptide-conjugates for cancer therapy in drug discovery.^{210,211} Later on, the *dis* biosynthetic gene cluster was identified in 2005 by two independent groups through transposon mutagenesis.^{212,213} The whole disorazol gene cluster was larger than 60 kb with four main genes which were named *disA-D*.²¹² After comparison with databases, the anticipated *disA-C* genes encoded hybrid *trans*-AT type I PKS/NRPS megaenzymes, and the last gene *disD* encoded an additional acyl transferase protein. Our findings are in agreement with these results.

In this work, we reconstituted the 58-kb *dis* core gene cluster from BACs²¹² into a p15A replication origin (*p15A ori*) via Red/ET recombineering and expressed in *M. xanthus* DK1622. Gene clusters with moderate sequence complexity are usually stable in the p15A plasmid.¹⁵⁵ Additionally, disorazol was highly toxic to the host cell due to its biological activity. All the *E. coli* strains harboring the core *dis* gene cluster with native promoter were found to carry mutations after recombineering. Therefore, to solve the issue, an inducible promoter P_{tet} was used to regulate gene expression because of its achievements in enabling several mixed PKS/NRPS natural products in many diverse hosts unrelated to the native producing organisms, including *E. coli*, *M. xanthus* and *P. putida*^{116,129,168,214,215}.

The *dis* gene cluster was randomly transposed into the chromosome of the heterologous host *M. xanthus* DK1622 by electroporation and several recombinants were verified by PCR¹²⁶ to confirm that the *dis* gene cluster had been integrated into the *M. xanthus* chromosome in each case. After fermentation of mutants *M. xanthus*::*p15A-dis*, we demonstrated that the main compound disorazol A₂ was produced at 5-fold higher levels than described in the native producer strain So ce12.^{196,216} The reason for this enhancement could be the effect of promoter P_{tet} which could raise transcription rate of the *dis* gene cluster.

Disorazol was characterized to be a typical *trans*-AT type PKSs. Based on the successful heterologous expression model, more research had been focused on the special AT domain (*disD* gene) of this *trans*-AT type PKS. According to the results of

overexpression the discrete *disD* gene, the yield of disorazol increased approximately 2.5-fold when compared to the ones without overexpression. The event obviously indicated and confirmed the crucial position of the special AT domain in disorazol biosynthetic pathway. Enough supplementation of DisD could boost metabolite quantities to a modest extent. It was worth mentioning that the production of disorazol was currently limiting further progress of the compounds as neither synthetic nor fermentative methods had resulted in sufficient production strategies. Notably, abundant substrates consisting of sufficient ATs would facilitate the PKS module efficiency for polyketide chain extension of disorazol biosynthesis leading to elevated production.

Furthermore, successful heterologous expression of known full-length disorazol gene cluster in *M. xanthus* DK1622 is another considerable mirror for Red/ET recombineering application in engineering metabolites biosynthetic gene clusters in the myxobacteria which own an ample source of natural products with biological activity. Disorazol, a novel macrocyclic compound with two oxazol rings, has almost highest inhibitory effects on mammalian cells ever recorded for a natural product. Clearly, it seems that disorazol has great potential development and market value. However, the first limitation of disorazol promotion is the drug production. The native natural product producer So ce12 grow poor and slowly even in optimized laboratory conditions. In this case, in order to increase the yields and industrialize development of disorazols, a surrogate heterologous host must be invested for the reconstitution and genetic manipulation of *dis* biosynthetic pathways. A multitude of shared heterologous hosts are chosen to express such potential clinic compound because of theirs fast growth rate and the ease of achieving genetic manipulations, including *M. xanthus* DK1622 here. All sorts of trials are provided towards a total synthesis of disorazol and to expand a natural derivative as an anticancer drug.

2.2 Salinomycin

Salinomycin, an antibiotic potassium ionophore with an unique tricyclic spiroketal ring system and an unsaturated six-membered ring isolated from *Streptomyces*

albus,²⁰¹ has been described to exhibit high antimicrobial activity against Gram-positive bacteria and murder breast cancer stem cells in mice at least 100 times higher effectively than paclitaxel.²¹⁷⁻²¹⁹ Previous studies have stated that the polyketide chain of salinomycin was synthesized by an assembly line of nine PKS multienzymes (named *salAI*, *salAII*, *salAIII*, *salAIV*, *salAV*, *salAVI*, *salAVII*, *salAVIII* and *salAIX*).^{220,221} Here, the 106 kb salinomycin gene cluster (*salO-orf18*) was cloned from the genomic DNA of *Streptomyces albus* DSM41398 by three rounds of direct cloning (LLHR) followed by assembly and successfully expression in a heterologous host *S. coelicolor* A3 (2), which resulted in the identification of salinomycin and its derivatives. All of the genes are oriented in the same direction and under the original promoters.

At the beginning, we attempted to directly clone the 106 kb *sal* biosynthetic gene cluster (*salO-orf18*) using one and two-step recombination reactions¹¹⁶ with the BAC vector but were unsuccessful. The failure to this case might have resulted from several issues. Firstly, the direct cloning efficiency, both in transformation and recombineering, was quite low for large DNA fragments, especially with high GC content. Co-transformation of two large linear molecules inside the cell was difficult as well as the recombineering efficiency would also drop for sequences with GC-rich content (data not shown). Secondly, it was arduous to enrich the target DNA after extracting the genomic DNA whose stability could be damaged under the mechanical destruction and degradation by nuclease activity. Consequently, it was challenging to gain the intact *sal* biosynthesis gene cluster from *S. albus* DSM 41398 straight.

Streptomyces is the largest genus of *Actinobacteria* who produce the large majority of characterized natural products.⁸ Over 500 species of *Streptomyces* bacteria have been described. With the purpose to analyze the known natural products biosynthetic gene clusters and discover the silent biosynthetic gene clusters in these precious resources, lots of genetic tools and approaches are developed for *Streptomyces* strains. Target secondary metabolite genes from *Streptomyces* were constructed and manipulated into bifunctional vectors in traditional *E. coli* species by the management of the λ Red

recombination system. Afterwards, the vectors were transformed into *Streptomyces* by conjugation and site-specific integrated into bacteriophage attachment (*attB*) sites for stable maintenance of the points. Consequently, target genes were expressed in model heterologous hosts for natural product production in modern biotechnology.

In summary, our work represents a powerful approach to mine the function of the individual genes and identify novel and potentially valuable analogues of the complex natural products through module exchange in the recipient.

2.3 Magnetosome products

Magnetotactic bacteria (MTB), well known to synthesize magnetic nanocrystals with uniform shapes and sizes at physiological conditions, serve as a source of multiple biological macromolecules taken for the biomimetic synthesis of a whole host of magnetic nanomaterials.⁷⁶ Only a limited number of MTB have been isolated in pure culture so far, including our target *M. gryphiswaldense* strain.²²² According to the 4.3 Mb genome draft sequence of *M. gryphiswaldense*,²²³ magnetosome-related *mam* and *mms* genes are organized as clusters in close proximity to each other.^{76,224}

These clusters are organized as a larger unit, the so-called genomic magnetosome island (MAI), in some species. However, although the gene clusters within the magnetosome island that are required for biomineralization have already been identified in 2010,²²⁸ successfully transferring these specific gene clusters or indeed the whole island to a different bacterium has remained an elusive aim till now.

In our work, a minimal set of genes from the magnetotactic bacterium *M. gryphiswaldense* linked to magnetosome biosynthesis has been successfully expressed in the photosynthetic model organism *Rhodospirillum rubrum* (very close biological relationship to *M. gryphiswaldense*, whose 16S rRNA similarity to *M. gryphiwaldense* is 90%) using powerful Red/ET recombineering technology. These cassettes consist of four chief gene clusters on the magnetosome island that play either vital (*mamAB* gene, for magnetite biomineralization²²⁵) or regulatory (*mamGFDC* gene, for involving in controlling the size of magnetite crystals,²²⁶ *mms6* gene, for the magnetosome membrane protein²²⁷ and *mamXY* gene) roles in magnetosome

formation. These expression cassettes were transformed into *R. rubrum* and cultivated under the same conditions (iron ions in solution, microaerobic or anaerobic environment) as *M. gryphiswaldense*. The host cells *R. rubrum_ABG6* were found to be able to produce iron oxide particles of varying quality depending on which gene clusters were transferred. Consequently, the successful synthesis of magnetosomes within another organism expands the feasibility of commercialization of modified magnetosome production within bacteria which breaks the inexorable laws of nanomagnets under the strict control of magnetotactic bacterial genes. Similarly, depending on the use of Red/ET technology, a crucial following procedure would be integrated magnetosome biosynthetic gene clusters in *E. coli* and other easy-to-grow model bacterium. If fast-growing microbes could be utilized in the future to manufacture nanomagnets in a satisfied yield, higher value-added and greener industries for nanomagnets might emerge. Accompanied by a mass production of nanomagnets in a well-known model organism which is with the advantage of easy-control and stabilization, it could be widely used in development of targeted drugs, kits of early-diagnosis disease, heat treatment for tumor magnetic, molecular environment monitoring, and even the sealing materials for aviation helmet seals.

In a word, the Red/ET recombineering art mediated activation and expression of complex biosynthetic gene clusters in various heterologous hosts is exhibited to be a cogent tool for synthetic biology, not only for antibiotic in PKS/NRPS but also for other type natural products.

3. New molecular technologies are required for construction and modification of large gene clusters in microbial genomes

It is well known that the development of recombinant DNA technology in *E. coli* occurred in the early 1970s while natural products was playing an increasing important part in its progress as all vectors used for cloning depended on the use of genes that conferred resistance to antibiotics (such as penicillin, aureomycin, streptomycin, etc.).¹⁰⁰ Subsequently, multifunctional plasmids, such as P1 vectors, BACs, harboring the specialized secondary metabolite genes were constructed and

engineered in *E. coli* under the use of λ Red recombination genetic engineering methods.²²⁹⁻²³¹ Afterwards, the modified target constructs would be transformed and expressed in a host that was closely associated to its native producer. In addition, all analytical means were in a state of rapid advance with the developing of determining gene expression (transcriptomics, RNA-Seq), enzyme levels (proteomics), precursor supply (metabolomics) in *E. coli* and other well-characterized heterologous hosts.

Cloning, engineering and expression of long microbial genomic sequences in the chosen heterologous host is an effective approach in synthetic biology and genome engineering for natural products discovery and optimization, especially if the genomic sequences are derived from slow-growing bacteria or such one for which genetics are only poorly or not at all established. However, such large sequences (invariably more than 20 kb) are often arduous to acquire directly by traditional PCR or restriction enzyme digestion, and therefore the cloning of these sequences has remained a technical obstacle in molecular biology.

Much of the research in the last two decades has reported several synthetic biology tools which have already been developed to directly capture entire biosynthetic gene clusters from complex genomic DNA sources, circumventing the laborious construction and screening of genomic libraries.¹⁶³ RecET-mediated linear-linear homologous recombination (LLHR)¹¹⁶ or transformation-associated recombination (TAR),¹⁷⁵ CRISPR/Cas9-mediated TAR,²³³ Cas9-assisted targeting of chromosome segments (CATCH),²³⁴ and ϕ BT1 integrase-mediated site-specific recombination²³⁵ are the present popular and powerful methods for direct capture of large DNA fragments from bacteria chromosome. Based on these advanced technologies, now gene cloning is not limiting genome mining anymore. Furthermore, with the continued technological and conceptual advances in bioinformatics, mass spectrometry, proteomics, transcriptomics, metabolomics and gene expression, the new field of microbial genome mining for applications in natural product discovery and development are gradually opening to scientists. Therefore, we predict a second “Golden Age for Antibiotics” and natural products discovery is coming.

D. References

- 1 Cragg, G. M. & Newman, D. J. Natural products: a continuing source of novel drug leads. *Biochim. Biophys. Acta* **1830**, 3670-3695 (2013).
- 2 Chin, Y. W., Balunas, M. J., Chai, H. B., & Kinghorn, A. D. Drug discovery from natural sources. *AAPS Journal* **8**, E239-E253 (2006).
- 3 Firn, R. D. J., C. G. Natural products - a simple model to explain chemical diversity. *Nat. Prod. Rep.* **20**, 382-391 (2003).
- 4 Ganesan, A. The impact of natural products upon modern drug discovery. *Curr. Opin. Chem. Biol.* **12**, 306-317 (2008).
- 5 Cantrell, C. L., Dayan, F. E., & Duke, S. O. Natural products as sources for new pesticides. *J. Nat. Prod.* **75**, 1231-1242 (2012).
- 6 Florey, H. W. Penicillin: A Survey. *British Medical Journal* **2**, 169-171. (1944).
- 7 D. J. Newman, G. M. C., K. M. Snader. The influence of natural products upon drug discovery. *Nat. Prod. Rep.* **17**, 215-234 (2000).
- 8 Katz, L. & Batlz, R. H. Natural product discovery: past, present, and future. *J. Ind. Microbiol. Biotechnol.* **43**, 1-22 (2016).
- 9 Luo, Y., Cobb, R. E., & Zhao H. Recent advances in natural product discovery. *Curr. Opin. Biotechnol.* **30**, 230-237 (2014).
- 10 Agarwal, V. & Nair, S. K. Antibiotics for Emerging Pathogens. *Science* **325**, 1089-1093 (2009).
- 11 Demain, A. L. From natural products discovery to commercialization: a success story. *J. Ind. Microbiol. Biotechnol.* **33**, 486-495 (2006).
- 12 H. Gross, V. O. S., M. D. Henkels, B. Nowak-Thompson, J. E. Loper, & W. H. Gerwick. The Genom isotopic Approach: A Systematic Method to Isolate Products of Orphan Biosynthetic Gene Clusters. *Chem. Biol.* **14**, 53-63 (2007).
- 13 T. A. Gulder, & B. S. Moore. Salinosporamide natural products: Potent 20S proteasome inhibitors as promising cancer chemotherapeutics. *Angew. Chem. Ed. Engl.* **49**, 9346-9367 (2010).
- 14 Li, J. W. V., J. C. Drug discovery and natural products: end of an era or an endless frontier? *Science* **325**, 161-165 (2009).
- 15 Bode, H. B. & Müller, R. The impact of bacterial genomics on natural product research. *Angew. Chem. Int. Ed. Engl.* **44**, 6828-6846 (2005).
- 16 Cordier C., M. D., Murrison S., Nelson A., & O'Leary-Steele C. Natural products as an inspiration in the diversity-oriented synthesis of bioactive compound libraries. *Nat. Prod. Rep.* **25**, 719-737 (2008).
- 17 Winter, J. M. & Tang, Y. Synthetic biological approaches to natural product biosynthesis. *Curr. Opin. Biotech.* **23**, 736-743 (2012).
- 18 Hertweck, C. The biosynthetic logic of polyketide diversity. *Angew. Chem. Ed. Engl.* **48**, 4688-4716 (2009).
- 19 Fischbach, M. A. & Walsh, C. T. Assembly-line enzymology for polyketide and nonribosomal Peptide antibiotics: logic, machinery, and mechanisms. *Chemical reviews* **106**, 3468-3496 (2006).

D. References

- 20 Marahiel, M. A. Working outside the protein-synthesis rules: insights into non-ribosomal peptide synthesis. *Journal of peptide science : an official publication of the European Peptide Society* **15**, 799-807 (2009).
- 21 Knaggs, A. R. The biosynthesis of shikimate metabolites. *Nat. Prod. Rep.* **18**, 334-355 (2001).
- 22 Knaggs, A. R. The biosynthesis of shikimate metabolites. *Nat. Prod. Rep.* **20**, 119-136 (2003).
- 23 Dewick, P. M. The biosynthesis of C5-C25 terpenoid compounds. *Nat. Prod. Rep.* **19**, 181-222 (2002).
- 24 Schwarzer, D. & Marahiel, M. A. Multimodular biocatalysts for natural product assembly. *Naturwissenschaften* **88**, 93-101 (2001).
- 25 Walsh, C. T. Polyketide and nonribosomal peptide antibiotics: modularity and versatility. *Science* **303**, 1805-1810 (2004).
- 26 Moore, B. S. & Hertweck, C. Biosynthesis and attachment of novel bacterial polyketide synthase starter units. *Nat. Prod. Rep.* **19**, 70-99 (2002).
- 27 Schwarzer, D., Finking, R. & Marahiel, M. A. Nonribosomal peptides: from genes to products. *Nat. Prod. Rep.* **20**, 275 (2003).
- 28 Du, L., Sanchez, C., Chen, M., Edwards, D. J. & Shen, B. The biosynthetic gene cluster for the antitumor drug bleomycin from *Streptomyces verticillus* ATCC15003 supporting functional interactions between nonribosomal peptide synthetases and a polyketide synthase. *Chem. Biol.* **7**, 623-642 (2000).
- 29 Miao V., C.-L. M., Brian P., Brost R., Penn J., Whiting A., et al., Daptomycin biosynthesis in *Streptomyces roseosporus*: cloning and analysis of the gene cluster and revision of peptide stereochemistry. *Microbiology* **151**, 1507-1523 (2005).
- 30 Sattely, E. S., Fischbach, M. A. & Walsh, C. T. Total biosynthesis: in vitro reconstitution of polyketide and nonribosomal peptide pathways. *Nat. Prod. Rep.* **25**, 757-793 (2008).
- 31 Staunton, J. & Weissman, K. J. Polyketide biosynthesis: a millennium review. *Nat. Prod. Rep.* **18**, 380-416 (2001).
- 32 Hopwood, D. A. Genetic Contributions to Understanding Polyketide Synthases. *Chem. Rev.* **97**, 2465-2497 (1997).
- 33 Kopp, F. & Marahiel, M. A. Macrocyclization strategies in polyketide and nonribosomal peptide biosynthesis. *Nat. Prod. Rep.* **24**, 735-749 (2007).
- 34 Wenzel, S. C. & Müller., R. The impact of genomics on the exploitation of the myxobacterial secondary metabolome. *Nat. Prod. Rep.* **26**, 1385-1407 (2009).
- 35 Schäberle, T. F., Lohr, F., Schmitz, A., & König, G.M. Antibiotics from myxobacteria. *Nat. Prod. Rep.* **31**, 953-972 (2014).
- 36 Ralph H Lambalot, A. M. G., Roger S Flugel, Peter Zuber, Michael LaCelle, Mohamed A Marahiel, Ralph Reid, Chaitan Khosia, Christopher T Walsh. A new enzyme superfamily - the phosphopantetheinyl transferases. *Chem. Biol.* **3**, 923-936 (1996).
- 37 Mercer, A. C. & Burkart, M. D. The ubiquitous carrier protein--a window to metabolite biosynthesis. *Nat. Prod. Rep.* **24**, 750-773 (2007).
- 38 Chan, Y. A., Boyne, M.T., Podevels, A.M., Klimowicz, A.K., Handelsman, J.,

D. References

- Kelleher, N.L., and Thomas, M.G. Hydroxymalonyl-acyl carrier protein (ACP) and aminomalonyl-ACP are two additional type I polyketide synthase extender units. *Proc. Natl. Acad. Sci. USA* **103**, 14349-14354 (2006).
- 39 Caboche, S., Pupin, M., Leclère, V., Fontaine, A., Jacques, P., Kucherov, G. . NORINE: a database of nonribosomal peptides. *Nucleic Acids Res.* **36**, D326–D331 (2008).
- 40 Das, A., and Khosla, C. Biosynthesis of aromatic polyketides in bacteria. *Accounts of chemical research* **42**, 631-639 (2009).
- 41 Shen, B. Polyketide biosynthesis beyond the type I, II and III polyketide synthase paradigms. *Curr. Opin. Chem. Biol.* **7**, 285-295 (2003).
- 42 Yu, D., Xu, F., Zeng, J., & Zhan, J. Type III polyketide synthases in natural product biosynthesis. *IUBMB Life* **64**, 285-295 (2012).
- 43 Yuzaw, S., Kim, W., Katz, L., & Keasling, J. D. Heterologous production of polyketides by modular type I polyketide synthases in *Escherichia coli*. *Curr. Opin. Biotechnol.* **23**, 727-735 (2012).
- 44 Zhang, W., and Tang, Y. In vitro analysis of type II polyketide synthase. *Methods in Enzymology* **459**, 367-393 (2009).
- 45 Masschelein, J., Mattheus, W., Gao, L.-J., Moons, P., Houdt, R.V., Uytterhoeven, B., Lamberigts, C., Lescrinier, E., Rozenski, J., Herdewijn, P., et al. A PKS/NRPS/FAS hybrid gene cluster from *Serratia plymuthica* RVH1 encoding the biosynthesis of three broad spectrum, zeamine-related antibiotics. *PLoS One* **8**, e54143 (2013).
- 46 Mcdaniel, R., Ebert-Khosla, S., A.Hopwood, D., & Khosla, C. Rational design of aromatic polyketide natural products by recombinant assembly of enzymatic subunits. *Nature* **375**, 549-554 (1995).
- 47 Fu, H., Hopwood, D.A., & Khosla, C. Engineered biosynthesis of novel polyketides: evidence for temporal, but not regiospecific, control of cyclization of an aromatic polyketide precursor. *Chem. Biol.* **1**, 205-210 (1994).
- 48 Abe, I., & Morita, H. . Structure and function of the chalcone synthase superfamily of plant type III polyketide synthases. *Nat. Prod. Rep.* **27**, 809-838 (2010).
- 49 Austin, M. B., & Noel, J.P. The chalcone synthase superfamily of type III polyketide synthases. *Nat. Prod. Rep.* **20**, 79-110 (2003).
- 50 Schow, S. G., Buchholz, T.J., Seufert, W., Dordick, J.S., & Sherman, D.H. Substrate profile analysis and ACP-mediated acyl transfer in *Streptomyces coelicolor* Type III polyketide synthases. *Chembiochem* **8**, 863-868 (2007).
- 51 Li, Y. Y. & Müller, R. Non-modular polyketide synthases in myxobacteria. *Phytochemistry* **70**, 1850-1857 (2009).
- 52 Albertini, A.M., Scoffone, F., Scotti, C., & Galizzi, A. Sequence around the 159-degrees region of the *Bacillus subtilis* genome - the PKS-X locus spans 33.6 kb. *Microbiology* **141**, 299–309 (1995).
- 53 Piel, J. A polyketide synthase-peptide synthetase gene cluster from an uncultured bacterial symbiont of *Paederus* beetles. *Proc. Natl. Acad. Sci. USA* **99**, 14002-14007 (2002).
- 54 Cheng, Y. Q, & Shen, B. Type I polyketide synthase requiring a discrete acyltransferase for polyketide biosynthesis. *Proc. Natl. Acad. Sci. USA* **100**, 3149–

D. References

- 3154 (2003).
- 55 El-Sayed, A.K., Cooper, S.M., Stephens, E., Simpson, T.J., & Thomas, C.M. Characterization of the mupirocin biosynthesis gene cluster from *Pseudomonas fluorescens* NCIMB 10586. *Chem. Biol.* **10**, 419–430 (2003).
- 56 Piel, J. Biosynthesis of polyketides by trans-AT polyketide synthases. *Nat. Prod. Rep.* **27**, 996-1047 (2010).
- 57 Helfrich, E. J. & Piel, J. Biosynthesis of polyketides by trans-AT polyketide synthases. *Nat. Prod. Rep.* (2015).
- 58 Nguyen T, I. K., Jenke-Kodama H, Dittmann E, Gurgui C, Hochmuth T, Taudien S, Platzer M, Hertweck C, & Piel J. Exploiting the mosaic structure of trans-acyltransferase polyketide synthases for natural product discovery and pathway dissection. *Nat. Biotechnol.* **26**, 225–233 (2008).
- 59 Olano, C., Méndez, C., and Salas, J.A. Molecular insights on the biosynthesis of antitumour compounds by actinomycetes. *Microbial Biotechnology* **4**, 144-164 (2011).
- 60 Brakhage, A. Molecular Regulation of β -Lactam Biosynthesis in *Filamentous Fungi*. *Microbiology and Molecular Biology Reviews* **62**, 547–585 (1998).
- 61 T. J. Wolpert, V. M., W. Acklin, B. Jaun, J. Seibl, J. Meiliand & D. Arigoni. Structure of victorin C, the major host-selective toxin from *Cochliobolus victoriae*. *Experientia.* **41**, 1524-1529 (1985).
- 62 Brachmanna, A. O., Kirchnera, F., Keglera, C., Kinskia, S.C., Schmittb, I., & Bode, H.B. Triggering the production of the cryptic blue pigment indigoidine from *Photorhabdus luminescens*. *Journal of Biotechnology* **157**, 96-99 (2012).
- 63 Carroll, P. A., Calderwood, S.B., Butterson, J.R., Choi, M.H., & Watnick, P.I. . *Vibrio cholerae* VibF Is Required for Vibriobactin Synthesis and Is a Member of the Family of Nonribosomal Peptide Synthetases. *Journal of Bacteriology* **182**, 1731–1738 (2000).
- 64 W.W. Carmichael, S. M. F. O. A., J. S. An, et al.,. Human Fatalities from Cyanobacteria: Chemical and Biological Evidence for Cyanotoxins. *Environmental Health Perspectives* **109**, 663-668 (2001).
- 65 Cane, D. E. & Walsh, C. T. The parallel and convergent universes of polyketide synthases and nonribosomal peptide synthetases. *Chem. Biol.* **6**, R319-325 (1999).
- 66 Eustáquio, A. S. et al. Biosynthesis of the salinosporamide A polyketide synthase substrate chloroethylmalonyl-coenzyme A from S-adenosyl-L-methionine. *Proc. Natl. Acad. Sci. USA* **106**, 12295–12300 (2009).
- 67 B. Silakowski, H. U. S., H. Ehret, B. Kunze, S. Weinig, G. Nordsiek, P. Brandt, H. Blöcker, G. Höfle, S. Beyer, & R. Müller. New Lessons for Combinatorial Biosynthesis from Myxobacteria. *J. Biol. Chem.* **274**, 37391-37399 (1999).
- 68 S. Weinig, H. J. H., T. Mahmud, R. Müller. Melithiazol biosynthesis: further insights into myxobacterial PKS/NRPS systems and evidence for a new subclass of methyl transferases. *Chem. Biol.* **10**, 939-952 (2003).
- 69 Y. Paitan, G. A., E. Orr, E. Z. Ron, E. Rosenberg. The first gene in the biosynthesis of the polyketide antibiotic TA of *Myxococcus xanthus* codes for a unique PKS module coupled to a peptide synthetase. *J. Mol. Biol.* **286**, 465-474 (1999).

D. References

- 70 B. Silakowski, G. N., B. Kunze, H. Blöcker, & R. Müller. Novel features in a combined polyketide synthase/non-ribosomal peptide synthetase: the myxalamid biosynthetic gene cluster of the myxobacterium *Stigmatella aurantiaca* Sga15. *Chem. Biol.* **8**, 59-69 (2001).
- 71 Shen, B. *et al.* The biosynthetic gene cluster for the anticancer drug bleomycin from *Streptomyces verticillus* ATCC15003 as a model for hybrid peptide-polyketide natural product biosynthesis. *J. Ind. Microbiol. Biotechnol.* **27**, 378-385 (2001).
- 72 Huang, T., Wang, Y., Yin, J., Du, Y., Tao, M., Xu, J., Chen, W., Lin, S., & Deng, Z. Identification and characterization of the pyridomycin biosynthetic gene cluster of *Streptomyces pyridomyceticus* NRRL B-2517. *J. Biol. Chem.* **286**, 20648-20657 (2011).
- 73 N. Gaitatzis, A. H., R. Müller, & S. Beyer. The *mtaA* gene of the myxothiazol biosynthetic gene cluster from *Stigmatella aurantiaca* DW4/3-1 encodes a phosphopantetheinyl transferase that activates polyketide synthases and polypeptide synthetases. *J. Biochem.* **129**, 119-124 (2001).
- 74 L. E. Quadri, P. H. W., M. Lei, M. M. Nakano, P. Zuber, & C. T. Walsh. Characterization of Sfp, a *Bacillus subtilis* phosphopantetheinyl transferase for peptidyl carrier protein domains in peptide synthetases. *Biochemistry* **37**, 1585-1595 (1998).
- 75 Sanchez, C., Du, L., Edwards, D. J., Toney, M. D. & Shen, B. Cloning and characterization of a phosphopantetheinyl transferase from *Streptomyces verticillus* ATCC15003, the producer of the hybrid peptide-polyketide antitumor drug bleomycin. *Chem. Biol.* **8**, 725-738 (2001).
- 76 Prozorov, T., Bazylinski, D. A., Mallapragada, S. K. & Prozorov, R. Novel magnetic nanomaterials inspired by magnetotactic bacteria: topical review. *Mater. Sci. Eng. R.* **74**, 133–172 (2013).
- 77 Blakemore, R. P. Magnetotactic bacteria. *Science* **190**, 377-379 (1982).
- 78 Komeili, A., Zhuo Li & D. K. Newman. Magnetosomes Are Cell Membrane Invaginations Organized by the Actin-Like Protein MamK. *Science* **311**, p. 242-245 (2006).
- 79 Pollithy, A. *et al.* Magnetosome expression of functional camelid antibody fragments (nanobodies) in *Magnetospirillum gryphiswaldense*. *Appl. Environ. Microbiol.* **77**, 6165–6171 (2011).
- 80 Ullrich, S., Kube, M., Schübbe, S., Reinhardt, R. & Schüller, D. A hypervariable 130-kilobase genomic region of *Magnetospirillum gryphiswaldense* comprises a magnetosome island which undergoes frequent rearrangements during stationary growth. *J. Bacteriol.* **187**, 7176–7184 (2005).
- 81 Muyrers, J.P., Zhang, Y., Testa, G., & Stewart, A.F. Rapid modification of bacterial artificial chromosomes by ET-recombination. *Nucleic Acids Res.* **27**, 1555-1557 (1999).
- 82 Youming Zhang, J. P. P. Muyrers, Giuseppe Testa, & A. Francis Stewart. DNA cloning by homologous recombination in *Escherichia coli*. *Nature biotechnol.* **18**, 1314-1317 (2000).
- 83 Zhang Y., Muyrers J.P. and Stewart A.F. A new logic for DNA engineering using

D. References

- recombination in *Escherichia coli*. *Nature Genetics*. **20**, 123-128 (1998).
- 84 Yu, D. *et al.* An efficient recombination system for chromosome engineering in *Escherichia coli*. *Proc. Natl. Acad. Sci. USA* **97**, 5978-5983 (2000).
- 85 Junping Wang, M. S., Jeanette Rientjes, Jun Fu, Heike Hollak, Harald Kranz, Wei Xie, A. Francis Stewart & Youming Zhang. An improved recombinering approach by adding RecA to lambda Red recombination. *BMC Mol. Biotechnolo.***32**, 43-54 (2006).
- 86 Copeland, N. G., Jenkins, N. A. & Court, D. L. Recombineering: a powerful new tool for mouse functional genomics. *Nature reviews. Genetics* **2**, 769-779 (2001).
- 87 Sharan, S. K., Thomason, L. C., Kuznetsov, S. G. & Court, D. L. Recombineering: a homologous recombination-based method of genetic engineering. *Nature protocols* **4**, 206-223 (2009).
- 88 Muyrers, J.P., Zhang, Y., Buchholz, F., & Stewart A.F. RecE/RecT and Reda/Redb initiate double stranded break repair by specifically interacting with their respective partners. *Genes & Dev.* **14**, 1971-1982 (2000).
- 89 Zhang Y. M., J., Rientjes, J. and Stewart, A.F. Phage annealing proteins promote oligonucleotide-directed mutagenesis in *Escherichia coli* and mouse ES cells. *BMC molecular biology* **4**, 1-14 (2003).
- 90 Kovall, R. & Matthews, B. W. Toroidal structure of lambda-exonuclease. *Science* **277**, 1824-1827 (1997).
- 91 Erler, A. *et al.* Conformational adaptability of Redbeta during DNA annealing and implications for its structural relationship with Rad52. *J. Mol. Biol.* **391**, 586-598 (2009).
- 92 Iyer, L. M., Koonin, E. V. & Aravind, L. Classification and evolutionary history of the single-strand annealing proteins, RecT, Redbeta, ERF and RAD52. *BMC Genomics* **3**, 8 (2002).
- 93 Muniyappa, K. & M., E. Phage $\lambda\beta$ protein, a component of general recombination, is associated with host ribosomal S1 protein. *Biochem. Mol. Biol. Int.* **31**, 1-11 (1993).
- 94 Venkatesh, T. V. & R., C.M. Ribosomal protein S1 and NusA protein complexed to recombination protein β of phage λ . *J. Bacteriol.* **175**, 1844-1846 (1993).
- 95 Shulman, M. J., Hallick, L.M., Echols, H. & Signer, E.R. Properties of recombination-deficient mutants of bacteriophage lambda. *J. Mol. Biol.* **52**, 501-520 (1970).
- 96 Zagursky, R. J. & H., J.B. Expression of the phage λ recombination genes *exo* and *bet* under *lacPO* control on a multi-copy plasmid. *Gene* **23**, 277-292 (1983).
- 97 Hall, S. D. & K., R.D. Homologous pairing and strand exchange promoted by the *Escherichia coli* RecT protein. *Proc. Natl. Acad. Sci. USA* **91**, 3205-3209 (1994).
- 98 Muniyappa, K. & R., C.M. The homologous recombination system of phage λ . Pairing activities of β protein. *J. Biol. Chem.* **261**, 7472-7478 (1986).
- 99 Kmiec, E. & H., W. K. Beta protein of bacteriophage lambda promotes renaturation of DNA. *J. Biol. Chem.* **256**, 12636-12639 (1981).
- 100 STANLEY N. COHEN, A. C. Y. C., HERBERT W. BOYER, AND ROBERT B. HELLING. Construction of Biologically Functional Bacterial Plasmids *In Vitro*. *Proc. Nat. Acad. Sci. USA* **70**, 3240-3244 (1973).
- 101 Mullis, K. *et al.* Specific enzymatic amplification of DNA in vitro: the polymerase

D. References

- chain reaction. *Cold Spring Harbor symposia on quantitative biology* **51 Pt 1**, 263-273 (1986).
- 102 Collins, J. & Hohn, B. Cosmids: a type of plasmid gene-cloning vector that is packageable in vitro in bacteriophage lambda heads. *Proc. Nat. Acad. Sci. USA* **75**, 4242-4246 (1978).
- 103 Pierce, J. C., Sauer, B. & Sternberg, N. A positive selection vector for cloning high molecular weight DNA by the bacteriophage P1 system: improved cloning efficacy. *Proc. Nat. Acad. Sci. USA* **89**, 2056-2060 (1992).
- 104 Shizuya, H. *et al.* Cloning and stable maintenance of 300-kilobase-pair fragments of human DNA in *Escherichia coli* using an F-factor-based vector. *Proc. Nat. Acad. Sci. USA* **89**, 8794-8797 (1992).
- 105 O'Connor, M., Peifer, M. & Bender, W. Construction of large DNA segments in *Escherichia coli*. *Science* **244**, 1307-1312 (1989).
- 106 Kim, U. J., Shizuya, H., de Jong, P. J., Birren, B. & Simon, M. I. Stable propagation of cosmid sized human DNA inserts in an F factor based vector. *Nucleic Acids Res.* **20**, 1083-1085 (1992).
- 107 Orr-Weaver, T. L., Szostak, J. W. & Rothstein, R. J. Genetic applications of yeast transformation with linear and gapped plasmids. *Methods Enzymol.* **101**, 228-245 (1983).
- 108 Szostak, J. W., Orr-Weaver, T. L., Rothstein, R. J. & Stahl, F. W. The double-strand-break repair model for recombination. *Cell* **33**, 25-35 (1983).
- 109 Moerschell, R. P., Tsunasawa, S. & Sherman, F. Transformation of yeast with synthetic oligonucleotides. *Proc. Nat. Acad. Sci. USA* **85**, 524-528 (1988).
- 110 Hamilton, C. M., Aldea, M., Washburn, B. K., Babitzke, P. & Kushner, S. R. New method for generating deletions and gene replacements in *Escherichia coli*. *J. Bacteriol.* **171**, 4617-4622 (1989).
- 111 Ellis, H. M., Yu, D., DiTizio, T. & Court, D. L. High efficiency mutagenesis, repair, and engineering of chromosomal DNA using single-stranded oligonucleotides. *Proc. Nat. Acad. Sci. USA* **98**, 6742-6746 (2001).
- 112 Joep P.P. Muylers, Y. Zhang, Vladimir Benes, Giuseppe Testa, Wilhelm Ansorge & A. Francis Stewart. Point mutation of bacterial artificial chromosomes by ET recombination. *EMBO reports.* **1**, 239-243 (2000).
- 113 Warming, S., Costantino, N., Court, D. L., Jenkins, N. A. & Copeland, N. G. Simple and highly efficient BAC recombineering using galK selection. *Nucleic Acids Res.* **33**, e36 (2005).
- 114 Wong, Q. N. *et al.* Efficient and seamless DNA recombineering using a thymidylate synthase A selection system in *Escherichia coli*. *Nucleic Acids Res.* **33**, e59 (2005).
- 115 DeVito, J. A. Recombineering with tolC as a selectable/counter-selectable marker: remodeling the rRNA operons of *Escherichia coli*. *Nucleic Acids Res.* **36**, e4 (2008).
- 116 Fu, J. *et al.* Full-length RecE enhances linear-linear homologous recombination and facilitates direct cloning for bioprospecting. *Nature Biotechnol.* **30**, 440-446 (2012).
- 117 Hu, S. *et al.* Genome engineering of *Agrobacterium tumefaciens* using the lambda Red recombination system. *Appl. Microbiol. Biotechnol.* **98**, 2165-2172 (2014).
- 118 van Kessel, J. C. & Hatfull, G. F. Recombineering in *Mycobacterium tuberculosis*.

D. References

- Nat. methods* **4**, 147-152 (2007).
- 119 van Kessel, J. C. & Hatfull, G. F. Mycobacterial recombineering. *Methods Mol. Biol.* **435**, 203-215 (2008).
- 120 Yin, J. *et al.* A new recombineering system for *Phototrhobdus* and *Xenorhabdus*. *Nucleic Acids Res.* **43**, e36 (2015).
- 121 Bunny, K., Liu, J. & Roth, J. Phenotypes of *lexA* mutations in *Salmonella enterica*: evidence for a lethal *lexA* null phenotype due to the Fels-2 prophage. *J. Bacteriol.* **184**, 6235-6249 (2002).
- 122 Derbise, A., Lesic, B., Dacheux, D., Ghigo, J. M. & Carniel, E. A rapid and simple method for inactivating chromosomal genes in *Yersinia*. *FEMS Immunology & Medical Microbiology* **38**, 113-116 (2003).
- 123 Kang, Y. *et al.* Knockout and pullout recombineering for naturally transformable *Burkholderia thailandensis* and *Burkholderia pseudomallei*. *Nat. protocols* **6**, 1085-1104 (2011).
- 124 Lynn Thomason, D. L. C., Mikail Bubunencko, Nina Costantino, & Helen Wilson, S. D., & Amos Oppenheim. Recombineering, genetic engineering in bacteria using homologous recombination. *Current Protocols in Molecular Biology*, 1.16.11-11.16.24 (2007).
- 125 Maresca, M. *et al.* Single-stranded heteroduplex intermediates in lambda Red homologous recombination. *BMC molecular biology* **11**, 54 (2010).
- 126 Fu, J. *et al.* Efficient transfer of two large secondary metabolite pathway gene clusters into heterologous hosts by transposition. *Nucleic Acids Res.* **36**, e113 (2008).
- 127 Wenzel, S. C. *et al.* Heterologous expression of a myxobacterial natural products assembly line in *pseudomonads* via red/ET recombineering. *Chem. Biol.* **12**, 349-356 (2005).
- 128 Ongley, S. E., Bian, X., Neilan, B. A. & Müller, R. Recent advances in the heterologous expression of microbial natural product biosynthetic pathways. *Nat. Prod. Rep.* **30**, 1121-1138 (2013).
- 129 Bian, X., Plaza, A., Zhang, Y. & Müller, R. Luminmycins A-C, cryptic natural products from *Phototrhobdus luminescens* identified by heterologous expression in *Escherichia coli*. *J. Nat. Prod.* **75**, 1652-1655 (2012).
- 130 Bian, X. *et al.* Heterologous production of glidobactins/luminmycins in *Escherichia coli* Nissle containing the glidobactin biosynthetic gene cluster from *Burkholderia* DSM7029. *Chembiochem* **15**, 2221-2224 (2014).
- 131 Hanahan, D., Jessee, J. & Bloom, F. R. Plasmid transformation of *Escherichia coli* and other bacteria. *Methods Enzymol.* **204**, 63-113 (1991).
- 132 Dower, W. J., Miller, J. F. & Ragsdale, C. W. High efficiency transformation of *E. coli* by high voltage electroporation. *Nucleic Acids Res.* **16**, 6127-6145 (1988).
- 133 Fiedler, S. & Wirth, R. Transformation of bacteria with plasmid DNA by electroporation. *Anal Biochem.* **170**, 38-44 (1988).
- 134 Taketo, A. DNA transfection of *Escherichia coli* by electroporation. *Biochim. Biophys. Acta* **949**, 318-324 (1988).
- 135 Sambrook, J. R., D.W. *Molecular Cloning: A Laboratory Manual. 3rd ed.* Vol. Vol. 1 & 3 (Cold Spring Harbor Laboratory Press, 2001).

D. References

- 136 Andreason, G. L. & Evans, G. A. Introduction and expression of DNA molecules in eukaryotic cells by electroporation. *BioTechniques* **6**, 650-660 (1988).
- 137 Chassy, B. M. F., J. L. Transformation of *Lactobacillus casei* by electroporation. *FEMS Microbiol. Lett.* **44**, 173-177 (1987).
- 138 Yoshida, N. & Sato, M. Plasmid uptake by bacteria: a comparison of methods and efficiencies. *Appl. Microbiol. Biotechnol.* **83**, 791-798 (2009).
- 139 Aune, T. E. & Aachmann, F. L. Methodologies to increase the transformation efficiencies and the range of bacteria that can be transformed. *Appl. Microbiol. Biotechnol.* **85**, 1301-1313 (2010).
- 140 Cong, L. *et al.* Multiplex genome engineering using CRISPR/Cas systems. *Science* **339**, 819-823 (2013).
- 141 Wiedenheft, B., Sternberg, S. H. & Doudna, J. A. RNA-guided genetic silencing systems in bacteria and archaea. *Nature* **482**, 331-338 (2012).
- 142 Horvath, P. & Barrangou, R. CRISPR/Cas, the immune system of bacteria and archaea. *Science* **327**, 167-170 (2010).
- 143 Deltcheva, E. *et al.* CRISPR RNA maturation by trans-encoded small RNA and host factor RNase III. *Nature* **471**, 602-607 (2011).
- 144 Jiang, Y. *et al.* Multigene editing in the *Escherichia coli* genome via the CRISPR-Cas9 system. *Appl. Environ. Microbiol.* **81**, 2506-2514 (2015).
- 145 Pyne, M. E., Moo-Young, M., Chung, D. A. & Chou, C. P. Coupling the CRISPR/Cas9 System with Lambda Red Recombineering Enables Simplified Chromosomal Gene Replacement in *Escherichia coli*. *Appl. Environ. Microbiol.* **81**, 5103-5114 (2015).
- 146 Wenzel, S. C. & Müller, R. Recent developments towards the heterologous expression of complex bacterial natural product biosynthetic pathways. *Curr. Opin. Biotechnol.* **16**, 594-606 (2005).
- 147 Wenzel, S. C. & Müller, R. Myxobacterial natural product assembly lines: fascinating examples of curious biochemistry. *Nat. Prod. Rep.* **24**, 1211-1224 (2007).
- 148 Bode, H. B. & Müller, R. Analysis of myxobacterial secondary metabolism goes molecular. *J. Ind. Microbiol. Biotechnol.* **33**, 577-588 (2006).
- 149 Gross, F. *et al.* Bacterial type III polyketide synthases: phylogenetic analysis and potential for the production of novel secondary metabolites by heterologous expression in pseudomonads. *Archives of microbiology* **185**, 28-38 (2006).
- 150 Schmidt, E. W. *et al.* Patellamide A and C biosynthesis by a microcin-like pathway in *Prochloron didemni*, the cyanobacterial symbiont of *Lissoclinum patella*. *Proc. Natl. Acad. Sci. USA* **102**, 7315-7320 (2005).
- 151 Kodumal, S. J. *et al.* Total synthesis of long DNA sequences: synthesis of a contiguous 32-kb polyketide synthase gene cluster. *Proc. Natl. Acad. Sci. USA* **101**, 15573-15578 (2004).
- 152 Bode, H. B. & Muller, R. The impact of bacterial genomics on natural product research. *Angew. Chem. Int. Ed. Engl.* **44**, 6828-6846 (2005).
- 153 Sorensen, H. P. & Mortensen, K. K. Advanced genetic strategies for recombinant protein expression in *Escherichia coli*. *J. Biotechnol.* **115**, 113-128 (2005).
- 154 Li, Y. *et al.* Directed natural product biosynthesis gene cluster capture and expression

D. References

- in the model bacterium *Bacillus subtilis*. *Sci. Rep.* **5**, 9383 (2015).
- 155 Hailong Wang, Z. L., Ruonan Jia, Jia Yin, Xiaoying Bian, Aiyong Li, Rolf Müller, A Francis Stewart, Jun Fu & Youming Zhang. A concerted pipeline for direct cloning of biosynthetic gene clusters and engineering for heterologous expression. *Nature protocols* **accepted** (2016).
- 156 Tu, Q. *et al.* Genetic engineering and heterologous expression of the disorazol biosynthetic gene cluster via Red/ET recombineering. *Sci. Rep.* **6**, 21066 (2016).
- 157 Homburg, S., Oswald, E., Hacker, J. & Dobrindt, U. Expression analysis of the colibactin gene cluster coding for a novel polyketide in *Escherichia coli*. *FEMS Microbiol. Lett.* **275**, 255-262 (2007).
- 158 Watanabe, K. *et al.* Total biosynthesis of antitumor nonribosomal peptides in *Escherichia coli*. *Nat. Chem. Biol.* **2**, 423-428 (2006).
- 159 Fong, R. *et al.* Characterization of a large, stable, high-copy-number *Streptomyces* plasmid that requires stability and transfer functions for heterologous polyketide overproduction. *Appl. Environ. Microbiol.* **73**, 1296-1307 (2007).
- 160 Kakirde, K. S. *et al.* Gram negative shuttle BAC vector for heterologous expression of metagenomic libraries. *Gene* **475**, 57-62 (2011).
- 161 Aakvik, T. *et al.* A plasmid RK2-based broad-host-range cloning vector useful for transfer of metagenomic libraries to a variety of bacterial species. *FEMS Microbiol. Lett.* **296**, 149-158 (2009).
- 162 Ganusov, V. V. & Brilkov, A. V. Estimating the instability parameters of plasmid-bearing cells. I. Chemostat culture. *J. Theoretical Biology* **219**, 193-205 (2002).
- 163 Zhang, M. M., Wang, Y., Ang, E. L. & Zhao, H. Engineering microbial hosts for production of bacterial natural products. *Nat. Prod. Rep.* (2016).
- 164 Dahod, S. K. Dissolved carbon dioxide measurement and its correlation with operating parameters in fermentation processes. *Biotechnology progress* **9**, 655-660 (1993).
- 165 Gross, F. *et al.* Metabolic engineering of *Pseudomonas putida* for methylmalonyl-CoA biosynthesis to enable complex heterologous secondary metabolite formation. *Chem. Biol.* **13**, 1253-1264 (2006).
- 166 Wang, A. *et al.* High level expression and purification of bioactive human alpha-defensin 5 mature peptide in *Pichia pastoris*. *Appl. Microbiol. Biotechnol.* **84**, 877-884 (2009).
- 167 Liao, G. *et al.* Cloning, reassembling and integration of the entire nikkomycin biosynthetic gene cluster into *Streptomyces ansiochromogenes* lead to an improved nikkomycin production. *Microbial cell factories* **9**, 6 (2010).
- 168 Chai, Y. *et al.* Heterologous expression and genetic engineering of the tubulysin biosynthetic gene cluster using Red/ET recombineering and inactivation mutagenesis. *Chem. Biol.* **19**, 361-371 (2012).
- 169 Perlova, O. *et al.* Reconstitution of the myxothiazol biosynthetic gene cluster by Red/ET recombination and heterologous expression in *Myxococcus xanthus*. *Appl. Environ. Microbiol.* **72**, 7485-7494 (2006).
- 170 Yin, J. *et al.* Direct cloning and heterologous expression of the salinomycin

D. References

- biosynthetic gene cluster from *Streptomyces albus* DSM41398 in *Streptomyces coelicolor* A3(2). *Sci. Rep.* **5**, 15081 (2015).
- 171 Kolinko, I. *et al.* Biosynthesis of magnetic nanostructures in a foreign organism by transfer of bacterial magnetosome gene clusters. *Nature nanotechnology* **9**, 193-197 (2014).
- 172 Vladimir Larionov, N. K., & Michael, A. R. Direct isolation of human BRCA2 gene by transformation-associated recombination in yeast. *Proc. Natl. Acad. Sci. USA* **94**, 7384–7387 (1997).
- 173 Natalay, L. A., Joan, G., & Vladimir Larionov. Functional copies of a human gene can be directly isolated by transformation-associated recombination cloning with a small 3' end target sequence. *Proc. Natl. Acad. Sci. USA* **95**, 4469–4474 (1998).
- 174 Kouprina, N. & Larionov, V. Selective isolation of genomic loci from complex genomes by transformation-associated recombination cloning in the yeast *Saccharomyces cerevisiae*. *Nature protocols* **3**, 371-377 (2008).
- 175 Kouprina, N. & Larionov, V. TAR cloning insights into gene function, long-range haplotypes and genome structure and evolution. *Nature Reviews Genetics* **7**, 805-812 (2006).
- 176 Noskov, V. N. *et al.* A general cloning system to selectively isolate any eukaryotic or prokaryotic genomic region in yeast. *BMC Genomics* **4**, 16 (2003).
- 177 Kim, J. H. *et al.* Cloning large natural product gene clusters from the environment: piecing environmental DNA gene clusters back together with TAR. *Biopolymers* **93**, 833-844 (2010).
- 178 Kouprina, N. *et al.* Dynamic structure of the SPANX gene cluster mapped to the prostate cancer susceptibility locus HPCX at Xq27. *Genome research* **15**, 1477-1486 (2005).
- 179 Kouprina, N. *et al.* The SPANX gene family of cancer/testis-specific antigens: rapid evolution and amplification in African great apes and hominids. *Proc. Natl. Acad. Sci. USA* **101**, 3077-3082 (2004).
- 180 Gibson, D. G. *et al.* Enzymatic assembly of DNA molecules up to several hundred kilobases. *Nat. methods* **6**, 343-345 (2009).
- 181 Shao, Z., Zhao, H. & Zhao, H. DNA assembler, an in vivo genetic method for rapid construction of biochemical pathways. *Nucleic Acids Res.* **37**, e16 (2009).
- 182 Shao, Z., Luo, Y. & Zhao, H. Rapid characterization and engineering of natural product biosynthetic pathways via DNA assembler. *Mol. Biosyst.* **7**, 1056-1059 (2011).
- 183 Baltz, R. H. Molecular engineering approaches to peptide, polyketide and other antibiotics. *Nat. Biotechnol.* **24**, 1533-1540 (2006).
- 184 Galm, U. & Shen, B. Expression of biosynthetic gene clusters in heterologous hosts for natural product production and combinatorial biosynthesis. *Expert Opin. Drug Discov.* **1**, 409-437 (2006).
- 185 Ikeda, H. *et al.* Complete genome sequence and comparative analysis of the industrial microorganism *Streptomyces avermitilis*. *Nat. Biotechnol.* **21**, 526-531 (2003).
- 186 Onaka, H., Taniguchi, S., Igarashi, Y. & Furumai, T. Cloning of the staurosporine biosynthetic gene cluster from *Streptomyces* sp. TP-A0274 and its heterologous

D. References

- expression in *Streptomyces lividans*. *J. Antibiot. (Tokyo)* **55**, 1063-1071 (2002).
- 187 Bentley, S. D. *et al.* Complete genome sequence of the model actinomycete *Streptomyces coelicolor* A3(2). *Nature* **417**, 141-147 (2002).
- 188 Pope, M. R., Murrell, S. A. & Ludden, P. W. Covalent modification of the iron protein of nitrogenase from *Rhodospirillum rubrum* by adenosine diphosphoribosylation of a specific arginine residue. *Proc. Natl. Acad. Sci. USA* **82**, 3173-3177 (1985).
- 189 Mutka, S. C., Carney, J. R., Liu, Y. & Kennedy, J. Heterologous production of epothilone C and D in *Escherichia coli*. *Biochemistry* **45**, 1321-1330 (2006).
- 190 Krug, D. *et al.* Discovering the hidden secondary metabolome of *Myxococcus xanthus*: a study of intraspecific diversity. *Appl. Environ. Microbiol.* **74**, 3058-3068 (2008).
- 191 Stevens, D. C., Henry, M. R., Murphy, K. A. & Boddy, C. N. Heterologous expression of the oxytetracycline biosynthetic pathway in *Myxococcus xanthus*. *Appl. Environ. Microbiol.* **76**, 2681-2683 (2010).
- 192 Oliynyk, M. *et al.* Complete genome sequence of the erythromycin-producing bacterium *Saccharopolyspora erythraea* NRRL23338. *Nat. Biotechnol.* **25**, 447-453 (2007).
- 193 Baltz, R. H. *Streptomyces* and *Saccharopolyspora* hosts for heterologous expression of secondary metabolite gene clusters. *J. Ind. Microbiol. Biotechnol.* **37**, 759-772 (2010).
- 194 Butzin, N. C., Owen, H. A. & Collins, M. L. A new system for heterologous expression of membrane proteins: *Rhodospirillum rubrum*. *Protein expression and purification* **70**, 88-94 (2010).
- 195 Klask, C. Heterologous Expression of Various PHA Synthase Genes in *Rhodospirillum rubrum*. *Chemical and Biochemical Engineering Quarterly* **29**, 75-85 (2015).
- 196 Rolf Jansen, H. I., Hans Reichenbach, Victor Wray, & Gerhard Höfle. Disorazoles, Highly Cytotoxic Metabolites from the Sorangicin-Producing Bacterium *Sorangium Cellulosum*, Strain So ce12. *Liebigs Ann. Chem.*, 759-773 (1994).
- 197 Elnakady, Y. A., Sasse, F., Lünsdorf, H. & Reichenbach, H. Disorazol A1, a highly effective antimitotic agent acting on tubulin polymerization and inducing apoptosis in mammalian cells. *Biochemical Pharmacology* **67**, 927-935 (2004).
- 198 Schackel, R., Hinkelmann, B., Sasse, F. & Kalesse, M. The synthesis of novel disorazoles. *Angew. Chem. Int. Ed. Engl.* **49**, 1619-1622 (2010).
- 199 Lee, C., An, D., Lee, H. & Cho, K. Correlation between *Sorangium cellulosum* subgroups and their potential for secondary metabolite production. *J. Microbiol. Biotechnol.* **23**, 297-303 (2013).
- 200 Frankel, R.B, et al. Structure and function of the bacterial magnetosome. *ASM News* **61**, 337-343 (1995).
- 201 Mitani, M., Yamanishi, T. & Miyazaki, Y. Salinomycin: a new monovalent cation ionophore. *Biochemical and biophysical research communications* **66**, 1231-1236 (1975).
- 202 Singh, M., Yadav, A., Ma, X., & Amoah, E. Plasmid DNA Transformation in *Escherichia Coli* Effect of Heat Shock Temperature, Duration, and Cold Incubation of

D. References

- CaCl₂ Treated Cells. *International Journal of Biotechnology and Biochemistry* **6**, 561–568. (2010).
- 203 Miller, J. F., Dower, W.J., & Tompkins, L.S. High-voltage electroporation of bacteria: genetic transformation of *Campylobacter jejuni* with plasmid DNA. *Proc. Natl. Acad. Sci. USA* **85**, 856-860. (1988).
- 204 Zhang Y. M., Testa G and Stewart AF. DNA cloning by homologous recombination in *Escherichia coli*. *Nat. Biotechnol.* **18**, 1314-1317 (2000).
- 205 Kandušer, M., Šentjurc, M. & Miklavčič, D. The temperature effect during pulse application on cell membrane fluidity and permeabilization. *Bioelectrochemistry* **74**, 52-57 (2008).
- 206 Quinn. A lipid-phase separation model of low-temperature damage to biological membranes. *Cryobiology* **22**, 128-146 (1985).
- 207 Gray, M. H., et al. Effect of chromosomal locus, GC content and length of homology on PCR-mediated targeted gene replacement in *Saccharomyces*. *Nucleic Acids Res.* **29**, 5156-5162 (2001).
- 208 Cobb, R. E. & Zhao, H. Direct cloning of large genomic sequences. *Nat. Biotechnol.* **30**, 405-406 (2012).
- 209 Lee, C., An, D., Lee, H., & Cho, K. Correlation between *Sorangium cellulosum* subgroups and their potential for secondary metabolite production. *J. Microbiol. Biotechnol.* **23**, 297-303 (2013).
- 210 Hopkins, C. D. & Wipf, P. Isolation, biology and chemistry of the disorazoles: new anti-cancer macrodiolides. *Nat. Prod. Rep.* **26**, 585-601 (2009).
- 211 Elisângela Soares Gomes, V. S., & Eliana Gertrudes de Macedo Lemos. Biotechnology of polyketides: New breath of life for the novel antibiotic genetic pathways discovery through metagenomics. *Brazilian Journal of Microbiology* **44**, 1007-1034 (2013).
- 212 Kopp, M., Irschik, H., Pradella, S. & Müller, R. Production of the tubulin destabilizer disorazol in *Sorangium cellulosum*: biosynthetic machinery and regulatory genes. *Chembiochem* **6**, 1277-1286 (2005).
- 213 Carvalho, R., Reid, R., Viswanathan, N., Gramajo, H. & Julien, B. The biosynthetic genes for disorazoles, potent cytotoxic compounds that disrupt microtubule formation. *Gene* **359**, 91-98 (2005).
- 214 Stevens, D. C., Hari, T. P. & Boddy, C. N. The role of transcription in heterologous expression of polyketides in bacterial hosts. *Nat. Prod. Rep.* **30**, 1391-1411 (2013).
- 215 Bian, X. *et al.* Direct cloning, genetic engineering, and heterologous expression of the syringolin biosynthetic gene cluster in *E. coli* through Red/ET recombineering. *Chembiochem* **13**, 1946-1952 (2012).
- 216 Herbert Irschik, R. J., Klaus Gerth, Gerhard Hofle & Hans Reichenbach. Disorazol A, an Efficient Inhibitor of Eukaryotic Organisms Isolated from *Myxobacteria*. *J. Antibiot.* **48**, 21-25 (1995).
- 217 Miyazaki, Y. et al. Salinomycin, a new polyether antibiotic. *J. Antibiot.* **27**, 814–821 (1974).
- 218 Gupta PB, O. T., Jiang G, Tao K, Kuperwasser C, Weinberg RA, & Lander ES. Identification of selective inhibitors of cancer stem cells by high-throughput

D. References

- screening. *Cell* **138**, 645-659 (2009).
- 219 Huczynski, A. Salinomycin: a new cancer drug candidate. *Chemical biology & drug design* **79**, 235-238 (2012).
- 220 Jiang, C., Wang, H., Kang, Q., Liu, J. & Bai, L. Cloning and characterization of the polyether salinomycin biosynthesis gene cluster of *Streptomyces albus* XM211. *Appl. Environ. Microbiol.* **78**, 994-1003 (2012).
- 221 Yurkovich, M. E. *et al.* A late-stage intermediate in salinomycin biosynthesis is revealed by specific mutation in the biosynthetic gene cluster. *Chembiochem* **13**, 66-71 (2012).
- 222 Arakaki A, N. H., Nemoto M, Mori T, & Matsunaga T. Formation of magnetite by bacteria and its application. *J. R. Soc. Interface.* **5**, 977-999 (2008).
- 223 Richter M, K. M., Bazylnski DA, Lombardot T, Glöckner FO, Reinhardt R, & Schüler D. Comparative genome analysis of four magnetotactic bacteria reveals a complex set of group-specific genes implicated in magnetosome biomineralization and function. *J. Bacteriol.* **189**, 4899-4910 (2007).
- 224 Yan L, Z. S., Chen P, Liu H, Yin H, & Li H. Magnetotactic bacteria, magnetosomes and their application. *Microbiol Res.* **167**, 507-519 (2012).
- 225 Grünberg K., Tebo B.M., Schüler D. A large gene cluster encoding several magnetosome proteins is conserved in different species of magnetotactic bacteria. *Appl. Environ. Microbiol.* **67**, 4573-4582 (2001).
- 226 Scheffel A, et al. The acidic repetitive domain of the *Magnetospirillum gryphiswaldense* MamJ protein displays hypervariability but is not required for magnetosome chain assembly. *J. Bacteriol.* **189**, 6437-6446 (2007).
- 227 Schübbe S, K. M., Scheffel A, Wawer C, Heyen U, Meyerdierks A, Madkour MH, Mayer F, Reinhardt R, & Schüler D. Characterization of a spontaneous nonmagnetic mutant of *Magnetospirillum gryphiswaldense* reveals a large deletion comprising a putative magnetosome island. *J. Bacteriol.* **185**, 5779-5790 (2003).
- 228 Murat D, Q. A., Vali H, & Komeili A. Comprehensive genetic dissection of the magnetosome gene island reveals the step-wise assembly of a prokaryotic organelle. *Proc. Natl. Acad. Sci. USA* **107**, 5593-5598 (2010).
- 229 Alexander D, R. J., He X, Miao V, Brian P, & Baltz RH. Development of a genetic system for lipopeptide combinatorial biosynthesis in *Streptomyces fradiae* and heterologous expression of the A54145 biosynthetic gene cluster. *Appl. Environ. Microbiol.* **76**, 6877-6887 (2010).
- 230 RH, Bode. Combinatorial biosynthesis of cyclic lipopeptide antibiotics: a model for synthetic biology to accelerate the evolution of secondary metabolite biosynthetic pathways. *ACS Synth. Biol.* **3**, 748-759 (2014).
- 231 Nguyen K, R. D., Gu JQ, Alexander D, Chu M, Miao V, Brian P, & Baltz RH. Combinatorial biosynthesis of lipopeptide antibiotics related to daptomycin. *Proc. Natl. Acad. Sci. USA* **103**, 17462-17467 (2006).
- 232 Jun Fu. Difference between two phage-mediated homologous recombination systems and their application. Ph.D Dissertation. (2012).
- 233 Lee, N. C., Larionov, V. & Kouprina, N. Highly efficient CRISPR/Cas9-mediated TAR cloning of genes and chromosomal loci from complex genomes in yeast.

D. References

- Nucleic Acids Res.* **43**, e55 (2015).
- 234 Jiang, W. & Zhu, T. F. Targeted isolation and cloning of 100-kb microbial genomic sequences by Cas9-assisted targeting of chromosome segments. *Nat. protocols* **11**, 960-975 (2016).
- 235 Du, D., W. L., Tian, Y, Liu, H., Tan, H., Niu, G. Genome engineering and direct cloning of antibiotic gene clusters via phage ϕ BT1 integrase-mediated site-specific recombination in *Streptomyces*. *Sci. Rep.* **5**, 8740 (2015).
- 236 Zhang, Q., Pang, B., Ding, W., & Liu, W. Aromatic polyketides produced by bacterial iterative Type I polyketide synthases. *Acs Catalysis*, 3(7): 1439-1447 (2013).
- 237 Qiang Tu, Jun Fu, Francis A. Stewart, Rolf Mueller and Youming Zhang. A new method for DNA transformation. United States of America patent application No: US 61/730,772 (2012). International patent application No: PCT/IB2013/071546 (2013)
- 238 Gerth K, Bedorf N, Höfle G, Irschik H. & Reichenbach H. Epothilons A and B: antifungal and cytotoxic compounds from *Sorangium cellulosum* (myxobacteria). *Production. J. Antibiot.* 49: 560–563 (1996).
- 239 Sasse, F., Steinmetz, H, Heil, J., Höfle, G.& Reichenbach H. Tubulysins, new cytostatic peptides from myxobacteria acting on microtubuli. *J. Antibiot.* 53: 879–885 (2000).
- 240 Piel, J. A polyketide synthase-peptide synthetase gene cluster from an uncultured bacterial symbiont of *Paederus* beetles. *Proc. Natl. Acad. Sci.* 99: 14002–14007 (2002).
- 241 Calderone, C. T. Isoprenoid-like alkylations in polyketide biosynthesis, *Nat. Prod. Rep.* 25: 845–853 (2008).

E. Appendix

Author's efforts in publications presented in this work

Publication I:

Genetic engineering and heterologous expression of the disorazol biosynthetic gene cluster via Red/ET recombineering.

Q.T., S.H. and Y.Z. planned and performed cloning experiments. **Q.T.** and X.B. performed genetic transfers, cultivation experiments and data analysis. **Q.T.** and R.R. performed HPLC and compound isolation. R.R. performed NMR experiments and data analysis. J.H. performed biological functional studies. **Q.T.**, Y.Z. and R.M. designed the study and wrote the paper. All authors discussed the results and commented on the manuscript.

Publication II:

Room temperature electrocompetent bacterial cells improve DNA transformation and recombineering efficiency.

Q.T. and J.Y. participated in the design of this study, performed data collection analysis, and drafted the manuscript; J.F, J.H, Y.L. and Y.Y. participated in interpretation data; A.F.S. and R.M. gave the advice for experimental design and discussed the data, also helped in the revision of the final manuscript. Y.Z. designed and oversaw the study, performed data interpretation and drafted the manuscript. All authors read and approved the final manuscript.

Publication III:

Biosynthesis of magnetic nanostructures in a foreign organism by transfer of bacterial magnetosome gene clusters.

I.K., D.S., Y.Z., **Q.T.**, C.J. and R.M. planned and performed cloning experiments. I.K.

and A.L. performed genetic transfers and cultivation experiments. G.W. prepared cryo- and chemically fixed cells. S.B., O.R. and G.W. performed TEM and I.K. analyzed the data. J.P. and O.R. performed cryo-electron tomography experiments. E.T. and M.P. took high-resolution TEM micrographs and analyzed the data. I.K. and A.L. took fluorescence micrographs and performed phenotypization experiments. I.K. performed western blot experiments and analyzed proteomic data. A.B. performed Illumina genome sequencing and I.K. analyzed the data. I.K. and D.S. designed the study and wrote the paper. All authors discussed the results and commented on the manuscript.

Publication IV:

Direct cloning and heterologous expression of the salinomycin biosynthetic gene cluster from *Streptomyces albus* DSM41398 in *S. coelicolor*A3 (2).

J.Y. participated in the design of this study, performed data collection analysis, and drafted the manuscript; H.M., X.Y., T.Q., F.Y., L.Q. and X.Z. participated in interpretation data; A.F.S. and R.M. helped with the revision of the final manuscript. J.F. and Y.Z. designed and oversaw the study, performed data interpretation and drafted the manuscript.

Publication I


Genetic engineering and heterologous expression of the disorazol biosynthetic gene cluster via Red/ET recombineering.


Qiang Tu, Jennifer Herrmann, Shengbiao Hu, Ritesh Raju, Xiaoying Bian, Youming Zhang[†] & Rolf Müller[†]


Author Contributions


Q.T., S.H. and Y.Z. planned and performed cloning experiments. **Q.T.** and X.B. performed genetic transfers, cultivation experiments and data analysis. **Q.T.** and R.R. performed HPLC and compound isolation. R.R. performed NMR experiments and data analysis. J.H. performed biological functional studies. **Q.T.**, Y.Z. and R.M. designed the study and wrote the paper. All authors discussed the results and commented on the manuscript.

Signatures:


Qiang Tu: 

Jennifer Herrmann: 

Shengbiao Hu: 

Ritesh Raju: 

Xiaoying Bian: 

Youming Zhang: 

Rolf Müller: 

Publication II


Room temperature electrocompetent bacterial cells improve DNA transformation and recombineering efficiency.

Qiang Tu*, Jia Yin*, Jun Fu, Jennifer Herrmann, Yuezhong Li, Yulong Yin, A. Francis Stewart[‡], Rolf Müller[‡] and Youming Zhang[‡]

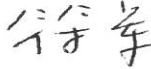
Author Contributions

Q.T. and **J.Y.** participated in the design of this study, performed data collection analysis, and drafted the manuscript; **J.F.**, **J.H.**, **Y.L.** and **Y.Y.** participated in interpretation data; **A.F.S.** and **R.M.** gave the advice for experimental design and discussed the data, also helped in the revision of the final manuscript. **Y.Z.** designed and oversaw the study, performed data interpretation and drafted the manuscript. All authors read and approved the final manuscript.

Signatures:


Qiang Tu: 


Jia Yin: 

Jun Fu: 


Jennifer Herrmann: 

Yuezhong Li: 

Yulong Yin: 

A. Francis Stewart: 

Rolf Müller: 

Youming Zhang: 

Publication III


Biosynthesis of magnetic nanostructures in a foreign organism by transfer of bacterial magnetosome gene clusters.

Isabel Kolinko, Anna Lohße, Sarah Borg, Oliver Raschdorf, Christian Jogler, **Qiang Tu**, Mihály Pósfai, Éva Tompa, Jürgen M. Plitzko, Andreas Brachmann, Gerhard Wanner, Rolf Müller, Youming Zhang[‡] and Dirk Schüler[‡]

Author contributions

I.K., D.S., Y.Z., Q.T., C.J. and R.M. planned and performed cloning experiments. I.K. and A.L. performed genetic transfers and cultivation experiments. G.W. prepared cryo- and chemically fixed cells. S.B., O.R. and G.W. performed TEM and I.K. analysed the data. J.P. and O.R. performed cryo-electron tomography experiments. E.T. and M.P. took highresolution TEM micrographs and analysed the data. I.K. and A.L. took fluorescence micrographs and performed phenotypization experiments. I.K. performed western blot experiments and analysed proteomic data. A.B. performed Illumina genome sequencing and I.K. analysed the data. I.K. and D.S. designed the study and wrote the paper. All authors discussed the results and commented on the manuscript.

Signatures:

Isabel Kolinko: 

Anna Lohße: 

Sarah Borg: 


Oliver Raschdorf: 

Christian Jogler: 

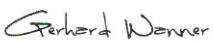
Qiang Tu: 

Mihály Pósfai: 


Éva Tompa: 

Jürgen M. Plitzko: 

Andreas Brachmann: 

Gerhard Wanner: 

Rolf Müller: 

Youming Zhang: 

Dirk Schüler: 

Publication IV

Direct cloning and heterologous expression of the salinomycin biosynthetic gene cluster from *Streptomyces albus* DSM41398 in *S. coelicolor*A3(2).

Jia Yin, Michael Hoffmann, Xiaoying Bian, **Qiang Tu**, Fu Yan, Liqiu Xia, Xuezhi Ding, A. Francis Stewart, Rolf Müller[†], Jun Fu[†] & Youming Zhang[†]

Author Contributions

J.Y. participated in the design of this study, performed data collection analysis, and drafted the manuscript; H.M., X.Y., T.Q., F.Y., L.Q. and X.Z. participated in interpretation data; A.F.S. and R.M. helped with the revision of the final manuscript. J.F. and Y.Z. designed and oversaw the study, performed data interpretation and drafted the manuscript.

Signatures:

Jia Yin: 尹佳

Michael Hoffmann:

Xiaoying Bian:

Qiang Tu:

Fu Yan:

Liqiu Xia:

Xuezhi Ding:

A. Francis Stewart:

Rolf Müller:

Jun Fu:

Youming Zhang: